Anomalous Couplings, Resonances and Unitarity in Vector Boson Scattering

Dissertation
zur Erlangung des Grades eines Doktors
der Naturwissenschaften

vorgelegt von
MSc. Marco Sekulla

eingereicht bei der Naturwissenschaftlich-Technischen Fakultät
der Universität Siegen
Siegen 2015

Gutachter:

- Prof. Dr. Wolfgang Kilian
- Prof. Dr. Thomas Mannel

Datum der mündlichen Prüfung: 04.12.2015
Prüfer:

- Prof. Dr. Ivor Fleck
- Prof. Dr. Otfried Gühne
- Prof. Dr. Wolfgang Kilian (Vorsitz der Prüfungskommision)
- Prof. Dr. Thomas Mannel

Zusammenfassung

Das Standardmodell der Teilchenphysik hat sich als verlässliche Theorie bewährt, um Wechselwirkungen elementarer Teilchen zu beschreiben. Jedoch sind viele Fragen bezüglich des Higgs-Sektors und der zugehörigen elektroschwachen Symmetriebrechung weiterhin unbeantwortet, obwohl (oder gerade weil) ein leichtes Higgs-Boson entdeckt wurde. Die Streuamplitude zweier schwacher Vektorbosonen ist im Standardmodell zusätzlich durch den Higgs-Boson Austausch unterdrückt. Daher können selbst geringe Beiträge neuer Physik zu großen Abweichungen des Vektorboson-Streuprozesses führen. Um mögliche Abweichungen durch neue Physik modellunabhängig zu analysieren, können höherdimensionale Operatoren einer effektiven Feldtheorie verwendet werden.

In dieser Doktorarbeit wird ein kompletter Satz von Dimension sechs und acht Operatoren, welche den Streuprozess zweier Vektorbosonen direkt beeinflussen, systematisch aufgestellt und diskutiert. Unter der Annahme, dass die neue Physik des Higgs/Goldstoneboson Sektors im Hochenergielimes vom Fermionen- und Eichsektor entkoppelt, wird der Einfluss des Dimension sechs Operators $\mathcal{L}_{HD}$ und der Dimension acht Operatoren $\mathcal{L}_{S,0}$ und $\mathcal{L}_{S,1}$ auf den Vektorboson Streuprozess separat untersucht. Eine Betrachtung mithilfe konventioneller effektiver Feldtheorie wird jedoch die Unitarität der Streumatrix ab einer gewissen Energie verletzen. Um eine Analyse der Dimension acht Operatoren konsistent mit quantenmechanischen Grundsätzen durchzuführen, wird das T-matrix Unitarisierungsverfahren entwickelt. Da dieses Schema theoretische Vorhersagen, welche nicht die Unitarität verletzen, invariant lässt, kann dieses Unitarisierungsverfahren präventiv zu jedem beliebiges Modell eingesetzt werden.

Die effektive Feldtheorie wird zusätzlich um generische Resonanzen, die an den Higgs/Goldstoneboson Sektor koppeln, erweitert und zwar den Isoskalar-Skalar, den Isoskalar-Tensor, den Isotensor-Skalar und den Isotensor-Tensor. Im Falle der Tensorresonanzen wird der Stückelberg-Formalismus benutzt, um die einzelnen Freiheitsgrade des Tensors und deren Einfluss auf die Vektorboson-Streuamplitude separat zu untersuchen. Bei einem Vergleich mit der effektiven Theorie bei niedrigen Energien, wo die Resonanzen ausintegriert sind, zeigt sich die Notwendigkeit der Einführung dieser zusätzlichen Freiheitsgrade. Für verschie-

dene Parametersätze werden die Verteilungen der Streuung zweier Vektorboson am Large Hadron Collider bei einer Schwerpunktsenergie von $\sqrt{s} = 14\,\text{TeV}$ mit Hilfe des Monte-Carlo Generators `WHIZARD` berechnet.

Im Rahmen der Doktorarbeit werden die Resonanzmodelle und die besprochenen Operatoren in der effektiven Feldtheorie inklusive der T-matrix Unitarisierungsverfahren in `WHIZARD` implementiert. Mit den `WHIZARD` Modellen SSC_2, SSC_AltT und SM_ul werden somit Werkzeuge für eine phänomenologische Analyse neuer Physik im Goldstoneboson/Higgs-Sektors bereit gestellt, um Vektorboson-Streuprozesse zu untersuchen.

Abstract

The Standard Model of particle physics has proved itself as a reliable theory to describe interactions of elementary particles. However, many questions concerning the Higgs sector and the associated electroweak symmetry breaking are still open, even after (or because) a light Higgs boson has been discovered. The $2 \to 2$ scattering amplitude of weak vector bosons is suppressed in the Standard Model due to the Higgs boson exchange. Therefore, weak vector boson scattering processes are very sensitive to additional contributions beyond the Standard Model. Possible new physics deviations can be studied model-independently by higher dimensional operators within the effective field theory framework.

In this thesis, a complete set of dimension six and eight operators are discussed for vector boson scattering processes. Assuming a scenario where new physics in the Higgs/Goldstone boson decouples from the fermion-sector and the gauge-sector in the high energy limit, the impact of the dimension six operator $\mathcal{L}_{HD}$ and dimension eight operators $\mathcal{L}_{S,0}$ and $\mathcal{L}_{S,1}$ to vector boson scattering processes can be studied separately for complete processes at particle colliders. However, a conventional effective field theory analysis will violate the S-matrix unitarity above a certain energy limit. The direct T-matrix scheme is developed to allow a study of effective field theory operators consistent with basic quantum-mechanical principles in the complete energy reach of current and future colliders. Additionally, this scheme can be used preventively for any model, because it leaves theoretical predictions invariant, which already satisfies unitarity.

The effective field theory approach is further extended by allowing additional generic resonances coupling to the Higgs/Goldstone boson sector, namely the isoscalar-scalar, isoscalar-tensor, isotensor-scalar and isotensor-tensor. In particular, the Stückelberg formalism is used to investigate the impact of the tensor degree of freedoms, separately. The necessity of these additional resonance, especially for weakly coupled resonances, are manifest by comparing vector boson scattering distributions of the resonance model and of the corresponding effective field theory operators, where the resonance is integrated out. For different parameter sets, the distributions of vector boson scattering processes for the large hadron collider at center of mass energy of $\sqrt{s} = 14\,\text{TeV}$ are calculated with the Monte-Carlo generator `WHIZARD`.

As part of this thesis, the resonance model and the effective field operators including the T-matrix unitarization scheme are implemented in WHIZARD. With the WHIZARD models SSC_2, SSC_AltT and SM_ul, a tool-set is provided to study new physic in the Goldstone boson/Higgs sector within complete experimental analysis at the large hadron collider or other future colliders.

Contents

Chapter 1

Introduction

The Standard Model of particle physics has proven to be a very successful quantum field theory for describing processes on an elementary level. Three of four known forces, the electromagnetic, the weak and the strong forces, are described by the Standard Model. These forces are mediated by gauge bosons, the photon γ for the electromagnetic force, the vector boson $W^{\pm}$ and Z for the weak force and the gluons for the strong force. Their interactions are formulated within the gauge symmetry group

$$SU(3)_C \times SU(2)_L \times U(1)_Y \,. \tag{1.1}$$

In addition to bosons, the Standard Model describes fermions as the elementary components of matter. The gauge group quantum numbers and representations of the three flavor generations of quark field $U = (u, c, t)$, $D = (d, s, b)$, and lepton fields $\widetilde{E} = (e, \mu, \tau)$, $N = \left(\nu_e, \nu_\mu, \nu_\tau\right)$ are listed in Table 1.1. Whereas, the gauge bosons transform according to the adjoint representation of their associated gauge group and are singlets under the other gauge groups.

To formulate a Lagrangian for the theory which is invariant under local transformations of the Standard Model gauge group (1.1), it is necessary that all particles are massless due to the chiral nature of the particle representations. However, a scheme to introduce massive particles into a gauge theory was first proposed in [1–3]. In particular, an additional elementary scalar particle, the Higgs boson, with non-vanishing vacuum expectation value was added to the Standard Model. Its vacuum expectation value spontaneously breaks the electroweak symmetry group $SU(2)_L \times U(1)_Y$ to the electromagnetic $U(1)_{\text{em}}$ and generates masses for all charged fermions and the weak vector bosons $W^{\pm}$ and Z.

Although, the Higgs plays an important role in the Standard Model, its mass was unknown for a long time. Even its existence was not proved. A positive result for the Higgs boson search was achieved only three year ago in 2012; the experiments ATLAS [4] and CMS [5] at the Large Hadron Collider (LHC) at CERN (Geneva, Switzerland) announced the discovery

field	$SU(3)_C$	$SU(2)_L$	$U(1)_Y$
$Q = \begin{pmatrix} U_L \\ D_L \end{pmatrix}$	**3**	**2**	$+1/6$
$L = \begin{pmatrix} N_L \\ \widetilde{E}_L \end{pmatrix}$	**1**	**2**	$-1/2$
U_R	$\bar{\mathbf{3}}$	**1**	$+2/3$
D_R	$\bar{\mathbf{3}}$	**1**	$-1/3$
$\widetilde{E}_R$	**1**	**1**	$+1$

Table 1.1.: The representation of the strong $SU(3)_C$ and weak $SU(2)_L$ for the fermion fields and their hypercharge $U(1)_Y$.

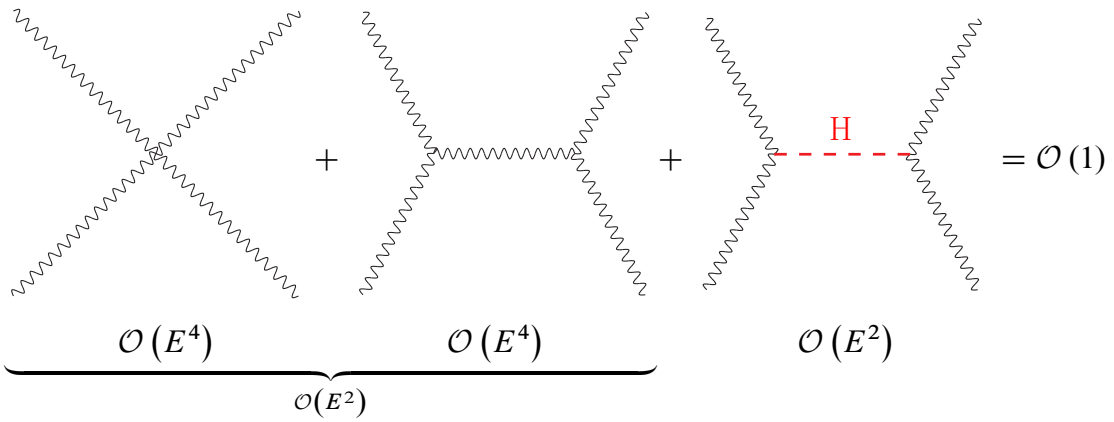

Figure 1.1.: Vector boson ($W^{\pm}, Z$) scattering: Higgs contribution cancels E^2 energy dependence of both gauge boson self interaction diagrams.

of a Higgs-like resonance with a mass of 125 GeV. It has to be a boson, because it was discovered in the photon-photon and two weak vector boson decay channels. More detailed experimental studies of the spin of the new resonance favor the Standard Model assumption that the new resonance has spin zero [6, 7]. Therefore, this resonance can be identified as the weakly interacting scalar Higgs boson predicted by the Standard Model.

Further insights into the Higgs boson properties and its role in a fundamental theory can be achieved by studying the quasi-elastic scattering of two weak gauge bosons. The Higgs contribution is crucial for the tree level Standard Model amplitude for this process. Without the Higgs, the vector boson scattering amplitude at high energies would be dominated by the scattering of the longitudinal weak vector bosons $W^{\pm}$ and Z, which are associated with the Goldstone bosons of the broken electroweak symmetry. Each weak gauge boson self interaction diagram shown in Figure 1.1 will rise with the energy as E^4. Summing over all vector boson self interaction contributions will cancel the leading energy dependence, but will leave an amplitude proportional to E^2/v^2 at leading order, where v is the electroweak energy scale $v = 246$ GeV. Therefore, the electroweak interaction would become strong in the TeV range.

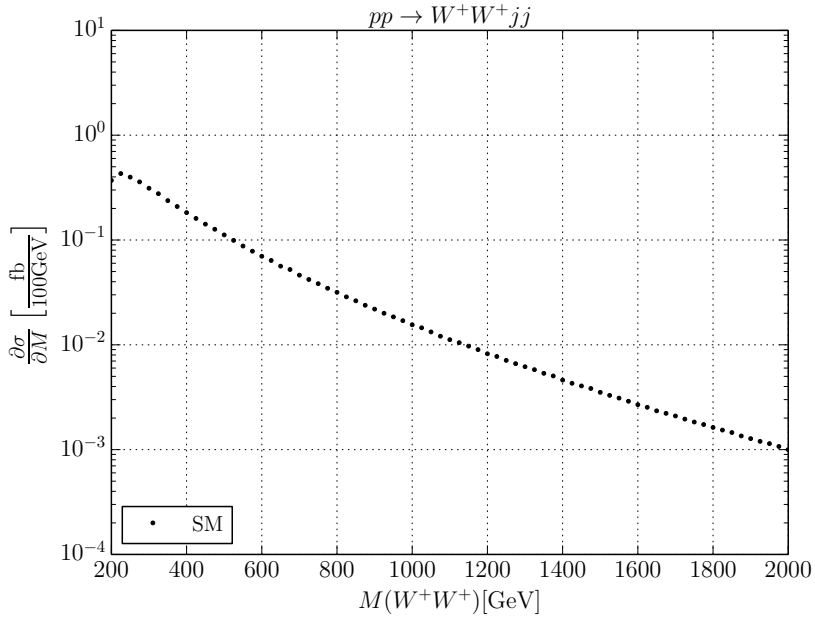

Figure 1.2.: $pp \to W^+W^+jj$ at $\sqrt{s} = 14\,\text{TeV}$.
Differential cross section as function of the invariant mass of the final state on-shell Ws calculated with `WHIZARD` using vector boson fusion cuts:
$M_{jj} > 500$ GeV; $\Delta y_{jj} > 2.4$; $p_T^j > 20$ GeV; $|\eta_j| > 4.5$.

However, the Standard Model Higgs contribution to the Goldstone scattering amplitude induces an exact cancellation of the rising energy behavior and leads to an asymptotically small tree level amplitude proportional to $m_h^2/v^2 = 0.25$. In other words, the Higgs exchange suppresses the longitudinal vector boson scattering amplitude, and instead of a strongly interacting model, the Standard Model describes a weakly interacting Higgs sector.

At the LHC, the Standard Model like vector boson scattering of two vector bosons was experimentally confirmed in proton-proton collisions just recently [8, 9]. Due to its small cross section, as shown in Figure 1.2, the sensitivity for vector boson scattering is not very high at the LHC. Further upgrades for the LHC and future linear colliders, including the International Linear Collider, will improve the accuracy and energy reach of the measurement [10].

Because the contribution of longitudinally polarized weak vector bosons is highly suppressed, the complete vector boson scattering amplitude is dominated by the transverse degrees of freedom of the gauge boson $W^\pm$ and Z. Therefore, the longitudinal channel is sensitive to a possible excess, which could be caused by new physics in the electroweak breaking sector.

In this thesis, a tool set is introduced to execute a phenomenological study for full vector boson scattering processes at particle colliders. Starting point is the discussion of suitable representations of the electroweak breaking sector and the definition of the corresponding Lagrangian in Chapter 2. With a chosen representation, a complete basis of effective field

theory operators is then defined in Chapter 3, which parameterizes the low energy behavior of possible new physics contributions without knowledge of the full theory. Considering fundamental mathematical properties of the scattering matrix and difficulties of separating low-energy from high-energy scattering observables at hadron colliders, the phenomenological description of vector boson scattering processes should smoothly interpolate low-energy behavior and any possible high-energy asymptotic. For a meaningful analysis of the experimental data, searching for new physics contributions, the parameterized high-energy behavior has to be consistent with the universal principles of quantum physics. As it will be discussed at the end of Chapter 3, a naive low energy effective field theory analysis will not fulfill this demand. Instead, a framework, namely the direct T-matrix unitarization, is presented in Chapter 4, which will accompany any generic model to provide an interpolation between low-energy effects and the high energy behavior. As part of this thesis, the T-matrix unitarization scheme is implemented in the Monte Carlo generator `WHIZARD`[11, 12] for vector boson scattering processes in the presence of a light Higgs. `WHIZARD` can then generate events, which can be used in phenomenological studies of realistic scattering processes with fermions as external probes of off-shell vector bosons. In Chapter 4, an extended approach for modeling new physics contributions in vector boson scattering is introduced by including generic resonances. Finally, a conclusion is presented at the end of this thesis.

Chapter 2

Representations of the Standard Model

The theoretical description of weak particle interactions starts with the specification of a Lagrangian which includes the particle content and their interactions. There is some freedom of choice in the definition of a Lagrangian. These choices are only of mathematical nature and will not affect experimental observables such as cross sections. Nevertheless, the use of a particular representation can be more or less beneficial for the calculation and discussion of those observables.

A model which describes the spontaneous breaking of the electroweak symmetry does not necessarily need an elementary Higgs. Instead, the breaking of the electroweak symmetry group can originate from strongly interacting physics in analogy to chiral symmetry breaking by vacuum condensates in quantum chromodynamics (QCD). A scalar Higgs boson can then be additionally added as an electroweak singlet to the Lagrangian. It is therefore formally separated from the Goldstone boson sector in contrary to the usual Standard Model representation, where it is embedded with the Goldstone bosons in a linear representation as Higgs doublet. This linear representation is favorable to describe a weakly interacting Higgs sector.

Both representations, the nonlinear and the linear Higgs doublet, have some beneficial features for the analysis of vector boson scattering. In this thesis, the linear Higgs matrix representation is introduced to combine these advantageous features into one representation, which is particularly suited to analyze weak vector boson scattering processes.

Some basic definitions for the electroweak gauge theory will be given in this chapter. Three different representation, the nonlinear and the linear Higgs doublet representation and the linear Higgs matrix representation are considered. The parts of the Lagrangian which directly contribute to the vector boson scattering process will be discussed as well. The fermionic sector and the strong interaction have no leading order impact on vector boson scattering and will therefore not be reviewed. Descriptions of these can be found in many textbooks of quantum field theory, for example [13, 14].

2.1. Basic Definitions

Interactions of weak vector bosons are described by the electroweak $SU(2)_L \times U(1)_Y$ gauge group. The generators in the fundamental representation of the $SU(2)_L$ are given by the Pauli-matrices τ_i $(i = 1, 2, 3)$ and the hypercharge Y represents the $U_Y(1)$ generator. Furthermore, the interaction of each gauge group is described by gauge fields, W_i^μ and B^μ for $SU(2)_L$ and $U(1)_Y$, respectively. A simplification of the notation is achieved by introducing the definitions

$$\mathbf{W}^\mu \equiv W_i^\mu \frac{\tau_i}{2}, \tag{2.1a}$$

$$\mathbf{B}^\mu \equiv \frac{Y}{2} B^\mu. \tag{2.1b}$$

For a gauge theory the Lagrangian has to be invariant under local gauge transformations. These gauge transformations, V_L for $SU(2)_L$ and V_Y for $U(1)_Y$, are defined by arbitrary, smooth complex functions of space-time $\alpha_i(x)$ and $\beta(x)$ as

$$V_L(x) = \exp\left(-\mathrm{i}\alpha_i(x)\frac{\tau_i}{2}\right) = 1 - \mathrm{i}\alpha_i(x)\frac{\tau_i}{2} + \mathcal{O}(\alpha_i^2), \tag{2.2a}$$

$$V_Y(x) = \exp\left(-\mathrm{i}\frac{Y}{2}\beta(x)\right) = 1 - \mathrm{i}\frac{Y}{2}\beta(x) + \mathcal{O}(\beta^2). \tag{2.2b}$$

To fulfill gauge invariance the covariant derivative, instead of the usual partial derivative, has to be used. Within this definition a first choice arises. In line with the definition in the Monte Carlo generator `WHIZARD` [15] (see Appendix (C.2.1) for details) the covariant-derivative-sign-convention '–' ("CD–") is chosen, i.e.

$$\mathbf{D}_W^\mu = \partial^\mu - \mathrm{i}g\mathbf{W}^\mu, \tag{2.3a}$$

$$\mathbf{D}_B^\mu = \partial^\mu - \mathrm{i}g'\mathbf{B}^\mu, \tag{2.3b}$$

$$\mathbf{D}^\mu = \partial^\mu - \mathrm{i}g\mathbf{W}^\mu - \mathrm{i}g'\mathbf{B}^\mu. \tag{2.3c}$$

The formulation of gauge invariant kinetic terms for gauge bosons is simplified by introducing the field strength tensors

$$\begin{aligned}\mathbf{W}^{\mu\nu} \equiv W_i^{\mu\nu}\frac{\tau_i}{2} &= +\frac{\mathrm{i}}{g}\left[\mathbf{D}_W^\mu, \mathbf{D}_W^\nu\right] = \left(\partial^\mu W_k^\nu - \partial^\nu W_k^\mu + g\varepsilon_{ijk}W_i^\mu W_j^\nu\right)\frac{\tau_k}{2} \\ &= \partial_\mu \mathbf{W}_\nu - \partial_\nu \mathbf{W}_\mu - \mathrm{i}g\left[\mathbf{W}_\mu, \mathbf{W}_\nu\right], \end{aligned} \tag{2.4a}$$

$$\begin{aligned}\mathbf{B}^{\mu\nu} \equiv \frac{Y}{2}B^{\mu\nu} &= +\frac{\mathrm{i}}{g'}\left[\mathbf{D}_B^\mu, \mathbf{D}_B^\nu\right] = \frac{Y}{2}\left(\partial^\mu B^\nu - \partial^\nu B^\mu\right) \\ &= \partial_\mu \mathbf{B}_\nu - \partial_\nu \mathbf{B}_\mu. \end{aligned} \tag{2.4b}$$

Therefore, a minimal Lagrangian for the gauge bosons can now be written as

$$\mathcal{L}_{\text{kin}} = -\frac{1}{2}\mathrm{tr}\left[\mathbf{W}_{\mu\nu}\mathbf{W}^{\mu\nu}\right] - \frac{1}{2}\mathrm{tr}\left[\mathbf{B}_{\mu\nu}\mathbf{B}^{\mu\nu}\right]. \tag{2.5}$$

Besides the kinetic terms for the gauge bosons W^i and B, the Lagrangian (2.5) also contains triple and quartic gauge boson self interactions.

Experimental results show that the non-zero mass eigenstates of W and B, i.e. the weak vector bosons $W^\pm$ and Z, have different masses. However, mass terms for the weak vector bosons are not included in (2.5). The easiest way to write down mass terms for for $W^\pm$ and Z is to simply add a mass term of the form

$$\mathcal{L}_{\text{mass}} = m_Z^2 Z_\mu Z^\mu + m_W^2 W_\mu^+ W^{-\mu}\,, \tag{2.6}$$

but these terms break the $SU(2)_L \times U(1)_Y$ gauge symmetry explicitly and violate the demand that the Lagrangian should be invariant under gauge transformations (2.2).

A way to solve this dilemma has been found with the Higgs mechanism for the electroweak theory [1–3, 16–19]. Only the ground state of the theory breaks the symmetry, but the Lagrangian itself maintains the electroweak symmetry. The electromagnetic and weak interactions can be described correctly by an unified electroweak symmetry at high energies, which is spontaneously broken at the electroweak energy scale v. This has the advantage, that less free parameters are needed for the theoretical description and the renormalizability of the theory with massive vector bosons is guaranteed [20]. Spontaneous symmetry breaking of the electroweak symmetry group

$$SU(2)_L \times U(1)_Y \to U(1)_{\text{em}} \tag{2.7}$$

gives rise to three Goldstone bosons w^i. These are massless spin zero fields and mix with the gauge fields W^i and B. Diagonalizing this mixing, mass eigenstates can be found, where the Goldstone bosons are absorbed by the gauge bosons and become the longitudinal degree of freedom of the massive mass eigenstates $W^\pm$ and Z.

The mechanism originally proposed by Higgs uses a scalar field acquiring a vacuum expectation value [1]. Nevertheless, a gauge invariant Lagrangian can also be written down with a very heavy or non-elementary Higgs field. A nonlinear realization of the Higgs sector is necessary for this scenario.

2.2. Nonlinear Realization of Electroweak Symmetry Breaking

Nonlinear representations have been originally introduced in particle physics for chiral symmetry breaking [21], where the chiral symmetry is broken by the strong dynamics of quantum chromodynamics.

Possible scenarios of electroweak symmetry breaking by a heavy Higgs or a new strong interacting sector (non-elementary Higgs) analogous to chiral symmetry breaking have been investigated. For these cases a nonlinear realization of the electroweak breaking sector has been introduced [22, 23]. If the Higgs is heavy, it can be decoupled from the Goldstone boson sector and integrated out.

2.2.1. The Goldstone Boson Sector

The Goldstone boson sector is represented by an auxiliary dimensionless field

$$\mathbf{U} = \mathbf{U}\left(\frac{w^1}{v}\tau^1, \frac{w^2}{v}\tau^2, \frac{w^3}{v}\tau^3\right). \tag{2.8}$$

It is a nonlinear function of all three electroweak Goldstone bosons w^i and can be represented as a unitary 2×2-matrix. The associated electroweak breaking scale v for the Goldstone bosons is explicitly contained in the definition (2.8). Under the gauge transformation (2.2) the field $\mathbf{U}$ transforms as

$$\mathbf{U}(w^i(x)) \to V_L(x)^\dagger \mathbf{U}(w^i(x)) V_Y(x). \tag{2.9}$$

A possible and convenient nonlinear representation of the Goldstone boson sector is the exponential representation [24, 25]

$$\mathbf{U}(x) = \exp\left(-\mathrm{i}\frac{w^i(x)}{v}\tau^i\right). \tag{2.10}$$

This representation is used for arbitrary, strongly interacting models within a chiral Lagrangian. However, many different representations are used in the literature. For example, another nonlinear representation is

$$\mathbf{U}(x) = \sqrt{1 - \frac{w^i(x)w^i(x)}{v^2}} + \mathrm{i}\frac{w^i(x)}{v}\tau^i\,, \tag{2.11}$$

which is used after integrating out a heavy strongly interacting Higgs within a linear representation of the Higgs sector in [22].

To formulate the interaction of the auxiliary field in a more general approach, the auxiliary field $\mathbf{U}$ is extended to the field $\mathbf{U}'$ by including non-unitary 2×2-matrices. This field couples to the gauge bosons through the covariant derivative

$$\mathbf{D}^\mu \mathbf{U} \equiv \partial^\mu \mathbf{U} - \mathrm{i}g\mathbf{W}^\mu \mathbf{U}\,. - \mathrm{i}g'\mathbf{U}\mathbf{B}^\mu \tag{2.12}$$

The covariant derivative is needed for a gauge invariant formulation of the kinetic term

$$\mathcal{L}_{\mathrm{U,kin}} = \frac{v^2}{4}\mathrm{tr}\left[\left(\mathbf{D}_\mu \mathbf{U}'\right)^\dagger \mathbf{D}^\mu \mathbf{U}'\right]. \tag{2.13}$$

To generate mass terms with the kinetic term for the weak vector bosons, the operator $\mathrm{tr}\left[\mathbf{U}'^\dagger \mathbf{U}'\right]$ has to receive a nonzero vacuum expectation value. This is achieved by adding the potential

$$\mathcal{L}_{\mathrm{U,pot}} = \frac{1}{4}\lambda\left(\frac{v^2}{4}\mathrm{tr}\left[\mathbf{U}'^\dagger \mathbf{U}'\right] - \frac{\mu^2}{\lambda}\right)^2, \tag{2.14}$$

which is invariant under $SU(2)_Y \times U(1)_L$. Therefore, a nonzero vacuum expectation value is generated for the composite operator

$$\left\langle \frac{1}{2}\mathrm{tr}\left[\mathbf{U}'^{\dagger}(x)\mathbf{U}'(x)\right]\right\rangle = 1. \tag{2.15}$$

The field $\mathbf{U}'$ is normalized in such a way, that it will give rise to the correct masses of the $W^{\pm}$ and Z gauge bosons [1]. Additionally, the equation (2.15) results in an infinite degeneracy of equivalent ground states for $\mathbf{U}'$ [26]. A convenient choice for the ground state to obtain the spontaneous breaking of the electroweak symmetry group to the electromagnetic $U(1)_{\mathrm{em}}$ is

$$\left\langle \mathbf{U}'(x)\right\rangle = 1\,, \qquad \text{for} \qquad x \to \infty. \tag{2.16}$$

However, there is an additional degree of freedom in the fluctuation of the composite field $\left\langle \frac{1}{2}\mathrm{tr}\left[\mathbf{U}'^{\dagger}(x)\mathbf{U}'(x)\right]\right\rangle$. This degree of freedom can be represented by introducing an additional particle, the Higgs boson.

2.2.2. Introduction of the Higgs

Contrary to the scenarios with non or heavy Higgs, a scalar resonance with mass of the same order of W and Z mass has been detected in 2012 [4, 5]. Therefore, a light Higgs boson has to be included. The most generic way to introduce the Higgs boson h into the model is by rewriting the Goldstone boson sector as

$$\mathbf{U}' \equiv \left(1 + \sum_{i=1}^{\infty} f_{h,i}\left(\frac{h}{v}\right)^i\right)\mathbf{U}\,, \tag{2.17}$$

with independent couplings $f_{h,i}$ and $\mathbf{U}^{\dagger}\mathbf{U} = \mathbb{1}$. Without fine-tuned Higgs couplings in (2.17), the amplitude of weak vector boson scattering is dominated by longitudinal vector boson scattering and will rise with the center of mass energy s/v^2. Therefore, the validity of the theory is restricted to a cut-off scale $\Lambda_c \sim 4\pi f$, whereas no cut-off scale is present in the linear Higgs-realization. This representation automatically provides the correct Higgs coupling strength, that will suppress the $VV \to VV$ amplitude at high energies [27], where V represents the weak gauge bosons $W^{\pm}$ and Z.

2.3. The Linear Matrix Representation

The Higgs can be directly included into the auxiliary field $\mathbf{U}'$. In this case, the field $\mathbf{U}'$ can be represented by the linear form

$$\mathbf{U}' = -\mathrm{i}\frac{w^i}{v}\tau^i + \frac{h}{v}\mathbb{1}\,. \tag{2.18}$$

[1] This will be discussed in more detail for the linear Higgs matrix representation in Section 2.3

To distinguish the nonlinear representation and linear representation, a linear 2×2 field containing the massless Goldstone bosons $w^{\pm} = \left(w^1 \mp \mathrm{i}w^2\right)/\sqrt{2}$, w^3 and the scalar Higgs h is introduced to represent the Higgs sector

$$\mathbf{H} \equiv \frac{1}{2}\begin{pmatrix} v + h - \mathrm{i}w^3 & -\mathrm{i}\sqrt{2}w^+ \\ -\mathrm{i}\sqrt{2}w^- & v + h + \mathrm{i}w^3 \end{pmatrix}. \tag{2.19}$$

This new field has similar properties as the auxiliary field $\mathbf{U}'$, but its mass dimension is one. Furthermore, the matrix representation (2.19) transforms like the auxiliary field $\mathbf{U}$ in equation (2.9), namely

$$\mathbf{H}(x) \to V_L(x)^{\dagger}\mathbf{H}(x)V_Y(x). \tag{2.20}$$

In the definition (2.19) the Higgs h is explicitly expanded around its vacuum expectation value. The expectation value originates from the potential [2]

$$\mathcal{L}_{\mathrm{H,pot}} = -\mu^2 \mathrm{tr}\left[\mathbf{H}^{\dagger}\mathbf{H}\right] + \frac{\lambda}{2}\left(\mathrm{tr}\left[\mathbf{H}^{\dagger}\mathbf{H}\right]\right)^2, \tag{2.21}$$

where the values of the parameters μ^2 and λ will be set to give the necessary potential for spontaneous symmetry breaking of the electroweak group. Therefore, the expectation value is set to the electroweak scale v. Vector boson masses are then generated by the kinetic term of the Higgs field

$$\mathcal{L}_{\mathrm{H,kin}} = \mathrm{tr}\left[\left(\mathbf{D}_{\mu}\mathbf{H}\right)^{\dagger}\mathbf{D}^{\mu}\mathbf{H}\right]. \tag{2.22}$$

Within the covariant derivative of the Higgs

$$\mathbf{D}_{\mu}\mathbf{H} = \partial_{\mu}\mathbf{H} - \mathrm{i}g\mathbf{W}_{\mu}\mathbf{H} - \mathrm{i}g'\mathbf{H}\mathbf{B}_{\mu}, \tag{2.23}$$

the operator Y is defined as

$$\mathbf{H}Y \equiv -\mathbf{H}\tau_3. \tag{2.24}$$

The vector bosons interact with the vacuum expectation value due to the coupling by the covariant derivative (2.23) of the Higgs matrix field in (2.22). These interactions lead to mass terms for the weak vector bosons,

$$\mathcal{L}_{\mathrm{mass}} = \frac{1}{2}\frac{v^2}{4}\left(g^2\left(W_{1\,\mu} - \mathrm{i}W_{2\,\mu}\right)\left(W_1^{\mu} + \mathrm{i}W_2^{\mu}\right) + \left(gW_{3\,\mu} - g'B_{\mu}\right)\left(gW_3^{\mu} - g'B^{\mu}\right)\right). \tag{2.25}$$

It is obvious that they mix in the electroweak basis of the gauge bosons. A diagonalized basis can be found by introducing the Weinberg angle θ_w as

$$c_w \equiv \cos(\theta_w) = \frac{g}{\sqrt{g^2 + g'^2}} \quad \text{and} \quad s_w \equiv \sin(\theta_w) = \frac{g'}{\sqrt{g^2 + g'^2}}. \tag{2.26}$$

[2] Note that terms proportional to $\mathrm{tr}\left[\left(\mathbf{H}^{\dagger}\mathbf{H}\right)^2\right]$ can decomposed to $\mathrm{tr}\left[\mathbf{H}^{\dagger}\mathbf{H}\right]^2$ by (A.6).

The mass eigenstates are identified with the weak vector bosons $W^{\pm}$ and Z, and can be written as a linear combination of W_i^{μ} and B^{μ},

$$W_{\mu}^{\pm} = \frac{1}{\sqrt{2}} \left(W_{\mu\,1} \mp \mathrm{i} W_{\mu\,2} \right), \tag{2.27a}$$

$$Z_{\mu} = c_w W_{3\,\mu} - s_w B_{\mu}. \tag{2.27b}$$

Additionally, there is one orthogonal and massless eigenstate remaining, the photon

$$A_{\mu} = s_w W_{3\,\mu} + c_w B_{\mu}, \tag{2.27c}$$

which represents the gauge boson of the unbroken $U_{\mathrm{em}}(1)$. To get a closer look at the electromagnetic interactions, the relations (2.27) are inverted

$$W_{1\,\mu} = \frac{1}{\sqrt{2}} \left(W_{\mu}^{+} + W_{\mu}^{-} \right), \tag{2.28a}$$

$$W_{2\,\mu} = \frac{\mathrm{i}}{\sqrt{2}} \left(W_{\mu}^{+} - W_{\mu}^{-} \right), \tag{2.28b}$$

$$W_{3\,\mu} = s_w A_{\mu} + c_w Z_{\mu}, \tag{2.28c}$$

$$B_{\mu} = c_w A_{\mu} - s_w A_{\mu}. \tag{2.28d}$$

Combining equations (2.28) and (2.3) the covariant derivative can be rewritten as

$$\begin{aligned} \mathbf{D}_{\mu} = \partial_{\mu} - \mathrm{i} \frac{g}{\sqrt{2}} \left(W_{\mu}^{+} \tau^{+} + W_{\mu}^{-} \tau^{-} \right) - \mathrm{i} Z_{\mu} \left(c_w g \frac{\tau_3}{2} - s_w g' \frac{Y}{2} \right) \\ - \mathrm{i} s_w g A_{\mu} \left(\frac{\tau_3}{2} + \frac{Y}{2} \right) \end{aligned} \tag{2.29}$$

with $\tau^{\pm} = \frac{1}{2} (\tau_1 \pm \mathrm{i}\tau_2)$. Representing the covariant derivative in the mass eigenstate basis gives a better insight into interactions of the physical particles $W^{\pm}$, Z and γ. One can easily read off the electromagnetic coupling e and its generator, the charge operator Q,

$$e = s_w g, \tag{2.30}$$

$$Q = \frac{\tau_3 + Y}{2}. \tag{2.31}$$

As mentioned above, the focus of this thesis lies on the Higgs sector, which will be investigated using vector boson scattering. All Standard Model interactions for vector boson scattering are described by the Lagrangian

$$\begin{aligned} \mathcal{L}_{\mathrm{min}} = &- \frac{1}{2} \mathrm{tr} \left[\mathbf{W}_{\mu\nu} \mathbf{W}^{\mu\nu} \right] - \frac{1}{2} \mathrm{tr} \left[\mathbf{B}_{\mu\nu} \mathbf{B}^{\mu\nu} \right] \\ &+ \mathrm{tr} \left[\left(\mathbf{D}_{\mu} \mathbf{H} \right)^{\dagger} \mathbf{D}^{\mu} \mathbf{H} \right] + \mu^2 \mathrm{tr} \left[\mathbf{H}^{\dagger} \mathbf{H} \right] - \frac{\lambda}{2} \left(\mathrm{tr} \left[\mathbf{H}^{\dagger} \mathbf{H} \right] \right)^2 . \end{aligned} \tag{2.32}$$

The coupling strengths are given by the parameters μ^2, λ, g and g'. There are some theoretical constraints for these parameters, especially for the Higgs potential parameters μ^2 and λ. The relation $\mu^2 > 0$ has to be fulfilled to get a non-zero local minimum for the potential, which will break the electroweak symmetry spontaneously. Furthermore, λ has to be positive to guarantee vacuum stability.

2.3.1. Tree-level Normalization

The couplings in (2.32) should be represented by physical parameters to get a better understanding of their scaling and interpretation. This is done by an expression of these parameters in terms of physical quantities, like the masses of the weak vector bosons m_W and m_Z, the Higgs mass m_h and the electroweak scale v. The normalization will only include tree level contributions. Higher order corrections result in a renormalization of those couplings and fields. They are important for a precise calculation of the electroweak parameters [28]. However, for simplicity they will be neglected in this thesis.

The Lagrangian (2.32) contains three degrees of freedom, which are related directly to gauge symmetry breaking. By choosing a particular gauge called unitary gauge, the massless Goldstone bosons can be decoupled [29, 30]. Therefore, the Goldstone boson fields can be omitted in this gauge.

The Higgs matrix field becomes diagonal

$$\mathbf{H} = \frac{1}{2}\begin{pmatrix} v+h & 0 \\ 0 & v+h \end{pmatrix}. \tag{2.33}$$

Because the Operator τ_3 commutes with the diagonal Higgs matrix field, the covariant derivate (2.23) can be simplified to

$$\mathbf{D}_\mu \mathbf{H} = \left(\partial_\mu - \mathrm{i}g\left(\frac{1}{\sqrt{2}}\left(W_\mu^+\tau^+ + W_\mu^-\tau^-\right) + \frac{1}{c_w}Z_\mu\frac{\tau_3}{2}\right)\right)\mathbf{H}. \tag{2.34}$$

The Higgs matrix field does not interact with the photon field in unitary gauge, because it is not charged. Using the mass eigenstate basis defined in (2.29), the Lagrangian (2.32) can be rewritten as

$$\begin{aligned}\mathcal{L}_{\min} =& -\frac{1}{2}\mathrm{tr}\left[\mathbf{W}_{\mu\nu}\mathbf{W}^{\mu\nu}\right] - \frac{1}{2}\mathrm{tr}\left[\mathbf{B}_{\mu\nu}\mathbf{B}^{\mu\nu}\right] \\ &+ \frac{1}{2}\partial_\mu h\partial^\mu h - \frac{g^2}{4}(h+v)^2 W_\mu^- W^{+\mu} - \frac{g^2}{8c_w^2}(h+v)^2 Z_\mu Z^\mu \\ &- \frac{H^4\lambda}{8} - v\lambda H^3 - \frac{\lambda}{8}H^2\left(3v^2 - 4\frac{\mu^2}{\lambda}\right) - v\frac{\lambda}{2}H\left(v^2 - \frac{\mu^2}{\lambda}\right) \\ &- \frac{\lambda v^2}{8}\left(v^2 - 4\frac{\mu^2}{\lambda}\right).\end{aligned} \tag{2.35}$$

The parameters λ, μ, g^2 and c_w will be fixed by the physical masses of the bosons m_W, m_Z and m_h and the coefficients of the related kinetic terms c_{dH}, c_{dW}, c_{dB} using the Lagrangian

$$\begin{aligned}\mathcal{L}_{\mathrm{fix}} =& c_{dW}\mathrm{tr}\left[\mathbf{W}_{\mu\nu}\mathbf{W}^{\mu\nu}\right] + c_{dB}\mathrm{tr}\left[\mathbf{B}_{\mu\nu}\mathbf{B}^{\mu\nu}\right] \\ &+ c_{dh}\partial_\mu h\partial^\mu h + m_W^2 W_\mu^- W^{+\mu} + \frac{1}{2}m_Z^2 Z_\mu Z^\mu \\ &- \frac{1}{2}m_h^2 h^2 + c_{th}H.\end{aligned} \tag{2.36}$$

To fulfill the standard propagator definitions, the coefficients of kinetic terms have to be $c_{dH} = -c_{dW} = -c_{dB} = \frac{1}{2}$. A change in these coefficients would lead to different mass definitions. Additionally, the vacuum expectation value for the physical Higgs h should vanish, i.e. $c_{th} = 0$. Comparing equations (2.35) and (2.36) results in the coefficient relations,

$$0 = v^2 - 2\frac{\mu^2}{\lambda}, \tag{2.37a}$$

$$m_h^2 = \frac{\lambda}{4}\left(3v^2 - 4\frac{\mu^2}{\lambda}\right), \tag{2.37b}$$

$$m_W^2 = \frac{g^2 v^2}{4}, \tag{2.37c}$$

$$m_Z^2 = \frac{g^2 v^2}{4c_w^2}. \tag{2.37d}$$

The parameters μ, λ, g and g' can be traded for physical parameters by equations (2.37) and become functions of m_h, m_W, m_Z and v,

$$\lambda = 4\frac{m_h^2}{v^2}\,, \tag{2.38a}$$

$$\mu^2 = 2m_h^2\,, \tag{2.38b}$$

$$g^2 = \frac{4m_W^2}{v^2}\,, \tag{2.38c}$$

$$c_w^2 = \frac{m_W^2}{m_Z^2} \tag{2.38d}$$

$$g'^2 = 4\frac{m_Z^2 - m_W^2}{v^2}\,. \tag{2.38e}$$

The Z mass is heavier than the W mass, because of the contribution of the B-boson coupling to the Higgs vacuum expectation value, which is proportional to g'. This results in a small deviation between $m_W = 80.385 \pm 0.015$ GeV and $m_Z = 91.1876 \pm 0.0021$ GeV [31], which is parametrized in the Standard Model by the Weinberg angle θ_w. Additional contributions to the mass difference of the weak vector bosons beyond leading order of the Standard Model are described by the $\hat{\rho}$-paramter,

$$\hat{\rho} \equiv \frac{m_W^2}{c_w^2 m_Z^2}. \tag{2.39}$$

The Standard Model prediction, including radiative correction, is $\hat{\rho}_{\mathrm{SM}} = 1.01031 \pm 0.00011$ and experimental data does not suggest significant deviations from this prediction [31],

$$\frac{\hat{\rho}_{\mathrm{exp}}}{\hat{\rho}_{\mathrm{SM}}} = 1.00040 \pm 0.00024. \tag{2.40}$$

Therefore, new physics contributions to $\hat{\rho}$ are strongly constrained. The next section will explain how to suppress any deviation of the Standard Model $\hat{\rho}$-parameter by introducing an additional approximate symmetry.

2.3.2. Custodial Symmetry

The effective operator, that models beyond Standard Model deviations from the $\hat{\rho}$-parameter, is defined in nonlinear theories [23, 32] as

$$\mathcal{L}_{\beta'} = -\beta' \frac{v^2}{8} \mathrm{tr}\left[\mathbf{U}^\dagger \frac{\tau_3}{2} \mathbf{D}_\mu \mathbf{U}\right] \mathrm{tr}\left[\mathbf{U}^\dagger \frac{\tau_3}{2} \mathbf{D}^\mu \mathbf{U}\right]. \tag{2.41}$$

This term will only contribute to the two point function of the Z-boson and has to be suppressed to agree with experimental data. Extending the electroweak symmetry $SU(2)_L \times U(1)_Y$ to a chiral symmetry $SU(2)_L \times SU(2)_R$ will forbid this term entirely [33]. Gauge bosons are then singlets under $SU(2)_R$ and the auxiliary field in the nonlinear representation and the Higgs matrix field will transform as

$$\mathbf{U}(x) \to V_L^\dagger(x) \mathbf{U}(x) V_R(x)\,, \tag{2.42a}$$

$$\mathbf{H}(x) \to V_L^\dagger(x) \mathbf{H}(x) V_R(x)\,, \tag{2.42b}$$

with $SU(2)$ gauge transformations

$$V_L(x) = \exp\left(-\mathrm{i}\alpha_i(x)\frac{\tau_i}{2}\right) = 1 - \mathrm{i}\alpha_i(x)\frac{\tau_i}{2} + \mathcal{O}(\alpha_i^2)\,, \tag{2.43a}$$

$$V_R(x) = \exp\left(-\mathrm{i}\beta_i(x)\frac{\tau_i}{2}\right) = 1 - \mathrm{i}\beta_i(x)\frac{\tau_i}{2} + \mathcal{O}(\beta_i^2)\,. \tag{2.43b}$$

The vacuum expectation value of the Higgs breaks the chiral symmetry to the custodial symmetry group

$$SU(2)_L \times SU(2)_R \to SU(2)_C. \tag{2.44}$$

The custodial symmetry group prevents deviations from the $\hat{\rho}$-parameter beyond Standard Model. Only the $U(1)_Y$ gauge field $\mathbf{B}$ contributes to $SU(2)_C$ breaking in the gauge boson sector of the Standard Model. These contribution are proportional to

$$s_w^2 = \frac{m_Z^2 - m_W^2}{m_Z^2}. \tag{2.45}$$

This is very small compared to deviations in the fermion sector, where the top-quark is two orders of magnitude heavier than the bottom quark. Fermion masses originate from the Yukawa terms, which strongly violate custodial symmetry. An introduction of custodial symmetry in this sector is unnecessary, because even the Standard Model terms do not conserve this symmetry.

However, the custodial symmetry will prove to be advantageous in the case of modeling generic new physics effects to high energy vector boson scattering. This is one of the reasons for introducing the Higgs matrix representation and not using the linear Higgs doublet representation. The implicit custodial breaking property of the linear Higgs doublet representation is manifest in the relation

$$\mathbf{H} = \left(\tilde{\phi}, \phi\right) = \left(\tilde{\phi}, 0\right) + (0, \phi) = \mathbf{H}\frac{1}{2}\left(\mathbb{1} + \tau_3\right) + \mathbf{H}\frac{1}{2}\left(\mathbb{1} - \tau_3\right). \tag{2.46}$$

Using the doublet presentation for higher dimensional operators introduces $SU(2)_C$ violating terms implicitly, whereas $SU(2)_C$ breaking is manifest in the Higgs matrix representation by inserting the operator τ_3 between two Higgs fields $\mathbf{H}$. As examples serves the operator analogue to (2.41),

$$\mathcal{L}_{F,\beta} = F'_\beta \mathrm{tr}\left[\mathbf{H}^\dagger \frac{\tau_3}{2} \mathbf{D}_\mu \mathbf{H}\right] \mathrm{tr}\left[\mathbf{H}^\dagger \frac{\tau_3}{2} \mathbf{D}^\mu \mathbf{H}\right]. \tag{2.47}$$

It can be easily seen, that the Lagrangian (2.47) is not invariant under the custodial symmetry (2.42). Furthermore, the effective operator $\mathcal{L}_{F,\beta}$ has dimension six in the linear representation[3] and is therefore naturally suppressed by an unknown scale Λ^2. This scale is included in the coupling F'_β of(2.47), which has mass dimension -2.

A systematic discussion of effective field theory operators for vector boson scattering is given in the next chapter. The custodial symmetry is helpful to categorize the effective field theory operator basis.

[3]This is also true for the linear Higgs doublet representation.

Chapter 3

Effective Quantum Field Theories

Contributions from physics beyond the Standard Model can be experimentally constrained in two ways. The usual approach is to take a complete model with new particle content beyond the Standard Model and calculate its contributions to experimental observables. However, it is a tedious work to execute the whole calculation sequence from Feynman rules over the Monte Carlo integration to the final data analysis for every new physics model.

Alternatively, one can quantify deviation from the Standard Model using effective couplings, which describe low-energy effects from possible new particles. The Lagrangian has to be defined as generic as possible to model every possible new physics effect. In [34] this is done for triple gauge couplings[1]

$$\begin{aligned}
\mathcal{L}_{\mathbf{WWV}} = -e\Big[&\mathrm{i}g_1^A\left(W^{+\mu\nu}W^{-\mu}A^{\nu} - W^{+\mu}A^{\nu}W^{-\mu\nu}\right) + \mathrm{i}\kappa_A W_\mu^+ W_\nu^- A^{\mu\nu} \\
&+ \mathrm{i}\frac{\rho_A}{m_W^2} W^+{}_{\rho\mu} W^{-\mu}{}_{\nu} A^{\nu\rho} - g_4^A W_\mu^+ W_\nu^- \left(\partial^\mu A^\nu + \partial^\nu A^\mu\right) \\
&+ g_5^A \varepsilon^{\mu\nu\rho\sigma}\left(W_\mu^+\left(\partial_\rho W_\nu^-\right)A_\rho\right) + \mathrm{i}\tilde{\kappa}_A W_\mu^+ W_\nu^- \tilde{A}^{\mu\nu} \\
&+ \mathrm{i}\frac{\tilde{\rho}_A}{m_W^2} W^+{}_{\rho\mu} W^{-\mu}{}_{\nu} \tilde{A}^{\nu\rho}\Big] \\
-\frac{c_w e}{s_w}\Big[&\mathrm{i}g_1^Z\left(W^{+\mu\nu}W^{-\mu}Z^{\nu} - W^{+\mu}Z^{\nu}W^{-\mu\nu}\right) + \mathrm{i}\kappa_Z W_\mu^+ W_\nu^- Z^{\mu\nu} \\
&+ \mathrm{i}\frac{\rho_Z}{m_W^2} W^+{}_{\rho\mu} W^{-\mu}{}_{\nu} Z^{\nu\rho} - g_4^Z W_\mu^+ W_\nu^- \left(\partial^\mu Z^\nu + \partial^\nu Z^\mu\right) \\
&+ g_5^Z \varepsilon^{\mu\nu\rho\sigma}\left(W_\mu^+\left(\partial_\rho W_\nu^-\right)Z_\rho\right) + \mathrm{i}\tilde{\kappa}_Z W_\mu^+ W_\nu^- \tilde{Z}^{\mu\nu} \\
&+ \mathrm{i}\frac{\tilde{\rho}_Z}{m_W^2} W^+{}_{\rho\mu} W^{-\mu}{}_{\nu} \tilde{Z}^{\nu\rho}\Big],
\end{aligned} \tag{3.1}$$

[1] The Bjorken-Drell convention with $\varepsilon_{0123} = -\varepsilon^{0123} = +1$ is used.

with the abbreviations $X_{\mu\nu} = \partial_\mu X_\nu - \partial_\nu X_\mu$ and $\tilde{X}_{\mu\nu} = \frac{1}{2}\varepsilon_{\mu\nu\rho\sigma}X^{\rho\sigma}$ for vector bosons $X = \{W^-, W^+, A, Z\}$. The couplings are characterized by independently C- and P-conserving parameters g_1^A, g_1^Z, κ_A, κ_Z, λ_A, λ_Z and C- or P-violating parameters g_4^A, g_4^Z, g_5^A, g_5^Z, $\tilde{\kappa}_A$, $\tilde{\kappa_Z}$, $\tilde{\lambda}_A$, $\tilde{\lambda}_Z$. Three couplings $g_1^A = 1$ and $g_4^A = g_5^A = 0$ have to be fixed to satisfy electromagnetic gauge invariance. However (3.1) is not as generic as possible, additional extra derivatives can be added to all operators. Another representation of effective vertices in momentum space is introduced in [34], which shows the Lorentz structure of the anomalous couplings explicitly.

Writing down effective couplings like in the Lagrangian (3.1) will in general not respect the electroweak $SU(2)_L \times U(1)_Y$ gauge group, and it is not eased to calculate radiative corrections within this framework. Another approach should be chosen, which does not have these issues. Furthermore, additional features can be added, that a model-independent approach to search for new physic effects should fulfill. A list of desirable feature has been given in [35]:

- Any extension of the Standard Model should satisfy the S-matrix axioms of unitary, analyticity, etc.
- The symmetries of the Standard Model, namely Lorentz invariance and $SU(3)_C \times SU(2)_L \times U(1)_Y$ gauge symmetry, should be respected.
- It should be possible to recover the Standard Model in an appropriate limit.
- The extended theory should be general enough to capture any physics beyond the Standard Model, but [might] give some guidance as to the most likely place to see the effects of new physics.
- It should be possible to calculate radiative corrections at any order in the Standard Model interactions in the extended theory.
- It should be possible to calculate radiative corrections to any order in the new interactions of the extended theory.

All of these features are fulfilled by an effective quantum field theory. A power counting procedure in effective field theories provides a guidance where new physics is most likely to be be discovered. The choice of representation automatically implies a power counting. A linear representation would favor new physic effects of a weakly interacting Higgs sector, whereas a nonlinear representation advocates new Higgs interactions which originate from a strongly interacting sector.

Two different types of effective field theories can be distinguished, top-down effective field theories and bottom-up effective field theories. The first approach starts with a full theory and then effective operators are calculated in a certain energy limes. For example heavy degree of freedoms can be integrated out, matching the full theory to a low energy effective field theory [36]. This can be useful to get better insights into the model by separating long distance effects from short distance effects.

The bottom up approach can be used, even if the underlying new physics is unknown. Starting point is the minimal Lagrangian $\mathcal{L}_{\text{min}}$ and it will be extended by additional effective operators.

They are suppressed by some power of a high energy mass scale Λ,

$$\mathcal{L}_{\text{EFT}} = \mathcal{L}_{\text{min}} + \sum_i \frac{c_i}{\Lambda_i^n} \mathcal{O}_i \,, \tag{3.2}$$

with an unknown coupling c_i. Operator contributions can in general originate from different new physics sources, therefore the related suppressing mass scales can vary for each operator $\mathcal{O}_i$.

3.1. Example: Fermi Theory

In 1933, Enrico Fermi described the β-decay without knowledge of the weak vector bosons W and Z [37, 38]. Therefore, the Fermi theory can be formulated as an effective field theory for the weak interaction.

In this section, the Fermi theory is used as an example to explain the procedure of a bottom-up effective field theory. In contrast to the detailed discussion in [26], quark fields and the chiral structure of fermions are neglected. The starting point is the minimal Lagrangian of quantum electrodynamics

$$\mathcal{L}_{QED} = \bar{l} \mathrm{i} \not{D} l + \bar{\nu}_l \mathrm{i} \not{D} \nu_l - \frac{1}{4} A^{\mu\nu} A_{\mu\nu}, \tag{3.3}$$

where charged lepton fields $l = e, \mu, \tau$ and neutrino fields $\nu_l = \nu_e, \nu_\mu, \nu_\tau$ are introduced as massless fermions for simplicity. Furthermore, the convention $\not{D} = D_\mu \gamma^\mu$ with Dirac matrices γ^μ as defined in (A.11) is used. To describe all possible new physics interactions, the quantum electrodynamic Lagrangian has to be extended by the most general additional terms. The leading order contributions to the effective field theory expansion are a priori dimension five operators with independent couplings $\mu_{ll'}$ and $\lambda_{ll'}$,

$$\mathcal{L}_5 = \mu_{ll'} \bar{l} \sigma_{\mu\nu} A^{\mu\nu} l' + \lambda_{ll'} \bar{\nu}_l \sigma_{\mu\nu} A^{\mu\nu} \nu_l'. \tag{3.4}$$

These couplings have mass dimension -1, so they are suppressed by some high energy scale and contain all possible flavor combinations. Additional radiative correction to the electromagnetic interaction will only contribute to flavor conserving couplings μ and λ, since flavor changing effects cannot originate from the $U(1)_{\text{em}}$. Therefore, the observation of flavor changing processes indicates automatically new physics beyond quantum electrodynamics.

Additionally, the next order of operators has also to be included, because they contain contributions, which are not loop suppressed. These dimension six operators describe effective four fermion couplings

$$\mathcal{L}_6 = \sum_{f=l,\nu_l} s_{ijkl} \left(\bar{f}^i f^j\right) \left(\bar{f}^k f^l\right) + v_{ijkl} \left(\bar{f}^i \gamma_\mu f^j\right) \left(\bar{f}^k \gamma^\mu f^l\right). \tag{3.5}$$

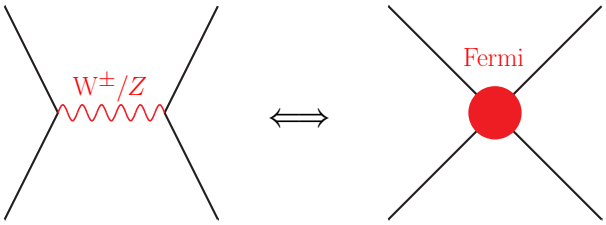

Figure 3.1.: Matching the effective quartic fermion vertex of the Fermi theory to the full theory with weak vector bosons.

Again, to be general, the couplings v and s with mass dimension -2 are a priori independent for all possible lepton combinations. For simplicity, some Dirac structures which are discussed in [26] are omitted.

Using the operators defined in (3.5) and (3.4) as a low energy effective field theory extension of quantum electrodynamics, possible experimental deviations can be quantitatively related. Experimental observations from flavor physics shows, that the dimension six operators can be formulated as a sum of products of charged and neutral currents

$$\mathcal{L}_6 = -4\sqrt{2}G_F \left(2J_\mu^+ J^{\mu-} + J_\mu^0 J^{\mu 0}\right). \tag{3.6}$$

Omitting the neutral currents, the interactions of the charged currents can be written as Fermi interactions

$$\mathcal{L}_{\text{Fermi}} = -2\sqrt{2}G_F \left[\bar{\nu}_l \gamma^\mu l\right] \left[\bar{\nu}_{l'} \gamma^\mu l'\right]^\dagger + h.c.\,. \tag{3.7}$$

The reduced number of independent parameters and the current-current structure of (3.7) in comparison to (3.5) lead to the assumption, that an underlying symmetry is present. This symmetry was identified as the weak interaction, which was then included in the Standard Model of electroweak interactions [17–19].

The effective field theory operators are the low energy contribution of a weak vector boson exchange as pictured in Figure 3.1. Matching the weak interactions contribution to the Fermi interaction operator within a top-down effective field theory approach will give the relation of the Fermi constant to the electroweak scale

$$G_F = \frac{1}{\sqrt{2}v^2}. \tag{3.8}$$

3.2. Effective Field Theory Operator Bases

Different bottom-up effective field theories bases have been introduced to analyze the electroweak symmetry breaking sector. They can be categorized in terms of the representations

chosen for the Higgs, which are introduced in Chapter 2. Further subcategories arise depending on the assumed underlying new physics, which influence the power counting procedure used for the operators.

New strongly interacting physics was assumed in the case of the nonlinear realization of the Goldstone-boson sector without a light Higgs as described in Section 2.2. These new contributions to vector boson scattering are modeled by a set of effective field operators in a bottom-up approach. To build a complete basis, two additional abbreviations are introduced

$$\mathbf{V}^\mu = \mathbf{U}\left(\mathbf{D}^\mu \mathbf{U}\right)^\dagger \tag{3.9a}$$

$$\mathbf{T} = \mathbf{U}\tau^3\mathbf{U}^\dagger, \tag{3.9b}$$

where the field $\mathbf{V}$ represents the longitudinal degrees of freedoms and the operator $\mathbf{T}$ models additional $SU(2)_C$ breaking contributions. Using the operators $\mathbf{V}$ and $\mathbf{T}$, the field strength tensors $\mathbf{W}^{\mu\nu}$ and $\mathbf{B}^{\mu\nu}$, and the auxiliary Field $\mathbf{U}$ a complete effective operator set for boson scattering can be constructed to lowest order [22, 23, 32],

$$\begin{aligned}
\mathcal{L}_{\alpha_1} &= \alpha_1 g g' \mathrm{tr}\left[\mathbf{U}\mathbf{B}_{\mu\nu}\mathbf{U}^\dagger\mathbf{W}^{\mu\nu}\right], & \mathcal{L}_{\alpha_6} &= \alpha_6 \mathrm{tr}\left[\mathbf{V}_\mu\mathbf{V}_\nu\right]\mathrm{tr}\left[\mathbf{T}\mathbf{V}^\mu\right]\mathrm{tr}\left[\mathbf{T}\mathbf{V}^\nu\right], \\
\mathcal{L}_{\alpha_2} &= \mathrm{i}\alpha_2 g' \mathrm{tr}\left[\mathbf{U}\mathbf{B}_{\mu\nu}\mathbf{U}^\dagger[\mathbf{V}^\mu,\mathbf{V}^\nu]\right], & \mathcal{L}_{\alpha_7} &= \alpha_7 \mathrm{tr}\left[\mathbf{V}_\mu\mathbf{V}^\mu\right]\mathrm{tr}\left[\mathbf{T}\mathbf{V}_\nu\right]\mathrm{tr}\left[\mathbf{T}\mathbf{V}^\nu\right], \\
\mathcal{L}_{\alpha_3} &= \alpha_3 \mathrm{i}\mathrm{tr}\left[\mathbf{W}_{\mu\nu}[\mathbf{V}^\mu,\mathbf{V}^\nu]\right], & \mathcal{L}_{\alpha_8} &= \tfrac{1}{4}\alpha_8 \mathrm{tr}\left[\mathbf{T}\mathbf{W}_{\mu\nu}\right]\mathrm{tr}\left[\mathbf{T}\mathbf{W}^{\mu\nu}\right], \\
\mathcal{L}_{\alpha_4} &= \alpha_4 \mathrm{tr}\left[\mathbf{V}_\mu\mathbf{V}_\nu\right]\mathrm{tr}\left[\mathbf{V}^\mu\mathbf{V}^\nu\right], & \mathcal{L}_{\alpha_9} &= \tfrac{\mathrm{i}}{2}\alpha_9 \mathrm{tr}\left[\mathbf{T}\mathbf{W}_{\mu\nu}\right]\mathrm{tr}\left[\mathbf{T}[\mathbf{V}^\mu,\mathbf{V}^\nu]\right], \\
\mathcal{L}_{\alpha_5} &= \alpha_5 \mathrm{tr}\left[\mathbf{V}_\mu\mathbf{V}^\mu\right]\mathrm{tr}\left[\mathbf{V}_\nu\mathbf{V}^\nu\right], & \mathcal{L}_{\alpha_{10}} &= \alpha_{10}\tfrac{1}{2}\left(\mathrm{tr}\left[\mathbf{T}\mathbf{V}_\mu\right]\mathrm{tr}\left[\mathbf{T}\mathbf{V}^\mu\right]\right)^2, \\
\mathcal{L}_{\alpha_{11}} &= \alpha_{11} g \varepsilon^{\mu\nu\rho\lambda}\mathrm{tr}\left[\mathbf{T}\mathbf{V}_\mu\right]\mathrm{tr}\left[\mathbf{V}_\nu\mathbf{W}_{\rho\lambda}\right], & \mathcal{L}_{\beta'} &= \beta'\frac{v^2}{4}\mathrm{tr}\left[\mathbf{T}\mathbf{V}_\mu\right]\mathrm{tr}\left[\mathbf{T}\mathbf{V}^\mu\right].
\end{aligned} \tag{3.10}$$

Besides the operator $\mathcal{L}_{\beta'}$, which is of mass dimension two, the operators of (3.10) have all canonical dimension four. The terms $\mathcal{L}_{\beta'}$, $\mathcal{L}_{\alpha_6}\ldots\mathcal{L}_{\alpha_{11}}$ have to be additionally suppressed, because of their custodial symmetry violating nature. To estimate the contribution strength of the operators in a nonlinear effective field theory, the naive dimensional analysis method was introduced in [39–41].

Another approach to model physics without knowledge of the exact Higgs boson properties is to formulate an effective field theory below the electroweak symmetry scale. Then the operators need to be invariant under the local electromagnetic $U_{\mathrm{em}}(1)$ only. Additionally, the global custodial $SU(2)_C$ is introduced to forbid contributions to the $\hat{\rho}$-parameter. A complete basis was examined in [42, 43] to analyze generic quartic gauge couplings. The LEP II studies of anomalous contributions to the $WW\gamma\gamma$-vertex and $ZZ\gamma\gamma$-vertex in [44, 45] used the two operators

$$\mathcal{L}^0 = -\frac{e^2}{16\pi\Lambda^2}a_0 A_{\mu\nu}A^{\mu\nu}\overrightarrow{W}_\rho\overrightarrow{W}^\rho, \tag{3.11a}$$

$$\mathcal{L}^c = -\frac{e^2}{16\pi\Lambda^2}a_c A_{\mu\nu}A^{\mu\rho}\overrightarrow{W}^\nu\overrightarrow{W}_\rho \tag{3.11b}$$

with an unknown new physics energy scale Λ and

$$\overrightarrow{W}_\mu = \begin{pmatrix} \frac{1}{\sqrt{2}}\left(W_\mu^+ + W_\mu^-\right) \\ \frac{\mathrm{i}}{\sqrt{2}}\left(W_\mu^+ - W_\mu^-\right) \\ \frac{1}{c_w} Z_\mu \end{pmatrix}. \tag{3.12}$$

In recent LHC studies by CMS [46], the anomalous couplings, a_0 and a_c have been constrained experimentally. A transformation to convert the measured constraints in the basis (3.11) directly to constraints of the operators in the nonlinear representation (3.10) can be formulated [47]. However, the nonlinear basis respects the full chiral symmetry group and therefore implies different dependencies between the gauge bosons and their couplings on lowest order.

After the Higgs discovery, a scalar boson has to be included in the effective field theory. Unless the theory is used at energies much below the Higgs mass, bounds on effective field theory operators of Higgs-less models are not valid. Because no critical deviations from the Standard Model prediction have been experimentally discovered, the electroweak symmetry should be considered as a fundamental symmetry. In other words, it is conserved at energies above the electroweak scale $v \approx 246$ GeV and should therefore be respected when defining an effective field theory. Furthermore, using the complete gauge group reduces the number of parameters and guarantees the renormalizability of the effective field theory. A most generic way to extend the operators of the nonlinear realization is to add a Higgs scalar in (3.10) analogously to (2.17). A complete discussion of a nonlinear basis including a Higgs scalar with boson and fermion operators is given in [48]. This basis is often advertised, when one assumes an underlying model that includes the Higgs as a pseudo-Goldstone boson. In some models it originates from a strongly interaction sector at energy scales above $\Lambda \gtrsim 4\pi v$. In contrary to the Standard Model, the Higgs couplings are independent and additional parameters are present at leading order in the effective field theory. Chiral dimensional analysis was introduced in [49] as power counting procedure for a strongly interacting Higgs sector. In this scenario, the new physic scale is defined as $\Lambda = 4\pi f \sim 4\pi v$. Taking the decoupling limit of the Higgs ($\frac{v}{f} \to 0$) will reproduce the operators belonging to the effective field theory basis within a linear Higgs, the strongly interacting light Higgs (SILH) basis, which is presented in [50].

When a weakly interacting Standard Model like Higgs sector is assumed, a linear realization is preferable. The Higgs couplings are then fixed at leading order, because the Higgs is embedded in the Goldstone boson sector. Anomalous Higgs couplings will enter first at higher orders in the effective field theory expansion. Compared to the nonlinear representation, the numbers of parameters to describe the couplings of the lowest dimension operators is therefore smaller. Furthermore, a simple canonical dimensional analysis can be used for the power counting of the operators. First contributions of new physics could be generated by dimension six operators in an effective field approach, which originate mainly from integrating out loop corrections of heavy new particles. An analysis of the complete dimension six basis within the linear Higgs doublet realization was conducted in [51]. The basis consists of 16 operators, which contribute to anomalous gauge and Higgs couplings, 29 operators which consists of four fermion fields and 35 mixed operators which have only two fermion fields. In total this sums

up to 80 operators. A more relevant study [52] showed that many of the operators with two fermion fields are redundant and the full basis can be reduced to 59 independent operators. The list of the complete set of independent dimension six operators only containing bosons is

$$\begin{aligned}
\mathcal{O}_W &= \epsilon^{ijk} W_\mu^{i\,\nu} W_\nu^{j\,\rho} W_\rho^{k\,\mu}, & \mathcal{O}_{\widetilde{W}} &= \epsilon^{ijk} \widetilde{W}_\mu^{i\,\nu} W_\nu^{j\,\rho} W_\rho^{k\,\mu}, \\
\mathcal{O}_\Phi &= \left(\Phi^\dagger \Phi\right)^3, & \mathcal{O}_{\Phi\partial^2} &= \left(\Phi^\dagger \Phi\right) \partial^2 \left(\Phi^\dagger \Phi\right), \\
\mathcal{O}_{\Phi D} &= \left(\Phi^\dagger D^\mu \Phi\right)^* \left(\Phi^\dagger D_\mu \Phi\right), & \mathcal{O}_{\Phi B} &= \left(\Phi^\dagger \Phi\right) B_{\mu\nu} B^{\mu\nu}, \\
\mathcal{O}_{\Phi W} &= \left(\Phi^\dagger \Phi\right) W^i{}_{\mu\nu} W^{i\,\mu\nu}, & \mathcal{O}_{\Phi\widetilde{W}} &= \left(\Phi^\dagger \Phi\right) \widetilde{W}^i{}_{\mu\nu} W^{i\,\mu\nu}, \\
\mathcal{O}_{\Phi WB} &= \left(\Phi^\dagger \tau^i \Phi\right) W^i{}_{\mu\nu} B^{\mu\nu}, & \mathcal{O}_{\Phi\widetilde{W}B} &= \left(\Phi^\dagger \tau^i \Phi\right) \widetilde{W}^i{}_{\mu\nu} B^{\mu\nu}.
\end{aligned} \tag{3.13}$$

Here, following [52], the convention 'CD+' is used for the covariant derivative

$$D_\mu \Phi = \left(\partial_\mu + \mathrm{i} g W_\mu^i \frac{\tau^i}{2} + i \frac{g'}{2} B_\mu\right) \Phi, \tag{3.14a}$$

$$W_{\mu\nu}^i = \partial_\mu W_\nu^i - \partial_\nu W_\mu^i - g \varepsilon^{ijk} W_\mu^j W_\nu^k, \tag{3.14b}$$

$$B_{\mu\nu}^i = \partial_\mu B_\nu^i - \partial_\nu B_\mu^i. \tag{3.14c}$$

The dimension six operators in (3.13) will affect the anomalous triple gauge couplings (3.1) as described in [53, 54]. When converting constraints from anomalous couplings to effective field theory operators the linear combinations of all operators have to be considered.

Operators contributing to anomalous quartic, but not triple gauge couplings, can originate from tree level new physics contributions [55]. These cannot be modeled by dimension six operators, and therefore dimension eight operators are needed. However, a full study regarding a complete and minimal dimension eight operator basis has not yet been published. The set of dimension eight operators introduced in [56] is a first step to build a minimal dimension eight basis. In particular, the building blocks in (3.14) are used to write down all possible combinations for an operator set. A revised list, where some linear dependent operators are already dropped, is given in [57] and listed in Appendix A.5. A linear relation of the quartic gauge couplings (3.11) to an incomplete set of electroweak symmetry conserving operators is introduced in [58]. Recent experimental studies, e.g. in [46], used this incomplete conversion to set limits on the dimension eight operators. Respecting the complete operator list, the conversion for the $WW\gamma\gamma$-vertex and the $ZZ\gamma\gamma$-vertex for anomalous couplings a_c and a_0 to couplings $f_{M,l}$ for $l = 0, 1, 2, 3, 4, 5, 7$ of operators, defined in the appendix in (A.64), can be derived

$$\frac{a_0}{\Lambda^2} \frac{1}{g^2 v^2} \equiv \frac{1}{\Lambda^4} \left(f_{M,0} + \frac{f_{M,2}}{2} \mp f_{M,4}\right), \tag{3.15a}$$

$$\frac{a_c}{\Lambda^2} \frac{1}{g^2 v^2} \equiv \frac{1}{\Lambda^4} \left(-f_{M,1} - \frac{f_{M,3}}{2} \mp \frac{f_{M,5}}{2} + \frac{f_{M,7}}{2}\right). \tag{3.15b}$$

The different sign in front of $f_{M,4}$ and $f_{M,5}$ for the $WW\gamma\gamma$-vertex (upper) and the $ZZ\gamma\gamma$-vertex (lower) arise, because the effective operators (3.15) respects custodial symmetry, while the operators $\mathcal{O}_{M,4}$ and $\mathcal{O}_{M,5}$ do not. A first conversion, which still includes the redundant operator $\mathcal{O}_{M,6}$, is given in [57]. After building up a full effective Lagrangian, the operators are checked for linear dependencies to find the minimal operator set.

3.2.1. Minimizing the Operator Set

Mainly two techniques are used to reduce the operator set of the effective field theory: Employing the equations of motion and field redefinitions leave the S-matrix invariant and change only intermediate mathematical quantities [59, 60]. Therefore, the operators with two derivatives acting on one field can be rewritten as interaction terms. Equations of motion for effective field operators of dimension $n+4$ that are used to study linear dependencies of operators of the same or lower dimension can be neglected, because they are proportional to terms with an additional suppression factor of $1/\Lambda^n$. To reduce the dimension six operator set, the equations of motion for vector boson scattering are deduced from the minimal Lagrangian (2.32) only

$$\left(\mathbf{D}^2\mathbf{H}\right) = -\mu^2\mathbf{H} + \lambda \mathrm{tr}\left[\mathbf{H}^\dagger\mathbf{H}\right]\mathbf{H}, \tag{3.16a}$$

$$\left(\mathbf{D}^2\mathbf{H}\right)^\dagger = -\mu^2\mathbf{H}^\dagger + \lambda \mathrm{tr}\left[\mathbf{H}^\dagger\mathbf{H}\right]\mathbf{H}^\dagger, \tag{3.16b}$$

$$\mathbf{D}_\mu \mathbf{W}^{\mu\nu} \equiv \left[\mathbf{D}_\mu^W, \mathbf{W}^{\mu\nu}\right] = -\mathrm{i}\frac{g}{2}\left(\mathbf{H}\left(\mathbf{D}^\nu\mathbf{H}\right)^\dagger - \mathbf{D}^\nu\mathbf{H}\mathbf{H}^\dagger\right), \tag{3.16c}$$

$$\mathbf{D}_\mu \mathbf{B}^{\mu\nu} \equiv \quad \partial_\mu \mathbf{B}^{\mu\nu} = -\mathrm{i}\frac{g'}{2}\left(\left(\mathbf{D}^\nu\mathbf{H}\right)^\dagger \mathbf{H} - \mathbf{H}^\dagger\mathbf{D}^\nu\mathbf{H}\right). \tag{3.16d}$$

The fermion currents are omitted here. Further details of the calculation are shown in Appendix A.4.3. With the equation of motion, all operators, which include a double derivative acting on the Higgs field or a derivative acting on a field strength tensor, are redundant. To reduce the operator set even more, other reduction procedures have to be used. A basic set of techniques for the reduction of an operator basis is listed in the analysis of anomalous triple gauge couplings of dimension 8 operators given in [61]:

- Equation of motion (3.16) and field redefinitions;
- Integration by part;
- Bianchi identities

$$\mathbf{D}^\mu\widetilde{\mathbf{W}}_{\mu\nu} = 0 = \mathbf{D}^\mu\widetilde{\mathbf{B}}_{\mu\nu}; \tag{3.17}$$

- Jacobi identities

$$\mathbf{D}_\mu\mathbf{W}_{\nu\rho} + \mathbf{D}_\nu\mathbf{W}_{\rho\mu} + \mathbf{D}_\rho\mathbf{W}_{\mu\nu} = 0 = \mathbf{D}_\mu\mathbf{B}_{\nu\rho} + \mathbf{D}_\nu\mathbf{B}_{\rho\mu} + \mathbf{D}_\rho\mathbf{B}_{\mu\nu}; \tag{3.18}$$

- Using the definition of field strength tensors in (2.4): the commutator of two covariant derivatives is a linear combination of field strength tensors.

It is noted in [62] that field redefinitions are necessary to eliminate redundant operators at higher order calculations in $1/\Lambda$ by showing explicitly the impact of renormalization group evolution to a redundant basis. Additional arbitrary parameters would appear in the

anomalous dimension matrix, which describes the operator evolution and mixing due to loop corrections.

Next-to-leading order corrections to the effective field theory basis with a linear Higgs doublet realization are discussed in [62–65]. Using gauge symmetry and minimal flavor violation, operator mixing is suppressed by weak couplings and loop factors [66]. Therefore, the full effective field theory model decomposes at energies E with $\Lambda > E \gg v$ into the left- and right-handed fermion sector, the gauge boson sector and the Goldstone boson sector. Hence, higher dimensional operators containing fermions can be neglected in the discussion of the effective field theory basis for vector boson scattering.

3.3. Dimension Six Operators

The starting point of the bottom up effective field theory is the minimal Lagrangian (2.32) using the Higgs matrix representation. The dimension six operator basis is then build up systematically with the building blocks $\mathbf{W}^{\mu\nu}$, $\mathbf{B}^{\mu\nu}$, $\mathbf{D}^{\mu}$ and $\mathbf{H}$. Additionally, the operators have to be invariant under the $SU(2)_L \times SU(2)_R$ symmetry group of the minimal Lagrangian. A manifest $SU(2)_C$ breaking term corresponding to $\mathbf{T}$ can be included in the operators, but it will increase the dimensionality of the operator as described in Section 2.3.2. Therefore, these operators are additionally suppressed and will be neglected. Only breaking of the custodial symmetry proportional to the hypercharge gauge field $\mathbf{B}^{\mu}$ is allowed. Furthermore, C and/or P violating operators are omitted for the time being. Their construction is similar and they can be added later. Combining all possible combinations results in the first set of a dimension six operator basis:

$$\mathcal{L}^0_{WWW} = -\mathrm{i}g^3 F^0_{WWW} \operatorname{tr}\left[\mathbf{W}_{\mu\nu}\mathbf{W}^{\nu\rho}\mathbf{W}^{\mu}_{\rho}\right], \tag{3.19a}$$

$$\mathcal{L}^0_{W} = \mathrm{i}g F^0_{W} \operatorname{tr}\left[\left(\mathbf{D}_{\mu}\mathbf{H}\right)^{\dagger}\mathbf{W}^{\mu\nu}\left(\mathbf{D}_{\nu}\mathbf{H}\right)\right], \tag{3.19b}$$

$$\mathcal{L}^0_{B} = \mathrm{i}g' F^0_{B} \operatorname{tr}\left[\left(\mathbf{D}_{\mu}\mathbf{H}\right)\mathbf{B}^{\mu\nu}\left(\mathbf{D}_{\nu}\mathbf{H}\right)^{\dagger}\right], \tag{3.19c}$$

$$\mathcal{L}^0_{WB} = -gg' F^0_{WB} \operatorname{tr}\left[\mathbf{H}^{\dagger}\mathbf{W}_{\mu\nu}\mathbf{H}\mathbf{B}^{\mu\nu}\right], \tag{3.19d}$$

$$\mathcal{L}^0_{HW} = -g^2 F^0_{HW} \operatorname{tr}\left[\mathbf{H}^{\dagger}\mathbf{H}\right]\operatorname{tr}\left[\mathbf{W}_{\mu\nu}\mathbf{W}^{\mu\nu}\right], \tag{3.19e}$$

$$\mathcal{L}^0_{HB} = -g'^2 F^0_{HB} \operatorname{tr}\left[\mathbf{H}^{\dagger}\mathbf{H}\right]\operatorname{tr}\left[\mathbf{B}_{\mu\nu}\mathbf{B}^{\mu\nu}\right], \tag{3.19f}$$

$$\mathcal{L}^0_{HD} = F^0_{HD} \operatorname{tr}\left[\mathbf{H}^{\dagger}\mathbf{H}\right]\operatorname{tr}\left[\left(\mathbf{D}_{\mu}\mathbf{H}\right)^{\dagger}\left(\mathbf{D}^{\mu}\mathbf{H}\right)\right], \tag{3.19g}$$

$$\mathcal{L}^0_{HD'} = F^0_{HD'} \operatorname{tr}\left[\mathbf{H}^{\dagger}\left(\mathbf{D}_{\mu}\mathbf{H}\right)\right]\operatorname{tr}\left[\left(\mathbf{D}^{\mu}\mathbf{H}\right)^{\dagger}\mathbf{H}\right], \tag{3.19h}$$

$$\mathcal{L}^0_{HD''} = F^0_{HD''} \operatorname{tr}\left[\mathbf{H}^{\dagger}\left(\mathbf{D}_{\mu}\mathbf{H}\right)\right]\operatorname{tr}\left[\mathbf{H}^{\dagger}\left(\mathbf{D}^{\mu}\mathbf{H}\right)\right], \tag{3.19i}$$

$$\mathcal{L}^0_{HD'''} = F^0_{HD'''} \operatorname{tr}\left[\left(\mathbf{D}_{\mu}\mathbf{H}\right)^{\dagger}\mathbf{H}\right]\operatorname{tr}\left[\left(\mathbf{D}^{\mu}\mathbf{H}\right)^{\dagger}\mathbf{H}\right], \tag{3.19j}$$

$$\mathcal{L}^0_{H\partial} = F^0_{H\partial} \partial_{\mu}\left(\operatorname{tr}\left[\mathbf{H}^{\dagger}\mathbf{H}\right]\right)\partial^{\mu}\left(\operatorname{tr}\left[\mathbf{H}^{\dagger}\mathbf{H}\right]\right), \tag{3.19k}$$

$$\mathcal{L}^0_{HHH} = F^0_{HHH} \operatorname{tr}\left[\mathbf{H}^{\dagger}\mathbf{H}\right]\operatorname{tr}\left[\mathbf{H}^{\dagger}\mathbf{H}\right]\operatorname{tr}\left[\mathbf{H}^{\dagger}\mathbf{H}\right]. \tag{3.19l}$$

All operators are accompanied by an effective coupling, which is suppressed by a new physics scale $F \sim 1/\text{TeV}^2$. Assuming weakly coupled new physics, the couplings g and g' accompany their appropriate field strength tensors. Operators including terms like $\mathbf{D^2H}$, $\mathbf{D}_\mu\mathbf{W}^{\mu\nu}$ and $\partial_\mu\mathbf{B}^{\mu\nu}$ have already been removed in (3.19). They are linearly dependent to the ones in (3.19) due to the equations of motion of the minimal Lagrangian (3.16) (see Appendix A.4.3 for details). As explicit example, an operator containing $\mathbf{D^2H}$ is reduced via equations of motion (A.53a) to a term proportional to the Standard Model quartic coupling of the Higgs and the dimension 6 operator $\mathcal{L}^0_{HHH}$

$$\text{tr}\left[\mathbf{H}^\dagger\mathbf{H}\right]\text{tr}\left[\mathbf{H}^\dagger\mathbf{D}^2\mathbf{H}\right] = -\mu^2\text{tr}\left[\mathbf{H}^\dagger\mathbf{H}\right]^2 + \lambda\text{tr}\left[\mathbf{H}^\dagger\mathbf{H}\right]^3. \tag{3.20}$$

A partial derivative acting on the gauge singlet $\text{tr}\left[\mathbf{H}^\dagger\mathbf{H}\right]$ yields

$$\partial_\mu\text{tr}\left[\mathbf{H}^\dagger\mathbf{H}\right] = \text{tr}\left[\left(\mathbf{D}_\mu\mathbf{H}\right)^\dagger\mathbf{H}\right] + \text{tr}\left[\mathbf{H}^\dagger\left(\mathbf{D}_\mu\mathbf{H}\right)\right] \tag{3.21}$$

and thus will not contribute to the anomalous gauge couplings. This is also true for the terms on the right hand side of (3.21). In unitary gauge, the operators $\mathcal{L}^0_{HD'}$, $\mathcal{L}^0_{HD''}$ and $\mathcal{L}^0_{HD'''}$ only contribute to anomalous Higgs couplings.

Terms in (3.19) including two Higgs fields and two derivative are linearly dependent. Applying (3.21) and integration by parts on $\mathcal{L}_{HD'''}$, it can be related to $\mathcal{L}^0_{HD'}$, $\mathcal{L}^0_{HD}$ and the reducible term of (3.20)

$$\begin{aligned}\text{tr}\left[\mathbf{H}^\dagger\left(\mathbf{D}_\mu\mathbf{H}\right)\right]\text{tr}\left[\mathbf{H}^\dagger\left(\mathbf{D}^\mu\mathbf{H}\right)\right] = &-\text{tr}\left[\mathbf{H}^\dagger\mathbf{H}\right]\text{tr}\left[\left(\mathbf{D}_\mu\mathbf{H}\right)^\dagger\left(\mathbf{D}^\mu\mathbf{H}\right)\right]\\ &-\text{tr}\left[\left(\mathbf{D}_\mu\mathbf{H}\right)^\dagger\mathbf{H}\right]\text{tr}\left[\mathbf{H}^\dagger\left(\mathbf{D}^\mu\mathbf{H}\right)\right]\\ &-\text{tr}\left[\mathbf{H}^\dagger\mathbf{H}\right]\text{tr}\left[\mathbf{H}^\dagger\mathbf{D}^2\mathbf{H}\right].\end{aligned} \tag{3.22}$$

This proofs the redundancy of $\mathcal{L}_{HD'''}$. These steps can be repeated analogously to show the linear dependence of the terms $\mathcal{L}^0_{HD''}$ and $\mathcal{L}^0_{H\partial}$.

For operators containing field strength tensors like $\mathcal{L}^0_W$ and $\mathcal{L}^0_B$ another approach is used. Exploiting the total derivative

$$\begin{aligned}&\partial_\mu\text{tr}\left[\mathbf{H}^\dagger\mathbf{W}^{\mu\nu}\left(\mathbf{D}_\nu\mathbf{H}\right)\right]\\ =&\text{tr}\left[\left(\mathbf{D}_\mu\mathbf{H}\right)^\dagger\mathbf{W}^{\mu\nu}\left(\mathbf{D}_\nu\mathbf{H}\right)\right] + \text{tr}\left[\mathbf{H}^\dagger\left(\mathbf{D}_\mu\mathbf{W}^{\mu\nu}\right)\left(\mathbf{D}_\nu\mathbf{H}\right)\right] + \text{tr}\left[\mathbf{H}^\dagger\mathbf{W}^{\mu\nu}\left(\mathbf{D}_\mu\mathbf{D}_\nu\mathbf{H}\right)\right],\end{aligned} \tag{3.23}$$

$\mathcal{L}^0_W$ can be related to operators with two covariant derivatives acting on one field. The second operator can be written as a sum of $\mathcal{L}^0_{HD}$ and $\mathcal{L}^0_{HD'}$ with the equation of motion (3.16) of the field strength tensor. The third operator in (3.23) can be written as a function of $\mathcal{L}^0_{HW}$ and $\mathcal{L}^0_{WB}$ using the antisymmetry of the field strength tensor and its definition (2.4)

$$\begin{aligned}\text{tr}\left[\mathbf{H}^\dagger\mathbf{W}^{\mu\nu}\left(\mathbf{D}_\mu\mathbf{D}_\nu\mathbf{H}\right)\right] &= \frac{1}{2}\text{tr}\left[\mathbf{H}^\dagger\mathbf{W}^{\mu\nu}\left(\left[\mathbf{D}_\mu,\mathbf{D}_\nu\right]\mathbf{H}\right)\right]\\ &= \frac{i}{2g}\text{tr}\left[\mathbf{H}^\dagger\mathbf{W}^{\mu\nu}\mathbf{W}_{\mu\nu}\mathbf{H}\right] - \frac{i}{2g'}\text{tr}\left[\mathbf{H}^\dagger\mathbf{W}^{\mu\nu}\mathbf{B}_{\mu\nu}\mathbf{H}\right].\end{aligned} \tag{3.24}$$

The operator $\mathcal{L}_W^0$ can therefore be expressed as a linear combination of $\mathcal{L}_{HD}^0$, $\mathcal{L}_{HD'}^0$, $\mathcal{L}_{HW}^0$ and $\mathcal{L}_{WB}^0$. Analogously $\mathcal{L}_B^0$ is a linear function of $\mathcal{L}_{HD}^0$, $\mathcal{L}_{HD'}^0$, $\mathcal{L}_{HB}^0$ and $\mathcal{L}_{WB}^0$.

Taking all these linear dependencies into account, the operator set (3.19) can be reduced to the independent operator set

$$\mathcal{L}_{WWW}^0 = -\mathrm{i}g^3 F_{WWW}^0 \operatorname{tr}\left[\mathbf{W}_{\mu\nu}\mathbf{W}^{\nu\rho}\mathbf{W}_{\rho}^{\mu}\right], \tag{3.25a}$$

$$\mathcal{L}_{WB}^0 = -gg' F_{WB}^0 \operatorname{tr}\left[\mathbf{H}^\dagger \mathbf{W}_{\mu\nu}\mathbf{H}\mathbf{B}^{\mu\nu}\right], \tag{3.25b}$$

$$\mathcal{L}_{HW}^0 = -g^2 F_{HW}^0 \operatorname{tr}\left[\mathbf{H}^\dagger\mathbf{H}\right]\operatorname{tr}\left[\mathbf{W}_{\mu\nu}\mathbf{W}^{\mu\nu}\right], \tag{3.25c}$$

$$\mathcal{L}_{HB}^0 = -g'^2 F_{HB}^0 \operatorname{tr}\left[\mathbf{H}^\dagger\mathbf{H}\right]\operatorname{tr}\left[\mathbf{B}_{\mu\nu}\mathbf{B}^{\mu\nu}\right], \tag{3.25d}$$

$$\mathcal{L}_{HD}^0 = F_{HD}^0 \operatorname{tr}\left[\mathbf{H}^\dagger\mathbf{H}\right]\operatorname{tr}\left[\left(\mathbf{D}_\mu\mathbf{H}\right)^\dagger\left(\mathbf{D}^\mu\mathbf{H}\right)\right], \tag{3.25e}$$

$$\mathcal{L}_{HD'}^0 = F_{HD'}^0 \operatorname{tr}\left[\mathbf{H}^\dagger\left(\mathbf{D}_\mu\mathbf{H}\right)\right]\operatorname{tr}\left[\left(\mathbf{D}^\mu\mathbf{H}\right)^\dagger\mathbf{H}\right], \tag{3.25f}$$

$$\mathcal{L}_{HHH}^0 = F_{HHH}^0 \operatorname{tr}\left[\mathbf{H}^\dagger\mathbf{H}\right]\operatorname{tr}\left[\mathbf{H}^\dagger\mathbf{H}\right]\operatorname{tr}\left[\mathbf{H}^\dagger\mathbf{H}\right]. \tag{3.25g}$$

3.3.1. Basis Redefinition

All operators (3.25) beside $\mathcal{L}_{WWW}^0$ give contribution to physical parameters defined in Section 2.3.1, because of the non-zero vacuum expectation value of the Higgs. They affect Standard Model masses or kinetic terms directly. To normalize these parameters to their physical values a renormalization procedure is needed, if the operator set (3.25) is used. The renormalization procedure can be simplified by redefining these operator in such a way, that the operator contributions to the corresponding standard parameters are minimal. The operators in $\mathcal{L}_{HW}^0$, $\mathcal{L}_{HB}^0$, $\mathcal{L}_{HD}^0$ and $\mathcal{L}_{HHH}^0$ give rise to deviations to Standard Model parameters directly proportional to the dimension four operators due to their $\operatorname{tr}\left[\mathbf{H}^\dagger\mathbf{H}\right]$ building block. Dimension four operators can therefore directly used as counter terms. Equivalently, the building blocks can be redefined by subtracting their vacuum expectation value [67]

$$\operatorname{tr}\left[\mathbf{H}^\dagger\mathbf{H}\right] \to \operatorname{tr}\left[\widehat{\mathbf{H}^\dagger\mathbf{H}}\right] := \operatorname{tr}\left[\mathbf{H}^\dagger\mathbf{H} - \frac{v^2}{4}\right]. \tag{3.26}$$

This redefinition does not affect $\mathcal{L}_{HD'}$, which influences the kinematic term of the Higgs. The only dimension four operator which contributes to the Higgs propagator is $\operatorname{tr}\left[\left(\mathbf{D}_\mu\mathbf{H}\right)^2\mathbf{D}_\mu\mathbf{H}\right]$. Using the kinetic energy term of the Higgs results in a redefined operator

$$\mathcal{L}'_{HD'} = F'_{HD'}\left(\operatorname{tr}\left[\mathbf{H}^\dagger\left(\mathbf{D}_\mu\mathbf{H}\right)\right]\operatorname{tr}\left[\left(\mathbf{D}^\mu\mathbf{H}\right)^\dagger\mathbf{H}\right] - \frac{v^2}{2}\operatorname{tr}\left[\left(\mathbf{D}_\mu\mathbf{H}\right)\mathbf{D}_\mu\mathbf{H}\right]\right). \tag{3.27}$$

The Lagrangian (3.27) will change vector boson masses, but a renormalization of the Higgs field, which would affect all Higgs couplings, is not needed. Additional couplings of at least one Higgs to two weak vector bosons similar to $\mathcal{L}_{HD}$ are also introduced by the linear combination $\mathcal{L}'_{HD'}$. Combining these anomalous couplings into one operator can be achieved

with the linear transformation

$$\mathcal{L}_{HD'} = F_{HD'} \left(\mathrm{tr}\left[\mathbf{H}^\dagger \left(\mathbf{D}_\mu \mathbf{H}\right)\right] \mathrm{tr}\left[\left(\mathbf{D}^\mu \mathbf{H}\right)^\dagger \mathbf{H}\right] + \mathrm{tr}\left[\mathbf{H}^\dagger \mathbf{H} - \frac{v^2}{2}\right] \mathrm{tr}\left[\left(\mathbf{D}_\mu \mathbf{H}\right) \mathbf{D}_\mu \mathbf{H}\right] \right). \quad (3.28)$$

Dealing with the $SU(2)_C$ violating operator $\mathcal{L}^0_{WB}$ turns out to be more problematic. It includes terms, which will result in a mixing of the Standard Model eigenstates basis of the vector bosons Z and A

$$\mathcal{L}^0_{WB} \to \frac{F^0_{WB} v^2}{4} \mathrm{tr}\left[\mathbf{W}_{\mu\nu} \mathbf{B}^{\mu\nu}\right]. \quad (3.29)$$

The mixing can be dealt with modifying the Lagrangian $\mathcal{L}^0_{WB}$ by adding a term proportional to the kinetic Lagrangian of the $\mathbf{B}$ field

$$\mathcal{L}_{WB} = -F_{WB} \left(g g' \mathrm{tr}\left[\mathbf{H}^\dagger \mathbf{W}_{\mu\nu} \mathbf{H} \mathbf{B}^{\mu\nu}\right] + \frac{v^2}{8} \left(g^2 - g'^2\right) \mathrm{tr}\left[\mathbf{B}_{\mu\nu} \mathbf{B}^{\mu\nu}\right] \right). \quad (3.30)$$

Instead of a mixing, the redefined operator (3.30) yields an expression, which affects the two-point function of the Z and photon field

$$\mathcal{L}_{WB} \to -\frac{F_{WB} v^2}{16} \left(g^2 \left(\partial_\mu A_\nu - \partial_\nu A_\mu\right)^2 - g'^2 \left(\partial_\mu Z_\nu - \partial_\nu Z_\mu\right)^2 \right). \quad (3.31)$$

A renormalization of the boson fields Z and A is needed to guarantee the invariance of the kinetic term

$$Z_\mu \to \frac{1}{1 - \frac{g'^2 v^2}{4} F_{WB}} Z_\mu, \quad (3.32a)$$

$$A_\mu \to \frac{1}{1 + \frac{g^2 v^2}{4} F_{WB}} A_\mu. \quad (3.32b)$$

The redefinition of the boson fields (3.32) influences every coupling to these bosons. Furthermore, it contributes to the Z boson mass and therefore to the $\hat{\rho}$-parameter as well.

With the redefinitions (3.26),(3.30) and (3.28) the complete dimension six basis of C and P conserving parameters from (3.25) can be rewritten as

$$\mathcal{L}_{WWW} = -\mathrm{i}g^3 F_{WWW} \mathrm{tr}\left[\mathbf{W}_{\mu\nu}\mathbf{W}^{\nu\rho}\mathbf{W}_{\rho}^{\mu}\right], \tag{3.33a}$$

$$\mathcal{L}_{WB} = -gg' F_{WB} \left(\mathrm{tr}\left[\mathbf{H}^{\dagger}\mathbf{W}_{\mu\nu}\mathbf{H}\mathbf{B}^{\mu\nu}\right] + \frac{v^2}{8}\frac{g^2 - g'^2}{gg'}\mathrm{tr}\left[\mathbf{B}_{\mu\nu}\mathbf{B}^{\mu\nu}\right]\right), \tag{3.33b}$$

$$\mathcal{L}_{HW} = -g^2 F_{HW} \mathrm{tr}\left[\widehat{\mathbf{H}^{\dagger}\mathbf{H}}\right]\mathrm{tr}\left[\mathbf{W}_{\mu\nu}\mathbf{W}^{\mu\nu}\right], \tag{3.33c}$$

$$\mathcal{L}_{HB} = -g'^2 F_{HB} \mathrm{tr}\left[\widehat{\mathbf{H}^{\dagger}\mathbf{H}}\right]\mathrm{tr}\left[\mathbf{B}_{\mu\nu}\mathbf{B}^{\mu\nu}\right], \tag{3.33d}$$

$$\mathcal{L}_{HD} = F_{HD} \mathrm{tr}\left[\widehat{\mathbf{H}^{\dagger}\mathbf{H}}\right]\mathrm{tr}\left[\left(\mathbf{D}_{\mu}\mathbf{H}\right)^{\dagger}\left(\mathbf{D}^{\mu}\mathbf{H}\right)\right], \tag{3.33e}$$

$$\mathcal{L}_{HD'} = F_{HD'} \left(\mathrm{tr}\left[\left(\mathbf{D}^{\mu}\mathbf{H}\right)^{\dagger}\mathbf{H}\right]\mathrm{tr}\left[\mathbf{H}^{\dagger}\left(\mathbf{D}_{\mu}\mathbf{H}\right)\right] + \mathrm{tr}\left[\mathbf{H}^{\dagger}\mathbf{H} - \frac{v^2}{2}\right]\mathrm{tr}\left[\left(\mathbf{D}_{\mu}\mathbf{H}\right)^{\dagger}\left(\mathbf{D}^{\mu}\mathbf{H}\right)\right]\right), \tag{3.33f}$$

$$\mathcal{L}_{HHH} = F_{HHH} \mathrm{tr}\left[\widehat{\mathbf{H}^{\dagger}\mathbf{H}}\right]\mathrm{tr}\left[\widehat{\mathbf{H}^{\dagger}\mathbf{H}}\right]\mathrm{tr}\left[\widehat{\mathbf{H}^{\dagger}\mathbf{H}}\right]. \tag{3.33g}$$

A list of vertices, which are affected by the dimension six operator basis (3.33), is shown in Table 3.1. Vector boson scattering receives no tree level contribution from $\mathcal{L}_{HD'}$ and $\mathcal{L}_{HHH}$, because they are not contributing to anomalous gauge couplings or to HVV couplings (see Table 3.1 (a) and (b)). The only operator affecting longitudinal weak vector boson scattering is $\mathcal{L}_{HD}$ due to HVV couplings.

Other operators contributing directly to longitudinal vector boson scattering without involving extra Higgs fields start to appear at dimension eight.

3.4. Dimension Eight Operator set

There are many possibilities to construct dimension eight operators, which conserve C, P and only break custodial $SU_C(2)$ proportionally to $\mathbf{B}^{\mu\nu}$. The operators can be categorized in the number of fields they consist of to systematically build up a complete set. In particular, the classes are distinguishable in the number of field strength tensor, covariant derivatives and Higgs fields. An even number of Higgs fields is necessary to guarantee gauge invariance. Furthermore, the amount of covariant derivatives has to be equal or lower than the quantity of Higgs fields, because integration by parts and equations of motion (3.16) can be used to relate them to a linear combination of operators with less derivatives. Following this criterion, the operator basis can be separated in eight different classes shown in Table 3.2. In case of the linear Higgs doublet representation, only categories with an equal number of covariant derivatives and Higgs fields are used for the dimension eight operators in [56]. The

	WWZ	WWA	$WWWW$	$WWZZ$	$WWZA$	$WWAA$
$\mathcal{L}_{WWW}$	✓	✓	✓	✓	✓	✓
$\mathcal{L}_{WB}$	✓	✓	–	–	–	–

(a) Anomalous gauge couplings.

	HWW	HZZ	HZA	HAA
$\mathcal{L}_{WB}$	–	✓	✓	✓
$\mathcal{L}_{HW}$	✓	✓	✓	✓
$\mathcal{L}_{HB}$	–	✓	✓	✓
$\mathcal{L}_{HD}$	✓	✓	–	–

(b) Anomalous coupling of Higgs to two gauge bosons.

	HHH	$HHHH$
$\mathcal{L}_{HD}$	✓	✓
$\mathcal{L}_{HD'}$	✓	✓
$\mathcal{L}_{HHH}$	✓	✓

(c) Anomalous Higgs self couplings.

	$HWWZ$	$HWWA$	$HHWW$	$HHZZ$	$HHZA$	$HHAA$
$\mathcal{L}_{WB}$	✓	✓	–	✓	✓	✓
$\mathcal{L}_{HW}$	✓	✓	✓	✓	✓	✓
$\mathcal{L}_{HB}$	–	–	–	✓	✓	✓
$\mathcal{L}_{HD}$	–	–	✓	✓	–	–
$\mathcal{L}_{HD'}$	–	–	✓	✓	–	–

(d) Anomalous quartic couplings involving Higgs and gauge bosons.

Table 3.1.: List of vertices which receive contributions from the dimension six operator basis defined in (3.33) up to four particle interactions.

complete list of this set is shown in the Appendix A.5 and is separated into operators, which only affect longitudinal vertices (S), transversal vertices (T) and mixed vertices (M). To ease the comparison between the Higgs doublet and Higgs matrix representation, the same labeling is used while creating a dimension eight operator set for the complete Higgs matrix representation.

For a detailed discussion of a minimal dimension eight operator basis all non-redundant dimension six operators have to be included when using equation of motion or field redefinitions for an operators basis reduction. However, a full analysis is beyond the scope of this thesis, but applying insights from Section 3.3 a set of redundant dimension eight operators can already be eliminated. Additionally, the linear redundancy of an operator set can also be checked by comparing Feynman rules of the operators for each affected vertex. This way may not seem mathematical satisfactory and may be insufficient to find a minimal operator set. However, if the Feynman rules of a subset of every operator show the same linear dependency for every affected vertex, the operators cannot be distinguished on S-matrix level and are therefore redundant. To calculate the Feynman Rules, the Mathematica package FeynRules [68] is used[2].

The list of independent operators with an unequal number of Higgs fields and derivatives,

[2]To check of linear redundancies of an operator subset only vertices up to four fields are included, because a vertex with five or more fields will not contribute to the tree level amplitude of vector boson scattering.

n_x \ n_D	0	2	4
4	$(4,0,0) \equiv T$		
3	$(3,2,0)$		
2	$(2,4,0)$	$(2,2,2) \equiv M$	
1		$(1,4,2)$	
0	$(0,8,0)$	$(0,6,2)$	$(0,4,4) \equiv S$

Table 3.2.: List of possible classes for dimension eight operators, categorized by the number of field strength tensor n_X, Higgs fields n_H and covariant derivatives n_D in the tuple (n_X, n_H, n_D)

includes seven operators, which can be related to the dimension 6 basis (3.33)

$$\mathcal{L}_{(3,2,0),0} = -\mathrm{i}g^3 F_{(3,2,0),0}\ \mathrm{tr}\left[\widehat{\mathbf{H}^\dagger\mathbf{H}}\right]\mathrm{tr}\left[\mathbf{W}_{\mu\nu}\mathbf{W}^{\nu\rho}\mathbf{W}^{\mu}_{\rho}\right], \tag{3.34a}$$

$$\mathcal{L}_{(3,2,0),1} = -\mathrm{i}g^2 g' F_{(3,2,0),1}\ \mathrm{tr}\left[\mathbf{H}^\dagger\mathbf{W}_{\mu\nu}\mathbf{W}^{\nu\rho}\mathbf{H}\mathbf{B}^{\mu}_{\rho}\right], \tag{3.34b}$$

$$\mathcal{L}_{(2,4,0),0} = -g^2 F_{(2,4,0),0}\ \mathrm{tr}\left[\widehat{\mathbf{H}^\dagger\mathbf{H}}\right]\mathrm{tr}\left[\widehat{\mathbf{H}^\dagger\mathbf{H}}\right]\mathrm{tr}\left[\mathbf{W}_{\mu\nu}\mathbf{W}^{\mu\nu}\right], \tag{3.34c}$$

$$\mathcal{L}_{(2,4,0),1} = -g'^2 F_{(2,4,0),1}\ \mathrm{tr}\left[\widehat{\mathbf{H}^\dagger\mathbf{H}}\right]\mathrm{tr}\left[\widehat{\mathbf{H}^\dagger\mathbf{H}}\right]\mathrm{tr}\left[\mathbf{B}_{\mu\nu}\mathbf{B}^{\mu\nu}\right], \tag{3.34d}$$

$$\mathcal{L}_{(2,4,0),2} = -gg' F_{(2,4,0),1}\ \mathrm{tr}\left[\widehat{\mathbf{H}^\dagger\mathbf{H}}\right]\mathrm{tr}\left[\mathbf{H}^\dagger\mathbf{W}_{\mu\nu}\mathbf{H}\mathbf{B}^{\mu\nu}\right], \tag{3.34e}$$

$$\mathcal{L}_{(1,4,2),0} = \mathrm{i}g F_{(1,4,2),2}\ \mathrm{tr}\left[\left(\mathbf{D}_\mu\mathbf{H}\right)^\dagger\mathbf{H}\right]\mathrm{tr}\left[\mathbf{H}^\dagger\mathbf{W}^{\mu\nu}\left(\mathbf{D}_\nu\mathbf{H}\right)\right], \tag{3.34f}$$

$$\mathcal{L}_{(1,4,2),1} = \mathrm{i}g F_{(1,4,2),3}\ \mathrm{tr}\left[\left(\mathbf{D}_\mu\mathbf{H}\right)^\dagger\mathbf{H}\right]\mathrm{tr}\left[\left(\mathbf{D}_\nu\mathbf{H}\right)\mathbf{B}^{\mu\nu}\mathbf{H}^\dagger\right], \tag{3.34g}$$

$$\mathcal{L}_{(0,8,0),0} = F_{(0,8,0),0}\ \mathrm{tr}\left[\widehat{\mathbf{H}^\dagger\mathbf{H}}\right]\mathrm{tr}\left[\widehat{\mathbf{H}^\dagger\mathbf{H}}\right]\mathrm{tr}\left[\widehat{\mathbf{H}^\dagger\mathbf{H}}\right]\mathrm{tr}\left[\widehat{\mathbf{H}^\dagger\mathbf{H}}\right], \tag{3.34h}$$

$$\mathcal{L}_{(0,6,2),0} = F_{(0,6,2),0}\ \mathrm{tr}\left[\widehat{\mathbf{H}^\dagger\mathbf{H}}\right]\mathrm{tr}\left[\widehat{\mathbf{H}^\dagger\mathbf{H}}\right]\mathrm{tr}\left[\left(\mathbf{D}_\mu\mathbf{H}\right)^\dagger\mathbf{D}^\mu\mathbf{H}\right], \tag{3.34i}$$

$$\mathcal{L}_{(0,6,2),1} = F_{(0,6,2),1}\ \mathrm{tr}\left[\widehat{\mathbf{H}^\dagger\mathbf{H}}\right]\mathrm{tr}\left[\left(\mathbf{D}^\mu\mathbf{H}\right)^\dagger\mathbf{H}\right]\mathrm{tr}\left[\mathbf{H}^\dagger\left(\mathbf{D}_\mu\mathbf{H}\right)\right]. \tag{3.34j}$$

Two additional Higgs matrix fields are added to the dimension six operator by multiplying (3.33) with (3.26). These dimension eight operators have a similar coupling structure as their corresponding dimension six operators with one or two additional Higgs fields. Therefore, the operators listed in (3.34) would have an additional Higgs loop suppression, when contributing to vector boson scattering, and are not relevant to a study of leading order vector boson scattering.

Because the field strength tensor represents the coupling to transversal gauge boson modes, all contributions to transversal vector boson scattering are described by operators with four field strength tensors

$$\mathcal{L}_{T,0} = g^4 F_{T,0} \mathrm{tr}\left[\mathbf{W}_{\mu\nu}\mathbf{W}^{\mu\nu}\right] \mathrm{tr}\left[\mathbf{W}_{\alpha\beta}\mathbf{W}^{\alpha\beta}\right], \tag{3.35a}$$

$$\mathcal{L}_{T,1} = g^4 F_{T,1} \mathrm{tr}\left[\mathbf{W}_{\alpha\nu}\mathbf{W}^{\mu\beta}\right] \mathrm{tr}\left[\mathbf{W}_{\mu\beta}\mathbf{W}^{\alpha\nu}\right], \tag{3.35b}$$

$$\mathcal{L}_{T,2} = g^4 F_{T,2} \mathrm{tr}\left[\mathbf{W}_{\alpha\mu}\mathbf{W}^{\mu\beta}\right] \mathrm{tr}\left[\mathbf{W}_{\beta\nu}\mathbf{W}^{\nu\alpha}\right], \tag{3.35c}$$

$$\mathcal{L}_{T,5} = g^4 F_{T,5} \mathrm{tr}\left[\mathbf{W}_{\mu\nu}\mathbf{W}^{\mu\nu}\right] \mathrm{tr}\left[\mathbf{B}_{\alpha\beta}\mathbf{B}^{\alpha\beta}\right], \tag{3.35d}$$

$$\mathcal{L}_{T,6} = g^4 F_{T,6} \mathrm{tr}\left[\mathbf{W}_{\alpha\nu}\mathbf{W}^{\mu\beta}\right] \mathrm{tr}\left[\mathbf{B}_{\mu\beta}\mathbf{B}^{\alpha\nu}\right], \tag{3.35e}$$

$$\mathcal{L}_{T,7} = g^4 F_{T,7} \mathrm{tr}\left[\mathbf{W}_{\alpha\mu}\mathbf{W}^{\mu\beta}\right] \mathrm{tr}\left[\mathbf{B}_{\beta\nu}\mathbf{B}^{\nu\alpha}\right], \tag{3.35f}$$

$$\mathcal{L}_{T,8} = g'^4 F_{T,8} \mathrm{tr}\left[\mathbf{B}_{\mu\nu}\mathbf{B}^{\mu\nu}\right] \mathrm{tr}\left[\mathbf{B}_{\alpha\beta}\mathbf{B}^{\alpha\beta}\right], \tag{3.35g}$$

$$\mathcal{L}_{T,9} = g'^4 F_{T,9} \mathrm{tr}\left[\mathbf{B}_{\alpha\mu}\mathbf{B}^{\mu\beta}\right] \mathrm{tr}\left[\mathbf{B}_{\beta\nu}\mathbf{B}^{\nu\alpha}\right]. \tag{3.35h}$$

It should be noted, that the operators $\mathcal{L}_{T,8}$ and $\mathcal{L}_{T,9}$ contribute only to couplings of neutral vector bosons.

Replacing two field strength tensors with two derivatives and two Higgs fields gives rise to seven independent dimension 8 operators

$$\mathcal{L}_{M,0} = -g^2 F_{M,0} \mathrm{tr}\left[\left(\mathbf{D}_\mu\mathbf{H}\right)^\dagger \left(\mathbf{D}^\mu\mathbf{H}\right)\right] \mathrm{tr}\left[\mathbf{W}_{\nu\rho}\mathbf{W}^{\nu\rho}\right], \tag{3.36a}$$

$$\mathcal{L}_{M,1} = -g^2 F_{M,1} \mathrm{tr}\left[\left(\mathbf{D}_\mu\mathbf{H}\right)^\dagger \left(\mathbf{D}^\rho\mathbf{H}\right)\right] \mathrm{tr}\left[\mathbf{W}_{\nu\rho}\mathbf{W}^{\nu\mu}\right], \tag{3.36b}$$

$$\mathcal{L}_{M,2} = -g'^2 F_{M,2} \mathrm{tr}\left[\left(\mathbf{D}_\mu\mathbf{H}\right)^\dagger \left(\mathbf{D}^\mu\mathbf{H}\right)\right] \mathrm{tr}\left[\mathbf{B}_{\nu\rho}\mathbf{B}^{\nu\rho}\right], \tag{3.36c}$$

$$\mathcal{L}_{M,3} = -g'^2 F_{M,3} \mathrm{tr}\left[\left(\mathbf{D}_\mu\mathbf{H}\right)^\dagger \left(\mathbf{D}^\rho\mathbf{H}\right)\right] \mathrm{tr}\left[\mathbf{B}_{\nu\rho}\mathbf{B}^{\nu\mu}\right], \tag{3.36d}$$

$$\mathcal{L}_{M,4} = -gg' F_{M,4} \mathrm{tr}\left[\left(\mathbf{D}_\mu\mathbf{H}\right)^\dagger \mathbf{W}_{\nu\rho} \left(\mathbf{D}^\mu\mathbf{H}\right) \mathbf{B}^{\nu\rho}\right], \tag{3.36e}$$

$$\mathcal{L}_{M,5} = -gg' F_{M,5} \mathrm{tr}\left[\left(\mathbf{D}_\mu\mathbf{H}\right)^\dagger \mathbf{W}_{\nu\rho} \left(\mathbf{D}^\rho\mathbf{H}\right) \mathbf{B}^{\nu\mu}\right], \tag{3.36f}$$

$$\mathcal{L}_{M,7} = -g^2 F_{M,7} \mathrm{tr}\left[\left(\mathbf{D}_\mu\mathbf{H}\right)^\dagger \mathbf{W}_{\nu\rho}\mathbf{W}^{\nu\mu} \left(\mathbf{D}^\rho\mathbf{H}\right)\right]. \tag{3.36g}$$

The operators (3.36) have mixed contributions to transversal and longitudinal modes, represented by the covariant derivative acting on the Higgs matrix field.

The complete list of independent dimension 8 operators, which affect purely the longitudinal vector boson scattering contains only two operators

$$\mathcal{L}_{S,0} = F_{S,0} \mathrm{tr}\left[\left(\mathbf{D}_\mu\mathbf{H}\right)^\dagger \mathbf{D}_\nu\mathbf{H}\right] \mathrm{tr}\left[\left(\mathbf{D}^\mu\mathbf{H}\right)^\dagger \mathbf{D}^\nu\mathbf{H}\right], \tag{3.37a}$$

$$\mathcal{L}_{S,1} = F_{S,1} \mathrm{tr}\left[\left(\mathbf{D}_\mu\mathbf{H}\right)^\dagger \mathbf{D}^\mu\mathbf{H}\right] \mathrm{tr}\left[\left(\mathbf{D}_\nu\mathbf{H}\right)^\dagger \mathbf{D}^\nu\mathbf{H}\right]. \tag{3.37b}$$

The operators in equations (3.34)–(3.37) represent a complete set of dimension eight operators for vector boson scattering, where some redundant operators are already eliminated. They could represent the effective coupling of a resonance, which is above the directly experimental accessible energy region. To study the effect of this operators to physical observables in collider experiments, an implementation in a Monte Carlo generator is necessary.

3.5. Vector Boson Scattering at the LHC

The Goldstone boson sector can be completely described by longitudinal vector bosons at high energies using the Goldstone boson equivalence theorem [27, 69–72]. This means, that the transversal sector decouples completely from the longitudinal in the high-energy limit [66]. In this thesis the focus lies on operators which affect the Goldstone boson sector only.

Contributing to the coupling of a Higgs to two longitudinal vector bosons, the operator $\mathcal{L}_{HD}$ given in (3.33e) regulates the Higgs exchange in vector boson scattering. The related operator of dimension eight $\mathcal{L}_{(0,6,2),0}$, defined in (3.34), describes the coupling of two longitudinal vector bosons to a Higgs pair. This operator can be neglected, because it will not contribute at leading order to longitudinal vector boson scattering processes. $\mathcal{L}_{S,0}$ and $\mathcal{L}_{S,1}$ in (3.37) are the only dimension eight operators which modify quartic couplings of longitudinal vector bosons. The Feynman rules for the relevant tree-level vector boson scattering vertices are given in Appendix B.2 for $\mathcal{L}_{S,0}$, $\mathcal{L}_{S,1}$ and $\mathcal{L}_{HD}$. This subset of operators is implemented in the Monte Carlo generator `WHIZARD` and is used to study their impact at lepton and proton colliders[66, 73].

Quasi-elastic vector boson scattering $VV \to VV$ can be investigated with the process

$$pp \to (V \to ff) + (V \to ff) + jj \tag{3.38}$$

at proton-proton colliders with two jets j. The light fermions f serve as external probes for vector bosons in this process. Possible higher dimensional light fermion operators, which could modify this process, are assumed to be suppressed due to minimal flavor violation. Because gluons and heavy fermions are not contained in (3.38), the complete fermion sector can be treated perturbatively.

To enhance the contribution of the partonic process $VV \to VV$, typical vector boson fusion cuts are used [8],

$$p_j^T > 20 \text{ GeV} , \tag{3.39a}$$
$$\left|\eta_j\right| > 4.5 , \tag{3.39b}$$
$$M_{jj} > 500 \text{ GeV} , \tag{3.39c}$$
$$\Delta y_{jj} > 2.4. \tag{3.39d}$$

The differential cross section of $pp \to W^+W^+jj$ is represented in Figure 3.2 as a function of the invariant mass of final state vector bosons at the design energy of the LHC of 14

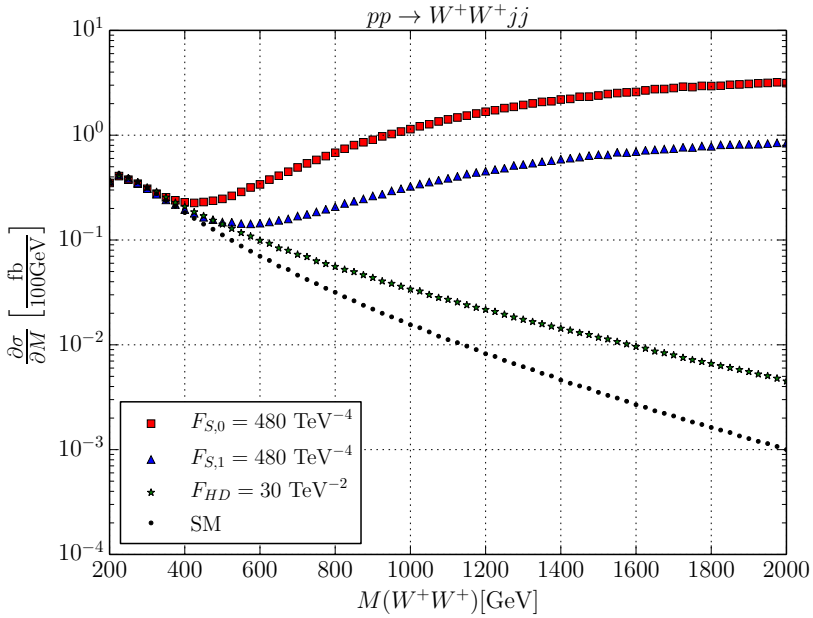

Figure 3.2.: $pp \to W^+W^+jj$, naive EFT results compared to the Standard Model, QCD contributions are neglected.
Cuts: $M_{jj} > 500$ GeV; $\Delta y_{jj} > 2.4$; $p_T^j > 20$ GeV; $|\eta_j| > 4.5$.

TeV. If only the Standard Model Lagrangian is considered, the vector boson scattering cross section is dominated by transversal gauge boson. Additionally to the higher multiplicity of transversal polarized vector boson, the impact of longitudinal vector bosons is suppressed. Besides the cancellation due to the Higgs exchange, the longitudinal production mechanism is small, because massless fermions only couple via helicity mixing to longitudinal vector bosons.

The probability that a quark or gluon is emitted from the proton, which is given by the parton distribution function, will quickly fall with the energy fraction of the parton. Therefore, the differential cross section of the Standard Model will be suppressed at high energies as shown in Figure 3.2. Although the dimension six operator contribution will rise with the invariant mass of the VV system, at couplings of $F_{HD} = 30\ \text{TeV}^{-2} \approx (0.18\ \text{TeV})^{-2}$ the PDF suppression is still present. However, anomalous quartic gauge couplings of $F_{S,0/1} = 480\ \text{TeV}^{-4} \approx (0.21\ \text{TeV})^{-4}$, which respect current experimental bounds [8], cancel the proton PDF suppression and the differential cross section rises with the invariant mass of the vector boson scattering system. A high energy extrapolation of the Standard Model is impossible in such an effective field theory [27, 74]. This is a clear hint, that the effective field theory is used beyond its validity.

3.6. The Goldstone Boson Scattering Amplitude

The energy behavior of the effective field theory operators affecting the longitudinal vector boson modes will be studied in more detail by discussing the related Goldstone boson scattering amplitudes. In the case of weak boson scattering, the Standard Model amplitudes are proportional to $m_H^2/(4\pi v)^2$ in the high energy limit [27, 74]. Therefore, the small Standard Model contribution can be neglected and is treated as zero during the determination of the energy behavior of the effective field theory operators. To determine the contributions of new physics operators to the vector boson scattering amplitudes at high energies the Goldstone boson equivalence theorem is used, and the Goldstone boson amplitudes are evaluated in the gaugeless limit $g \to 0$, $g' \to 0$.

When treating vector boson scattering as a $2 \to 2$ process of massless scalars at high energies, it is convenient to describe kinematic dependencies using Mandelstam variables

$$s + t + u = \sum_{i=1}^{4} m_i^2 \to 0 \tag{3.40a}$$

$$s = (k_1 + k_2)^2 = (k_3 + k_4)^2\,, \tag{3.40b}$$

$$t = (k_1 - k_3)^2 = (k_2 - k_4)^2\,, \tag{3.40c}$$

$$u = (k_1 - k_4)^2 = (k_2 - k_3)^2\,, \tag{3.40d}$$

with incoming momenta k_1, k_2, outgoing momenta k_3, k_4 and their associated masses $m_i^2 = k_i^2$. In the massless limit, the scattering angle between k_1 and k_3 can be written as

$$\cos\Theta = 2\frac{t}{s} + 1. \tag{3.41}$$

The amplitudes $\mathcal{A}(s,t,u)$ are usually displayed as functions of the three Mandelstam variables, but equation (3.40a) demonstrates a linear dependency of these variables. Therefore, the amplitudes are a function of two variables only, $\mathcal{A}(s,t)$, $\mathcal{A}(s,u)$ or $\mathcal{A}(u,t)$.

The Feynman rules in the gaugeless limit $g \to 0$, $g' \to 0$ for the dimension six and dimension eight operators are listed in Appendix B.3. They yield the goldstone boson scattering amplitudes

$$\begin{aligned}\mathcal{A}(w^+w^+ \to w^+w^+) = {} & \frac{1}{4}F_{S,0}(2s^2 + t^2 + u^2) + \frac{1}{2}F_{S,1}(t^2 + u^2) \\ & - \left(F_{HD}^2\frac{v^2}{4} + F_{HD}\right)\left(\frac{t^2}{t - m_H^2} + \frac{u^2}{u - m_H^2}\right),\end{aligned} \tag{3.42a}$$

$$\mathcal{A}(w^+z \to w^+z) = \frac{1}{4}F_{S,0}(s^2 + u^2) + \frac{1}{2}F_{S,1}t^2 - \left(F_{HD}^2\frac{v^2}{4} + F_{HD}\right)\frac{t^2}{t - m_H^2}, \tag{3.42b}$$

$$\begin{aligned}\mathcal{A}(w^+w^- \to w^+w^-) = {} & \frac{1}{4}F_{S,0}(s^2 + t^2 + 2u^2) + \frac{1}{2}F_{S,1}(s^2 + t^2) \\ & - \left(F_{HD}^2\frac{v^2}{4} + F_{HD}\right)\left(\frac{s^2}{s - m_H^2} + \frac{t^2}{t - m_H^2}\right),\end{aligned} \tag{3.42c}$$

$$\mathcal{A}(w^+w^- \to zz) = \frac{1}{4}F_{S,0}(t^2+u^2) + \frac{1}{2}F_{S,1}s^2 - \left(F_{HD}^2\frac{v^2}{4} + F_{HD}\right)\frac{s^2}{s-m_H^2}, \tag{3.42d}$$

$$\mathcal{A}(zz \to zz) = \frac{1}{2}\left(F_{S,0}+F_{S,1}\right)\left(s^2+t^2+u^2\right) - \left(F_{HD}^2\frac{v^2}{4} + F_{HD}\right)\left(\frac{s^2}{s-m_H^2} + \frac{t^2}{t-m_H^2} + \frac{u^2}{u-m_H^2}\right). \tag{3.42e}$$

For the high energy behavior of a general amplitude $\mathcal{A}(s,t,u)$ a bound was computed in [75, 76] which is known as the Froissart bound

$$\lim_{s\to\infty}\mathcal{A}\left(s,t,u\right) = \mathcal{O}\left(s\left(\log s\right)^2\right) \qquad \text{for fixed } t \leq 0 \text{ or } u \leq 0. \tag{3.43}$$

The dimension eight operators contribution to (3.42) are proportional to $\frac{s^2}{\Lambda^4}$ and will strongly violate this bound at high energies $s \gg \Lambda$. Because the mass scale of new physic Λ is unknown, it is impossible to know the exact validity limit of a bottom-up effective field theory a priori. However, the unitarity condition of the S-matrix can be used to study the theoretical validity of bottom-up effective field theories.

Chapter 4

Unitarity

The scattering matrix S plays a fundamental role in quantum field theory. It includes all information how an incoming state $|\text{in}\rangle$ at $t = -\infty$ evolves in time to an outgoing state $|\text{out}\rangle$ at $t = \infty$,

$$|\text{out}, t = \infty\rangle = \text{S}|\text{in}, t = -\infty\rangle. \tag{4.1}$$

Furthermore, the S-matrix can be separated into a noninteracting part and an interacting part represented by the transition operator T

$$\text{S} = \mathbb{1} + \text{iT}. \tag{4.2}$$

A complete discussion of general S-matrix principles can be found in [75, 77]. The focus of this chapter is the unitarity of the S-matrix, which is related to probability conservation

$$\mathbb{1} = S^\dagger S = \mathbb{1} - \text{iT}^\dagger + \text{iT} + \text{T}^\dagger\text{T}. \tag{4.3}$$

This implies the optical theorem for the transition operator

$$\text{T}^\dagger\text{T} = -\text{i}\left(\text{T} - \text{T}^\dagger\right), \tag{4.4}$$

which set bounds on amplitudes and can therefore be used to check the liability of an effective field theory.

Beside the determination of the validity bound of an effective field theory, a unitarization scheme is introduced in this chapter to allow a theoretical description consistent with the S-matrix unitarity at all energies. This part of the thesis has been published in [66].

4.1. Crossing symmetry

Crossing symmetry can be used to relate amplitudes by transforming ingoing particles into outgoing antiparticles and vice versa. A special case is the $2 \to 2$ scattering of four particles p_1, p_2, p_3 and p_4 with momenta k_i, which can be separated into different channels

$$\begin{aligned}
\text{s} - \text{channel}: \quad & p_1(k_1)p_2(k_2) \;\to\; p_3(k_3)p_4(k_4), && \text{(4.5a)}\\
& \bar{p}_3(-k_3)\bar{p}_4(-k_4) \to \bar{p}_1(-k_1)\bar{p}_2(-k_2), && \text{(4.5b)}\\
\text{t} - \text{channel}: \quad & p_1(k_1)\bar{p}_3(-k_3) \to \bar{p}_2(-k_2)p_4(k_4), && \text{(4.5c)}\\
& p_2(k_2)\bar{p}_4(-k_4) \to \bar{p}_1(-k_1)p_3(k_3), && \text{(4.5d)}\\
\text{u} - \text{channel}: \quad & p_1(k_1)\bar{p}_4(-k_4) \to \bar{p}_2(-k_2)p_3(k_3), && \text{(4.5e)}\\
& p_2(k_2)\bar{p}_3(-k_3) \to \bar{p}_1(-k_1)p_4(k_4), && \text{(4.5f)}
\end{aligned}$$

where $\bar{p}_i$ are the corresponding antiparticles. The channels in (4.5) describe physically non-overlapping regions of the Mandelstam variables defined in (3.40). In [2] these regions were analyzed for general $2 \to 2$ processes and can be qualitatively described by the inequalities

$$\begin{aligned}
\text{s} - \text{channel}: \quad & s > M_\text{f}^2 \text{ and } t, u < 0, && \text{(4.6a)}\\
\text{t} - \text{channel}: \quad & t > M_\text{f}^2 \text{ and } s, u < 0, && \text{(4.6b)}\\
\text{u} - \text{channel}: \quad & u > M_\text{f}^2 \text{ and } t, s < 0, && \text{(4.6c)}
\end{aligned}$$

where M_f^2 is the minimal energy needed to produce the final state particles. In the following, the abbreviations $\Theta(s - M_\text{f}^2)$, $\Theta(t - M_\text{f}^2)$ and $\Theta(u - M_\text{f}^2)$ are used to indicate which channel becomes physical.

As stated in Section 2.3.2, custodial symmetry is conserved at high energies. In this thesis the $SU(2)_C$ quantum number is referred as custodial isospin and can only take the values $I = 0, 1, 2$ in the vector boson scattering process. Following an analogous ansatz as [78] for pion-pion scattering, the quasi-elastic scattering amplitude of two Goldstone bosons w^i ($i = 1, 2, 3$) can therefore be written with three independent functions of s, t and u

$$\mathcal{A}_{\alpha\beta\gamma\delta}(s,t,u) = A(s,t,u)\delta_{\alpha\beta}\delta_{\gamma\delta} + B(s,t,u)\delta_{\alpha\gamma}\delta_{\beta\delta} + C(s,t,u)\delta_{\alpha\delta}\delta_{\gamma\beta}, \tag{4.7}$$

where $\alpha, \beta, \gamma, \delta$ represent the states w^1, w^2, w^3. These states are related to the mass eigenstates of the weak vector bosons by

$$\begin{aligned}
|w^+w^+\rangle &= \frac{1}{2}\left[|w^1w^1\rangle - |w^2w^2\rangle - \mathrm{i}\left(|w^1w^2\rangle + |w^2w^1\rangle\right)\right], && \text{(4.8a)}\\
|w^+w^-\rangle &= \frac{1}{2}\left[|w^1w^1\rangle + |w^2w^2\rangle + \mathrm{i}\left(|w^1w^2\rangle - |w^2w^1\rangle\right)\right], && \text{(4.8b)}\\
|w^+z\rangle &= \frac{1}{\sqrt{2}}\left[|w^1w^3\rangle - \mathrm{i}|w^2w^3\rangle\right], && \text{(4.8c)}\\
|zz\rangle &= |w^3w^3\rangle. && \text{(4.8d)}
\end{aligned}$$

Processes involving the Higgs field are omitted at first for simplification and will be considered as corrections later in Section 4.3.2. Inserting (4.8) in (4.7) leads to a decomposition of the Goldstone amplitudes

$$\mathcal{A}(w^+w^+ \to w^+w^+) = B(s,t,u) + C(s,t,u)\,, \tag{4.9a}$$
$$\mathcal{A}(w^+w^- \to w^+w^-) = A(s,t,u) + B(s,t,u) \tag{4.9b}$$
$$\mathcal{A}(w^+z \to w^+z) = B(s,t,u)\,, \tag{4.9c}$$
$$\mathcal{A}(w^+w^- \to zz) = A(s,t,u)\,, \tag{4.9d}$$
$$.\mathcal{A}(zz \to zz) = A(s,t,u) + B(s,t,u) + C(s,t,u)\,. \tag{4.9e}$$

Here, the amplitudes are formulated in the s-channel. Therefore, the Heaviside step function $\Theta\left(s - M_\mathrm{f}^2\right)$ should be added to (4.9) to point out the choice of channel. Using Heaviside step functions for the other Mandelstam variables, the amplitudes in (4.9) can be written including all channels like

$$\begin{aligned}\mathrm{A}(w^+w^-w^+w^-) =& \left(A(s,t,u) + B(s,t,u)\right)\Theta\left(s - M_\mathrm{f}^2\right)\\ &+ \left(B(s,t,u) + C(s,t,u)\right)\Theta\left(t - M_\mathrm{f}^2\right)\\ &+ \left(A(s,t,u) + C(s,t,u)\right)\Theta\left(u - M_\mathrm{f}^2\right),\end{aligned} \tag{4.10a}$$
$$\begin{aligned}\mathrm{A}(w^+w^-zz) =& A(s,t,u)\Theta\left(s - M_\mathrm{f}^2\right) + B(s,t,u)\Theta\left(t - M_\mathrm{f}^2\right)\\ &+ C(s,t,u)\Theta\left(u - M_\mathrm{f}^2\right),\end{aligned} \tag{4.10b}$$
$$\begin{aligned}\mathrm{A}(zzzz) =& \left[A(s,t,u) + B(s,t,u) + C(s,t,u)\right]\\ &\times\left[\Theta\left(s - M_\mathrm{f}^2\right) + \Theta\left(t - M_\mathrm{f}^2\right) + \Theta\left(u - M_\mathrm{f}^2\right)\right].\end{aligned} \tag{4.10c}$$

Every of these amplitudes has to respect crossing symmetry. Therefore, the amplitudes B and C can be related to A by interchanging $s \to t$ and $u \to t$, respectively,

$$B(s,t,u) = A(t,s,u), \tag{4.11a}$$
$$C(s,t,u) = A(u,s,t). \tag{4.11b}$$

With equations (4.11), the longitudinal vector boson scattering amplitudes can be formulated as functions of one master amplitude $A(s,t,u)$

$$\begin{aligned}\mathrm{A}(w^+w^-w^+w^-) =& \left(A(s,t,u) + A(t,s,u)\right)\Theta\left(s - M_\mathrm{f}^2\right)\\ &+ \left(A(t,s,u) + A(u,s,t)\right)\Theta\left(t - M_\mathrm{f}^2\right)\\ &+ \left(A(s,t,u) + A(u,s,t)\right)\Theta\left(u - M_\mathrm{f}^2\right),\end{aligned} \tag{4.12a}$$
$$\begin{aligned}\mathrm{A}(w^+w^-zz) =& A(s,t,u)\Theta\left(s - M_\mathrm{f}^2\right) + A(t,s,u)\Theta\left(t - M_\mathrm{f}^2\right)\\ &+ A(u,s,t)\Theta\left(u - M_\mathrm{f}^2\right),\end{aligned} \tag{4.12b}$$
$$\begin{aligned}\mathrm{A}(zzzz) =& \left(A(s,t,u) + A(t,s,u) + A(u,s,t)\right)\\ &\left(\Theta\left(s - M_\mathrm{f}^2\right) + \Theta\left(t - M_\mathrm{f}^2\right) + \Theta\left(u - M_\mathrm{f}^2\right)\right).\end{aligned} \tag{4.12c}$$

The crossing symmetry is manifest in (4.12). Furthermore, the Θ-function indicates which particle poles on the associated physical region can be reached. The particles poles fall into

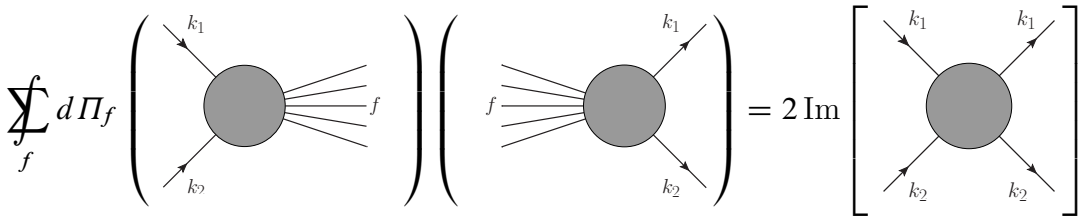

Figure 4.1.: Optical Theorem: The imaginary part of a forward scattering amplitude is equivalent to the sum of all possible intermediate state particle contributions.

two classes: stable particles, which generate a pole on the physical sheet at m^2 of the particle, and unstable particles, where the resonance pole is located on the unphysical Riemann sheet [79]. This unphysical Riemann sheet can only be reached through a branch cut above a certain threshold energy M_{th} in the corresponding physical region, which is related to an open decay channel of the resonance [80]. To guarantee that the crossing symmetric Breit-Wigner formulation of a resonance receives only a non-vanishing imaginary contribution in the resonant channel, an additional Θ-function multiplies the width Γ of the particle with mass m

$$\mathcal{A}_{\mathrm{BW}} = \frac{s}{s - m^2 + \mathrm{i}m\Gamma\Theta\left(s - M_{th}^2\right)}. \tag{4.13}$$

4.2. Optical Theorem

Introducing the matrix elements $\mathcal{T}_{fi} = \langle f\,|\mathrm{T}|i\rangle$ between final state $\langle f\,|$ and initial state $|i\rangle$ the optical theorem in (4.4) can be written as

$$\sigma_{\mathrm{tot}} = \frac{1}{64\pi^2 s}\int d\Omega \sum_f \left|\mathcal{T}_{fi}\right|^2 = \frac{2\,\mathrm{Im}\left[\mathcal{T}_{\mathrm{ii}}(\mathrm{t}=0)\right]}{s}. \tag{4.14}$$

The derivation for general processes is given in [13]. Figure 4.1 pictures that the optical theorem associates the total cross section σ_{tot} with the imaginary part of the elastic forward scattering amplitude. To make the angular distribution explicit on the left handed side of (4.14), the matrix elements can be decomposed into partial waves

$$\mathcal{T}_{fi}(s,t,u) = \sum_\ell (2l+1)\mathcal{T}_{fi}^\ell(s)\,P^\ell(\cos\Theta(s,t,u)), \tag{4.15a}$$

$$\mathcal{T}_{fi}^\ell(s) = \frac{1}{2}\int_{-s}^{0} \mathrm{d}t\,\frac{2}{s}\mathcal{T}_{fi}(s,t,u)\,P^\ell(\cos\Theta(s,t,u)), \tag{4.15b}$$

with Legendre polynomials P^ℓ (see Appendix A.2 for details) and scattering angle Θ. Using the partial wave decomposition (4.15) for the optical theorem (4.14) will result in a relation

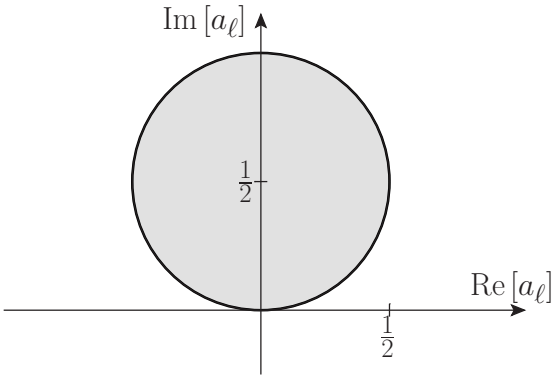

Figure 4.2.: Argand circle: A partial wave amplitude satisfying S-matrix unitarity has to lie on (inside) the circle for elastic (inelastic) scattering processes.

for the angular matrix elements

$$\sum_{f,\ell} \frac{2l+1}{64\pi s} \left|\mathcal{T}^\ell_{fi}\right|^2 = \sum_{\ell} \frac{2l+1}{s} \operatorname{Im}\left[\mathcal{T}^\ell_{ii}\right]. \tag{4.16}$$

Expressing (4.16) in terms of angular amplitudes $\mathcal{A}_\ell\,(i \to f) = \mathcal{T}^\ell_{fi}/2$ results in

$$\sum_{f,\ell} \frac{2l+1}{32\pi s} \left|\mathcal{A}_\ell\,(i \to f)\right|^2 = \sum_{\ell} \frac{2l+1}{s} \operatorname{Im}\left[\mathcal{A}_\ell\,(i \to i)\right]. \tag{4.17}$$

The Froissart bound (3.43) is obtained by a power analysis of the equation (4.17). A more accurate bound can be derived for the partial waves of elastic scattering processes. In that case, all off-diagonal amplitudes are zero and the optical theorem simplifies for normalized amplitudes $a = \frac{1}{32\pi}\mathcal{A}_{ii}$ to

$$|a_\ell|^2 = \operatorname{Im}\left[a_\ell\right]. \tag{4.18}$$

In case of inelastic amplitudes, the equality sign becomes an inequality. This bound for elastic and inelastic amplitudes can be graphically described in an Argand diagram by a circle with radius $\frac{1}{2}$ and center $\frac{\mathrm{i}}{2}$, the Argand circle, (see fig. 4.2)

$$\left|a_\ell - \frac{\mathrm{i}}{2}\right| \leq \frac{1}{2}. \tag{4.19}$$

Only amplitudes which lie on or inside of this circle fulfill the unitarity condition. However, tree-level amplitudes without a resonance are usually real, because they are only the leading order expansion of the full amplitude. Therefore, the boundary condition for the real part of (4.18) is used to check the unitarity of the amplitudes,

$$|\operatorname{Re}\left(a_\ell\right)| \leq \frac{1}{2}. \tag{4.20}$$

	$w^+w^+ \to w^+w^+$	$w^+z \to w^+z$	$w^+w^- \to w^+w^-$	$w^+w^- \to zz$	$zz \to zz$
$\mathcal{A}_0$	–	–	✓	✓	✓
$\mathcal{A}_1$	–	✓	✓	–	✓
$\mathcal{A}_2$	✓	✓	✓	✓	✓

Table 4.1.: Possible contributions of isospin eigenamplitudes to the vector boson scattering s-channel processes.

The relation (4.18) becomes exactly equal, if only elastic scattering is allowed. In contrary, the unitarity bound becomes weaker, if additional inelastic channels open up. The interaction matrix of vector boson scattering in the mass eigenstate basis (4.21) has also non-diagonal entries from inelastic channels

$$\mathcal{T}_{\mathrm{VBS}} \equiv \begin{pmatrix} \mathcal{A}_{w^+w^+\to w^+w^+} & 0 & 0 & 0 \\ 0 & \mathcal{A}_{w^+z\to w^+z} & 0 & 0 \\ 0 & 0 & \mathcal{A}_{w^+w^-\to w^+w^-} & \mathcal{A}_{w^+w^-\to zz} \\ 0 & 0 & \mathcal{A}_{zz\to w^+w^-} & \mathcal{A}_{zz\to zz} \end{pmatrix}. \tag{4.21}$$

4.3. Isospin Eigenamplitude

The custodial $SU(2)$-symmetry holds at high energies in the high p_T region, where no Coloumb singularities arise. Therefore, the $SU(2)$-symmetry can be used to diagonalize the interaction matrix (4.21), and the vector boson scattering amplitudes can be represented as a function of diagonal s-channel isospin eigenamplitudes $\mathcal{A}_I = \mathcal{A}_I(s,t,u)$ for $I = 0, 1, 2$. A detailed description of the isospin eigenbasis is shown in Appendix A.3. The decomposition to isospin eigenamplitudes in (A.31) can be rewritten in terms of the physical regions

$$\begin{aligned} \mathcal{A}(w^+w^-w^+w^-) = &\left(\frac{1}{3}\mathcal{A}_0 + \frac{1}{2}\mathcal{A}_1 + \frac{1}{6}\mathcal{A}_2\right)\Theta\left(s - M_{\mathrm{f}}^2\right) + \mathcal{A}_2\Theta\left(t - M_{\mathrm{f}}^2\right) \\ &+ \left(\frac{1}{3}\mathcal{A}_0 - \frac{1}{2}\mathcal{A}_1 + \frac{1}{6}\mathcal{A}_2\right)\Theta\left(u - M_{\mathrm{f}}^2\right), \end{aligned} \tag{4.22a}$$

$$\begin{aligned} \mathcal{A}(w^+w^-zz) = &\left(\frac{1}{3}\mathcal{A}_0 - \frac{1}{3}\mathcal{A}_2\right)\Theta\left(s - M_{\mathrm{f}}^2\right) + \left(\frac{1}{2}\mathcal{A}_1 + \frac{1}{2}\mathcal{A}_2\right)\Theta\left(t - M_{\mathrm{f}}^2\right) \\ &+ \left(-\frac{1}{2}\mathcal{A}_1 + \frac{1}{2}\mathcal{A}_2\right)\Theta\left(u - M_{\mathrm{f}}^2\right), \end{aligned} \tag{4.22b}$$

$$\mathcal{A}(zzzz) = \left(\frac{1}{3}\mathcal{A}_0 + \frac{2}{3}\mathcal{A}_2\right)\left(\Theta\left(s - M_{\mathrm{f}}^2\right) + \Theta\left(t - M_{\mathrm{f}}^2\right) + \Theta\left(u - M_{\mathrm{f}}^2\right)\right). \tag{4.22c}$$

An overview of possible channels contributing to certain processes according to equations (4.22) is given in Table 4.1. That means the isospin of a resonance can be determined by its appearance in the vector boson scattering channels. For example, when a resonance is detected in the $w^+w^+ \to w^+w^+$ process, it has to be originated from the isospin-two eigenamplitude.

To satisfy crossing invariance, equations (4.22) and (4.12) have to be compared. This comparison leads to a relation between isospin eigenamplitudes and the master amplitude $A(s,t,u)$

$$\mathcal{A}_0 = 3A(s,t,u) + A(t,s,u) + A(u,s,t)\,, \tag{4.23a}$$
$$\mathcal{A}_1 = A(t,s,u) - A(u,s,t)\,, \tag{4.23b}$$
$$\mathcal{A}_2 = A(t,s,u) + A(u,s,t)\,. \tag{4.23c}$$

4.3.1. Spin-Isospin Eigenamplitudes

The Goldstone boson scattering amplitudes can now be written as functions of isospin-spin eigenamplitudes $\mathcal{A}_{I\ell}$ by decomposing the isospin amplitudes further in partial waves[1] as defined in (4.15)

$$\begin{aligned}
\mathcal{A}(w^+w^+ \to w^+w^+) =& \mathcal{A}_{20}(s) - 10\mathcal{A}_{22}(s) \\
&+ 15\mathcal{A}_{22}(s)\frac{t^2+u^2}{s^2}\,, && (4.24a)\\
\mathcal{A}(w^+w^- \to zz) =& \frac{1}{3}\left(\mathcal{A}_{00}(s) - \mathcal{A}_{20}(s)\right) - \frac{10}{3}\left(\mathcal{A}_{02}(s) - \mathcal{A}_{22}(s)\right) \\
&+ 5\left(\mathcal{A}_{02}(s) - \mathcal{A}_{22}(s)\right)\frac{t^2+u^2}{s^2}\,, && (4.24b)\\
\mathcal{A}(w^+z \to w^+z) =& \frac{1}{2}\mathcal{A}_{20}(s) - 5\mathcal{A}_{22}(s) + \frac{15}{2}\mathcal{A}_{22}(s)\frac{t^2+u^2}{s^2} \\
&- \frac{3}{2}\mathcal{A}_{11}(s)\frac{t^2-u^2}{s^2}\,, \\
\mathcal{A}(w^+w^- \to w^+w^-) =& \frac{1}{6}\left(2\mathcal{A}_{00}(s) + \mathcal{A}_{20}(s)\right) - \frac{5}{3}\left(2\mathcal{A}_{02}(s) + \mathcal{A}_{22}(s)\right) \\
&+ \left(5\mathcal{A}_{02}(s) + \frac{5}{2}\mathcal{A}_{22}(s)\right)\frac{t^2+u^2}{s^2} \\
&- \frac{3}{2}\mathcal{A}_{11}(s)\frac{t^2-u^2}{s^2}\,, && (4.24c)\\
\mathcal{A}(zz \to zz) =& \frac{1}{3}\left(\mathcal{A}_{00}(s) + 2\mathcal{A}_{20}(s)\right) - \frac{10}{3}\left(\mathcal{A}_{02}(s) + 2\mathcal{A}_{22}(s)\right) \\
&+ 5\left(\mathcal{A}_{02}(s) + 2\mathcal{A}_{22}(s)\right)\frac{t^2+u^2}{s^2}\,. && (4.24d)
\end{aligned}$$

Because all scattering amplitudes in (4.24) are formulated only in the physical region of the Mandelstam variable s, the factor $\Theta\left(s - M_{\text{th}}^2\right)$ is omitted. When exchanging $t \leftrightarrow u$ in the amplitudes of equations (4.24), it will also affect the isospin-spin eigenamplitude

$$\mathcal{A}_{11}(s,t,u) = -\mathcal{A}_{11}(s,u,t). \tag{4.25}$$

[1] The angular momenta of the vector boson scattering system is assumed to be zero, therefore only amplitudes up to $\ell = 2$ will contribute.

Thus, the crossing invariance of $t \leftrightarrow u$ is apparent. However, the crossing invariance is not manifest for other exchanges like $s \leftrightarrow t$. A complete analysis of crossing invariance of isospin-spin amplitude for pion-pion scattering to study a generic analytical function for the partial waves is performed in [81–83]. However, in this thesis the isospin-spin eigenamplitudes are by construction in (4.23) symmetric under crossing .

4.3.2. Including the Higgs

The effective operators $\mathcal{L}_{S,0}$, $\mathcal{L}_{S,1}$ and $\mathcal{L}_{HD}$ will also contribute to quartic Higgs self interaction $hh \to hh$ process and to the amplitudes $w^+w^- \to hh$, $zz \to hh$, which can affect the vector boson scattering cross section via back-scattering. The inclusion of the Higgs contribution can be achieved by treating z as complex scalar

$$z \to z + \mathrm{i}h. \tag{4.26}$$

The substitution (4.26) into the isospin-spin formulation of the s-channel scattering amplitudes in (4.24) leads to the amplitudes

$$\begin{aligned}
\mathcal{A}(w^+w^- \to hh) = \mathcal{A}(zz \to hh) =& \frac{1}{3}\left(\mathcal{A}_{00}(s) - \mathcal{A}_{20}(s)\right) - \frac{10}{3}\left(\mathcal{A}_{02}(s) - \mathcal{A}_{22}(s)\right) \\
&+ 5\left(\mathcal{A}_{02}(s) - \mathcal{A}_{22}(s)\right)\frac{t^2+u^2}{s^2}, && \text{(4.27a)} \\
\mathcal{A}(w^+h \to w^+h) = \mathcal{A}(zh \to zh) =& \frac{1}{2}\mathcal{A}_{20}(s) - 5\mathcal{A}_{22}(s) \\
&+ \frac{15}{2}\mathcal{A}_{22}(s)\frac{t^2+u^2}{s^2} && \text{(4.27b)} \\
&- \frac{3}{2}\mathcal{A}_{11}(s)\frac{t^2-u^2}{s^2}, \\
\mathcal{A}(hh \to hh) =& \frac{1}{3}\left(\mathcal{A}_{00}(s) + 2\mathcal{A}_{20}(s)\right) - \frac{10}{3}\left(\mathcal{A}_{02}(s) + 2\mathcal{A}_{22}(s)\right) \\
&+ 5\left(\mathcal{A}_{02}(s) + 2\mathcal{A}_{22}(s)\right)\frac{t^2+u^2}{s^2}. && \text{(4.27c)}
\end{aligned}$$

At first sight the amplitudes in (4.27) seem to be incorrect, because they include contributions of isospin amplitudes $\mathcal{A}_1$ and $\mathcal{A}_2$. However the custodial $SU(2)_C$ is only the subgroup of the broken chiral $SU(2)_L \times SU(2)_R$. In presence of a Higgs, the amplitudes should be characterized in terms of the full $SU(2)_L \times SU(2)_R$ symmetry group instead of the weak isospin. Therefore, contributions with higher isospin will never occur isolated. A detailed discussion about this phenomena is given in Section 5.1.2. In this section it is satisfactory to state, that the amplitudes of the Higgs scattering processes agree with the amplitudes calculated with the relations in (4.27) for all anomalous operators $\mathcal{L}_{HD}$, $\mathcal{L}_{S,0}$, $\mathcal{L}_{S,1}$.

4.4. Unitarity Bound for Effective Operators

The isospin-spin amplitudes of the effective operators in (3.42) include integrals of non-resonant particle exchange in the t- and u-channel. To shorten the notation of the logarithmic terms of the partial wave decomposition the abbreviations $\mathcal{S}_i(s, m_h)$ introduced in (A.33) are used for the isospin-spin eigenamplitudes

$$\begin{aligned}
\mathcal{A}_{00} =& \frac{1}{6}\left(7F_{S,0} + 11F_{S,1}\right)s^2 \\
&- \left(F_{HD}^2\frac{v^2}{4} + F_{HD}\right)\left(\frac{3s^2}{s-m_h^2} + 2\mathcal{S}_0(s, m_h)\right), && \text{(4.28a)}\\
\mathcal{A}_{02} =& \frac{1}{30}\left(2F_{S,0} + F_{S,1}\right)s^2 - \left(F_{HD}^2\frac{v^2}{4} + F_{HD}\right)2\mathcal{S}_2(s, m_h), && \text{(4.28b)}\\
\mathcal{A}_{11} =& \frac{1}{12}\left(F_{S,0} - 2F_{S,1}\right)s^2 - \left(F_{HD}^2\frac{v^2}{4} + F_{HD}\right)2\mathcal{S}_1(s, m_h), && \text{(4.28c)}\\
\mathcal{A}_{20} =& \frac{1}{3}\left(2F_{S,0} + F_{S,1}\right)s^2 - \left(F_{HD}^2\frac{v^2}{4} + F_{HD}\right)2\mathcal{S}_0(s, m_h), && \text{(4.28d)}\\
\mathcal{A}_{22} =& \frac{1}{60}\left(F_{S,0} + 2F_{S,1}\right)s^2 - \left(F_{HD}^2\frac{v^2}{4} + F_{HD}\right)2\mathcal{S}_2(s, m_h). && \text{(4.28e)}
\end{aligned}$$

Because the isospin-spin basis is diagonal, every isospin-spin amplitude has to satisfy the Argand circle condition as defined in (4.18)

$$\sqrt{\mathrm{Re}\left(a_{I\ell}\right)^2 + \mathrm{Im}\left(a_{I\ell} - \frac{\mathrm{i}}{2}\right)^2} \leq \frac{1}{2}. \tag{4.29}$$

If the couplings F_{HD}, $F_{S,0}$ and $F_{S,1}$ are real and the small Higgs width is neglected, the real bound for the isospin-spin amplitudes (4.20) should be used instead. Depending on the linear combination of the couplings F_{HD}, $F_{S,0}$ and $F_{S,1}$ different isospin-spin channels will give the strongest limit for the effective field theory description. Additionally, not all isospin-spin amplitudes affect every vector boson scattering amplitude as described in (4.27). Therefore, noncontributing isospin-spin amplitudes can be effectively neglected for the effective field theory limit determination.

In case of the $w^+w^+ \to w^+w^+$ amplitude the amplitude $\mathcal{A}_{20}$ gives the strongest bound, if only one effective coupling is nonzero at a time. The corresponding limits for the effective field theory coupling values plotted in Figure 3.2 ($F_{S,0}, F_{S,1} = 480\ \mathrm{TeV}^{-4}$, $F_{HD} = 30\ \mathrm{TeV}^{-2}$)

are given by

$$\sqrt{s} \leq \left(\frac{24\pi}{F_{S,0}}\right)^{\frac{1}{4}} \lesssim 630 \text{ GeV}\,, \tag{4.30a}$$

$$\sqrt{s} \leq \left(\frac{48\pi}{F_{S,1}}\right)^{\frac{1}{4}} \lesssim 750 \text{ GeV}\,, \tag{4.30b}$$

$$\sqrt{s} \leq \left(\frac{16\pi}{F_{HD}^2 \frac{v^2}{4} + F_{HD}}\right)^{\frac{1}{2}} \lesssim 1070 \text{ GeV}. \tag{4.30c}$$

However, the bounds in (4.30) are not valid for complex amplitudes. The absolute value of the amplitude can become maximal, when the amplitude is purely imaginary, $a_{I\ell} = \mathrm{i}$. Therefore, the absolute value can be used to get a real valued bound on the complex amplitudes

$$|a_{I\ell}| \leq 1. \tag{4.31}$$

This bound is looser for $w^+w^+ \to w^+w^+$ scattering than the one represented in (4.30), but can also be used for complex couplings

$$\sqrt{s} \leq \left(\frac{48\pi}{|F_{S,0}|}\right)^{\frac{1}{4}} \lesssim 750 \text{ GeV}, \tag{4.32a}$$

$$\sqrt{s} \leq \left(\frac{96\pi}{|F_{S,1}|}\right)^{\frac{1}{4}} \lesssim 890 \text{ GeV}, \tag{4.32b}$$

$$\sqrt{s} \leq \left(\frac{32\pi}{\left|F_{HD}^2 \frac{v^2}{4} + F_{HD}\right|}\right)^{\frac{1}{2}} \lesssim 1530 \text{ GeV}. \tag{4.32c}$$

4.4.1. Isospin-Spin Amplitudes in WHIZARD

The unitarity bound has to be extended to off-shell vector boson scattering to describe scattering processes like proton-proton collisions at the LHC completely. This is implemented in the Monte Carlo generator WHIZARD for weak boson and associated Higgs scattering processes. To calculate the cross section bounds from the Argand circle condition of a process, additional quartic coupling terms are added as form factor like effective vertices. Starting with the Goldstone bosons, a Lagragian is defined to model the isospin-spin amplitude from (4.24) with form factors $f(s,t,u)$

$$\mathcal{L}_{\text{effV}} = \partial_{\mu_1} w_1 \partial_{\mu_2} w_2 f^{\mu_1\mu_2}_{\mu_3\mu_4}(s,t,u) \partial^{\mu_3} w_3 \partial^{\mu_4} w_4. \tag{4.33}$$

Therefore, the contribution of the Lagrangian $\mathcal{L}_{\text{effV}}$ is proportional to a linear combination of the momenta of the four interacting Goldstone bosons. Only three different Lorentz invariant

combinations are possible, which can be described by the Mandelstam variables and in the massless limit

$$(k_1 \cdot k_2)\,(k_3 \cdot k_4) = \frac{s^2}{4}, \tag{4.34a}$$

$$(k_1 \cdot k_3)\,(k_2 \cdot k_4) = \frac{t^2}{4}, \tag{4.34b}$$

$$(k_1 \cdot k_4)\,(k_1 \cdot k_4) = \frac{u^2}{4}. \tag{4.34c}$$

The form factors can therefore be determined from isospin-spin amplitudes in (4.24) by substituting

$$\frac{s^2}{s^2} \to \frac{4}{s^2} g^{\mu_1\mu_2} g_{\mu_3\mu_4}, \tag{4.35a}$$

$$\frac{t^2}{s^2} \to \frac{4}{s^2} g^{\mu_1}_{\ \mu_3} g^{\mu_2}_{\ \mu_4}, \tag{4.35b}$$

$$\frac{u^2}{s^2} \to \frac{4}{s^2} g^{\mu_1}_{\ \mu_4} g^{\mu_2}_{\ \mu_3}. \tag{4.35c}$$

In contrary to (4.33) the amplitudes are usually determined in unitary gauge within `WHIZARD`. To calculate the impact to massive longitudinal vector bosons, the Goldstone boson contribution has to be related to the equivalent longitudinal gauge boson contribution. In other words, the term $\mathbf{D}_\mu\mathbf{H}$ has to include equivalent terms in the gaugeless limit and unitary gauge. Comparing the partial derivative acting on the Goldstone bosons with the associated term of the longitudinal vector boson within the covariant derivative in (2.34) leads to the relations

$$\partial_\mu w^\pm \to \frac{g\,v}{2} W^\pm_\mu, \tag{4.36a}$$

$$\partial_\mu z \to \frac{g\,v}{2c_w} Z_\mu. \tag{4.36b}$$

By combining the relation in (4.35) and (4.36), the Feynman rules of the effective vertices are formulated for the physical region of the s-channel

$$W^{\pm}_{\mu_1}W^{\pm}_{\mu_2} \to W^{\pm}_{\mu_3}W^{\pm}_{\mu_4}: \quad \frac{g^4v^4}{4}\Bigg[\left(\Delta\mathcal{A}_{20}(s) - 10\Delta\mathcal{A}_{22}(s)\right)\frac{g_{\mu_1\mu_2}g_{\mu_3\mu_4}}{s^2} + 15\Delta\mathcal{A}_{22}(s)\frac{g_{\mu_1\mu_3}g_{\mu_2\mu_4} + g_{\mu_1\mu_4}g_{\mu_2\mu_3}}{s^2}\Bigg], \tag{4.37a}$$

$$W^{\pm}_{\mu_1}W^{\mp}_{\mu_2} \to Z_{\mu_3}Z_{\mu_4}: \quad \frac{g^4v^4}{4c_w^2}\Bigg[\left(\frac{1}{3}\left(\Delta\mathcal{A}_{00}(s) - \Delta\mathcal{A}_{20}(s)\right) - \frac{10}{3}\left(\Delta\mathcal{A}_{02}(s) - \Delta\mathcal{A}_{22}(s)\right)\right)\frac{g_{\mu_1\mu_2}g_{\mu_3\mu_4}}{s^2} + 5\left(\Delta\mathcal{A}_{02}(s) - \Delta\mathcal{A}_{22}(s)\right)\frac{g_{\mu_1\mu_3}g_{\mu_2\mu_4} + g_{\mu_1\mu_4}g_{\mu_2\mu_3}}{s^2}\Bigg], \tag{4.37b}$$

$$W^{\pm}_{\mu_1}Z_{\mu_2} \to W^{\pm}_{\mu_3}Z_{\mu_4}: \quad \frac{g^4v^4}{4c_w^2}\Bigg[\left(\frac{1}{2}\Delta\mathcal{A}_{20}(s) - 5\Delta\mathcal{A}_{22}(s)\right)\frac{g_{\mu_1\mu_2}g_{\mu_3\mu_4}}{s^2} + \left(-\frac{3}{2}\Delta\mathcal{A}_{11}(s) + \frac{15}{2}\Delta\mathcal{A}_{22}(s)\right)\frac{g_{\mu_1\mu_3}g_{\mu_2\mu_4}}{s^2} + \left(\frac{3}{2}\Delta\mathcal{A}_{11}(s) + \frac{15}{2}\Delta\mathcal{A}_{22}(s)\right)\frac{g_{\mu_1\mu_4}g_{\mu_2\mu_3}}{s^2}\Bigg], \tag{4.37c}$$

$$W^{\pm}_{\mu_1}W^{\mp}_{\mu_2} \to W^{\pm}_{\mu_3}W^{\mp}_{\mu_4}: \quad \frac{g^4v^4}{4}\Bigg[\left(\frac{1}{6}\left(2\Delta\mathcal{A}_{00}(s) + \Delta\mathcal{A}_{20}(s)\right) - \frac{5}{3}\left(2\Delta\mathcal{A}_{02}(s) + \Delta\mathcal{A}_{22}(s)\right)\right)\frac{g_{\mu_1\mu_2}g_{\mu_3\mu_4}}{s^2} + \left(5\Delta\mathcal{A}_{02}(s) - \frac{3}{2}\Delta\mathcal{A}_{11}(s) + \frac{5}{2}\Delta\mathcal{A}_{22}(s)\right)\frac{g_{\mu_1\mu_3}g_{\mu_2\mu_4}}{s^2} + \left(5\Delta\mathcal{A}_{02}(s) + \frac{3}{2}\Delta\mathcal{A}_{11}(s) + \frac{5}{2}\Delta\mathcal{A}_{22}(s)\right)\frac{g_{\mu_1\mu_4}g_{\mu_2\mu_3}}{s^2}\Bigg], \tag{4.37d}$$

$$Z_{\mu_1}Z_{\mu_2} \to Z_{\mu_3}Z_{\mu_4}: \quad \frac{g^4v^4}{4c_w^4}\Bigg[\left(\frac{1}{3}\left(\Delta\mathcal{A}_{00}(s) + 2\Delta\mathcal{A}_{20}(s)\right) - \frac{10}{3}\left(\Delta\mathcal{A}_{02}(s) + 2\Delta\mathcal{A}_{22}(s)\right)\right)\frac{g_{\mu_1\mu_2}g_{\mu_3\mu_4}}{s^2} + 5\left(\Delta\mathcal{A}_{02}(s) + 2\Delta\mathcal{A}_{22}(s)\right)\frac{g_{\mu_1\mu_3}g_{\mu_2\mu_4} + g_{\mu_1\mu_4}g_{\mu_2\mu_3}}{s^2}\Bigg]. \tag{4.37e}$$

Scattering processes involving a Higgs boson have a different off-shell extrapolation. Therefore, the Higgs momentum is included in the Feynman rules for the analogous effective vertices

given by

$$W^{\pm\mu_1}W^{\mp\mu_2} \to hh : -g^2v^2 \quad \left[\left(\frac{1}{3}\left(\Delta\mathcal{A}_{00}(s) - \Delta\mathcal{A}_{20}(s)\right)\right.\right.$$
$$\left. -\frac{10}{3}\left(\Delta\mathcal{A}_{02}(s) - \Delta\mathcal{A}_{22}(s)\right)\right)\frac{g^{\mu_1\mu_2}\left(k_3\cdot k_4\right)}{s^2}$$
$$\left. +5\left(\Delta\mathcal{A}_{02}(s) - \Delta\mathcal{A}_{22}(s)\right)\frac{k_3^{\mu_3}k_4^{\mu_2} + k_4^{\mu_1}k_3^{\mu_2}}{s^2}\right], \tag{4.37f}$$

$$Z^{\mu_1}Z^{\mu_2} \to hh : -\frac{g^2v^2}{c_w^2} \quad \left[\left(\frac{1}{3}\left(\Delta\mathcal{A}_{00}(s) - \Delta\mathcal{A}_{20}(s)\right)\right.\right.$$
$$\left. -\frac{10}{3}\left(\Delta\mathcal{A}_{02}(s) - \Delta\mathcal{A}_{22}(s)\right)\right)\frac{g^{\mu_1\mu_2}\left(k_3\cdot k_4\right)}{s^2}$$
$$\left. +5\left(\Delta\mathcal{A}_{02}(s) - \Delta\mathcal{A}_{22}(s)\right)\frac{k_3^{\mu_3}k_4^{\mu_2} + k_4^{\mu_1}k_3^{\mu_2}}{s^2}\right], \tag{4.37g}$$

$$W^{\pm\mu_1}h \to W^{\pm\mu_3}h : -g^2v^2 \quad \left[\left(\frac{1}{2}\Delta\mathcal{A}_{20}(s) - 5\Delta\mathcal{A}_{22}(s)\right)\frac{k_2^{\mu_1}k_4^{\mu_3}}{s^2}\right.$$
$$+\left(-\frac{3}{2}\Delta\mathcal{A}_{11}(s) + \frac{15}{2}\Delta\mathcal{A}_{22}(s)\right)\frac{g^{\mu_1\mu_3}\left(k_2\cdot k_4\right)}{s^2}$$
$$\left. +\left(\frac{3}{2}\Delta\mathcal{A}_{11}(s) + \frac{15}{2}\Delta\mathcal{A}_{22}(s)\right)\frac{k_4^{\mu_1}k_2^{\mu_3}}{s^2}\right], \tag{4.37h}$$

$$Z^{\mu_1}h \to Z^{\mu_3}h : -\frac{g^2v^2}{c_w^2} \quad \left[\left(\frac{1}{2}\Delta\mathcal{A}_{20}(s) - 5\Delta\mathcal{A}_{22}(s)\right)\frac{k_2^{\mu_1}k_4^{\mu_3}}{s^2}\right.$$
$$+\left(-\frac{3}{2}\Delta\mathcal{A}_{11}(s) + \frac{15}{2}\Delta\mathcal{A}_{22}(s)\right)\frac{g^{\mu_1\mu_3}\left(k_2\cdot k_4\right)}{s^2}$$
$$\left. +\left(\frac{3}{2}\Delta\mathcal{A}_{11}(s) + \frac{15}{2}\Delta\mathcal{A}_{22}(s)\right)\frac{k_4^{\mu_1}k_2^{\mu_3}}{s^2}\right], \tag{4.37i}$$

$$hh \to hh : \quad 4\left[\left(\frac{1}{3}\left(\Delta\mathcal{A}_{00}(s) + 2\Delta\mathcal{A}_{20}(s)\right)\right.\right.$$
$$\left. -\frac{10}{3}\left(\Delta\mathcal{A}_{02}(s) + 2\Delta\mathcal{A}_{22}(s)\right)\right)\frac{\left(k_1\cdot k_2\right)\left(k_3\cdot k_4\right)}{s^2} \tag{4.37j}$$
$$\left. +5\left(\Delta\mathcal{A}_{02}(s) + 2\Delta\mathcal{A}_{22}(s)\right)\frac{\left(k_1\cdot k_4\right)\left(k_2\cdot k_3\right) + \left(k_1\cdot k_4\right)\left(k_2\cdot k_3\right)}{s^2}\right].$$

The maximal absolute value each isospin-spin value can have is achieved, when it becomes purely imaginary (see Figure 4.2)

$$a_{I\ell} = \mathrm{i}. \tag{4.38}$$

To transfer this bound onto the cross section, the corresponding counter terms have to be included in (4.37) and are defined as

$$\Delta\mathcal{A}_{I\ell} = 32\pi\mathrm{i} - \mathcal{A}_{I\ell}. \tag{4.39}$$

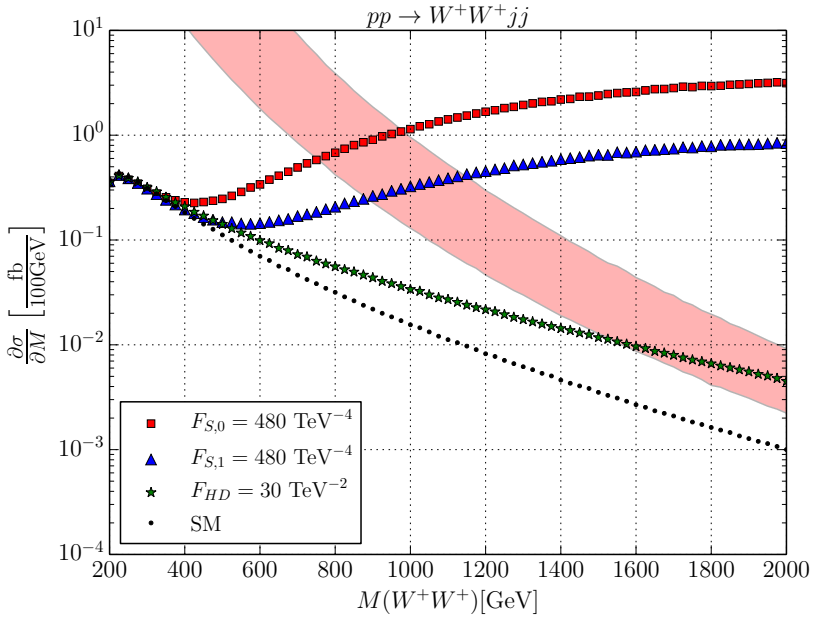

Figure 4.3.: $pp \to W^+W^+jj$, naive EFT results that violate unitarity, QCD contributions neglected. The band describes maximal allowed values, due to unitarity constraints, for the differential cross section. The lower bound describes the saturation of $\mathcal{A}_{20}$ and the upper bound describes the simultaneous saturation of $\mathcal{A}_{20}$ and $\mathcal{A}_{22}$, cf. (4.37).
Cuts: $M_{jj} > 500$ GeV; $\Delta y_{jj} > 2.4$; $p_T^j > 20$ GeV; $|\eta_j| > 4.5$.

The `WHIZARD` implementation of these effective vertices has been included within the file `./omega/src/target_Kmatrix_2.ml` belonging to the matrix generator `O'MEGA`[11]. Additionally, a new model `SM_ul` has been added to `WHIZARD`, where the impact of the bounds of weak isospin-spin amplitudes to arbitrary cross sections will be individually determined.

The $W^+W^+ \to W^+W^+$ amplitude is a function of two independent isospin-spin channels as shown in (4.24). To determine when the cross section of a process involving vector boson scattering will violate unitarity, all combinations of isospin-spin amplitudes bounds have to be taken into account. For the proton-proton collision, which includes the $W^+W^+ \to W^+W^+$ process, bounds on a combination of $\mathcal{A}_{20}$ and $\mathcal{A}_{22}$ have to be checked. As displayed in Figure 4.3, it leads to a band where the Argand circle condition is fulfilled. The lower limit arise from the $\mathcal{A}_{20}$ amplitude only, whereas the higher limit originates from the bound of simultaneous saturating $\mathcal{A}_{20}$ and $\mathcal{A}_{22}$. Every cross section above the band will not satisfy the unitarity condition and is unphysical. When a cross section is within the bound, single isospin spin eigenamplitudes could already break unitarity, but do not necessary have to.

The invariant cross section of the effective operators in Figure 4.3 will violate the $\mathcal{A}_{20}$ bound at invariant mass energies of the WW-system as calculated in (4.32). The differential cross section of the dimension six operator stays inside the region, which satisfies unitarity. At the point, where the dimension six operator could violate unitarity, the simulated numbers

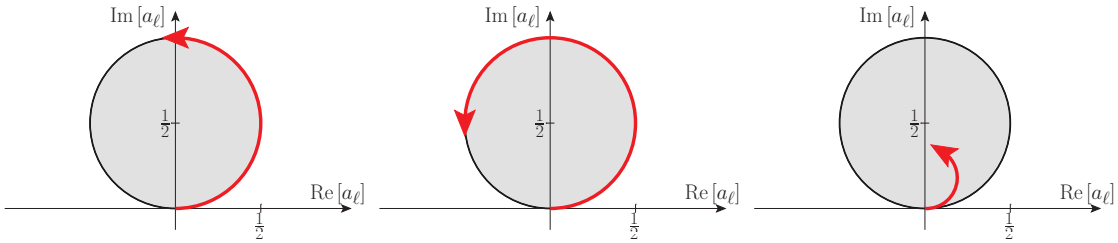

(a) Saturation (b) Resonance (c) Inelastic channels

Figure 4.4.: Possible situations for scattering amplitudes respecting the Argand circle.

of events are already too low to be significant in this analysis. This behavior of dimension six operators was already discovered in [35, 84]. Because the dimension six operators can be investigated via production and decay process, the effective field theory is mostly used in a limited energy range.

In contrast, the dimension eight operators can only be studied using scattering processes. They will always violate unitarity above a certain energy. Except for the rare decay $ZZ \rightarrow 4l$ the invariant mass of a general vector boson scattering process cannot be experimentally reconstructed completely. An energy cut cannot be applied on the data, which would remove those unphysical events on the generated sample. Therefore, a naive effective field theory approach cannot be used to study anomalous quartic gauge couplings at high energy colliders.

4.5. Unitarization

The diagonal isospin-spin amplitudes have to stay on the Argand circle as long as no additional inelastic channels appear. However, the raw amplitudes of the dimension eight operators will leave the Argand circle at a certain energy. This is obviously the wrong description of possible new physics effects. The possible behavior of an elastic scattering amplitude can be put in five categories [66]:

1. The Standard Model case: The amplitude is close to zero, and the imaginary part is small compared to the real part. Therefore, the amplitude is in a perturbative regime.
2. Strongly interacting regime: The amplitude rises and receives a bigger imaginary part.
3. Saturation: The amplitude asymptotically approaches its maximum absolute value (fig. 4.4a).
4. The resonant case: The amplitude flips over after saturation (fig. 4.4b).
5. Inelastic case: New inelastic channels open up (fig. 4.4c). The extra channels can be modeled by an effective form-factor suppression. In case of vector boson scattering these extra channels can be related to observable multi vector boson production [85, 86].

The physical amplitude has to follow one of these five possibilities. There are different unitarization prescriptions available to extrapolate the effective field theory beyond its valid energy regime. They are mostly inspired from the requirement of a full analytic S-matrix.

The Padé-formalism was introduced in [87–89] to reorder a non convergent perturbative series and was used to study the vector-boson scattering process in the no-Higgs or heavy-Higgs limit [90–94]. This unitarization model gives rise to additional resonances at higher energy, which were not included in the effective field theory. Additional resonance generating unitarization prescriptions are the inverse-amplitude [95–99] and the N/D unitarization scheme [96, 100]. These schemes are mainly used in pion-pion scattering, where the amplitude contains those resonances in the correct UV completion.

The suppression of unitarity violating amplitudes with an energy dependent form factor is studied in [101–104]. The form factors are dependent on additional parameters, which are associated with mixing of new resonances or additional open channels. Therefore, a certain knowledge of physical contributions is necessary, because it is not a prediction that can be derived from unitarity [35].

These introduced schemes demand a UV completion of the effective theory, in contrary to the unitarization scheme, which is presented in the next section. It will saturate the amplitude without needing additional parameters to give a possible upper limit of the effective field theory contribution.

4.5.1. K-Matrix Unitarization

Heitler [105] and Schwinger [106] defined the unitary scattering operator S in terms of a self-adjoint K operator to have a closer relation to the interaction hamiltonian operator

$$S = \frac{\mathbb{1} + \mathrm{i}K/2}{\mathbb{1} - \mathrm{i}K/2}\,. \tag{4.40}$$

The K operator is thus the Cayley transform of the S-operator, where a factor $1/2$ is added for later convenience. The corresponding interaction operator T can be evaluated with relation (4.2) to be

$$T = \frac{K}{\mathbb{1} - \mathrm{i}K/2}\,. \tag{4.41}$$

This T automatically satisfies the optical theorem (4.4), because the unitarity of S is respected by the Cayley transformation (4.40). The K-operator in terms of T is obtained by inverting equation (4.41),

$$K = 2\mathrm{i}\frac{1 - S}{1 + S} = \frac{T}{1 + \mathrm{i}T/2}\,. \tag{4.42}$$

If the theory is perturbatively calculable, the K-matrix can be determined pertubartively as long as $T - 2\mathrm{i}$ is non-singular. It is apparent from (4.42), that K and T are identical to lowest order.

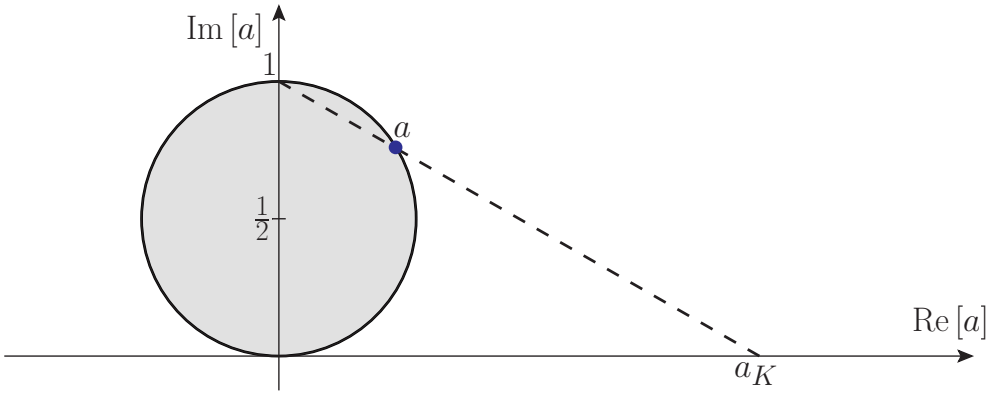

Figure 4.5.: Stereographic projection of unitary scattering amplitude on the Argand circle to the real axis (K-matrix eigenvalue)

The optical theorem for partial waves in (4.17) can be generalized for diagonalizable interaction operators with eigenvalues $t = 2a$. In this case, every a lies on the Argand circle, which is displayed in Figure 4.4,

$$|a - \mathrm{i}/2| = 1/2\,. \tag{4.43}$$

The corresponding eigenvalue a_k of the Cayley-transform K-matrix can be related to a as an stereographic projection from the Argand circle onto the real axis

$$a_K = \frac{a}{1 + \mathrm{i}a}\,. \tag{4.44}$$

The K-matrix can therefore be understood as the stereographic projection of the transition matrix T onto the space of Hermitian matrices.

Instead of starting with a unitary scattering matrix and then calculating the Hermitian operator K, the construction as introduced above was reversed by Gupta and collaborators, and in subsequent studies [107–111]. In doing so, the Hermitian K-matrix is interpreted as an incompletely calculated approximation to the true scattering matrix S. The T-matrix is then determined as a non-perturbative completion of this approximation.

To translate this formalism to the amplitude level the starting point is a diagonalized K-matrix with its real eigenamplitude a_K. The corresponding unitarized amplitudes a that enters the T-matrix are determined by inverting equation (4.44)

$$a = \frac{a_K}{1 - \mathrm{i}a_K}. \tag{4.45}$$

This transformation can be pictured as the inverse stereographic projection in Figure 4.5.

For a non-diagonal, but Hermitian K-matrix the inverse stereographic projection of the unitarized transition matrix K is defined by formula (4.41). The standard K-matrix unitarization

formalism acts only on the perturbative series of the T-matrix. If the n-th order approximation $T_0^{(n)}$ of the T-matrix is represented by the eigenamplitude $a_0^{(n)}$, the corresponding real K-matrix amplitude $a_K^{(n)}$ can be constructed by (4.44)

$$\begin{aligned} a_K^{(n)} &= \frac{a_0^{(n)}}{1 + \mathrm{i}a_0^{(n)}} = a_0^{(1)} + \mathrm{Re}\, a_0^{(2)} + \mathrm{i}(\mathrm{Im}\, a_0^{(2)} - (a_0^{(1)})^2) + \dots \\ &= a_0^{(1)} + \mathrm{Re}\, a_0^{(2)} + \dots \end{aligned} \tag{4.46}$$

where $a_0^{(1)}$ is assumed to be real and at lowest order the optical theorem is satisfied by $\mathrm{Im}\, a_0^{(2)} = (a_0^{(1)})^2$. If the original perturbation series is correct, the imaginary parts will cancel at each order. Inserting the truncated perturbation series for $a_K^{(n)}$ into equation (4.45) gives the unitarized amplitude

$$a^{(n)} = \frac{a_0^{(1)} + \mathrm{Re}\, a_0^{(2)} + \dots}{1 - \mathrm{i}(a_0^{(1)} + \mathrm{Re}\, a_0^{(2)} + \dots)}\,. \tag{4.47}$$

This prescription amounts to a partial resummation of the perturbation series for perturbatively calculable, exact scattering matrix. Furthermore, the construction guarantees that the computed S matrix is unitary, and the perturbation theory is reproduced order by order.

Physical singularities, such as Coulomb singularities should not be handled by an ad-hoc unitarization scheme. Instead, the charged particle singularities in the scattering matrix need a proper definition of the asymptotic states of charged particles [112–115]. Therefore, the Coulomb singularities have to be subtracted before applying the chosen unitarization prescription to the S-matrix, and then the Coulomb singularities are added together with appropriate corrections for the asymptotic states.

To summarize the unitarization routine for a given non-unitary perturbative approximation of the transition matrix T: The corresponding truncated perturbative expansion of the Hermitian K matrix is constructed by (4.42) and inserted back into the unitarization formula (4.41), to obtain the corresponding unitarized T matrix. Regardless to which order the K-matrix in (4.42) is calculated, by inserting an nth order approximation of the S-matrix will result in a unitary S-matrix to all orders. Contrary, expanding the unitarized S-matrix to nth order will reproduce the original nth order expression, which is unitary up to terms of order $n + 1$.

Example

As a concrete example a non-unitary $2 \to 2$ scattering process with a scalar particle exchange within the s-channel is chosen. The scalar pole is represented by a $J = 0$ partial-wave eigenamplitude

$$a_K^{(0)}(s) = \frac{\lambda}{s - m^2}. \tag{4.48}$$

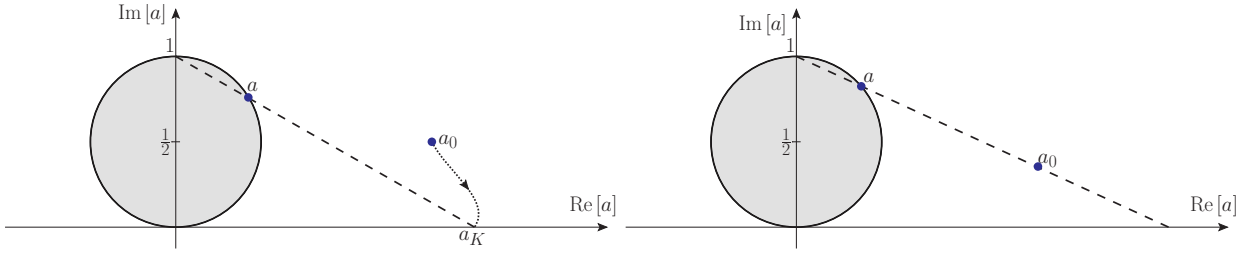

(a) K-matrix projection: (Pertubartive) construction of a real a_k in the first step.

(b) Linear Projection: Direct determination of the unitarized a.

Figure 4.6.: Geometrical representation of the K-matrix procedure and the linear projection starting with a complex amplitude a_0.

Using the K-matrix transformation the amplitude becomes

$$a^{(0)}(s) = \frac{\lambda}{s - m^2 - \mathrm{i}\lambda}, \tag{4.49}$$

the Breit-Wigner form of a scalar resonance. Thus, the K-matrix transformation implements the Dyson resummation of the resonant propagator.

4.5.2. Direct T-Matrix Unitarization I: Linear Projection

The K-matrix procedure as introduced above will lead to an exact reconstruction of the unitary S-matrix in perturbation theory, but it has the drawback, that the self-adjoint K-matrix has to be reconstructed as an intermediate step as shown in Figure 4.6a. This unnecessary detour can become significantly complicated, if the scattering matrix cannot be diagonalized or if non-perturbative effects need to be considered. Therefore, it would be more practical to skip this intermediate step and unitarize the T-matrix directly. Then this framework can be used for arbitrary models of the scattering matrix, which may or may not admit a perturbative expansion.

Starting on the amplitude level, a generalization of the K-matrix prescription is presented that operates on the T-matrix directly. The unitarized amplitude a is constructed directly from the complex approximation to an eigenvalue of the true T-matrix by the same geometric procedure as before. As pictured in Figure 4.6b, the point a_0 is connected with the point i by a straight line and the resulting intersection with the Argand circle becomes the unitarized amplitude a

$$a = \frac{\mathrm{Re}\, a_0}{1 - \mathrm{i}a_0^*}\,. \tag{4.50}$$

There is no need to construct the real amplitude a_K. The formula in (4.50) fulfills the properties that

1. a lies on the Argand circle,

2. real amplitudes a_0 reproduce (4.45),

3. amplitudes a_0, which already satisfies the Argand-circle condition stay invariant.

This guarantees the invariance of the correct perturbative series, up to higher orders. Nevertheless, the actual expression in (4.50) differs from the standard K-matrix formula in (4.47), when evaluated in perturbation theory,

$$a^{(n)} = \frac{a_0^{(1)} + \operatorname{Re} a_0^{(2)} + \dots}{1 - \mathrm{i}(a_0^{(1)} + \operatorname{Re} a_0^{(2)} - \mathrm{i} \operatorname{Im} a_0^{(2)} + \dots)} \,. \tag{4.51}$$

Due to the truncation of the necessary intermediate perturbative expansion of the scattering matrix in the K-matrix formulation, higher orders are treated differently in these two approaches. The direct unitarization formula in (4.50) does not rely on a perturbative expansion. It is thus applicable to a more general set of models. In the case of vector-boson scattering with a light Higgs, the leading term $a_0^{(1)}$ is suppressed, which leads to an ill-behaved K-matrix construction, whereas the modified version in (4.50) does not encounter this problem.

However, other difficulties can arise in the formula in (4.50): If the imaginary part of a_0 becomes larger than i, the selected intersection point a appears beyond the fixed point $a = \mathrm{i}$, on the complex half-plane opposite to the location of a_0. As a consequence the model amplitude with a resonance of the form

$$a_0(s) = \frac{\lambda'}{s - m^2 - i\lambda} \tag{4.52}$$

with $\lambda' > \lambda$, would be transformed into an unitarized version that revolves twice around the Argand circle. Therefore it will split the resonance at m^2 into two separate peaks. Although, this ansatz to describe a resonance is rather pathological, such a behavior is undesirable. This problem can be avoided by fixing the unitarized amplitude a for $\operatorname{Im} a_0 \geq 1$

$$a = \begin{cases} \dfrac{\operatorname{Re} a_0}{1 - \mathrm{i} a_0^*} & \text{if } \operatorname{Im} a_0 < 1, \\ \mathrm{i} & \text{otherwise}\,. \end{cases} \tag{4.53}$$

The transformation in (4.53) is generalized to a unitarization prescription for an scattering matrix T_0, which needs not satisfy the optical theorem. Choosing the scattering operator to be normal, $T_0^\dagger T_0 = T_0 T_0^\dagger$, and not having eigenvalues with an imaginary part larger than one, the unitarization transformation is given by

$$T = \frac{\operatorname{Re} T_0}{\mathbb{1} - \frac{\mathrm{i}}{2} T_0^\dagger}. \tag{4.54}$$

If the scattering matrix T_0 is non-normal, the operator ordering in the fraction must be

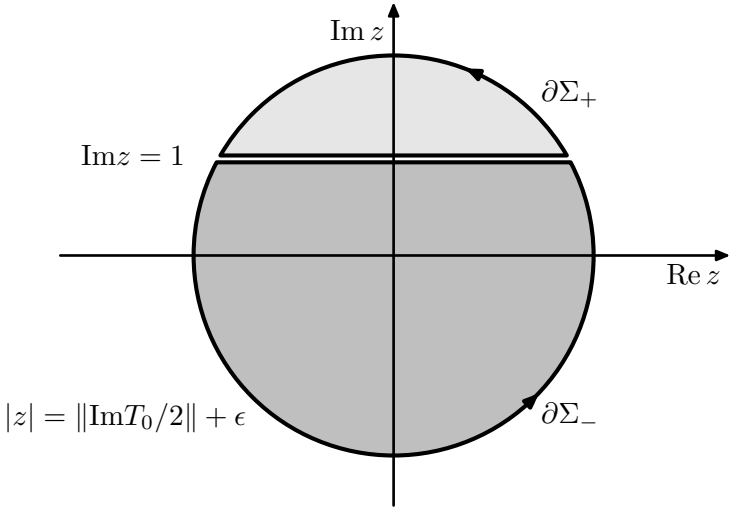

Figure 4.7.: Integration contours used for projecting on the subspaces corresponding to $\mathrm{Im}\, T_0/2 < 1$ and $\mathrm{Im}\, T_0/2 > 1$ for a bounded operator $\mathrm{Im}\, T_0/2$ in (4.55).

defined, which leads to the following two equivalent formulations

$$\begin{aligned} T &= \frac{1}{\sqrt{\mathbb{1} - \frac{1}{2}\,\mathrm{Im}\, T_0}}\,\mathrm{Re}\, T_0 \frac{1}{\mathbb{1} - \frac{\mathrm{i}}{2} T_0^\dagger} \sqrt{\mathbb{1} - \frac{1}{2}\,\mathrm{Im}\, T_0}, \\ &= \sqrt{\mathbb{1} - \frac{1}{2}\,\mathrm{Im}\, T_0} \frac{1}{\mathbb{1} - \frac{\mathrm{i}}{2} T_0^\dagger}\,\mathrm{Re}\, T_0 \frac{1}{\sqrt{\mathbb{1} - \frac{1}{2}\,\mathrm{Im}\, T_0}}\,. \end{aligned} \tag{4.55}$$

For any matrix T_0 with imaginary part of its eigenvalue satisfying $\mathrm{Im}\,(a_0) \leq 1$, the matrix T from (4.55) is related to a unitary S-matrix. If T_0 already respects the optical theorem, it will stay invariant under the transformation in (4.55). That means also, that the reconstructed matrix T reproduces the perturbative expansion of T_0, if it represents already the correct pertubartive series of T.

If perturbation expansion is not applicable to T, the matrix has either to be diagonalized, and the transformation in (4.53) has to be executed afterwards in order to extract eigenvalues with imaginary part greater than one, or a projection can be used for a well defined transformation of (4.55). For this purpose, functions of matrices can be defined by their power series expansion. More generally, a function $f : D \subseteq \mathbf{C} \to \mathbf{C}$ can be associated with another function $\hat{f}$ which maps matrices to matrices with a functional calculus

$$\widehat{\alpha f + \beta g} = \alpha \hat{f} + \beta \hat{g}\,, \tag{4.56a}$$

$$\widehat{fg} = \hat{f}\,\hat{g}\,, \tag{4.56b}$$

$$\widehat{f \circ g} = \hat{f} \circ \hat{g}\,. \tag{4.56c}$$

The Riesz-Dunford functional calculus, which is introduced in [116–119], defines $\hat{f}(A)$ by a

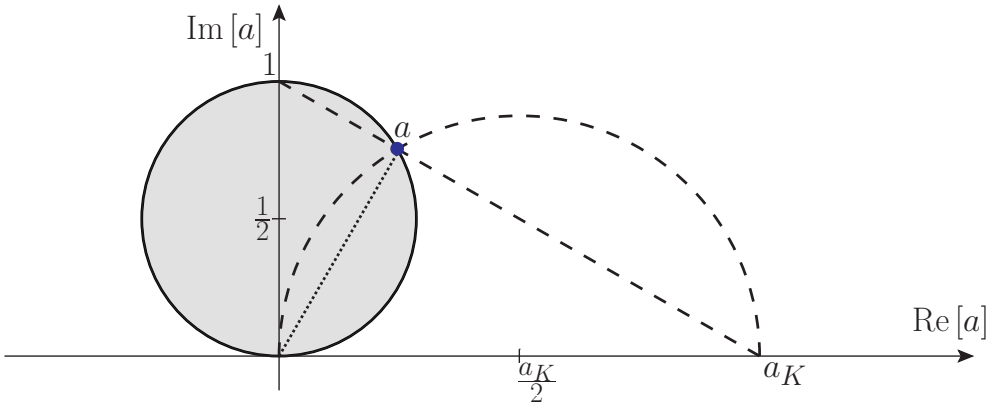

Figure 4.8.: Geometrical representation of Thales projection.

contour integral encircling the spectrum $\sigma(A)$

$$\hat{f}(A) = \int_{\partial\Sigma:\sigma(A)\subseteq\Sigma} \frac{\mathrm{d}z}{2\pi\mathrm{i}} \frac{f(z)}{z\mathbb{1} - A} \tag{4.57}$$

using the fact that the resolvent matrix $1/(z\mathbb{1} - A)$ is well defined whenever $z \notin \sigma(A)$. This functional calculus can therefore be used unchanged for all bounded operators on a Hilbert space. An extension to certain classes of unbounded operaters is possible, but not needed in the present work, because the scattering amplitudes with definite angular momentum are related to finite dimensional matrices. The functional calculus introduced in (4.57) is closely associated to the projections on the invariant subspace of A corresponding to a part $\Sigma \subseteq \sigma(A)$ of the spectrum

$$P_{A,\Sigma} = \int_{\partial\Sigma} \frac{\mathrm{d}z}{2\pi\mathrm{i}} \frac{1}{z\mathbb{1} - A}\,. \tag{4.58}$$

In particular,using the contours $\Sigma_\pm$ as described in Figure 4.7 to generalize the prescription (4.53) for $\mathrm{Im}\, T > 2$ projections $P_{\mathrm{Im}\, T_0/2,\Sigma_\pm}$ can be defined by

$$\mathbb{1} = P_{\mathrm{Im}\, T_0/2,\Sigma_+} + P_{\mathrm{Im}\, T_0/2,\Sigma_-}\,. \tag{4.59}$$

4.5.3. Direct T Matrix Unitarization II: Thales Projection

Thales' Theorem in elementary geometry suggests an alternative construction to the inverse stereographic projection from the real axis to the unitarity circle. Investigating Figure 4.8 reveals that the K matrix amplitude a_k coincides with the endpoint of a half-circle that connects the lower fixed point 0 with the unitary amplitude a. Consequently, for a given, arbitrary real amplitude $a_0 = a_k$, the Thales projection to a unitarized amplitude a is defined as the intersection point of the Argand circle and the half-circle that connects 0 and a_K. The Thales circle is characterized by its intersection a_K with the real axis and has its center on the positive real axis. Its points obeys

$$\left|a - \frac{a_K}{2}\right| = \frac{a_K}{2}. \tag{4.60}$$

Therefore, the projection of a real amplitude a_0 on the Argand circle coincides with the K-matrix description

$$a = \frac{a_K}{1 - \mathrm{i} a_K}. \tag{4.61}$$

When starting with a complex amplitude a_0, the corresponding a_k is determined from the condition, that both amplitudes have to be on the same Thales circle defined in (4.60)

$$\frac{1}{a_K} = \frac{\mathrm{Re}\,(a_0)}{|a_0|^2} = \mathrm{Re}\left(\frac{1}{a_0}\right). \tag{4.62}$$

There is no perurbative expansion necessary in this step. Furthermore, the intermediate calculation of the real amplitude a_K can be skipped by inserting (4.62) directly in (4.61), which leads to a unitarization formula for an arbitrary complex amplitude

$$a = \frac{1}{\mathrm{Re}\left(\frac{1}{a_0}\right) - \mathrm{i}}. \tag{4.63}$$

The corresponding prescription for the complete interaction matrix T, regardless of its perturbative expansion, is formulated analogously to one for the amplitudes in (4.63)

$$T(T_0) = \frac{1}{\mathrm{Re}\left(T_0{}^{-1}\right) - \frac{\mathrm{i}}{2}\mathbb{1}}. \tag{4.64}$$

In this case, an ordering prescription of the fraction is obviously not needed for the Thales projection. In Appendix A.4, it is proven in detail that the transformation in (4.64) leads to a unitary S matrix. Furthermore, it is shown that interaction matrices, which already satisfy the optical theorem stay invariant under the transformation (4.64).

This construction avoids the undesirable behaviors for a non-unitary amplitude above the Argand circle; the unitarized version of a single resonance is again a single resonance. However, this transformation encounters other drawbacks as it is not analytic in the vicinity of $a_0 = 0$. This disadvantage can be ignored, because the unitarization is only necessary for amplitudes, which violate the unitarity of the S-matrix and therefore clearly have $a_0 \neq 0$.

4.6. Physical Process

The Thales projection is chosen as the unitarization procedure to be implemented for weak boson scattering processes in the Monte-Carlo event generator `WHIZARD`[11, 12, 15] to numerically compute unitarized cross sections and generate corresponding event samples at colliders. The unitarization prescription is projected on the isospin-spin eigenamplitudes, because they provide a diagonal eigenbasis of the weak vector boson scattering process. Analogously to the implementation of the isospin-spin bounds in Section 4.4.1, the unitarization for full processes is implemented by including Feynman rules for the s-channel that correspond to

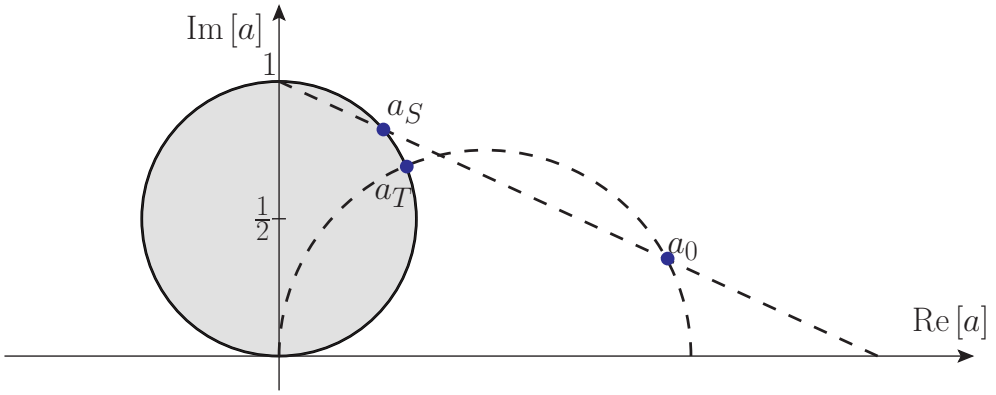

Figure 4.9.: Geometrical representation: stereographic projection vs Thales projection.

the energy-dependent counterterm operators[2]. The counterterms are calculated as shown in (4.37) from the unitarized isospin amplitudes

$$\Delta\mathcal{A}_{I\ell} = \hat{\mathcal{A}}_{I\ell} - \mathcal{A}_{I\ell}, \tag{4.65}$$

where $\hat{\mathcal{A}}_{I\ell}$ is the T-matrix transformed amplitude and fulfills the unitary condition. Up to the perturbative order that the scattering process is implemented, there is no difference between the T-matrix and K-matrix unitarization prescriptions. A difference would show up for higher-order or model-specific amplitudes that initially contain an imaginary part.

4.6.1. Numerical Results: On-Shell

The unitarized differential cross section of the vector boson scattering process within a proton-proton collision, $pp \to VVjj$ with jets j and weak vector bosons V, for the parameters $F_{HD}, F_{S,0}, F_{S,1}$ is calculated for the LHC configuration with $\sqrt{s} = 14$ TeV. Standard cuts for the dijet invariant mass $M_{jj} > 500$ GeV, the jet pseudorapidity distance $\Delta y_{jj} > 2.4$, a minimal jet transverse momentum of $p_T > 20$ GeV and a minimal (and opposite) jet rapidity of $|\eta_j| < 4.5$ are applied. The results are shown in Figure 4.10 for the distinct final states W^+W^+, W^+W^-, W^+Z, and ZZ taken to be on-shell. Comparing to the distributions in Figure 3.2, the plots clearly indicate that the naively calculated numbers with anomalous couplings and no unitarization (fig. 3.2) overshoot the more realistic T-matrix results (fig. 4.10a). The non-unitarized results rise with the invariant mass of the vector boson scattering system, whereas the unitarized results in Figure 4.10a have a kink at the calculated boundary energies for $\mathcal{A}_{20}$ (see eq. (4.32)). This kink originates from the T-matrix saturation prescription of the $\mathcal{A}_{20}$ amplitude. Furthermore, the effect of the dimension-eight operators (blue/red) is more pronounced for the chosen parameters than the effect of the anomalous Higgs coupling due to the dimension-six operator (green). In all channels, the

[2]Note, that it is not possible to use an automated tool for Feynman rules to include these rules here (like e.g. via the FeynRules interface for `WHIZARD` [120]), as one also needs a prescription to single out the s-channels.

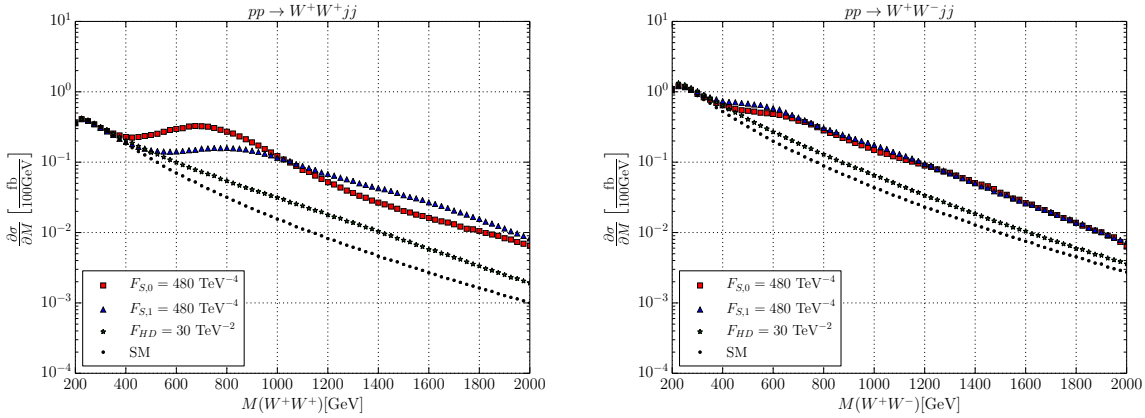

(a) $pp \to W^+W^+jj$ (b) $pp \to W^+W^-jj$

(c) $pp \to W^+Zjj$ (d) $pp \to ZZjj$

Figure 4.10.: $pp \to VVjj$, unitarized differential cross sections,
(QCD contributions neglected).
Cuts: $M_{jj} > 500$ GeV; $\Delta y_{jj} > 2.4$; $p_T^j > 20$ GeV; $|\eta_j| < 4.5$.

unitarized graphs have the same high energy behavior as the differential cross section of the Standard Model. They fall off with energy at the same rate, but are bigger by approximately one order of magnitude. A pure effective field theory description can be only meaningful, if it lies between the Standard Model curve and the saturated limit.

4.6.2. Numerical Results: Full Processes

For a full process simulation including W^+W^+-scattering at the LHC, the vector bosons will decay and the final state consists of six fermions, namely two forward jets and the decay products of the vector bosons

$$pp \to e^+\mu^+\nu_e\nu_\mu jj. \tag{4.66}$$

This process includes the vector boson scattering process and the complete irreducible background. The events have been generated with the WHIZARD event generator [15] in version 2.2 on the basis of the complete tree-level amplitude that connects the initial and final state. In Figure 4.11 the distribution of different observables for an unweighted partonic event sample that corresponds to 1 ab^{-1} at the nominal LHC energy of 14 TeV. Standard vector boson fusion cuts (listed in the caption of Figure 4.11) are used to suppress some background processes.

The observables shown in Figure 4.11 are the scalar sum of transverse momentum and the azimuthal distance of the charged lepton pair. It is manifest, that both observables are sensitive to the chosen values of the anomalous couplings. There is a significant difference between the Standard Model prediction (blue) and the prediction with nonzero operator coefficient and unitarization (red).The unphysical results that would be generated without unitarization (yellow/light) are also displayed for reference. If these non-unitarized samples were used to determine the experimental bounds for the dimension six and eight operators, they would be stronger constrained. More importantly, the results would be incorrect, and therefore possible new physic contributions would be falsely excluded. The T-matrix prescription ensures, that the computed results do not overshoot the limits. It does not have any further physical interpretation, but gives an upper limit, up to which an effective theory approach would be applicable.

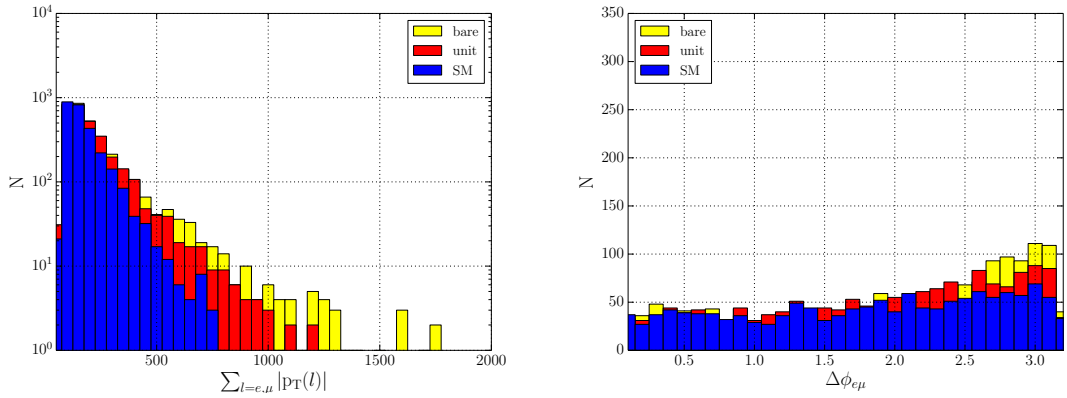

(a) $F_{HD} = 30\ \text{TeV}^{-2}$

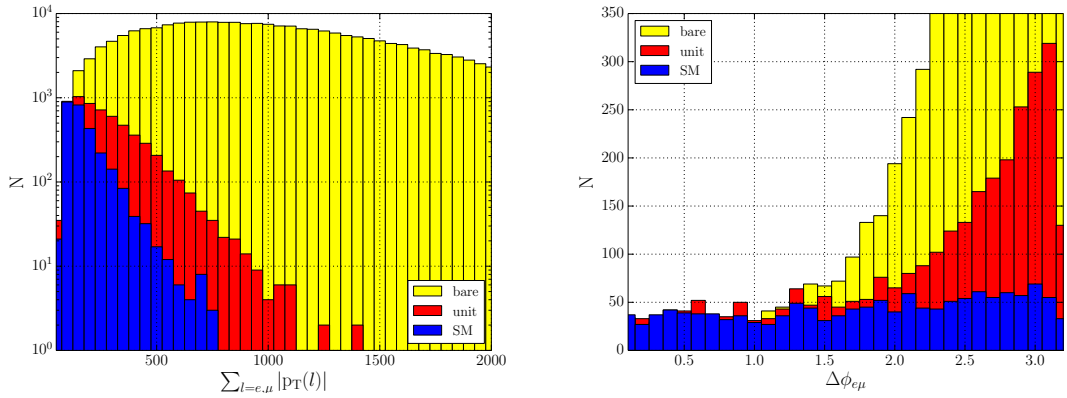

(b) $F_{S,0} = 480\ \text{TeV}^{-4}$

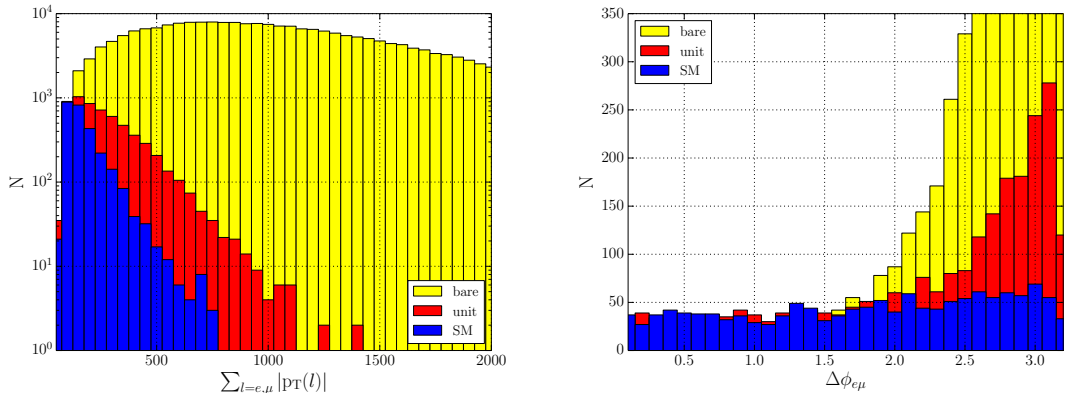

(c) $F_{S,1} = 480\ \text{TeV}^{-4}$

Figure 4.11.: $pp \to e^+\mu^+\nu_e\nu_\mu jj$, $\sqrt{s} = 14\,\text{TeV}, \text{L} = 1000\,\text{fb}^{-1}$
Cuts: $M_{jj} > 500$ GeV; $\Delta y_{jj} > 2.4$; $p_T^j > 20\,\text{GeV}$; $|\eta_j| < 4.5$; $p_T^\ell > 20\,\text{GeV}$

Chapter 5

Resonances

The saturization of an amplitude by the T-matrix description can be interpreted as a resonance at infinity. However, the high energy behavior of the amplitude differs from a resonance with finite mass. In the Argand circle picture of an elastic amplitude shown in Figure 5.1, the resonance amplitude will circle around the Argand circle. It will reach the highest absolute value at an energy equal to the mass of the corresponding new physics resonance. If the energy is not sufficient to access this point, only the rise of the amplitude is experimental measurable. In this case, the resonance description coincides with the description of the dimension eight operators like $\mathcal{L}_{S,0}$ and $\mathcal{L}_{S,1}$. Therefore, the origin of such dimension eight operators could be the Taylor expansion of a heavy resonance. As an example, a Higgs like scalar resonance can be expanded in terms of its heavy mass

$$\frac{s^2}{s-M^2} \to \frac{s^2}{M^2} + \mathcal{O}\left(\frac{1}{M^4}\right). \tag{5.1}$$

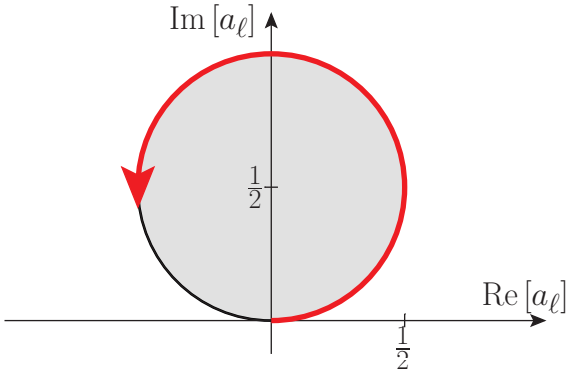

Figure 5.1.: A resonance circles around the Argand-circle.

At low energies compared to the particle mass, it is reasonable to use the effective field theory approach to describe an unknown new physics contribution. However, if the particle mass lies within the experimental reach of energy the typical bump of the resonance will not be described by the effective field theory approach. As described in Chapters 3 and 4, the effective field theory operators will break unitarity at high energies, because the Taylor expansion like in (5.1) will break down. The generic T-matrix unitarization scheme is then needed to reformulate the theoretical prediction, that is consistent at all energies. Beyond the resonance, the correct high energy behavior of an additional scalar resonance would be similar to a dimension six operator

$$\frac{s^2}{s - M^2} \to s + M^2 + \mathcal{O}\left(\frac{1}{s}\right) . \tag{5.2}$$

Therefore, the unitarity bound is shifted to higher energies from the bound of corresponding dimension eight operators. Modeling possible new physics degrees of freedom as generic resonances could be more feasible when their mass lies within the energy reach of the experiments.

In this chapter, the effective field theory approach to investigate new physics will be extended by a new set of generic resonances, which affect the vector boson scattering process. New resonances can appear as elementary particles and therefore interact weakly, or as strongly interacting resonances similar to mesons in quantum chromodynamics. Both scenarios will be covered by allowing a generic coupling of the resonance to the gauge and Higgs-Goldstone sectors [73]. As a first step, only couplings to the Higgs-Goldstone boson sector are assumed in this thesis. Thus, the calculation can be performed mainly in the gaugeless limit, where the gauge sector vanishes. Additionally, only partial derivatives instead of covariant derivatives acting on the resonance are considered, because the additional contribution of the covariant derivative would only lead to higher order corrections to a resonance propagating in the weak boson scattering process.

Because the Standard Model should be obtained as the low energy limit of this extension by new resonances, their interactions will be described by currents of canonical dimension four in an effective field theory approach to the Standard Model. Similar to dimension six operators, the theoretical description can become ill-defined at high energies again. Therefore, the T-matrix framework has to be used to avoid an unphysical prescription in this asymptotic regime.

A publication of this part of the thesis is in preparation [121].

5.1. Quantum Numbers

Additional resonances can be categorized according to their spin and gauge quantum numbers. As in Chapter 3, new degrees of freedom are introduced, which couple only to the Higgs sector, neglecting interactions to light fermion currents. In the asymptotic limit of high

masses, these are represented as dimension eight operators $\mathcal{L}_{S,0}$ and $\mathcal{L}_{S,1}$. Therefore, only color singlets which conserve charge-conjugation and parity are considered. In the following, the new resonances will be distinguished in terms of their spin and gauge quantum numbers, which will be referred to as isospin.

5.1.1. Spin

Starting with integer spin particles in the final state, only integer spin resonances are allowed. There are two possibilities for even-spin resonances in vector boson scattering: scalar and tensor resonances. Because even-spin fields switch the fermion helicity, only even-spin fields with Higgs doublet like quantum numbers couple directly to fermion currents. An example for a scalar extension of the Standard Model with these fields are two or multi Higgs doublet models. However, only resonances which couple directly to the Higgs sector are investigated in this thesis. To guarantee this behavior, the resonances must have quantum numbers different from the Higgs-doublet.

Resonances with odd spin in vector boson scattering, namely vector resonances, are also possible and have been studied extensively in the literature. Most studies about a vector resonance ρ in Higgs-less models are outdated in the presence of a light scalar Higgs, but the basic principles are the same. A vector-like resonance coupled to the Higgs sector will mix with the electroweak gauge bosons of the Standard Model. After diagonalization, heavy vector resonances mostly develop couplings to all fermions of the Standard Model, in particular to light fermions. Therefore, the vector resonances have a different phenomenology from the scalar and tensor resonances and are neglected in a first approach.

The case of a tensor resonance requires special consideration. While renormalizable weakly interacting theories cannot include elementary tensor particles, it is nevertheless possible to set up an effective theory which contains a tensor particle and remains weakly interacting over a considerable range of energies. This has been observed in the context of gravity in extra dimensions [122–124], where massive tensor particles arise in the low energy effective theory. Additionally, a method was introduced to receive further insights in the effective field theory properties of a massive graviton by restoring its gauge invariance [125]. In the detailed review about massive gravity, this is called Stückelberg trick [126].

Massive gravitons provide a very specific pattern of couplings to the Higgs doublet, gauge bosons and fermions. In this thesis, a more generic model where such relations are absent is introduced. Due to the construction of a Stückelberg type Lagrangian, a controlled high-energy behavior of the genuine tensor resonance can be separated from unrelated higher-dimensional operators that become asymptotically relevant.

5.1.2. Isospin

Scalar and tensor degrees of freedom are similar in their possible couplings to Standard Model particles. In addition to the spin, these even-spin resonances can be categorized

in their electroweak quantum number. Resonances in vector boson scattering have been categorized for Higgs-less models in terms of the custodial $SU(2)_C$ multiplets, namely the weak isospin. In a Higgs-less scenario, the electroweak symmetry breaking is caused by a strongly interacting sector with an electroweak breaking scale of $\Lambda_s = 4\pi v \approx 3$ TeV. Vector boson scattering would therefore only be measured below this scale, where only the (approximate) low-energy $SU(2)_C$ symmetry applies. This is not the case in the observed light Higgs scenario (see Section 4.3.2). Data from vector boson scattering can be accessed at TeV energies, which are above the masses of the physical Higgs and the electroweak gauge bosons. Therefore, the unbroken high-energy symmetry has to be considered for the theoretical description. Neglecting hypercharge, this is $SU(2)_L \times SU(2)_R$. The new resonance coupled to the Standard Model Higgs sector have to be categorized in terms of $SU(2)_L \times SU(2)_R$ multiplets.

Resonances of even-spin with couplings to Higgs-Goldstone pairs, must therefore reside in the decomposition of $\left(\frac{1}{2},\frac{1}{2}\right) \otimes \left(\frac{1}{2},\frac{1}{2}\right)$. This representation corresponds to a $\mathbf{H} \otimes \mathbf{H}^\dagger$ term in an effective interaction operator. There are only two possibilities:

1. $(0,0)$: a neutral singlet (isoscalar), or
2. $(1,1)$: a 3×3 matrix, which contains nine components. This multiplet decomposes into an isotensor with five components, an isovector with three components, and an isoscalar with one component after electroweak symmetry breaking. In terms of the $SU(2)_L \times U(1)_Y$ subgroup, the nonet is represented as a complex $SU(2)_L$ triplet with a doubly charged component and a real $SU(2)_L$ triplet, as described in [127]. The relative mass splitting between these states is of order $(M_W/M)^2$, where M is the average resonance mass. Assuming $M \gg M_W$, this splitting can be ignored. Therefore, the nonet contains degenerate resonance components.

Due to the existence of the light Higgs, the analogy between spin and isospin cannot be used, because tensor states have just five physical degrees of freedom, but an isotensor will never occur by itself. For any given resonance multiplet in a vector boson scattering, the chiral symmetry relates Goldstone pairs with Higgs pairs, i.e. the ZZ and HH pairs.

In this thesis, a scalar and a tensor resonances with $SU(2)_L \times SU(2)_R$ quantum numbers $(0,0)$ in addition to scalar and tensor $(1,1)$ resonances are considered. For brevity of notation, $(0,0)$ will be still denoted as isoscalar and the $(1,1)$ as isotensor, which is always accompanied by additional isovector and isoscalar components.

5.2. Isoscalar-Scalar Resonances

A new massive spin-zero isoscalar state σ might appear as another Higgs boson. For example a Higgs singlet ϕ can couple via the operator $\mathrm{tr}\left[\mathbf{H}^\dagger\mathbf{H}\right]\phi^2$, and a Higgs doublet $\mathbf{H}'$ can interact via $\mathrm{tr}\left[\mathbf{H}^\dagger\mathbf{H}'\right]^2$ and $\mathrm{tr}\left[\mathbf{H}^\dagger\mathbf{H}\right]\mathrm{tr}\left[\mathbf{H}'^\dagger\mathbf{H}'\right]$. However, these terms will only contribute to Higgs mixing and self-interactions, but not directly to vector boson scattering. If another light scalar

particle beside the Standard Model Higgs is present, the Standard Model cannot be obtained in the low energy limit and would contradict the effective field theory formalism. The observed Higgs boson is therefore the only light scalar which saturates the vector boson coupling in the dimension four part of the Lagrangian. To model an additional scalar resonance σ with mass m_σ in the vector boson scattering process, it has to be coupled to a current J_σ which contains two Higgs-field derivatives $\mathbf{D}_\mu\mathbf{H}$. Therefore, the interaction can be describe with an effective dimension-five operator

$$\mathcal{L}_\sigma = -\frac{1}{2}\sigma\left(m_\sigma^2 + \partial^2\right)\sigma + \sigma J_\sigma, \tag{5.3a}$$

$$\text{where} \quad J_\sigma = F_\sigma \mathrm{tr}\left[\left(\mathbf{D}_\mu\mathbf{H}\right)^\dagger \mathbf{D}^\mu\mathbf{H}\right], \tag{5.3b}$$

with effective coupling F_σ which is suppressed by the new physics scale Λ. However, new Higgses may eventually appear also in vector boson scattering process after diagonalization of a renormalizable extension of the Standard Model Higgs sector. In this case, the couplings are power suppressed equivalent to the effective field theory formalism due to the Higgs decoupling theorem [128–130]. Therefore, the renormalizable (possibly weakly interacting) case is a special case that is included in the general effective field theory framework. In particular, this applies to Higgs sector extensions by singlets and doublets, as long as the additional scalars can be considered heavy in the sense of the effective field theory formalism.

5.2.1. Goldstone Boson Amplitudes

Additional contributions to the weak boson scattering process arise due to the generic scalar resonance described by the Lagrangian (5.3). Using the corresponding Feynman rules derived in Appendix B.3, the Goldstone boson amplitudes are given in the gaugeless limit by

$$\mathcal{A}_\sigma\left(w^\pm w^\pm \to w^\pm w^\pm\right) = -\frac{1}{4}{F_\sigma}^2\left(\frac{t^2}{t-m_\sigma^2} + \frac{u^2}{u-m_\sigma^2}\right), \tag{5.4a}$$

$$\left.\begin{aligned}&\mathcal{A}_\sigma\left(w^\pm z \to w^\pm z\right)\\ &\mathcal{A}_\sigma\left(hw^\pm \to hw^\pm\right)\\ &\mathcal{A}_\sigma\left(hz \to hz\right)\end{aligned}\right\} = -\frac{1}{4}{F_\sigma}^2\frac{t^2}{t-m_\sigma^2}, \tag{5.4b}$$

$$\mathcal{A}_\sigma\left(w^\pm w^\mp \to w^\pm w^\mp\right) = -\frac{1}{4}{F_\sigma}^2\left(\frac{s^2}{s-m_\sigma^2} + \frac{t^2}{t-m_\sigma^2}\right), \tag{5.4c}$$

$$\left.\begin{aligned}&\mathcal{A}_\sigma\left(w^\pm w^\mp \to zz\right)\\ &\mathcal{A}_\sigma\left(hh \to w^\pm w^\mp\right)\\ &\mathcal{A}_\sigma\left(hh \to zz\right)\end{aligned}\right\} = -\frac{1}{4}{F_\sigma}^2\frac{s^2}{s-m_\sigma^2}, \tag{5.4d}$$

$$\left.\begin{aligned}&\mathcal{A}_\sigma\left(zz \to zz\right)\\ &\mathcal{A}_\sigma\left(hh \to hh\right)\end{aligned}\right\} = -\frac{1}{4}{F_\sigma}^2\left(\frac{s^2}{s-m_\sigma^2} + \frac{t^2}{t-m_\sigma^2} + \frac{u^2}{u-m_\sigma^2}\right). \tag{5.4e}$$

However, these amplitudes cannot be used in a numerical calculation, because they have a singularity at $s,t,u = m_\sigma^2$. Therefore, the resonance should be formulated as Breit-Wigner resonance by adding an imaginary term proportional to the width Γ_σ in the denominator

$$\frac{1}{s-m_\sigma^2} \to \frac{1}{s-m_\sigma^2+\mathrm{i}\Gamma_\sigma m_\sigma \Theta(s)}\,, \tag{5.5a}$$

$$\frac{1}{t-m_\sigma^2} \to \frac{1}{t-m_\sigma^2+\mathrm{i}\Gamma_\sigma m_\sigma \Theta(t)}\,, \tag{5.5b}$$

$$\frac{1}{u-m_\sigma^2} \to \frac{1}{u-m_\sigma^2+\mathrm{i}\Gamma_\sigma m_\sigma \Theta(u)}\,, \tag{5.5c}$$

where the Θ function has to be added, because of the analytical S-matrix features which has been discussed in Section 4.1. The width Γ_σ of the scalar resonance is related to its mass and coupling

$$\begin{aligned}\Gamma_\sigma(m_\sigma) &= \int d\Omega \frac{|\vec{p}|}{32\pi^2 m_\sigma^2}\left(|\mathcal{M}_{\sigma\to w^+w^-}|^2 + \frac{1}{2}|\mathcal{M}_{\sigma\to zz}|^2 + \frac{1}{2}|\mathcal{M}_{\sigma\to hh}|^2\right)\\ &= \frac{m_\sigma^3}{32\pi}F_\sigma^2\,,\end{aligned} \tag{5.6}$$

with $|\vec{p}| = \frac{m_\sigma}{2}$. Now, the master amplitude $\mathcal{A}\left(w^\pm w^\mp \to zz\right)$ in (5.4) will get an imaginary part when approaching the resonance. The isospin spin amplitude $\mathcal{A}_{00}$ should be saturated in a valid theoretical description at the resonance-mass (see fig. 5.1), i.e. this amplitude becomes purely imaginary.

5.2.2. Effective Field Theory Matching

If the mass of the scalar is similar to the Higgs mass, the behavior of the resonance is equivalent to the dimension six operator $\mathcal{L}_{HD}$ (see eq. (3.42))

$$F_\sigma = \sqrt{F_{HD}^2 v^2 + 4F_{HD}}\,, \tag{5.7a}$$

$$F_{\mathrm{HD}} = -\frac{2}{v^2}\left(1 \pm \sqrt{\frac{v^2}{4}F_\sigma^2 + 1}\right)\,. \tag{5.7b}$$

Especially, this is true for the high energy limit. Therefore, a combination of F_{HD} and F_σ can be chosen such, that a possible unitarity violation of the dimension six operator $\mathcal{L}_{HD}$ is canceled. If the pole of the scalar is beyond the energy reach, it can be integrated out and matched to higher dimensional operators in the low-energy effective field theory. The matching algorithm is displayed schematically for a generic even-spin resonance Φ with mass m_Φ and parameter z coupling to a current J

$$\mathcal{L}_\Phi = z\left[\Phi\left(m_\Phi^2 + \mathbf{DD}\right)\Phi + 2\Phi J\right]\,. \tag{5.8}$$

Integrating out Φ results in the effective Lagrangian

$$\mathcal{L}_{\Phi}^{\text{eff}} = -\frac{z}{m_{\Phi}^2} JJ + \frac{z}{m_{\Phi}^4} J(\mathbf{DD})J + \mathcal{O}(m_{\Phi}^{-6}) \,. \tag{5.9}$$

In case of a scalar resonance σ, the four weak boson fields will be truncated which yields an anomalous quartic gauge coupling

$$\mathcal{L}_{\sigma}^{\text{eff}} = \frac{F_{\sigma}^2}{2m_{\sigma}^2} \text{tr}\left[\left(\mathbf{D}_{\mu}\mathbf{H}\right)^{\dagger} \mathbf{D}^{\mu}\mathbf{H}\right] \text{tr}\left[\left(\mathbf{D}_{\nu}\mathbf{H}\right)^{\dagger} \mathbf{D}^{\nu}\mathbf{H}\right] . \tag{5.10}$$

This anomalous coupling can be matched to a dimension eight operator $\mathcal{L}_{S,1}$ (see eq. (3.37)) with an effective coupling of

$$F_{S,1} = \frac{F_{\sigma}^2}{2m_{\sigma}^2} \,. \tag{5.11}$$

5.2.3. Isospin-Spin Amplitudes

Analogously to the dimension eight and six operators, the contribution induced by a generic scalar resonance can violate the unitarity of the S-matrix. To avoid an unphysical theory description, the unitarization framework, namely the T-matrix scheme, which has been introduced in Chapter 4, is applied. Similar to the effective field theory approach described in Section 4.4.1 the counter terms corresponding to isospin-spin eigenamplitudes have to be calculated. For this purpose, the Goldstone boson scattering amplitudes (5.4) are decomposed in the isospin-spin eigenbasis

$$\mathcal{A}_{00} = F_{\sigma}^2 \left(-\frac{3}{4} \frac{s^2}{s - m_{\sigma}^2 + \mathrm{i} m_{\sigma} \Gamma_{\sigma}} - \frac{1}{2} \mathcal{S}_0 \left(s, m_{\sigma}\right) \right) , \tag{5.12a}$$

$$\mathcal{A}_{02} = -\frac{1}{2} F_{\sigma}^2 \mathcal{S}_2 \left(s, m_{\sigma}\right) , \tag{5.12b}$$

$$\mathcal{A}_{11} = -\frac{1}{2} F_{\sigma}^2 \mathcal{S}_1 \left(s, m_{\sigma}\right) , \tag{5.12c}$$

$$\mathcal{A}_{13} = -\frac{1}{2} F_{\sigma}^2 \mathcal{S}_3 \left(s, m_{\sigma}\right) , \tag{5.12d}$$

$$\mathcal{A}_{20} = -\frac{1}{2} F_{\sigma}^2 \mathcal{S}_0 \left(s, m_{\sigma}\right) , \tag{5.12e}$$

$$\mathcal{A}_{22} = -\frac{1}{2} F_{\sigma}^2 \mathcal{S}_2 \left(s, m_{\sigma}\right) , \tag{5.12f}$$

where the functions $\mathcal{S}_i \left(s, m_{\sigma}\right)$ are defined in the Appendix A.3.2. The resonance part of the eigenamplitude $\mathcal{A}_{00}$ could also be formulated without a width Γ_{σ}. Therefore, the amplitude would posses a pol at its mass on the real axis and would violate unitarity near the pol. The T-matrix scheme would act as Dyson resummation (see eq. (4.49)) and would transform the on-shell scattering amplitude automatically in the correct Breit-Wigner form. However, for a well behaved numerical calculation, the width has to be included in the Breit-Wigner form of the resonance.

5.3. Isoscalar-Tensor Resonances

The massive spin-two particle has five degrees of freedom, which can be represented by five component fields corresponding to an irreducible representation in the rest frame of the physical spin-two particle. No interacting model which posses an ultraviolet completion for a generic spin-two particle has been developed, yet. The main issue while modeling such a relativistic quantum field theory is to ensure a complete Hilbert space and a unitary scattering matrix. However, a massive spin-two particle can be embedded in an effective field theory approach to the Standard Model. Therefore, a generic spin two particle is introduced as relativistic extra field to the Standard Model in a Lagrangian formalism. These fields are coupled to currents build from Standard Model fields in a Lorentz- and gauge-invariant way.

Contrary to the spin-zero scenario, where the particle has only a single component, the spin-two case has five independent components in the appropriate Lorentz representation. A relativistic spin-two particle is represented by a symmetric Lorentz tensor with a priori ten components that mix under Lorentz transformations. The Lorentz symmetry is represented by the symmetry group $SU(2) \times SU(2)$ and is broken down to the diagonal $SU(2)$ algebra, the spin, in the rest frame of the tensor. In particular, the Lorentz decuplet decomposes into the irreducible spin states like

$$\text{symmetric Lorentz tensor} \rightarrow \text{spin states } (2) + (1) + (0) + (0)\,. \tag{5.13}$$

Looking at the symmetric rest-frame of the polarization tensor $\varepsilon^{\mu\nu}$, the irreducible parts correspond to one traceless spin-two component ε^{ij}, one spin-one component ε^{0i}, and two spin-zero components ε^{00} and $\sum \varepsilon^{ii}$. Under the full Lorentz group, the polarization tensor $\varepsilon^{\mu\nu}$ can be reduced to six degrees of freedom, particularly into the traceless tensor and the scalar which represents the trace. However, in the presence of interactions it is not straightforward to maintain this decomposition for off-shell amplitudes [131].

The extra degrees of freedom of a tensor with momentum k and mass m_f can be eliminated on-shell, $k = m_f^2$, by demanding the conditions

$$k_\mu \varepsilon^{\mu\nu} = 0\,, \tag{5.14a}$$

$$\varepsilon^{\mu}_{\ \mu} = 0\,. \tag{5.14b}$$

Thus, the independent degrees of freedom are reduced from ten to five. Using the real, symmetric and mutually orthogonal polarization tensors $\varepsilon_\lambda^{\mu\nu}$ the propagator for a single tensor can be written as [132]

$$G_f^{\mu\nu,\rho\sigma}(k) = \frac{\mathrm{i} \sum_\lambda \bar{\varepsilon}_\lambda^{\mu\nu} \varepsilon_\lambda^{\rho\sigma}}{k^2 - m_f^2 + i\epsilon} + \text{non-resonant}\,. \tag{5.15}$$

The non-resonant part has to vanish when k is on-shell. Explicitly summing over the five polarization tensors leads to a unique solution for the resonant part of the propagator [133]

$$G_f^{\mu_1\mu_2,\nu_1\nu_2} = \mathrm{i} \frac{P^{\mu_1\mu_2\nu_1\nu_2}(k, m_f)}{k^2 - m_f^2 + \mathrm{i}\epsilon} + \text{non-resonant}\,, \tag{5.16}$$

where the projection operator of spin two can be written in terms of the spin-one projection operators

$$\begin{aligned} P^{\mu_1\mu_2\nu_1\nu_2}(k,m_f) &= \sum_\lambda \bar{\varepsilon}^{\mu_1\mu_2}_\lambda(k,m_f)\,\varepsilon^{\nu_1\nu_2}_\lambda(k,m_f) \\ &= \frac{1}{2}\left[P^{\mu_1\nu_1}(k,m_f)P^{\mu_2\nu_2}(k,m_f) + P^{\mu_1\nu_2}(k,m_f)P^{\mu_1\nu_2}(k,m_f)\right] \\ &\quad - \frac{1}{3}P^{\mu_1\mu_2}(k,m_f)P^{\nu_1\nu_2}(k,m_f), \end{aligned} \tag{5.17}$$

which are given by

$$P^{\mu\nu}(k,m_f) = \sum_\lambda \bar{\varepsilon}^{\mu}_\lambda(k,m_f)\varepsilon^{\nu}_\lambda(k,m_f) = g^{\mu\nu} - \frac{k^\mu k^\nu}{m_f^2}. \tag{5.18}$$

A propagator with a vanishing non-resonant part follows from the well-known free Fierz-Pauli Lagrangian for the tensor field $f^{\mu\nu}$ [134, 135]

$$\begin{aligned} \mathcal{L} =& \frac{1}{2}\partial_\alpha f_{\mu\nu}\partial^\alpha f^{\mu\nu} - \frac{1}{2}m_f^2 f_{\mu\nu}f^{\mu\nu} \\ & - \partial^\alpha f_{\alpha\mu}\partial_\beta f^{\beta\mu} - f^\alpha_\alpha \partial^\mu\partial^\nu f_{\mu\nu} - \frac{1}{2}\partial_\alpha f^\mu_\mu \partial^\alpha f^\nu_\nu + \frac{1}{2}m_f^2 f^\mu_\mu f^\nu_\nu\,. \end{aligned} \tag{5.19}$$

This Lagrangian enforces conditions which are related to (5.14) on the symmetric spin-two field

$$\partial_\mu\partial_\nu f^{\mu\nu} = 0, \tag{5.20a}$$

$$\partial_\mu f^{\mu\nu} = 0, \tag{5.20b}$$

$$f^\mu_\mu = 0\,. \tag{5.20c}$$

Without the non-resonant terms, the tensor has more than five off-shell degrees of freedom and the propagator describes not a pure tensor. Additional different combinations of factors k^μ are included in the propagator (5.16) which projects out the proper spin-two part of the pole. At lower energies $s = k^2$, these factors vanish more rapidly than the $g^{\mu\nu}$ terms. In an effective field theory approach, this can be interpreted as the coupling to operators of higher dimensions. However, beyond the resonance, they could eventually rise more rapidly and therefore potentially provide the dominant part that enters the unitarization prescription.

5.3.1. Stückelberg Formulation

The additional momentum factors in the spin-two propagator represent the mismatch between the on-shell $SO(3)$ and off-shell Lorentz-group representations in a relativistic description. This is in analogy with a massive spin-one boson, which in the relativistic case acquires an extra zero component. To investigate the impact of these extra degrees of freedom for an spin-two field in an actual calculation, they have to be identified and separated first.

Analogously to the decomposition of the symmetric tensor field, an arbitrary symmetric polarization tensor $\varepsilon^{\mu\nu}$ can be written in terms of five polarization tensors $\varepsilon_f^{\mu\nu}$, three polarization vectors ε_A^μ and two polarization scalars ε_σ and ε_ϕ

$$\varepsilon^{\mu\nu} = \varepsilon_f^{\mu\nu} + \frac{1}{m}(k^\mu \varepsilon_A^\nu + k^\nu \varepsilon_A^\mu) + \frac{k^\mu k^\nu}{m_f^2}\varepsilon_\sigma + g^{\mu\nu}\varepsilon_\phi \,. \tag{5.21}$$

Using the on-shell conditions for the polarization tensor $\varepsilon_f^{\mu\nu}$ (5.14) and the constraint $k_\mu \varepsilon_v^\mu = 0$ at $k^2 = m_f^2$, the vector and scalar polarizations ε_A, ε_σ, ε_ϕ are given by contractions of the polarization tensor $\varepsilon^{\mu\nu}$

$$\varepsilon_A^\mu = \frac{1}{m_f}\left(k_\nu \varepsilon^{\mu\nu} - \frac{1}{m_f^2} k^\mu k_\nu k_\rho \varepsilon^{\nu\rho}\right), \tag{5.22a}$$

$$\varepsilon_\sigma = \frac{1}{3}\left(4\frac{k_\mu k_\nu}{m_f^2} - g_{\mu\nu}\right)\varepsilon^{\mu\nu}, \tag{5.22b}$$

$$\varepsilon_\phi = \frac{1}{3}\left(g_{\mu\nu} - \frac{k_\mu k_\nu}{m_f^2}\right)\varepsilon^{\mu\nu}. \tag{5.22c}$$

This decomposition yields a naturally extension for off-shell amplitudes. Using the prescription (5.22) will remove the k^μ factors of the tensor propagator (5.16), but introduces additional vector and scalar fields including their respective propagators. To extend the on-shell relations of the polarization degrees of freedom (5.22) off-shell, the interactions of the vector and scalar fields must be precisely related to the original tensor interactions. In field theory, a gauge symmetry can be introduced to automatically enforce such relations. The power-counting in the resulting Feynman rules will be explicit, in analogy with the 't Hooft-Feynman gauge of an ordinary gauge theory.

In the Lagrangian formalism, the Fierz-Pauli Lagrangian is related to the minimal single-field spin-two propagator. However, the propagators correspond to the pure tensor components only on-shell. To show explicitly the off-shell mixing of all ten degrees of freedom of a massive symmetric spin-two field, the Stückelberg mechanism is used [126]. This algorithm introduces additional fields and extra gauge symmetries simultaneously in the Lagrangian formalism [136–138]. Due to these extra gauge symmetries, the new degrees of freedom are redundant and the total number of observable degrees of freedom is not changed. Following the Stückelberg mechanism, the degrees of freedom which are eliminated on-shell by the conditions (5.20) can be shown explicit. The $f^{0\mu}$ components are separated from the tensor to the Stückelberg vector A^μ like

$$f^{\mu\nu} = f'^{\mu\nu} + \frac{1}{m_f}\partial^\mu A^\nu + \frac{1}{m_f}\partial^\nu A^\mu \,. \tag{5.23}$$

Analogously to the original Stückelberg algorithm for an abelian vector, the A^0 component which corresponds to f^{00} is extracted by introducing the scalar σ_f,

$$A^\mu = A_f^\mu + \frac{1}{m_f}\partial^\mu \sigma_f \,. \tag{5.24}$$

Finally, another Stückelberg scalar ϕ_f represents the trace of the massive tensor

$$f'^{\mu\nu} = f_f^{\mu\nu} + g^{\mu\nu}\phi_f \,. \tag{5.25}$$

This scheme guarantees that the interactions of the new fields in the Lagrangian are correctly related to the original interactions of the tensor field. The resulting Lagrangian exhibits several gauge symmetries that reflect the redundancy of the Stückelberg fields

$$\begin{aligned}
\mathcal{L} =& \frac{1}{2}\partial_\alpha f_{f\mu\nu}\partial^\alpha f_f^{\mu\nu} - \frac{1}{2}m_f^2 f_{f\mu\nu} f_f^{\mu\nu} - \partial^\alpha f_{f\alpha\mu}\partial_\beta f_f^{\beta\mu} - f_{f\ \alpha}^{\alpha}\partial^\mu\partial^\nu f_{f\mu\nu} \\
& - \frac{1}{2}\partial_\alpha f_{f\ \mu}^{\mu}\partial^\alpha f_{f\ \nu}^{\nu} + \frac{1}{2}m_f^2 f_{f\ \mu}^{\mu} f_{f\ \nu}^{\nu} - \partial_\mu A_{f\nu}\partial_\mu A_f^\nu + \partial_\mu A_f^\mu \partial_\nu A_f^\nu \\
& - 2m_f f_{f\mu\nu}\partial^\mu A_f^\nu + 2m_f f_{f\ \mu}^{\mu}\partial_\nu A_f^\nu + 6m_f\phi\partial_\mu A_f^\mu \\
& - 2f_{f\mu\nu}\partial^\mu\partial^\nu\sigma_f + 2f_{f\ \mu}^{\mu}\partial^2\sigma_f - 2f_{f\mu\nu}\partial^\mu\partial^\nu\phi_f + 2f_{f\ \mu}^{\mu}\partial^2\phi_f \\
& - 3\partial_\mu\phi_f\partial^\mu\phi_f + 6m_f^2\phi_f\phi_f + 3m_f^2 f_{f\ \mu}^{\mu}\phi_f \\
& + \left(f_{f\mu\nu} + g^{\mu\nu}\phi_f + \frac{2}{m_f}\partial_\mu A_{f\nu} + \frac{2}{m_f^2}\partial_\mu\partial_\nu\sigma_f\right) J_f^{\mu\nu} \,.
\end{aligned} \tag{5.26}$$

Choosing unitary gauge, where all Stückelberg fields vanish, recovers the Fierz-Pauli Lagrangian. The scheme simplifies slightly since both scalars are related to the original tensor, so their interactions are not independent and the gauge can be fixed by

$$\phi_f = -\sigma_f \,. \tag{5.27}$$

Adjusted by partial integration, the minimal Stückelberg Lagrangian is [139]

$$\begin{aligned}
\mathcal{L} =& \frac{1}{2}\partial_\alpha f_{f\mu\nu}\partial^\alpha f_f^{\mu\nu} - \frac{1}{2}m_f^2 f_{f\mu\nu} f_f^{\mu\nu} \\
& - \left(\partial^\alpha f_{f\alpha\mu} - \frac{1}{2}\partial_\mu f_{f\ \rho}^{\rho} - m_f A_{f\mu}\right)^2 \\
& - \frac{1}{4}\partial_\alpha f_{f\ \mu}^{\mu}\partial^\alpha f_{f\ \nu}^{\nu} + \frac{1}{4}m_f^2 f_{f\ \mu}^{\mu} f_{f\ \nu}^{\nu} - \partial_\mu A_{f\nu}\partial_\mu A_f^\nu + m_f^2 A_{f\mu} A_f^\mu \\
& + \left(\partial_\mu A_f^\mu - 3m_f\sigma_f + \frac{1}{2}m_f f_{f\ \mu}^{\mu}\right)^2 \\
& + 3\partial_\mu\sigma_f\partial^\mu\sigma_f - 3m_f^2\sigma_f\sigma_f \\
& + \left(f_{f\mu\nu} - g^{\mu\nu}\sigma_f + \frac{2}{m_f}\partial_\mu A_{f\nu} + \frac{2}{m_f^2}\partial_\mu\partial_\nu\sigma_f\right) J_f^{\mu\nu} \,.
\end{aligned} \tag{5.28}$$

For perturbative calculations, four additional gauge symmetries have to be fixed up to residual gauge transformations $\lambda(x)$ which decouple on-shell, i.e. satisfying the harmonic condition $(\partial^2 + m^2)\lambda = 0$. The Lagrangian (5.28) is already formulated in such a way, that the interaction terms between the different fields are grouped together. Choosing the linear

gauge fixing terms

$$\partial_\mu A_f^\mu - 3m_f\sigma_f + \frac{1}{2}m_f f_{f\,\mu}^{\mu} = 0\,, \tag{5.29}$$

$$\partial^\alpha f_{f\alpha\mu} - \frac{1}{2}\partial_\mu f_{f\,\rho}^{\rho} - m_f A_{f\mu} = 0\,, \tag{5.30}$$

results in the diagonalized Lagrangian

$$\begin{aligned}\mathcal{L} =& \frac{1}{2} f_{f\mu\nu}\left(-\partial^2 - m_f^2\right) f_f^{\mu\nu} + \frac{1}{2} f_{f\,\mu}^{\mu}\left(-\frac{1}{2}\left(-\partial^2 - m_f^2\right)\right) f_{f\,\nu}^{\nu} \\ &+ \frac{1}{2} A_{f\mu}\left(-\partial^2 - m_f^2\right) A_f^\mu + \frac{1}{2}\sigma_f\left(-\partial^2 - m_f^2\right)\sigma_f \\ &+ \left(f_{f\mu\nu} - \frac{1}{\sqrt{6}} g^{\mu\nu}\sigma_f + \frac{1}{\sqrt{2}m_f}\left(\partial_\mu A_{f\nu} + \partial_\nu A_{f\mu}\right) + \frac{\sqrt{2}}{\sqrt{3}m_f^2}\partial_\mu\partial_\nu\sigma_f\right) J_f^{\mu\nu}\,,\end{aligned} \tag{5.31}$$

where the fields are renormalized by $A_f^\mu \to A_f^\mu/\sqrt{2}$ and $\sigma_f \to \sigma_f/\sqrt{6}$). The corresponding scalar, vector and tensor degrees of freedom decouple from each other, but have a different coupling behavior to the effective current. If taking the massless limit $m_f \to 0$ in (5.31), the current $J_f^{\mu\nu}$ has to be conserved, i.e. $\partial_\mu J_f^{\mu\nu} = 0$. Otherwise the scalar and vector contributions proportional to $1/m_f$ become singular and the theory description breaks down. In this case the vector decouples completely and only the scalar corresponding to the trace and the tensor itself will affect the weak boson scattering amplitude. Note that, in this thesis, only heavy resonance are investigated, because the Standard Model should be obtained in the low energy limit. Therefore, the currents $J_f^{\mu\nu}$ receive a priori no further restrictions and all degrees of freedom could contribute to the weak vector boson scattering processes.

The kinetic terms of the pure tensor, vector and scalar lead to to their corresponding canonical propagators[1]

$$\Delta_{\mu\nu,\rho\sigma}(f_f) = \frac{\mathrm{i}}{k^2 - m_f^2}\left(\frac{1}{2}g_{\mu\rho}g_{\nu\sigma} + \frac{1}{2}g_{\mu\sigma}g_{\nu\rho} - g_{\mu\nu}g_{\rho\sigma}\right)\,, \tag{5.32a}$$

$$\Delta_{\mu\nu}(A_f) = \frac{-\mathrm{i}}{k^2 - m_f^2} g_{\mu\nu}\,, \tag{5.32b}$$

$$\Delta(\sigma_f) = \frac{\mathrm{i}}{k^2 - m_f^2}\,. \tag{5.32c}$$

[1]For a complete formulation at the quantum level, the gauge-fixed Lagrangian has to be embedded in a BRST formalism. Introducing appropriate Fadeev-Popov ghosts and auxiliary Nakanishi-Lautrup fields, the classical action can be rendered BRST invariant. The quantum effective action with resonance exchange is then defined as the solution to a Slavnov-Taylor equation, to all orders in the electroweak perturbative expansion. The gauge-fixing terms become BRST variations, which do not contribute to physical amplitudes, and the Stückelberg fields combine with the ghosts and auxiliary fields to BRST quartets that can be consistently eliminated from the Hilbert space. This procedure is shown in detail in [140] .

As desired, these propagators do not contain any momentum factors. This is advantageous in a Monte-Carlo calculation for physical processes, where in a generic momentum configuration all bosons are off-shell.

The Stückelberg formulation and the Fierz-Pauli Lagrangian are equivalent descriptions of a massive spin-two particle and result in identical on-shell amplitudes. Differences between those two approaches are manifest in the formulation for massive vector bosons, where the Stückelberg approach reproduces the usual reformulation as a spontaneously broken gauge theory. Although this is mathematically equivalent to the original model [141], a conceptual difference arises, when the accessible energy in a process exceeds the resonance mass within an effective field theory framework. In the gauge theory version, there is no higher dimensional operator with a $1/M$ coefficient. Any additional effects would come with a new cutoff $1/\Lambda$. Scattering amplitudes are bounded beyond the resonance as long as Λ is considered large. This is contrary in the formulation with massive gauge bosons, where k^μ/M terms are included in the propagator and could be naively estimated as order one in terms of power counting. These require the inclusion of a whole series of operators with $1/M$ factors. Thus, the model becomes strongly interacting by definition and looses predictivity. A possible weak interaction can only be described with fine-tuned cancellations between terms. Turning this argument around, if a vector boson is observed to interact weakly over a significant range of energies above its mass, it is natural to describe it as a gauge boson of some gauge symmetry. Analogously, only the Stückelberg approach provides a natural description for a weakly interacting tensor resonance over a significant range of scales above its mass.

In this thesis, the Stückelberg Lagrangian is therefore used as the basis of a tensor effective field theory with a minimum set of free parameters. Additional interactions which do not contribute to the resonance can be described with further free parameters. These unrelated new physics effects can be modeled by additional higher dimensional operators.

5.3.2. Currents

The lowest dimensional effective coupling of the isoscalar-tensor resonance to Goldstone boson/Higgs sector is described by a current which consists of two terms

$$J_f^{\mu\nu} = F_f \left(\mathrm{tr}\left[(\mathbf{D}^\mu \mathbf{H})^\dagger \mathbf{D}^\nu \mathbf{H} \right] - \frac{c_f}{4} g^{\mu\nu} \mathrm{tr}\left[\left(\mathbf{D}_\rho \mathbf{H}\right)^\dagger \mathbf{D}^\rho \mathbf{H} \right] \right) , \tag{5.33}$$

where the coupling F_f already contains the $1/\Lambda$ suppression. An additional independent coupling only to the trace of the tensor with the coefficient c_f is introduced in the second term. Because the trace of the tensor vanishes on-shell, the second term belongs to the non-resonant continuum and can be replaced by an higher dimensional effective field theory operator. For $c_f = 1$, the current $J_f^{\mu\nu}$ becomes traceless and decouples completely from the trace of the tensor. To investigate the effect of the second term further, the coefficient c_f is left undetermined.

The tensor-field coupling then reads in Fierz-Pauli formulation (5.19)

$$f_{\mu\nu} J_f^{\mu\nu} , \tag{5.34}$$

and in the Stückelberg formulation (5.31)

$$f_{f\mu\nu} J_f^{\mu\nu} - \sigma_f J_f{}^{\mu}_{\mu} - \frac{1}{m} A_{f\mu} \partial_\nu J_f^{\mu\nu} + \frac{2}{m^2} \sigma_f \partial_\mu \partial_\nu J_f^{\mu\nu} \,. \tag{5.35}$$

In the second formalism, the momentum factors in the Fierz-Pauli tensor propagator (5.16) have been converted to derivatives acting on the current. They are explicitly associated with the vector and scalar degrees of freedom. Besides the scalar coupling to the trace of the current, the vector and scalar couplings can be associated with dimension five and six operators, respectively. Thus, the formally dominant high-energy ($s \to \infty$) behavior of the amplitude is given by the exchange of the Stückelberg vector and scalar. These contributions will only vanish, if the current is conserved. However, evaluating the divergence using (2.4) and the equations of motion (A.53a) reveals that the current $J^{\mu\nu}$ is not conserved, even in the absence of electroweak symmetry breaking

$$\begin{aligned}
\partial_\mu J_f^{\mu\nu} =& F_f \operatorname{tr}\left[\left(\mathbf{D}^2\mathbf{H}\right)^\dagger \mathbf{D}^\nu \mathbf{H}\right] + \frac{F_f}{4}\left(c_f + 2\right) \operatorname{tr}\left[\left(\mathbf{D}_\mu \mathbf{H}\right)^\dagger \left[\mathbf{D}^\mu, \mathbf{D}^\nu\right] \mathbf{H}\right] \\
& - \frac{F_f}{4}\left(c_f - 2\right) \operatorname{tr}\left[\left(\mathbf{D}_\mu \mathbf{H}\right)^\dagger \left\{\mathbf{D}^\mu, \mathbf{D}^\nu\right\} \mathbf{H}\right] \\
=& F_f \left(\mu^2 - \frac{\lambda v^2}{2}\right) \operatorname{tr}\left[\mathbf{H}^\dagger \mathbf{D}^\nu \mathbf{H}\right] - F_f \lambda \operatorname{tr}\left[\widehat{\mathbf{H}^\dagger \mathbf{H}}\right] \operatorname{tr}\left[\mathbf{H}^\dagger \mathbf{D}^\nu \mathbf{H}\right] \\
& - \frac{\mathrm{i} g F_f}{4}\left(c_f + 2\right) \operatorname{tr}\left[\left(\mathbf{D}_\mu \mathbf{H}\right)^\dagger \mathbf{W}^{\mu\nu} \mathbf{H}\right] - \frac{\mathrm{i} g F_f}{4}\left(c_f + 2\right) \operatorname{tr}\left[\mathbf{H}\mathbf{B}^{\mu\nu} \left(\mathbf{D}_\mu \mathbf{H}\right)^\dagger\right] \\
& - \frac{F_f}{4}\left(c_f - 2\right) \operatorname{tr}\left[\left(\mathbf{D}_\mu \mathbf{H}\right)^\dagger \left\{\mathbf{D}^\mu, \mathbf{D}^\nu\right\} \mathbf{H}\right] .
\end{aligned} \tag{5.36}$$

Besides the term proportional to $\left(c_f - 2\right)$ all non vanishing terms of the derivatives contain at least three fields and therefore do not contribute to the $VV \to VV$ process at high energies, where the electroweak symmetry is conserved. After electroweak symmetry breaking the Higgs fields receives a vacuum expectation value v and the divergence of the current contains terms with just two particles. In combination with g, g' and λ, these new terms are proportional to the the masses of W, Z and the Higgs. They describe the interaction of the Stückelberg vector coupling to a longitudinal and a transversal vector boson, which are accompanied by a factor $1/m_f$. In the limit of a heavy resonance, the Stückelberg terms are thus parametrically suppressed and become only relevant for energies significantly beyond the resonance mass. Conversely, if the resonance mass is similar to the electroweak scale, the Stückelberg terms are significant.

The contributions of the Stückelberg scalar related to double derivative acting on the current

possess an energy behavior analogue to the Stückelberg vector

$$\begin{aligned}
\partial_\nu\partial_\mu J_f^{\mu\nu} =& F_f \mathrm{tr}\left[\left(\mathbf{D}_\mu\mathbf{H}\right)^\dagger\left(\mathbf{D}_\nu\mathbf{D}^\mu\mathbf{D}^\nu\mathbf{H}+\mathbf{D}^\mu\mathbf{D}^2\mathbf{H}-\frac{c_f}{2}\mathbf{D}^2\mathbf{D}^\mu\mathbf{H}\right)\right]\\
&+F_f\mathrm{tr}\left[\left(\mathbf{D}^2\mathbf{H}\right)^\dagger\mathbf{D}^2\mathbf{H}\right]+F_f\mathrm{tr}\left[\left(\mathbf{D}_\mu\mathbf{D}_\nu\mathbf{H}\right)^\dagger\mathbf{D}^\nu\mathbf{D}^\mu\mathbf{H}\right]\\
&-\frac{c_f}{2}F_f\mathrm{tr}\left[\left(\mathbf{D}_\mu\mathbf{D}_\nu\mathbf{H}\right)^\dagger\mathbf{D}^\mu\mathbf{D}^\nu\mathbf{H}\right]\\
=&-F_f\lambda\mathrm{tr}\left[\widehat{\mathbf{H}^\dagger\mathbf{H}}\right]\mathrm{tr}\left[\mathbf{D}_\mu\mathbf{H}^\dagger\mathbf{D}^\mu\mathbf{H}\right]-F_f\lambda\mathrm{tr}\left[\widehat{\mathbf{H}^\dagger\mathbf{H}}\right]\mathrm{tr}\left[\mathbf{H}^\dagger\mathbf{D}^2\mathbf{H}\right]\\
&-2F_f\lambda\mathrm{tr}\left[\mathbf{H}^\dagger\mathbf{D}_\mu\mathbf{H}\right]\mathrm{tr}\left[\mathbf{H}^\dagger\mathbf{D}^\mu\mathbf{H}\right]\\
&+\frac{g^2F_f}{8}\left(c_f+2\right)\left(\mathrm{tr}\left[\left(\mathbf{D}_\mu\mathbf{H}\right)^\dagger\mathbf{H}\left(\mathbf{D}^\mu\mathbf{H}\right)^\dagger\mathbf{H}\right]-\mathrm{tr}\left[\left(\mathbf{D}\mathbf{H}\right)^\dagger\left(\mathbf{D}^\mu\mathbf{H}\right)\mathbf{H}^\dagger\mathbf{H}\right]\right)\\
&+\frac{g'^2F_f}{8}\left(c_f+2\right)\left(\mathrm{tr}\left[\left(\mathbf{D}_\mu\mathbf{H}\right)^\dagger\mathbf{H}\left(\mathbf{D}^\mu\mathbf{H}\right)^\dagger\mathbf{H}\right]-\mathrm{tr}\left[\left(\mathbf{D}\mathbf{H}\right)^\dagger\left(\mathbf{D}^\mu\mathbf{H}\right)\mathbf{H}^\dagger\mathbf{H}\right]\right)\\
&+\frac{g^2F_f}{8}\left(c_f+2\right)\mathrm{tr}\left[\mathbf{H}^\dagger\mathbf{W}_{\mu\nu}\mathbf{W}^{\mu\nu}\mathbf{H}\right]+\frac{g'^2F_f}{8}\left(c_f+2\right)\mathrm{tr}\left[\mathbf{H}\mathbf{B}_{\mu\nu}\mathbf{B}^{\mu\nu}\mathbf{H}^\dagger\right]\\
&+\frac{gg'F_f}{4}\left(c_f+2\right)\mathrm{tr}\left[\mathbf{H}^\dagger\mathbf{W}_{\mu\nu}\mathbf{H}\mathbf{B}^{\mu\nu}\right]\\
&-\frac{\mathrm{i}gF_f}{4}\left(c_f+2\right)\mathrm{tr}\left[\left(\mathbf{D}_\mu\mathbf{H}\right)^\dagger\mathbf{W}^{\mu\nu}\mathbf{D}_\nu\mathbf{H}\right]\\
&-\frac{\mathrm{i}gF_f}{4}\left(c_f+2\right)\mathrm{tr}\left[\left(\mathbf{D}_\mu\mathbf{H}\right)\mathbf{B}^{\mu\nu}\left(\mathbf{D}_\mu\mathbf{H}\right)^\dagger\right]\\
&-\frac{F_f}{4}\left(c_f-2\right)\mathrm{tr}\left[\left(\left\{\mathbf{D}_\mu,\mathbf{D}_\nu\right\}\mathbf{H}\right)^\dagger\left\{\mathbf{D}^\mu,\mathbf{D}^\nu\right\}\mathbf{H}\right]\\
&-\frac{F_f}{4}\left(c_f-2\right)\mathrm{tr}\left[\left(\mathbf{D}_\mu\mathbf{H}\right)^\dagger\mathbf{D}_\nu\left\{\mathbf{D}^\mu,\mathbf{D}^\nu\right\}\mathbf{H}\right].
\end{aligned}\tag{5.37}$$

Again, by choosing $c_f = 2$ the double derivative acting on the current will only induce terms to weak boson/Higgs scattering after spontaneous electroweak symmetry breaking. These terms are therefore proportional to higher powers of the electroweak breaking scale v. Similar to (5.36), these contributions to the coupling of the scalar are suppressed by $1/m_f^2$. Thus the scalar couplings to two longitudinal or two transversal vector bosons described by the double derivative of the current can be neglected for heavy tensor resonances in the high energy limit.

5.3.3. On-shell Amplitudes

The contributions from (5.36) and (5.37) proportional to the masses m_W, m_Z and m_h of the scattered bosons would be automatically neglected in the gaugeless limit. Additional terms are expected for on-shell vector boson scattering amplitudes by the scalar and vector degrees of freedom in the Stückelberg parametrization. Contrary to the scalar resonance, the on-shell amplitudes have to be calculated for longitudinal vector bosons in unitary gauge for a complete discussion. A complete set of Feynman rules for the Stückelberg parametrization

in unitary gauge is given in Appendix B.2. Starting with the tensor degrees of freedom, the $W^+W^- \to ZZ$ scattering amplitudes reads

$$\begin{aligned}\mathcal{A}_f^f\left(W^+W^- \to ZZ\right) =& \frac{(c_f-2)F_f^2}{s-m_f^2}\cdot\frac{c_f\left(s-2m_W^2\right)\left(s-2m_Z^2\right)}{16} \\ &-\frac{F_f^2}{s-m_f^2}\cdot\frac{\left(P_2\left(\cos\Theta\right)-1\right)s^2+12m_W^2m_Z^2}{24}\,,\end{aligned} \tag{5.38}$$

with $P_2\left[\cos(\Theta)\right] = \frac{1}{2}\left[3\left(\cos\Theta\right)^2-1\right]$. Every term not proportional to s^2 can be neglected in the high energy limit. The amplitude then coincides with the gaugeless limit regardless of the parameter c_f and the mass of the tensor resonance. Although the amplitude has a dependence on the scattering angle Θ, its rise with the energy is comparable to a scalar resonance. Deviating behavior in the rise of the amplitude for longitudinal vector boson scattering is first introduced by the vector parametrization of the tensor resonance

$$\begin{aligned}\mathcal{A}_f^A\left(W^+W^- \to ZZ\right) =& \frac{(c_f-2)F_f^2}{s-m_f^2}\cdot\frac{s}{32m_f^2}\left[(c_f-2)s^2-2(c_f-4)\left(m_W^2+m_Z^2\right)s\right. \\ &\left.+4(c_f-6)m_W^2m_Z^2\right] \\ &+\frac{F_f^2}{s-m_f^2}\cdot\frac{m_W^2m_Z^2s}{2m_f^2}\,.\end{aligned} \tag{5.39}$$

The numerators grow with s^3 unlike the amplitude of the tensor part. This growth is caused by the last term of (5.36), which includes three partial derivatives acting on the Higgs field. By choosing $c_f = 2$ this rise of the amplitude vanishes. Furthermore, the vector contribution converges to a constant value in the high energy limit and can be neglected as it would be automatically in the gaugeless limit for $c_f = 2$.

Due to the coupling of the scalar part of the resonance to the current trace and the double derivative of the current (5.37), the longitudinal on-shell scattering amplitude contains mixing terms of these couplings

$$\begin{aligned}\mathcal{A}_f^\sigma\left(W^+W^- \to ZZ\right) =& -\frac{(c_f-2)F_f^2}{s-m_f^2}\cdot\left[\frac{c_f\left(s-2m_W^2\right)\left(s-2m_Z^2\right)}{24}\right. \\ &+\frac{s^2}{96m_f^4}\left((c_f-2)s^2-2(c_f-4)\left(m_W^2+m_Z^2\right)s+4(c_f-6)m_W^2m_Z^2\right) \\ &\left.+\frac{s}{24m_f^2}\left((c_f-1)s^2-2(c_f-2)\left(m_W^2+m_Z^2\right)s+4(c_f-3)m_W^2m_Z^2\right)\right] \\ &-\frac{F_f^2}{s-m_f^2}\cdot\left[\frac{\left(s-2m_W^2\right)\left(s-2m_Z^2\right)}{24}+\frac{m_W^2m_Z^2s^2}{6m_f^4}\right. \\ &\left.+\frac{\left(m_W^2+m_Z^2\right)s^2-4m_Z^2m_W^2s}{12m_f^2}\right].\end{aligned} \tag{5.40}$$

Terms proportional to $1/m_f^4$ originate from the double derivative acting on the current $J_f^{\mu\nu}$, terms without a suppression by m_f^2 arise due to the coupling to the trace of the current, and the remaining terms suppressed by $1/m_f^2$ indicate mixing between these two contributions. The parameter c_f has to be set to two again to avoid an unphysical behavior from the factor s^4 in the numerator. This would be even worse than in the vector case (5.39). Analogously to the tensor contribution, the remainder of the numerator will rise with s^2, but some terms are proportional to powers of v^2/m_f^2. These terms will be completely neglected, if the amplitude is calculated in the gaugeless limit for Goldstone boson scattering with Feynman rules given in Appendix B.3

$$\begin{aligned}\mathcal{A}_f\left(w^+w^-\to zz\right) = &-\frac{F_f^2}{96}\left(c_f-2\right)^2\frac{s^3}{m_f^4}-\frac{F_f^2}{48}\left(c_f-2\right)c_f\frac{s^2}{m_f^2}\\ &-\frac{F_f^2}{24}\frac{s^2}{s-m_f^2}P_2\left(s,t,u\right)\ ,\end{aligned} \tag{5.41}$$

with $P_2\left(s,t,u\right) = \left[3\left(t^2+u^2\right)-2s^2\right]/s^2$. An approximation of the longitudinal scattering amplitude with the Goldstone boson scattering amplitude, namely the Goldstone boson equivalence theorem, is therefore only valid for small ratios m_Z^2/m_f^2.

Due to the coupling to the derivatives of the scalar and vector degrees of freedom, also amplitudes in channels with transversal polarization rise with the energy of the vector boson scattering system. A full list of these channels in the high energy limit is displayed in Table 5.1. It is manifest that all channels which include at least one transversal polarized vector boson are suppressed by m_W^2/m_f^2 due to the coupling of the vector and/or scalar degrees of freedom. In case of a heavy tensor resonance, all channels beside the purely longitudinal polarized channel can be neglected regardless of the choice of c_f. Therefore, a calculation within the gaugeless limit is sufficient to estimate the high energy behavior for heavy tensor resonances.

$(+,+,+,+)$ $(+,+,-,-)$ $(-,-,+,+)$ $(-,-,-,-)$	$-\frac{c_f^2 m_W^2 m_Z^2}{24 m_f^2} F_f^2 s$
$(+,0,0,+)$ $(0,+,+,0)$ $(0,-,-,0)$ $(-,0,0,-)$	$\frac{m_W m_Z}{8 m_f^2} F_f^2 t$
$(+,0,+,0)$ $(0,+,0,+)$ $(0,-,0,-)$ $(-,0,-,0)$	$\frac{m_W m_Z}{8 m_f^2} F_f^2 u$
$(+,0,-,0)$ $(0,+,0,-)$ $(0,-,0,+)$ $(-,0,+,0)$	$-\frac{m_W m_Z}{8 m_f^2} F_f^2 t$
$(+,0,0,-)$ $(0,+,-,0)$ $(0,-,+,0)$ $(-,0,0,+)$	$-\frac{m_W m_Z}{8 m_f^2} F_f^2 u$
$(+,+,0,0)$ $(-,-,0,0)$	$(c_f-2)c_f \frac{m_W^2}{48 m_f^2} F_f^2 \left(\frac{s^2}{m_f^2} + 2s - 2\frac{m_Z^2}{m_f^2} s\right)$ $+ \frac{m_W^2}{12 m_f^2} F_f^2 \left(1 + c_f \frac{m_Z^2}{m_f^2}\right) s$
$(0,0,+,+)$ $(0,0,-,-)$	$(c_f-2)c_f \frac{m_Z^2}{48 m_f^2} F_f^2 \left(\frac{s^2}{m_f^2} + 2s - 2\frac{m_W^2}{m_f^2} s\right)$ $+ \frac{m_Z^2}{12 m_f^2} F_f^2 \left(1 + c_f \frac{m_W^2}{m_f^2}\right) s$
$(0,0,0,0)$	$-\frac{c_f-2}{96 m_f^4} F_f^2 \left[(c_f-2)s^3 - 2(c_f-4)\left(m_w^2 + m_Z^2\right)s^2 + 4(c_f-6)m_W^2 m_Z^2 s\right]$ $-\frac{\left(c_f-2\right)c_f}{48 m_f^2} F_f^2 \left[s^2 - 2\left(m_W^2 + m_Z^2\right)s\right]$ $-\frac{1}{24} F_f^2 \left[P_2\left(\cos\left(\Theta\right)\right) + 2\frac{m_W^2 + m_Z^2}{m_f^2} + 4\frac{m_W^2 m_Z^2}{m_f^4}\right] s$

Table 5.1.: High energy limit of the $W^+W^- \to ZZ$ amplitude for each polarization channel that rises with energy due to a isoscalar-tensor resonance.

5.3.4. Goldstone Boson Amplitudes

Choosing $c_f = 2$, the amplitude will rise asymptotically proportional to s/m_f^2 only, because the remaining s^2 term cancels partially with the denominator. Qualitatively, this is similar to a scalar resonance. Assuming a heavy tensor resonance, the high-energy behavior of the amplitude for all weak boson/Higgs channels is given by the Goldstone boson/Higgs amplitudes in the gaugeless limit without having to account for transversal gauge bosons

$$\mathcal{A}_f\left(w^\pm w^\pm \to w^\pm w^\pm\right) = -\frac{1}{24}{F_f}^2\left(\frac{t^2}{t-m_f^2}P_2(t,s,u) + \frac{u^2}{u-m_f^2}P_2(u,s,t)\right), \tag{5.43a}$$

$$\left.\begin{aligned}&\mathcal{A}_f\left(w^\pm z \to w^\pm z\right)\\ &\mathcal{A}_f\left(hw^\pm \to hw^\pm\right)\\ &\mathcal{A}_f\left(hz \to hz\right)\end{aligned}\right\} = -\frac{1}{24}{F_f}^2\frac{t^2}{t-m_f^2}P_2\left(t,s,u\right), \tag{5.43b}$$

$$\mathcal{A}_f\left(w^\pm w^\mp \to w^\pm w^\mp\right) = -\frac{1}{24}{F_f}^2\left(\frac{s^2}{s-m_f^2}P_2(s,t,u) + \frac{t^2}{t-m_f}P_2(t,s,u)\right), \tag{5.43c}$$

$$\left.\begin{aligned}&\mathcal{A}_f\left(w^\pm w^\mp \to zz\right)\\ &\mathcal{A}_f\left(hh \to w^\pm w^\mp\right)\\ &\mathcal{A}_f\left(hh \to zz\right)\end{aligned}\right\} = -\frac{1}{24}{F_f}^2\frac{s^2}{s-m_f^2}P_2\left(s,t,u\right), \tag{5.43d}$$

$$\left.\begin{aligned}\mathcal{A}_f\left(zz \to zz\right)\\ \mathcal{A}_f\left(hh \to hh\right)\end{aligned}\right\} = -\frac{1}{24}{F_f}^2\left(\frac{s^2}{s-m_f^2}P_2(s,t,u) + \frac{t^2}{t-m_f^2}P_2(t,s,u) + \frac{u^2}{u-m_f^2}P_2(u,s,t)\right). \tag{5.43e}$$

For a correct numerical calculation, Breit-Wigner propagators with an additional term $+im_f\Gamma_f\Theta\left(p^2\right)$ in the denominator are used analogously to (5.5). When determining the matrix element of the decay of a tensor resonance, a factor $1/5$ has to be added for summing over the five possible physical polarization states

$$\begin{aligned}\Gamma_f\left(m_f\right) &= \int d\Omega\frac{\left|\vec{p}\right|}{32\pi^2 m_f^2}\left(\left|\mathcal{M}_{f\to w^+w^-}\right|^2 + \frac{1}{2}\left|\mathcal{M}_{f\to zz}\right|^2 + \frac{1}{2}\left|\mathcal{M}_{f\to hh}\right|^2\right)\\ &= \frac{m_f^3}{960\pi}F_f^2\,.\end{aligned} \tag{5.44}$$

5.3.5. Effective Field Theory Matching

In the case of a heavy resonance beyond experimental reach, only the rise of the resonance can be measured. This rise can be modeled analogously to the scalar resonance by higher dimensional operators. However, dimension ten and twelve operators would also be needed to describe the couplings to derivatives (5.36) and double derivatives (5.37) of the tensor current.

As discussed above, all of these contributions are additionally suppressed by higher powers of m_f when choosing $c_f = 2$. In this case, only the contributions of the scalar coupling to the trace of the current and the tensor coupling to the current have to be accounted for. Using the formulation (5.9) for both scalar and tensor, the effective Lagrangian with the tensor resonance integrated out reads

$$\mathcal{L}_f^{\text{eff}} = \frac{1}{2m_X^2}\left(\text{tr}\left[J_{f\mu\nu}\right]\text{tr}\left[J_f^{\mu\nu}\right] - \frac{1}{3}\text{tr}\left[J_{f\rho}^{\rho}\right]^2\right). \tag{5.45}$$

The latter term originates from the scalar contribution coupling to the trace of the current $J_f^{\mu\nu}$ and the ghost contributions of the tensor trace. Using equation (5.45), the tensor resonance can be matched in the low energy limit to an effective field theory parameterized by the dimension eight operators $\mathcal{L}_{S,0}$ and $\mathcal{L}_{S,1}$ defined in (3.37) with

$$F_{S,0} = \frac{F_f^2}{2m_f^2}, \tag{5.46a}$$

$$F_{S,1} = -\frac{F_f^2}{6m_f^2}. \tag{5.46b}$$

The tensor resonance will eventually violate unitarity at a certain energy regardless of the choice of c_f, and the T-matrix unitarization as described in section (4.5) is necessary to receive a theoretical valid description at high energies. However, the allowed values of resonance masses are restricted such that the Stückelberg terms discussed above remain numerically small within some finite energy range. Outside this range, the Higgs-Goldstone sector cannot be separated from the theory, and the vector boson scattering amplitudes are sensitive to unknown strong interactions that involve all channels of longitudinal, transversal, and Higgs exchange simultaneously. A different implementation of the T-matrix unitarization scheme (4.64) is necessary in that situation.

5.3.6. Isospin-Spin Amplitudes

In this thesis, contributions which influence only the Higgs-Goldstone sector are examined. Analogously, to the unitarization of the effective field theory, a projection of the T-matrix algorithm onto the isospin-spin eigenamplitudes can be used. The Goldstone boson scattering amplitude (5.41) is used for the decomposition into isospin-spin eigenamplitudes for the spin two resonance

$$\begin{aligned}
\mathcal{A}_{00} =& -\frac{1}{12}F_f^2\mathcal{D}_0\left(s,m_f\right) \\
&-\frac{11}{144}c_f\left(c_f-2\right)F_f^2\frac{s^2}{m_f^2}-\frac{5}{192}\left(c_f-2\right)^2F_f^2\frac{s^3}{m_f^4}\,, && (5.47a)\\
\mathcal{A}_{02} =& -\frac{1}{40}F_f^2\frac{s^2}{s-m_f^2+\mathrm{i}m_f\Gamma_f}-\frac{1}{12}F_f^2\left(1+6\frac{s}{m_f^2}+6\frac{s^2}{m_f^4}\right)\mathcal{S}_2\left(s,m_f\right) \\
&-\frac{1}{720}c_f\left(c_f-2\right)F_f^2\frac{s^2}{m_f^2}+\frac{1}{960}\left(c_f-2\right)^2F_f^2\frac{s^3}{m_f^4}\,, && (5.47b)\\
\mathcal{A}_{11} =& -\frac{1}{12}F_f^2\mathcal{D}_1\left(s,m_f\right) \\
&+\frac{1}{144}c_f\left(c_f-2\right)F_f^2\frac{s^2}{m_f^2}-\frac{1}{320}\left(c_f-2\right)^2F_f^2\frac{s^3}{m_f^4}\,, && (5.47c)\\
\mathcal{A}_{13} =& -\frac{1}{12}F_f^2\left(1+6\frac{s}{m_f^2}+6\frac{s^2}{m_f^4}\right)\mathcal{S}_3\left(s,m_f\right) \\
&-\frac{1}{6720}\left(c_f-2\right)^2F_f^2\frac{s^3}{m_f^4}\,, && (5.47d)\\
\mathcal{A}_{20} =& -\frac{1}{12}F_f^2\mathcal{D}_0\left(s,m_f\right) \\
&-\frac{1}{72}c_f\left(c_f-2\right)F_f^2\frac{s^2}{m_f^2}+\frac{1}{192}\left(c_f-2\right)^2F_f^2\frac{s^3}{m_f^4}\,, && (5.47e)\\
\mathcal{A}_{22} =& -\frac{1}{12}F_f^2\left(1+6\frac{s}{m_f^2}+6\frac{s^2}{m_f^4}\right)\mathcal{S}_2\left(s,m_f\right) \\
&-\frac{1}{720}c_f\left(c_f-2\right)F_f^2\frac{s^2}{m_f^2}+\frac{1}{960}\left(c_f-2\right)^2F_f^2\frac{s^3}{m_f^4}\,. && (5.47f)
\end{aligned}$$

Using the implementation via isospin-spin eigenamplitudes in the gaugeless limit (see Section 4.4.1) for the T-matrix scheme will not guarantee unitarity for all energies. The longitudinal on-shell amplitude (5.40) of the scalar degrees of freedom would still rise due to the double derivative contributions (5.37) like a scalar resonance with the coupling

$$F_\sigma = 2\sqrt{\frac{m_W^2+m_Z^2}{12m_f^2}+\frac{m_W^2m_Z^2}{6m_f^4}}F_f = \sqrt{\frac{2}{3}}\frac{m_{whz}\left(m_f\right)}{m_f}F_f\,. \tag{5.48}$$

For the generalization to arbitrary $2 \to 2$ scattering processes involving gauge/Higgs bosons with mass m_i, the parameter m_{whz} is introduced

$$m_{whz}^2\left(m_f\right) = \sum_{i=1}^{4} \frac{m_i^2}{4} + \frac{\prod_{i=1}^{4} m_i}{m_f^2}\,. \tag{5.49}$$

The high energy behavior of the scalar will violate the unitarity of the S-matrix eventually. As discussed in Section 4.4, the isospin-spin eigenamplitudes are constrained by (4.31). Taking the leading high energy terms into account, the eigenamplitudes $\mathcal{A}_{00}$ and $\mathcal{A}_{20}$ of a scalar resonance (5.12) give the strongest bound

$$\sqrt{s} \leq \left(\frac{192\pi}{m_{whz}^2\left(m_f\right) F_f^2}\right)^{\frac{1}{2}}\,. \tag{5.50}$$

Rewriting the coupling F_f in terms of the width of the tensor using (5.44), the tensor description in the T-matrix implementation as described in Section 4.4.1 is only valid up to invariant masses of the boson scattering system of

$$\sqrt{s} \lesssim \sqrt{\frac{1}{5}\frac{m_f}{\Gamma_f}}\frac{m_f^2}{m_{whz}\left(m_f\right)}\,. \tag{5.51}$$

In case of a broad tensor resonance with mass $m_f = 1\,\text{TeV}$ and a width of $\Gamma_f = 0.5\,\text{TeV}$, the theoretical description can only be used up to an invariant mass of $\sqrt{s} \sim 5\,\text{TeV}$ for quasi-elastic Higgs-Higgs scattering. The description for a weak vector boson scattering process with an exchange of a 1 TeV tensor resonance and a more realistic width of $\Gamma_f = 0.1\,\text{TeV}$ does not break down until an invariant WW-mass of $\sim 15.6\,\text{TeV}$. Thus, the T-matrix implementation using the gaugless Goldstone boson scattering amplitudes is sufficient for a study of heavy tensor resonances ($m_f \gtrsim 1$ TeV) within the reach of a 14 TeV proton-proton collider.

5.4. Isotensor-Scalar Resonances

The couplings of the isotensor-scalar are analogously to the isoscalar-scalar case introduced in Section 5.2 assumed to couple only to the Goldstone boson/Higgs sector via two Higgs-field derivatives $\mathbf{D}^\mu\mathbf{H}$. However, the resonance with chiral $SU(2)_L \times SU(2)_R$ quantum numbers $(1,1)$ has nine degrees of freedom. In the chiral representation, these nine degrees of freedom can be represented as the tensor Φ^{ab} with the indices $a, b \in \{1,2,3\}$. Hence, the Lagrangian describing the a isotensor resonance in the Goldstone/Higgs boson sector can be written as

$$\mathcal{L}_\Phi = \frac{1}{2}\partial_\mu \Phi^{ab}\partial_\mu \Phi^{ab} - \frac{m_\Phi^2}{2}\Phi^{ab}\Phi^{ab} + J_\Phi^{ab}\Phi^{ab}\,, \tag{5.52}$$

where the current has a $SU(2)_L$ and a $SU(2)_R$ index

$$J^{ab}_{\Phi} = F_{\phi}\mathrm{tr}\left[\left(\mathbf{D}_{\mu}\mathbf{H}\right)^{\dagger}\tau^{a}\mathbf{D}^{\mu}\mathbf{H}\tau^{b}\right]. \tag{5.53}$$

Analogously to the isoscalar case, the coupling F_{ϕ} is suppressed by a new physics scale Λ. To expose the coupling structure to the Goldstone/Higgs boson sector, the current can be expanded in the gaugeless limit

$$\begin{aligned}\mathrm{tr}\left[\left(\mathbf{D}_{\mu}\mathbf{H}\right)^{\dagger}\tau^{a}\mathbf{D}^{\mu}\mathbf{H}\tau^{b}\right] =& \frac{1}{2}\left(\partial_{\mu}h\partial^{\mu}h - \partial_{\mu}w^{i}\partial^{\mu}w^{i}\right)\delta^{ab} - \partial_{\mu}w^{i}\partial^{\mu}h\varepsilon^{abi} \\ &+ \partial_{\mu}w^{a}\partial^{\mu}w^{b}\,.\end{aligned} \tag{5.54}$$

Here, the decomposition into isotensor, isovector and isoscalar is already manifest. The first term proportional to δ^{ab} couples to the isoscalar. A pair of Higgs bosons interact only with the isoscalar degrees of freedom, whereas the second term contains a mixing of the Higgs and the Goldstone boson. Its proportionality to the Levi-Civita symbol indicates the coupling to an isovector. The third term involves only Goldstone bosons and is associated with the coupling to an isotensor. The coupling of the isoscalar to two Goldstone bosons could also be reformulated analogously to the spin two case as a coupling to the isotensor trace. Without the Higgs, four degrees of freedom of the nonet will vanish, namely the isoscalar and the isovector. Therefore, the resonance with quantum number $(1,1)$ can be represented completely by an isotensor [142].

The resonance Φ^{ab} can be formulated in a basis of tensor products of $SU(2)$ generators which are related to the decomposition

$$\mathbf{1}\otimes\mathbf{1} = \mathbf{2} + \mathbf{1} + \mathbf{0}\,, \tag{5.55}$$

where the associated orthonormal eigenvectors are evaluated via Clebsch-Gordon decomposition. Using this basis, the resonance Φ^{ab} is rewritten in terms of its $SU(2)_C$ components

$$\Phi^{ab} \to \Phi_t + \Phi_v + \Phi_s \tag{5.56}$$

with

$$\Phi_t = \phi_t^{++}\tau_t^{++} + \phi_t^{+}\tau_t^{+} + \phi_t^{0}\tau_t^{0} + \phi_t^{-}\tau_t^{-} + \phi_t^{--}\tau_t^{--}\,, \tag{5.57a}$$

$$\Phi_v = \phi_v^{+}\tau_v^{+} + \phi_v^{0}\tau_v^{0} + \phi_v^{-}\tau_v^{-}\,, \tag{5.57b}$$

$$\Phi_s = \phi_s\tau_s\,. \tag{5.57c}$$

A complete definition of the isospin basis τ_t, τ_v and τ_s is given in the Appendix A.1. All nine degrees of freedom are identified as unique particles, which do not mix with each other due to orthogonality. An equivalent Lagrangian to (5.52) can now be formulated in terms of the $SU(2)_C$ basis

$$\mathcal{L}_{\phi} = \frac{1}{2}\sum_{i=s,v,t}\mathrm{tr}\left[\partial_{\mu}\Phi_i\partial^{\mu}\Phi_i - m^2_{\Phi}\Phi_i^2\right] + \mathrm{tr}\left[\left(\Phi_t + \frac{1}{2}\Phi_v - \frac{2}{5}\Phi_s\right)J_{\phi}\right], \tag{5.58a}$$

$$\text{where}\qquad J_{\phi} = F_{\phi}\left(\left(\mathbf{D}_{\mu}\mathbf{H}\right)^{\dagger}\otimes\mathbf{D}^{\mu}\mathbf{H} + \frac{1}{8}\mathrm{tr}\left[\left(\mathbf{D}_{\mu}\mathbf{H}\right)^{\dagger}\mathbf{D}^{\mu}\mathbf{H}\right]\right)\tau^{aa}\,. \tag{5.58b}$$

In absence of the Higgs boson, the coefficient of the second term is chosen in such a way, that the trace of the current vanishes. In this scenario, the isovector and isoscalar degrees of freedom decouple from the model and only the isotensor is needed to describe this resonance. However, including a Higgs the Lagrangian (5.58) guarantees the amplitude relation between the Higgs and Goldstone bosons introduced in Section 4.3.

5.4.1. Goldstone Boson Amplitudes

The crossing relations are manifest in the scattering amplitudes for the Goldstone/Higgs boson, which are determined in the gaugeless limit via the Feynman rules given in the Appendix B.3

$$\mathcal{A}_\phi\left(w^\pm w^\pm \to w^\pm w^\pm\right) = -\frac{{F_\phi}^2}{8}\left(2\frac{s^2}{s-m_\phi^2} + \frac{1}{2}\frac{u^2}{u-m_\phi^2} + \frac{1}{2}\frac{t^2}{t-m_\phi^2}\right), \tag{5.59a}$$

$$\left.\begin{aligned}\mathcal{A}_\phi\left(w^\pm z \to w^\pm z\right)\\ \mathcal{A}_\phi\left(hw^\pm \to hw^\pm\right)\\ \mathcal{A}_\phi\left(hz \to hz\right)\end{aligned}\right\} = \frac{{F_\phi}^2}{8}\left(\frac{1}{2}\frac{t^2}{t-m_\phi^2} - \frac{u^2}{u-m_\phi^2} - \frac{s^2}{s-m_\phi^2}\right), \tag{5.59b}$$

$$\mathcal{A}_\phi\left(w^\pm w^\mp \to w^\pm w^\mp\right) = -\frac{{F_\phi}^2}{8}\left(\frac{1}{2}\frac{s^2}{s-m_\phi^2} + 2\frac{u^2}{u-m_\phi^2} + \frac{1}{2}\frac{t^2}{t-m_\phi^2}\right), \tag{5.59c}$$

$$\left.\begin{aligned}\mathcal{A}_\phi\left(w^\pm w^\mp \to zz\right)\\ \mathcal{A}_\phi\left(hh \to w^\pm w^\mp\right)\\ \mathcal{A}_\phi\left(hh \to zz\right)\end{aligned}\right\} = \frac{{F_\phi}^2}{8}\left(\frac{1}{2}\frac{s^2}{s-m_\phi^2} - \frac{u^2}{u-m_\phi^2} - \frac{t^2}{t-m_\phi^2}\right), \tag{5.59d}$$

$$\left.\begin{aligned}\mathcal{A}_\phi\left(zz \to zz\right)\\ \mathcal{A}_\phi\left(hh \to hh\right)\end{aligned}\right\} = -\frac{3{F_\phi}^2}{16}\left(\frac{s^2}{s-m_\phi^2} + \frac{u^2}{u-m_\phi^2} + \frac{t^2}{t-m_\phi^2}\right). \tag{5.59e}$$

The width $\Gamma_\phi\Theta(s)$ has to be added in the denominator for an s-channel exchange via the resonance analogously to (5.5). Besides the degenerated mass of isotensor, isovector and isoscalar, also the width of all nine particles is the same

$$\begin{aligned}\Gamma_\phi &= \int d\Omega \frac{|\vec{p}|}{32\pi^2 m_\phi}\left(\left|\mathcal{M}_{\phi_t^0\to w^+w^-}\right|^2 + \frac{1}{2}\left|\mathcal{M}_{\phi_t^0\to zz}\right|^2\right)\\ &= \int d\Omega \frac{|\vec{p}|}{32\pi^2 m_\phi}\left|\mathcal{M}_{\phi_t^\pm\to w^\pm z}\right|^2 = \int d\Omega \frac{|\vec{p}|}{64\pi^2 m_\phi}\left|\mathcal{M}_{\phi_t^{\pm\pm}\to w^\pm w^\pm}\right|^2\\ &= \int d\Omega \frac{|\vec{p}|}{32\pi^2 m_\phi}\left|\mathcal{M}_{\phi_v^0\to zh}\right|^2 = \int d\Omega \frac{|\vec{p}|}{32\pi^2 m_\phi}\left|\mathcal{M}_{\phi_v^\pm\to w^\pm h}\right|^2\\ &= \int d\Omega \frac{|\vec{p}|}{32\pi^2 m_\phi}\left(\left|\mathcal{M}_{\phi_s^0\to w^+w^-}\right|^2 + \frac{1}{2}\left|\mathcal{M}_{\phi_s^0\to hh}\right|^2\right) = \frac{m_\phi^3}{128\pi}F_\phi^2\,.\end{aligned} \tag{5.60}$$

5.4.2. Effective Field Theory Matching

Analogously to the isoscalar case, an isotensor with a high mass can be described by the dimension eight operators $\mathcal{L}_{S,0}$ and $\mathcal{L}_{S,1}$. Determining the impact to these effective field operators is a cross-check of the correct formulation for the Lagrangian (5.58). Integrating out the isotensor resonance in the chiral representation gives contributions proportional to

$$\mathrm{tr}\left[\left(\mathbf{D}_\mu \mathbf{H}\right)^\dagger \tau^a \mathbf{D}^\mu \mathbf{H} \tau^b\right] \mathrm{tr}\left[\left(\mathbf{D}_\mu \mathbf{H}\right)^\dagger \tau^a \mathbf{D}^\mu \mathbf{H} \tau^b\right] . \tag{5.61}$$

In the $SU(2)_C$ eigenbasis, all nine particles are integrated out explicitly and result in the effective Lagrangian

$$\mathcal{L}_\phi^{\text{eff}} = \frac{2}{m_\phi^2}\left[\sum_{\tau=\tau_t^{++},\tau_t^{+},\tau_t^{0},\tau_t^{-},\tau_t^{--}} \mathrm{tr}\left[\tau J_\phi\right]^2 + \frac{1}{4}\sum_{\tau=\tau_v^{+},\tau_v^{0},\tau_v^{-}} \mathrm{tr}\left[\tau J_\phi\right]^2 + \frac{4}{25}\mathrm{tr}\left[\tau_s J_\phi\right]^2\right] . \tag{5.62}$$

Both approaches yield the same matching coefficients for the low energy effective theory operators $\mathcal{L}_{S,0}$ and $\mathcal{L}_{S,1}$ (see eq. (3.37))

$$F_{S,0} = \frac{F_\phi^2}{2m_\phi^2} , \tag{5.63a}$$

$$F_{S,1} = -\frac{F_\phi^2}{8m_\phi^2} . \tag{5.63b}$$

5.4.3. Isospin-Spin Amplitudes

Contrary to the isoscalar resonance (5.12), the isotensor resonance has two isospin-spin channels with a resonant contribution. Besides the expected singular behavior in the $\mathcal{A}_{20}$ channel, the accompanied non-vanishing isoscalar causes a resonant behavior in the $\mathcal{A}_{00}$ amplitude

$$\mathcal{A}_{00} = F_\phi^2\left(-\frac{1}{16}\frac{s^2}{s-m_\phi^2+\mathrm{i}m_\phi\Gamma_\phi} - \frac{7}{8}\mathcal{S}_0\left(s,m_\phi\right)\right) , \tag{5.64a}$$

$$\mathcal{A}_{02} = -\frac{7}{8}F_\phi^2\mathcal{S}_2\left(s,m_\phi\right) , \tag{5.64b}$$

$$\mathcal{A}_{11} = \frac{3}{8}F_\phi^2\mathcal{S}_1\left(s,m_\phi\right) , \tag{5.64c}$$

$$\mathcal{A}_{13} = \frac{3}{8}F_\phi^2\mathcal{S}_3\left(s,m_\phi\right) , \tag{5.64d}$$

$$\mathcal{A}_{20} = F_\phi^2\left(-\frac{1}{4}\frac{s^2}{s-m_\phi^2+\mathrm{i}m_\phi\Gamma_\phi} - \frac{1}{8}\mathcal{S}_0\left(s,m_\phi\right)\right) , \tag{5.64e}$$

$$\mathcal{A}_{22} = -\frac{1}{8}F_\phi^2\mathcal{S}_2\left(s,m_\phi\right) . \tag{5.64f}$$

Due to this unique characteristic, the isotensor particle provides resonant contributions to every vector boson scattering channel, and can be clearly distinguished from an isoscalar resonance.

5.5. Isotensor-Tensor Resonances

To formulate a consistent interaction of the spin two resonance with chiral $SU(2)_L \times SU(2)_R$ quantum numbers $(1,1)$, the insights from the isoscalar-tensor (Section 5.3) and from the isotensor-scalar (Section 5.4) are combined. Each of the five tensor degrees of freedom has nine degrees of freedom associated with the $SU(2)_L \times SU(2)_R$ symmetry group. These 45 components are parameterized by the tensor field $X^{ab}_{\mu\nu}$ with Lorentz indices μ and ν and isospin indices $a, b \in \{1,2,3\}$. Analogously to the isoscalar-tensor resonance, the kinematic properties of the spin two resonance are defined via the Fierz-Pauli Lagrangian

$$\begin{aligned}\mathcal{L}_X =& \frac{1}{2}\partial_\alpha X^{ab}_{\mu\nu}\partial^\alpha X^{\mu\nu}_{ab} - \frac{1}{2}m^2 X^{ab}_{\mu\nu}X^{ab\mu\nu} - \frac{1}{2}\partial_\alpha X^{ab\mu}{}_{\mu}\partial^\alpha X^{ab\nu}{}_{\nu} \\ &+ \frac{1}{2}m^2 X^{ab\mu}{}_{\mu}X^{ab\nu}{}_{\nu} - \partial^\alpha X^{ab}_{\alpha\mu}\partial_\beta X^{ab\beta\mu} - X^{ab\alpha}{}_{\alpha}\partial^\mu\partial^\nu X^{ab}_{\mu\nu} \\ &+ X^{ab}_{\mu\nu}J_X^{ab\mu\nu} \,. \end{aligned} \tag{5.65}$$

The current $J_X^{ab\mu\nu}$ represents the coupling of the isotensor tensor to the Higgs/Goldstone boson sector. Additionally to the isoscalar-tensor current definition (5.33), the current has a $SU(2)_L$ and a $SU(2)_R$ index

$$J_X^{ab\mu\nu} = F_X\left(\mathrm{tr}\left[\left(\mathbf{D}^\mu\mathbf{H}\right)^\dagger \tau^a \mathbf{D}^\nu \mathbf{H}\tau^b\right] - \frac{c_X}{4}g^{\mu\nu}\mathrm{tr}\left[\left(\mathbf{D}_\rho\mathbf{H}\right)^\dagger \tau^a \mathbf{D}^\rho \mathbf{H}\tau^b\right]\right), \tag{5.66}$$

with an arbitrary parameter c_X corresponding to c_f. Consistent with the other resonances, the coupling F_X has mass dimension -1 and is suppressed by a new physics scale Λ. By expanding the first part of the current within the gaugeless limit, it is manifest, that the coupling structure of the isotensor-tensor to the Goldstone/Higgs boson sector is similar to the isotensor-scalar resonance

$$\begin{aligned}\mathrm{tr}\left[\left(\mathbf{D}_\mu\mathbf{H}\right)^\dagger \tau^a \mathbf{D}_\nu \mathbf{H}\tau^b\right] =& \frac{1}{2}\left(\partial_\mu h\partial_\nu h - \partial_\mu w^i\partial_\nu w^i\right)\delta^{ab} - \frac{1}{2}\left(\partial_\mu w^i\partial_\nu h + \partial_\nu w^i\partial_\mu h\right)\varepsilon^{abi} \\ &+ \frac{1}{2}\left(\partial_\mu w^a\partial_\nu w^b + \partial_\mu w^b\partial_\nu w^a\right). \end{aligned} \tag{5.67}$$

Here, the decomposition of the coupling structure into an isoscalar part proportional to δ^{ab}, an isovector part highlighted by ε^{abi} and an isotensor part is manifest. Analogously to the isotensor-scalar, the isotensor-tensor resonance can be rewritten into its $SU(2)_C$ components

$$X^{ab} \to X_t + X_v + X_s \,, \tag{5.68}$$

with the nine single components

$$X_t = X_t^{++}\tau_t^{++} + X_t^{+}\tau_t^{+} + X_t^{0}\tau_t^{0} + X_t^{-}\tau_t^{-} + X_t^{--}\tau_t^{--}\,, \tag{5.69a}$$
$$X_v = X_v^{+}\tau_v^{+} + X_v^{0}\tau_v^{0} + X_v^{-}\tau_v^{-}\,, \tag{5.69b}$$
$$X_s = X_s\tau_s\,. \tag{5.69c}$$

Due to the orthogonality property of the isospin basis, these nine degrees of freedom can be identified as unique tensor particles, which do not mix with each other. Rewriting the interaction Lagrangian (5.65) within the isospin $SU(2)_C$ basis leads to the decomposition into isoscalar(s), isovector(v) and isotensor(t)

$$\begin{aligned}\mathcal{L}_X =& \frac{1}{2}\sum_{i=s,v,t}\mathrm{tr}\Big[\partial_\alpha X_{i\mu\nu}\partial^\alpha X_i^{\mu\nu} - m^2 X_{i\mu\nu}X_i^{\mu\nu} - \partial_\alpha X_{i\ \mu}^{\mu}\partial^\alpha X_{i\ \nu}^{\nu} + m^2 X_{i\ \mu}^{\mu}X_{i\ \nu}^{\nu} \\ &\qquad - 2\partial^\alpha X_{i\alpha\mu}\partial_\beta X_i^{\beta\mu} - 2X_{i\ \alpha}^{\alpha}\partial^\mu\partial^\nu X_{i\mu\nu}\Big] \\ &+ \mathrm{tr}\left[\left(X_{t\mu\nu} + \frac{1}{2}X_{v\mu\nu} - \frac{2}{5}X_{s\mu\nu}\right)J_X^{\mu\nu}\right],\end{aligned} \tag{5.70a}$$

$$\begin{aligned}\text{where}\quad J_X^{\mu\nu} =& F_X\Bigg[\frac{1}{2}\Big((\mathbf{D}^\mu\mathbf{H})^\dagger\otimes\mathbf{D}^\nu\mathbf{H} + (\mathbf{D}^\nu\mathbf{H})^\dagger\otimes\mathbf{D}^\mu\mathbf{H}\Big) - \frac{c_X}{4}g^{\mu\nu}\left(\mathbf{D}_\rho\mathbf{H}\right)^\dagger\otimes\mathbf{D}^\rho\mathbf{H} \\ &+ \frac{1}{8}\Big(\mathrm{tr}\Big[(\mathbf{D}^\mu\mathbf{H})^\dagger\mathbf{D}^\nu\mathbf{H}\Big] - \frac{c_X}{4}g^{\mu\nu}\mathrm{tr}\Big[\left(\mathbf{D}_\rho\mathbf{H}\right)^\dagger\mathbf{D}^\rho\mathbf{H}\Big]\Big)\Bigg]\tau^{aa}\,.\end{aligned} \tag{5.70b}$$

The coefficient of the last term of the current is chosen in such a way, that the relations between the Higgs and Goldstone bosons introduced in Section 4.3 are guaranteed. In a Higgs-less scenario, this coefficient can be chosen such, that the current becomes traceless. Analogously to the scalar resonance, the isovector and isoscalar components would decouple and the interaction can be described with a pure isotensor resonance.

In analogy to the isoscalar-tensor, the spin two degrees of freedom can be decomposed via the Stückelberg formalism into a scalar (σ_i), vector (A_i) and tensor (X_i) component

$$\begin{aligned}\mathcal{L}_{X'} =& \frac{1}{2}\sum_{i=s,v,t}\mathrm{tr}\Big[X'_{i\mu\nu}\left(-\partial^2 - m_X^2\right)X_i'^{\mu\nu} + X'^{\mu}_{i\mu}\left(-\frac{1}{2}\left(-\partial^2 - m_X^2\right)\right)X'^{\nu}_{i\nu} \\ &\qquad + A_{i\mu}\left(-\partial^2 - m_X^2\right)A_i^\mu + \sigma_i\left(-\partial^2 - m_X^2\right)\sigma_i\Big] \\ &+ \mathrm{tr}\Bigg[\left(X'_{t\mu\nu} - \frac{g^{\mu\nu}}{\sqrt{6}}\sigma_t + \frac{\partial_\mu A_{t\nu} + \partial_\nu A_{t\mu}}{\sqrt{2}m_X} + \frac{\sqrt{2}}{\sqrt{3}m_X^2}\partial_\mu\partial_\nu\sigma_t\right)J_X^{\mu\nu} \\ &\quad + \frac{1}{2}\left(X'_{v\mu\nu} - \frac{g^{\mu\nu}}{\sqrt{6}}\sigma_v + \frac{\partial_\mu A_{v\nu} + \partial_\nu A_{v\mu}}{\sqrt{2}m_X} + \frac{\sqrt{2}}{\sqrt{3}m_X^2}\partial_\mu\partial_\nu\sigma_v\right)J_X^{\mu\nu} \\ &\quad - \frac{2}{5}\left(X'_{s\mu\nu} - \frac{g^{\mu\nu}}{\sqrt{6}}\sigma_s + \frac{\partial_\mu A_{s\nu} + \partial_\nu A_{s\mu}}{\sqrt{2}m_X} + \frac{\sqrt{2}}{\sqrt{3}m_X^2}\partial_\mu\partial_\nu\sigma_s\right)J_X^{\mu\nu}\Bigg],\end{aligned} \tag{5.71}$$

with $i = \{s, v, t\}$. In this representation all reducible 81 degrees of freedom of an isotensor-tensor resonance are shown. The properties of the additional Stückelberg components were thoroughly analyzed in Section 5.3 and can be analogously transfered to the isotensor-tensor resonance.

5.5.1. Goldstone Boson Amplitudes

Starting with the Goldstone boson scattering $ww \to zz$ amplitude in the gaugeless limit for arbitrary c_X, the contributions of the scalar degrees of freedom are identified by their $1/m_X^2$ suppression

$$\begin{aligned}\mathcal{A}_X\left(w^\pm w^\mp \to zz\right) = &(c_X-2)^2 \frac{{F_X}^2}{384 m_X^4}\left(s^3-2t^3-2u^3\right)\\ &+ (c_X-2)\, c_X \frac{{F_X}^2}{192 m_X^2}\left(s^2-2t^2-2u^2\right)\\ &+ \frac{F_X^2}{96}\left(\frac{s^2}{s-m_X^2}P_2(s,t,u) - \frac{2t^2}{t-m_X^2}P_2(t,s,u)\right.\\ &\left. - \frac{2u^2}{u-m_X^2}P_2(u,s,t)\right).\end{aligned} \tag{5.72}$$

The Feynman rules used in the calculation are given in Appendix B.3. As discussed in Section 5.3, the parameter c_X is set to $c_X = 2$ to avoid these divergent terms proportional to s^3 and s^2. Thus, the isotensor-tensor resonance rises only proportional to s similar to the dimension six operator. The scattering amplitudes for all Goldstone/Higgs boson scattering channels read

$$\begin{aligned}\mathcal{A}_X\left(w^\pm w^\pm \to w^\pm w^\pm\right) = &-\frac{{F_X}^2}{96}\left(\frac{4s^2}{s-m_X^2}P_2(s,t,u) + \frac{t^2}{t-m_X^2}P_2(t,s,u)\right.\\ &\left. + \frac{u^2}{u-m_X^2}P_2(u,s,t)\right),\end{aligned} \tag{5.73a}$$

$$\left.\begin{aligned}&\mathcal{A}_X\left(w^\pm z \to w^\pm z\right)\\ &\mathcal{A}_X\left(hw^\pm \to hw^\pm\right)\\ &\mathcal{A}_X\left(hz \to hz\right)\end{aligned}\right\} = \frac{{F_X}^2}{96}\left(-\frac{2s^2}{s-m_X^2}P_2(s,t,u) + \frac{t^2}{t-m_X^2}P_2(t,s,u)\right.$$
$$\left. - \frac{2u^2}{u-m_X^2}P_2(u,s,t)\right), \tag{5.73b}$$

$$\begin{aligned}\mathcal{A}_X\left(w^\pm w^\mp \to w^\pm w^\mp\right) = &-\frac{{F_X}^2}{96}\left(\frac{s^2}{s-m_X^2}P_2(s,t,u) + \frac{t^2}{t-m_X^2}P_2(t,s,u)\right.\\ &\left. + \frac{4u^2}{u-m_X^2}P_2(u,s,t)\right),\end{aligned} \tag{5.73c}$$

$$\left.\begin{array}{l}\mathcal{A}_X\left(w^\pm w^\mp \to zz\right)\\ \mathcal{A}_X\left(hh \to w^\pm w^\mp\right)\\ \mathcal{A}_X\left(hh \to zz\right)\end{array}\right\} = \frac{{F_X}^2}{96}\left(\frac{s^2}{s-m_X^2}P_2\left(s,t,u\right) - \frac{2t^2}{t-m_X^2}P_2\left(t,s,u\right) - \frac{2u^2}{u-m_X^2}P_2\left(u,s,t\right)\right), \tag{5.73d}$$

$$\left.\begin{array}{l}\mathcal{A}_X\left(zz \to zz\right)\\ \mathcal{A}_X\left(hh \to hh\right)\end{array}\right\} = -\frac{1}{32}{F_X}^2\left(\frac{s^2}{s-m_X^2}P_2\left(s,t,u\right) + \frac{t^2}{t-m_X^2}P_2\left(t,s,u\right) + \frac{u^2}{u-m_X^2}P_2\left(u,s,t\right)\right). \tag{5.73e}$$

Equivalent to the other resonances a width $\Gamma_X\Theta(s)$ has to be added in the denominators for the s-channel exchange as described in (5.5). Besides the degenerated mass of isotensor, isovector and isoscalar, the widths of all nine tensor fields coincide to

$$\begin{aligned}\Gamma_X &= \int d\Omega \frac{\left|\vec{p}\right|}{32\pi^2 m_X}\left(\left|\mathcal{M}_{X_t^0\to w^+w^-}\right|^2 + \frac{1}{2}\left|\mathcal{M}_{X_t^0\to zz}\right|^2\right) && (5.74a)\\ &= \int d\Omega \frac{\left|\vec{p}\right|}{32\pi^2 m_X}\left|\mathcal{M}_{X_t^\pm\to w^\pm z}\right|^2 && (5.74b)\\ &= \int d\Omega \frac{\left|\vec{p}\right|}{64\pi^2 m_X}\left|\mathcal{M}_{X_t^{\pm\pm}\to w^\pm w^\pm}\right|^2 && (5.74c)\\ &= \int d\Omega \frac{\left|\vec{p}\right|}{32\pi^2 m_X}\left|\mathcal{M}_{X_v^0\to zh}\right|^2 && (5.74d)\\ &= \int d\Omega \frac{\left|\vec{p}\right|}{32\pi^2 m_X}\left|\mathcal{M}_{X_v^\pm\to w^\pm h}\right|^2 && (5.74e)\\ &= \int d\Omega \frac{\left|\vec{p}\right|}{32\pi^2 m_X}\left(\left|\mathcal{M}_{X_s^0\to w^+w^-}\right|^2 + \frac{1}{2}\left|\mathcal{M}_{X_s^0\to hh}\right|^2\right) && (5.74f)\\ &= \frac{m_X^3}{3840\pi}F_X^2\,. && (5.74g)\end{aligned}$$

The amplitudes calculated in the gaugeless limit represent the high energy behavior only for heavy isotensor-tensor resonances. The corresponding on-shell vector boson scattering amplitude calculated with Feynman rules given in (B.2) possess additional contributions proportional to s and the masses of the involved particles

$$\begin{aligned}\mathcal{A}_X\left(W^\pm W^\mp \to ZZ\right) =& \frac{{F_X}^2}{96}\left(\frac{s^2}{s-m_X^2}P_2\left(s,t,u\right) - \frac{2t^2}{t-m_X^2}P_2\left(t,s,u\right) - \frac{2u^2}{u-m_X^2}P_2\left(u,s,t\right)\right)\\ &+ \frac{{F_X}^2}{24}\frac{m_{whz}^2\left(m_x\right)}{m_X^2}\left(\frac{s^2}{s-m_X^2} - \frac{2t^2}{t-m_X^2} - \frac{2u^2}{u-m_X^2}\right)\\ &- \frac{{F_X}^2}{48}\frac{\left(m_W^2-m_Z^2\right)^2}{m_X^4}\left(\frac{t^2}{t-m_X^2} + \frac{u^2}{u-m_X^2}\right) + \mathcal{O}\left(s^0\right)\,,\end{aligned} \tag{5.75}$$

with mass $m_{whz}(m_x)$ as defined in (5.49). These extra contributions are caused by the scalar degrees of freedom, which couples to the double derivative of the current as shown in the Stückelberg formalism (5.71). Neglecting small terms proportional to the mass difference $|m_W - m_Z|$, the deviation from the gaugeless limit can be described by an isotensor-scalar resonance with the coupling strength

$$F_\phi \approx \sqrt{\frac{2}{3}} \frac{m_{whz}\,(m_x)}{m_X} F_X \,. \tag{5.76}$$

5.5.2. Effective Field Theory Matching

The effects to the dimension eight operators $\mathcal{L}_{S,0}$ and $\mathcal{L}_{S,1}$ by integrating out the resonance are calculated analogously to the isotensor-scalar resonance. Using both definitions of the current (5.53) and (5.70) the results can be cross checked. It is important to consider the contributions of the Lorentz trace of the scalar degrees of freedom and the tensor ghost field, namely the trace of the tensor. The contributions can be easily determined within the chiral representation

$$\begin{aligned} \mathcal{L}_{S,0} + \mathcal{L}_{S,1} \sim \operatorname{tr}\Big[\big(\mathbf{D}_\mu \mathbf{H}\big)^\dagger \tau^a \mathbf{D}_\nu \mathbf{H} \tau^b\Big] \operatorname{tr}\Big[\big(\mathbf{D}^\mu \mathbf{H}\big)^\dagger \tau^a \mathbf{D}^\nu \mathbf{H} \tau^b\Big] \\ - \frac{1}{3}\operatorname{tr}\Big[\big(\mathbf{D}_\mu \mathbf{H}\big)^\dagger \tau^a \mathbf{D}^\mu \mathbf{H} \tau^b\Big] \operatorname{tr}\Big[\big(\mathbf{D}_\nu \mathbf{H}\big)^\dagger \tau^a \mathbf{D}^\nu \mathbf{H} \tau^b\Big] \,. \end{aligned} \tag{5.77}$$

In the $SU(2)_C$, representation all nine tensor fields have to be integrated out

$$\begin{aligned} \mathcal{L}_X^{\text{eff}} = \frac{1}{2m_X^2} \Bigg(& \sum_{\tau=\tau_t^{++},\tau_t^{+},\tau_t^{0},\tau_t^{-},\tau_t^{--}} \operatorname{tr}\Big[\tau J_X^{\mu\nu}\Big]^2 - \frac{1}{3}\operatorname{tr}\Big[\tau J_X^{\rho}{}_{\rho}\Big]^2 \\ & + \sum_{\tau=\tau_v^{+},\tau_v^{0},\tau_v^{-}} \frac{1}{4}\operatorname{tr}\Big[\tau J_X^{\mu\nu}\Big]^2 - \frac{1}{12}\operatorname{tr}\Big[\tau J_X^{\rho}{}_{\rho}\Big]^2 \\ & + \frac{4}{25}\operatorname{tr}\Big[\tau_s J_X^{\mu\nu}\Big]^2 - \frac{4}{75}\operatorname{tr}\Big[\tau_s J_X^{\rho}{}_{\rho}\Big]^2 \Bigg) \,. \end{aligned} \tag{5.78}$$

Both approaches coincide and result in the matching coefficients

$$F_{S,0} = \frac{F_X^2}{24 m_X^2} \,, \tag{5.79a}$$

$$F_{S,1} = -\frac{7 F_X^2}{24 m_X^2} \,. \tag{5.79b}$$

5.5.3. Isospin-Spin Amplitudes

Contrary to the isoscalar resonance (5.47), the isotensor resonance has two isospin-spin channels with a resonance contribution. Beside the expected singular behavior in the $\mathcal{A}_{22}$

channel, the accompanied non-vanishing isoscalar causes a resonant behavior in the $\mathcal{A}_{02}$ amplitude

$$\mathcal{A}_{00} = -\frac{7}{48} F_X^2 \mathcal{D}_0 \left(s, m_X\right) , \tag{5.80a}$$

$$\mathcal{A}_{02} = -\frac{1}{480} F_X^2 \frac{s^2}{s - m_X^2 + \mathrm{i} m_X \Gamma_X} - \frac{7}{48} F_X^2 \left(1 + 6\frac{s}{m_X^2} + 6\frac{s^2}{m_X^4}\right) \mathcal{S}_2 \left(s, m_X\right) , \tag{5.80b}$$

$$\mathcal{A}_{11} = \frac{1}{16} F_X^2 \mathcal{D}_1 \left(s, m_X\right) , \tag{5.80c}$$

$$\mathcal{A}_{13} = \frac{1}{16} F_X^2 \left(1 + 6\frac{s}{m_X^2} + 6\frac{s^2}{m_X^4}\right) \mathcal{S}_3 \left(s, m_X\right) , \tag{5.80d}$$

$$\mathcal{A}_{20} = -\frac{1}{48} F_X^2 \mathcal{D}_0 \left(s, m_X\right) , \tag{5.80e}$$

$$\mathcal{A}_{22} = -\frac{1}{120} F_X^2 \frac{s^2}{s - m_X^2 + \mathrm{i} m_X \Gamma_X} - \frac{1}{48} F_X^2 \left(1 + 6\frac{s}{m_X^2} + 6\frac{s^2}{m_X^4}\right) \mathcal{S}_2 \left(s, m_X\right) . \tag{5.80f}$$

Due to this unique characteristic, the isotensor particle provides resonant contributions to every vector boson scattering channel, and can be clearly distinguished from an isoscalar resonance. However, even with the unitarization scheme describe in Section 4.4.1, the unitarity of a tensor resonance is not guaranteed, because of terms rising with the energy proportional to the masses of the weak bosons. The high energy behavior after unitarization is described by an isotensor-scalar resonance with a determined coupling in (5.76). By studying the unitarity bound of the isospin eigenamplitudes (5.64), the validity of the isotensor-tensor description is constrained by

$$\sqrt{s} \lesssim \sqrt{\frac{1}{30} \frac{m_x}{\Gamma_x}} \frac{m_X^2}{m_{whz}} . \tag{5.81}$$

This bound is stronger than the corresponding one of the isoscalar-tensor resonance (5.51) and the mass of the isotensor resonance needs to be higher in comparison to the isoscalar resonance. For example, a mass of $m_X = 1.4\,\mathrm{TeV}$ and width of $\Gamma_X = 140\,\mathrm{GeV}$ is necessary for an isotensor-tensor resonance description which is valid up to $\sqrt{s} = 12.5\,\mathrm{TeV}$, whereas a isoscalar-tensor resonance with a $m_f = 1\,\mathrm{TeV}$ and $\Gamma_f = 100\,\mathrm{GeV}$ provides a valid description up to $\sqrt{s} = 15.7\,\mathrm{TeV}$ for vector boson scattering processes.

	σ	ϕ	f	X
$F_{S,0}$	$\frac{1}{2}$	2	15	5
$F_{S,1}$	–	$-\frac{1}{2}$	-5	-35

Table 5.2.: Relation of resonance width Γ and mass m to the corresponding dimension eight operator coefficients in the low-energy effective field theory, for all resonance types considered in this thesis. The factors listed in the table have to be multiplied by $32\pi\Gamma/m^5$.

5.6. Physical Processes

For experimental studies, it is insufficient to consider just the contributions of isoscalar-scalar, isoscalar-tensor, isotensor-scalar and isotensor-tensor resonances to on-shell vector boson scattering processes. To provide a tool to investigate the impact of these resonances in physical processes, new models were implemented into `WHIZARD` as part of this thesis. Details about these models and their implementation are given in Appendix C.3. The unitarity of the S-matrix in presence of these resonances without altering the physical content of the model is ensured by applying the T-matrix unitarization as described in Section 4.4.1.

Using the Monte-Carlo integration and event generation package `WHIZARD` the partonic amplitudes can be convoluted with the parton structure functions to compute complete processes including QCD contributions and all irreducible background for the generated final-state partons, not restricted to on-shell final states of W/Z. Furthermore, partons can be showered and hadronized, to produce realistic exclusive event samples.

In this section, some examples for vector boson scattering processes in the presence of resonances for complete events at the LHC will be discussed using `WHIZARD` 2.2.8 r7332 (trunk). Proton-proton induced scattering processes with on-shell vector bosons final states and complete partonic final states will be considered

$$pp \to VVjj\,, \tag{5.82}$$

where V denotes either $W^\pm$ or Z, and jj are two quark-final states, which are detected as jets in forward direction. In proton-proton collisions at 14 TeV, suitable vector boson fusion cuts enhance the signal-to-background ratio for the subprocess $VV \to VV$ significantly, analogously to Section 4.6. The vector boson scattering subprocess obtains contributions from resonance exchange and is affected by unitarization in the limit of high invariant masses of the vector boson scattering system.

Each resonance σ, ϕ, f and X is parameterized by its mass m and its coupling F. Using equations (5.6), (5.44), (5.60) and (5.74) the coupling F is substituted by the width as an experimentally detectable quantity. The physical process in a presence of an actual resonance will also be compared with a matched low energy effective field theory, where the resonances are integrated out. Matching coefficients are given in equations (5.11), (5.46), (5.63) and

(5.79). Combining these equations, the relation between the mass and width of the resonance and the dimension eight coefficients $F_{S,0}$ and $F_{S,1}$ are obtained and listed in Table 5.2.

5.6.1. Numerical Results: On-shell

The study of on-shell vector boson scattering gives first insights into the physical features of the resonance model. In the following, particular parameter sets are chosen, where one resonance at a time is added to the Standard Model contributions, namely an isoscalar-scalar, an isoscalar-tensor, an isotensor-scalar or an isotensor-tensor. All extra higher-dimensional operator coefficients are set to zero. By varying the resonance parameters within reasonable limits, an overview of the expected phenomenology for this generic resonance model will be obtained.

Distributions of the processes will be plotted as function of the invariant mass of the final state vector-boson pair system, which is the energy scale of the actual vector boson scattering process. Standard vector boson fusion cuts for the dijet invariant mass $M_{jj} > 500$ GeV, the jet pseudorapidity distance $\Delta y_{jj} > 2.4$, a minimal jet transverse momentum of $p_T > 20$ GeV and a minimal (and opposite) jet rapidity of $|\eta_j| < 4.5$ are applied to enhance the signal for proton-proton collisions at $\sqrt{s} = 14$ TeV. Final states W^+W^+ and ZZ are especially interesting. The latter is the *golden channel* of vector boson scattering, because the ZZ invariant mass can be reconstructed from the leptonic Z decays. This is not possible for the W^+W^+ final state, but the corresponding same-sign lepton channel has a good signal-to-background ratio. The vector-boson decay branching ratios have not been included in the following on-shell distributions.

Each invariant-mass plot contains the following distributions: the pure Standard Model (black curve), the unitarized resonance model (blue curve) and the unitarized matched low-energy effective field theory (red curve) predictions. Additionally, the unitarity bounds for the appropriate partial wave, extrapolated off-shell by the same algorithm, is displayed as a dashed curve (black). For illustrative purposes, each unitarized case is accompanied by the numerical results of the effective field theory without unitarization (red, dashed) and the resonance with correct width but no further unitarization (blue, dashed).

Isoscalar-Scalar

The simplest case is a isoscalar-scalar resonance. This is a single isolated resonance, as it could arise e.g. as the extra scalar particle in a singlet-doublet Higgs model or as a low-energy signal of a strongly interacting Higgs sector that is neutral under the SM gauge group.

In Figures 5.2a and 5.2b, a moderate mass of $m_\sigma = 800$ GeV with a rather narrow width of $\Gamma_\sigma = 80$ GeV corresponding to a weak coupling is selected. The isolated resonance generates a clear peak in the ZZ channel, while the W^+W^+ channel is barely affected. In the effective field theory approach, the resonance would correspond to a small coefficient $F_{S,1}$, which is two orders of magnitude below the current LHC run I limit [8]. Therefore, the effective field theory is not useful in this case, but the resonance should be detectable with a sufficient luminosity.

Turning to a stronger coupling, the corresponding distributions in the ZZ channel for $m_\sigma = 650$ GeV and $\Gamma_\sigma = 260$ GeV are shown in Figure 5.2c.

In this case, the corresponding effective field theory parameters are within the range that should become accessible at LHC run II. The effective field theory curve (red) appears correctly as the low-energy Taylor expansion of the resonance curve (blue). However, the energy region, where the effective field theory starts to deviate from the Standard Model, already coincides with the resonance peak region. Therefore, a unitarized effective field theory would predict an underestimated amount of events. Beyond the resonance, the effective field theory cannot describe the fall of the curve approaching the Standard Model prediction (black) from above.

Additionally, without unitarization the scalar resonance with a strong coupling would violate unitarity beyond the Breit-Wigner approximation with constant width (blue-dashed curve). This is even worse for the naive effective field theory prediction without unitarization (red-dashed). It is obvious, that this curve heavily overestimates the possible number of events, which is approximately displayed by the unitarity limit (black-dashed) for $\mathcal{A}_{00}$.

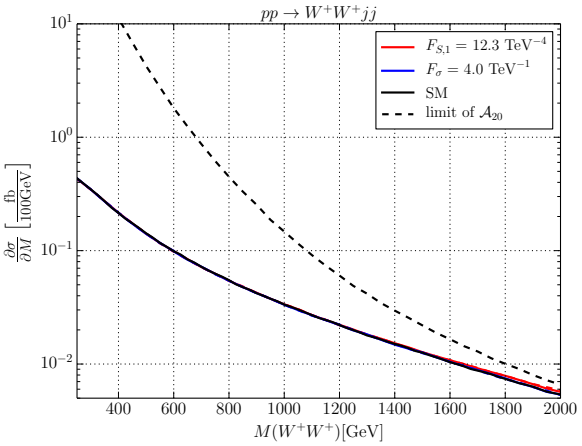

(a) $pp \to W^+W^+jj$, weakly coupled isoscalar-scalar with $m_\sigma = 800\,\text{GeV}$ and $\Gamma_\sigma = 80\,\text{GeV}$.

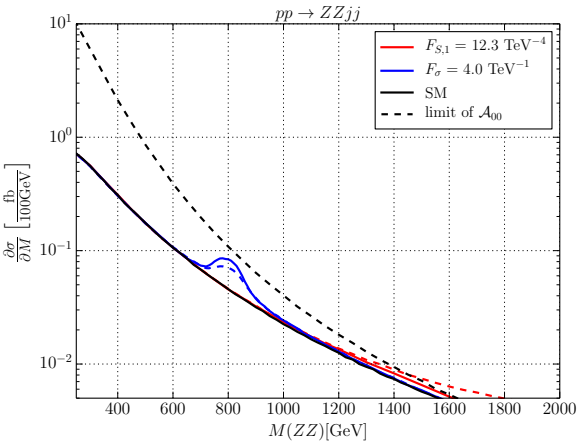

(b) $pp \to ZZjj$, weakly coupled isoscalar-scalar with $m_\sigma = 800\,\text{GeV}$ and $\Gamma_\sigma = 80\,\text{GeV}$.

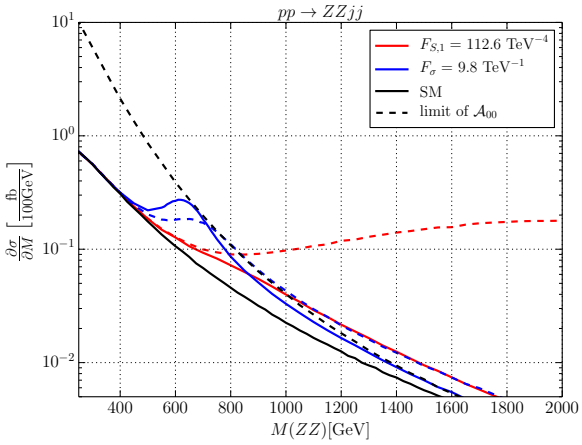

(c) $pp \to ZZjj$, low lying isoscalar-scalar with $m_\sigma = 650\,\text{GeV}$ and $\Gamma_\sigma = 240\,\text{GeV}$.

Figure 5.2.: Differential cross sections of an isoscalar-scalar resonance. Solid line: unitarized results, dashed lines: naive result, black dashed line: limit of saturation of $\mathcal{A}_{20}$ (W^+W^+) / $\mathcal{A}_{00}$ (ZZ). Cuts: $M_{jj} > 500$ GeV; $\Delta\eta_{jj} > 2.4$; $p_T^j > 20$ GeV; $|\eta_j| > 4.5$.

Isoscalar-Tensor

The tensor resonance has a stronger impact on the low-energy effective field theory than the scalar resonance of equal width (see Table 5.2). In Figure 5.3, the invariant mass distribution of tensor resonance with mass $m_f = 1$ TeV and width $\Gamma_f = 100$ GeV and of a strong interacting tensor resonance of $m_f = 1.2$ TeV and width $\Gamma_f = 480$ GeV is shown.

Even at energies below the mass of the tensor, the resonance starts to deviate visibly from the Standard Model. The deviation of the Standard Model is also manifest in the effective field energy approach, because it coincides with the tensor resonance in a wide energy region. However, the excess at the peak in the ZZ channel is sizable and would be neglected. Beyond the resonance, unitarization is essential in the tensor case.

In the W^+W^+ final state, the enhancement due to a t-channel exchange of the tensor resonance, is well described by the corresponding unitarized effective field theory. There is no large deviation between the tensor model and the effective field theory, because W^+W^+ is not resonant for the tensor. As in the scalar case, the models without unitarization do not provide a useful phenomenological description.

For a heavy isoscalar-tensor resonance with a strong coupling, the mass $m_f = 1.2$ TeV and width $\Gamma_f = 480$ GeV is chosen to provide the same Γ/m ratio as the isoscalar-scalar case in Figure 5.2c. Furthermore, this choice of parameters will not violate the unitarity bound of the additional couplings of the scalar degrees of freedom (5.51), which is not considered in the unitarization scheme. The resonance peak in Figure 5.3c appears as a broad enhancement at low and high energies and excesses the unitarity limit of the $\mathcal{A}_{02}$ amplitude, because of the non-unitarized scalar contribution in the isospin-spin 00 channel. Although the actual resonance curve shows a nontrivial threshold structure due to the interplay of all contributing partial waves, the effective field theory approximation is rather accurate in this case. In both models a unitarization scheme is necessary. However, the prediction for such a strong coupling is uncertain in any case.

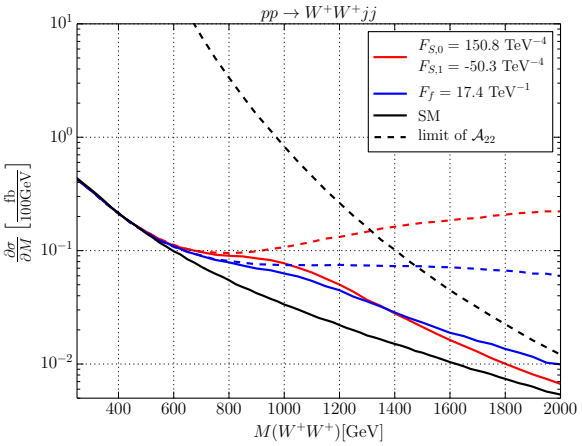

(a) $pp \to W^+W^+jj$, isoscalar-tensor with $m_f = 1000\,\text{GeV}$ and $\Gamma_f = 100\,\text{GeV}$.

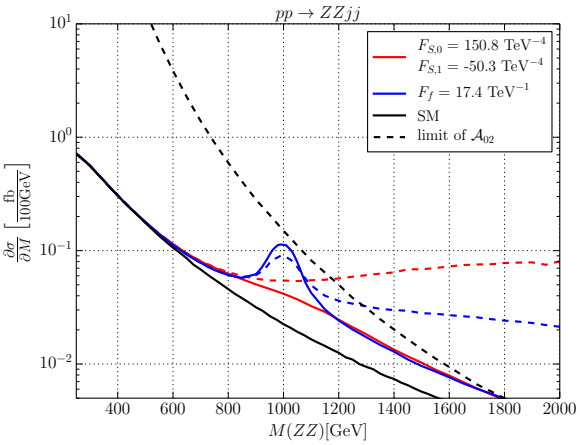

(b) $pp \to ZZjj$, isoscalar-tensor with $m_f = 1000\,\text{GeV}$ and $\Gamma_f = 100\,\text{GeV}$.

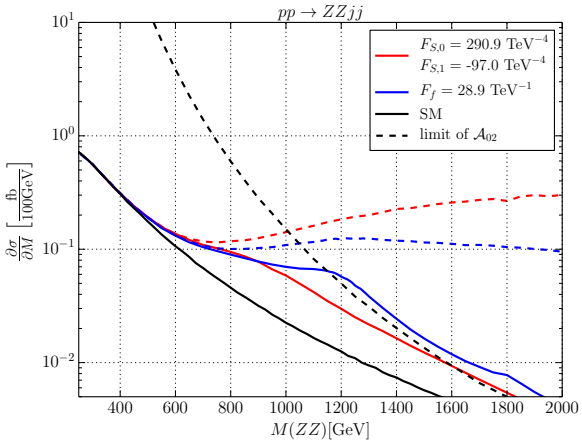

(c) $pp \to ZZjj$, strongly interacting isoscalar-tensor with $m_f = 1200\,\text{GeV}$ and $\Gamma_f = 480\,\text{GeV}$.

Figure 5.3.: Differential cross sections of an isoscalar-tensor resonance. Solid line: unitarized results, dashed lines: naive result, black dashed line: limit of saturation of $\mathcal{A}_{22}$ (W^+W^+) / $\mathcal{A}_{02}$ (ZZ). Cuts: $M_{jj} > 500$ GeV; $\Delta\eta_{jj} > 2.4$; $p_T^j > 20$ GeV; $|\eta_j| > 4.5$.

Isotensor-Scalar

The isotensor-scalar contains resonances in all vector boson scattering channels. As illustrated in Figure 5.4a for the W^+W^+ channel and Figure 5.4b for the the ZZ channel, the distributions of an isotensor-scalar with mass $m_\phi = 800$ GeV and width $\Gamma_\phi = 80$ GeV have a clear peak at the resonance in both channels.

Analogously to the isoscalar-scalar resonance, the effective field theory is not sensitive at energies below the mass of the resonance. Due to the nine scalar degrees of freedom with degenerate masses, the peak of the distribution is rather pronounced. The peak's value is slightly below (W^+W^+) and above (ZZ) the appropriate unitarity limit, because of additional t-channel exchanges in each channel. Even the non-unitarized resonance amplitudes do not violate unitarity and coincide with solid blue curves of the isotensor resonance with additional unitarization. However, in case of the effective field theory approach a unitarization description is necessary as it violates the unitarity bound of $\mathcal{A}_{22}$ for the W^+W^+ channel and $\mathcal{A}_{02}$ for the ZZ channel.

Contrary to the weakly interacting scenario, a non-unitarized low lying and strongly interacting isotensor-scalar with mass of $m_\phi = 650\,\text{GeV}$ and width $\Gamma_\phi = 260\,\text{GeV}$ violates the $\mathcal{A}_{20}$ slightly above the resonance as illustrated in Figure 5.4c. Therefore, a unitarization is needed for this strongly interacting resonance. The low energy effective field theory approach does only coincide in the unitarized case at high energies, because the eigenamplitudes of the isotensor-scalar as well as the dimension eight operators are already saturated through the T-matrix formalism. Although the coupling strength of the matched effective field theory operators are within current bounds of LHC run I, the corresponding isotensor-scalar resonance would have probably been detected.

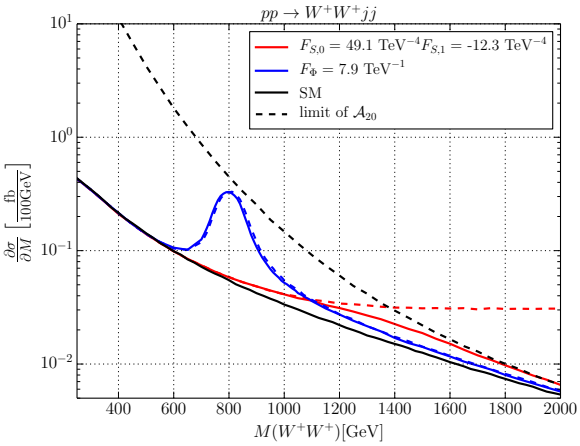

(a) $pp \to W^+W^+jj$, weakly coupled isotensor-scalar with $m_\phi = 800\,\text{GeV}$and $\Gamma_\phi = 80\,\text{GeV}$.

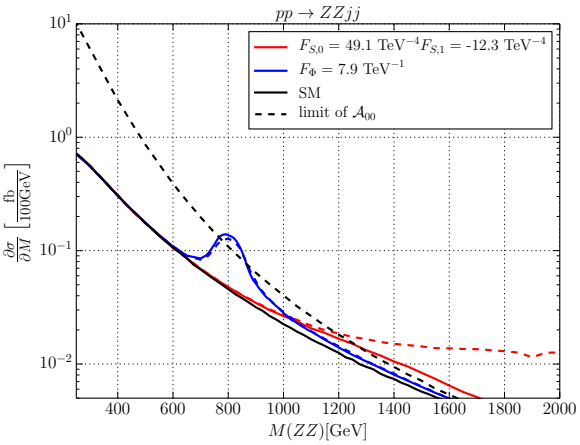

(b) $pp \to ZZjj$, weakly coupled isotensor-scalar with $m_\phi = 800\,\text{GeV}$and $\Gamma_\phi = 80\,\text{GeV}$.

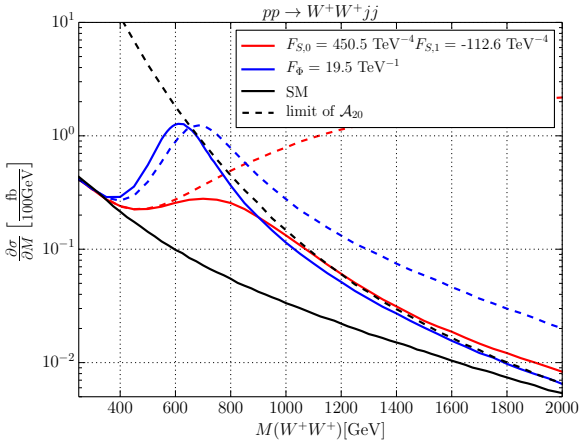

(c) $pp \to W^+W^+jj$, low lying isotensor-scalar with $m_\phi = 650\,\text{GeV}$and $\Gamma_\phi = 240\,\text{GeV}$.

Figure 5.4.: Differential cross sections of an isotensor-scalar resonance.
Solid line: unitarized results, dashed lines: naive result,
black dashed line: limit of saturation of $\mathcal{A}_{20}$ (W^+W^+) / $\mathcal{A}_{00}$ (ZZ).
Cuts: $M_{jj} > 500$ GeV; $\Delta\eta_{jj} > 2.4$; $p_T^j > 20$ GeV; $|\eta_j| > 4.5$.

Isotensor-Tensor

Similarly to the isotensor-scalar, every vector boson scattering channel receives a resonant contribution from the isotensor-tensor multiplet. The W^+W^+ and ZZ channel distributions of the isotensor-tensor resonance with mass $m_X = 1400\,\text{GeV}$ and width $\Gamma_X = 140\,\text{GeV}$ are plotted in Figures 5.5a and 5.5b, respectively. Due to the bound of equation (5.81), the mass of the isotensor-tensor has to be chosen slightly higher than the mass of the isoscalar-tensor in Figure 5.3 when leaving the ratio width and mass invariant.

The effective field theory with the dimension eight operators coincides with the onset of the isotensor-tensor peak. Starting slightly below the resonance, the resonant cross section deviates from the effective field theory description. Analogously to the isotensor-scalar, the very distinctive peak of the isotensor-tensor is not captured by the dimension eight operators. In the W^+W^+- channel, even the non-unitarized resonance contribution stays within the unitarity bound of $\mathcal{A}_{22}$. Contrary to the isotensor-scalar, the isotensor-tensor needs unitarization for the ZZ final state due to the large tensor contributions in the t- and $u-$channel. The non-unitarized amplitudes violate the $\mathcal{A}_{02}$ unitarity already below the mass of the resonance. Even the resonance peak is hardly visible. The unitarized resonance curve shows a peak, although it is slightly above the unitarity bound.

In a strongly interacting scenario ($\Gamma_X = 720\,\text{GeV}$), the unitarized isotensor-tensor resonance peaks below its actual mass at $m_X = 1800\,\text{GeV}$. This peak originates from the already saturated eigenamplitudes, which then falls due to the suppression of the parton distribution functions at high energies. Besides the resonance peak, the low energy effective field theory coincides with the isotensor-tensor for both unitarized and non-unitarized results.

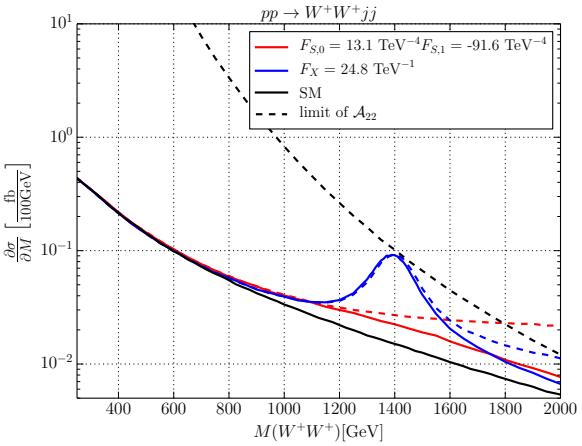

(a) $pp \to W^+W^+jj$, isotensor-tensor with $m_X = 1400\,\text{GeV}$ and $\Gamma_X = 140\,\text{GeV}$.

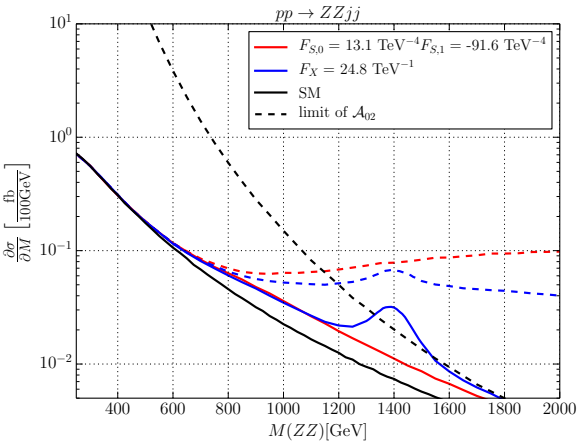

(b) $pp \to ZZjj$, isotensor-tensor with $m_X = 1400\,\text{GeV}$ and $\Gamma_X = 140\,\text{GeV}$.

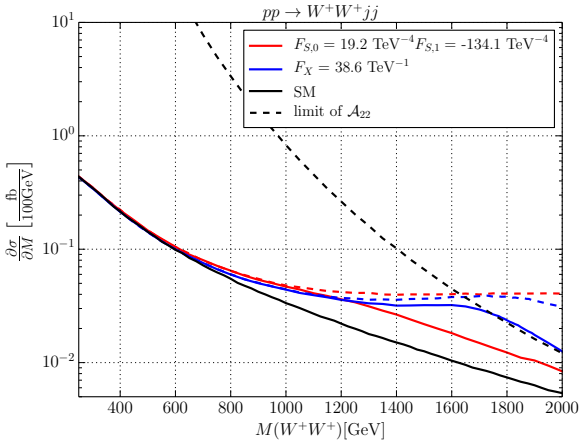

(c) $pp \to W^+W^+jj$, strongly interacting isotensor-tensor with $m_X = 1800\,\text{GeV}$ and $\Gamma_X = 720\,\text{GeV}$.

Figure 5.5.: Differential cross sections of an isotensor-tensor resonance. Solid line: unitarized results, dashed lines: naive result, black dashed line: limit of saturation of $\mathcal{A}_{22}$ (W^+W^+) / $\mathcal{A}_{02}$ (ZZ). Cuts: $M_{jj} > 500$ GeV; $\Delta\eta_{jj} > 2.4$; $p_T^j > 20$ GeV; $|\eta_j| > 4.5$.

5.6.2. Numerical Results: Full Processes

The actual analysis of the LHC data will have to exploit cross sections and distributions for the complete final state which consists of the two jets and the decay products of the vector bosons. A full analysis is beyond the scope of this thesis. To proof the applicability of the introduced methods, an example for a tensor resonance in the ZZ channel with its decay into four leptons, namely $e^+e^-\mu^+\mu^-$, is discussed.

The invariant mass of the four charged lepton final state can be easily determined, but it has a low leptonic branching ratio. For the simulation the high-luminosity mode of the LHC with integrated luminosity of 3 ab^{-1} is assumed. The result should considerably improve when additionally final states like leptonic WW and hadronic final states are taken into account.

The simulation generates event samples for the complete process with all Feynman graphs. There is no restriction that resonant vector bosons are the only origin for final-state leptons. To reduce the background, additional invariant mass cuts for e^+e^- and $\mu^+\mu^-$ are introduced between 80 GeV and 100 GeV to identify Z boson candidates. In Figure 5.6, various distributions for the Standard Model (blue) and a resonance model with a single unitarized isoscalar-tensor (red) are displayed.

As expected, the resonance with $m = 1$ TeV and $\Gamma = 100$ GeV appears in the invariant mass distribution of Figure 5.6. Additionally, the tensor resonance deviates from the Standard Model at high values of the scalar sum transversal momenta p_T of the vector boson candidates. Due to the favored coupling of the tensor resonance to longitudinal vector bosons, a deviation from the Standard Model arises also in the observable $\Delta\Theta^*$, the decay angle of μ^- in the rest frame of the reconstructed muon Z-boson candidate. This parameter set is at the margin of observability. The situation will be improved, if resonances with lower mass, larger coupling or in a higher isospin representation are considered and other analysis channels are added.

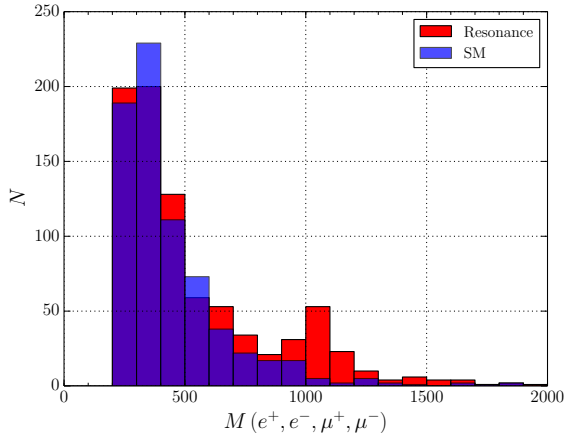

(a) $m\,(Z, Z)$

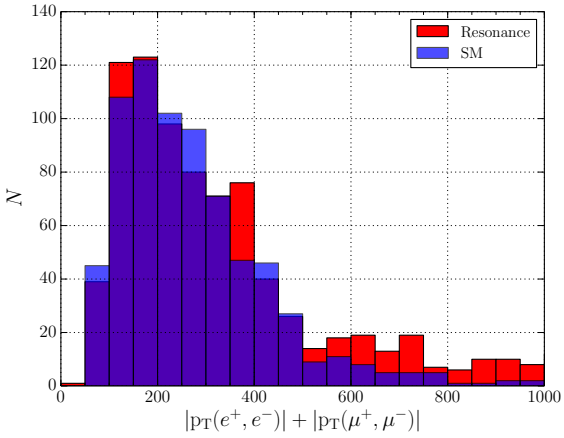

(b) P_t

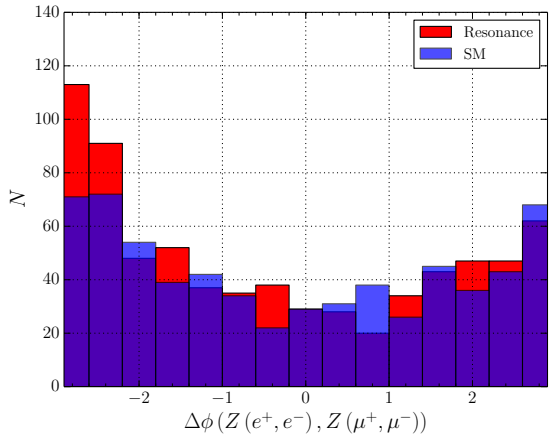

(c) $\Delta\phi$

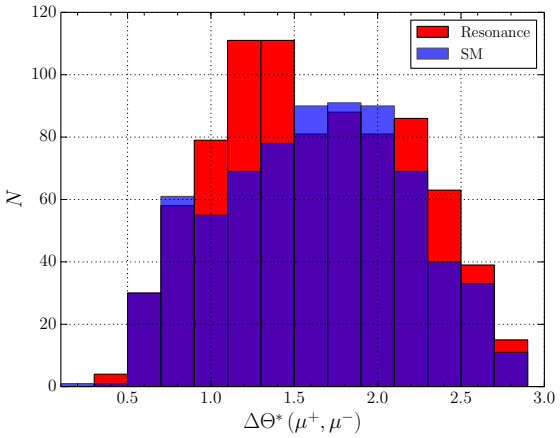

(d) Θ^*

Figure 5.6.: $pp \to e^+e^-\mu^+\mu^- jj$ at $\sqrt{s} = 14\,\text{TeV}$ with luminosity of $3000\,\text{fb}^{-1}$ with isoscalar-tensor at $m_f = 1000$ GeV and Γ_f=100 GeV
Cuts: $M_{jj} > 500$ GeV; $\Delta\eta_{jj} > 2.4$; $p_T^j > 20$ GeV; $|\eta_j| > 4.5$; 100 GeV $> M_{e^+e^-} > 80$ GeV; 100 GeV $> M_{\mu^+\mu^-} > 80$ GeV.

Conclusions

The discovery of a light Higgs boson completed the predicted particle content of the Standard Model and started a new era of experimental studies at the LHC and future colliders, namely the study of the Higgs sector. Vector boson scattering processes are suited to investigate the Higgs sector, because the weakly coupled Standard Model contributions are suppressed by the light Higgs exchange. Therefore, this process is very sensitive to additional new physics effects.

The bottom-up effective field theory formalism provides a model independent framework to quantify new physics contributions in vector boson scattering processes. In case of the Higgs/Goldstone boson sector, the electroweak symmetry $SU(2)_L \times U(1)_Y$ can be extended to the chiral symmetry group $SU(2)_L \times SU(2)_R$ to suppress additional contributions to the $\hat{\rho}$ parameter. A set of CP invariant dimension six and dimension eight operators relevant for vector boson scattering in the Higgs matrix representation has been introduced in Chapter 3. Redundant dimension six operators have been removed from the set to built a minimal dimension six operator basis. Assuming a scenario where new physics in the Higgs/Goldstone boson sector decouples from the fermion and gauge sector in the high energy limit, the impact of the the dimension six operator $\mathcal{L}_{HD}$ and dimension eight operators $\mathcal{L}_{S,0}$ and $\mathcal{L}_{S,1}$ to vector boson scattering processes can be studied separately for complete processes at particle colliders.

However, it has been shown in Chapter 4, that a naive effective field theory study for the dimension eight operators within the sensitivity level of run I at the LHC does not respect basic quantum field theory principles. In particular, it violates the unitarity of the S-matrix. Strong unitarity bounds can be calculated by analyzing effective theory contributions to the isospin-spin amplitudes of vector boson scattering. An exclusion of high invariant masses of the vector boson scattering system, where the effective field theory violates unitarity, is not viable due to the impossibility of experimental energy reconstruction for some final states. Furthermore, the interesting high energy region for possible new physic contribution would be automatically neglected. To provide a consistent description at high energies matching the low energy effective field theory, the direct T-matrix scheme has been introduced in Chapter 4. This framework can be used for any model and will project invalid, non-unitary theoretical descriptions to unitary ones. It has to be considered that the T-matrix unitarization is an arbitrary scheme to restore unitarity of a broken theory model and does not necessary predict the true high energy behavior. As a result, this introduces a model dependence. However, in the valid region of the effective field theory, the T-matrix projection leaves the theoretical prediction invariant and can always be used as a preventive procedure. In particular, the Thales projection T-matrix scheme has been implemented in the Monte-Carlo package `WHIZARD` for longitudinal vector boson/Higgs scattering as described in Section 4.4.1.

Extending the effective field theory by operators with additional resonances allows a more detailed analysis of new physics contributions. Assuming resonances only affect the gauge/Higgs boson sector directly, four resonances have been distinguished by their quantum numbers of the chiral symmetry group $SU(2)_L \times SU(2)_R$ and their spin. All four resonances, namely the isoscalar-scalar σ, the isoscalar-tensor f, the isotensor-scalar ϕ and the isotensor-tensor X, have been discussed in Chapter 5. Each resonance is parameterized by its coupling and its

mass. To avoid an overestimation of the event rates in the high-energy region, the T-matrix unitarization scheme, which can also be used for complex amplitudes, is applied for longitudinal vector boson/Higgs scattering. These resonance models can describe the contributions due to the decoupling limit of multi-Higgs models and certain aspects of massive-graviton models.

In detail, the isoscalar-tensor resonance introduced here does not coincide with the tensor resonance state in massive-graviton models as discussed in the literature. Contrary to these models, the generic tensor considered in this thesis couples mainly to the Higgs sector and therefore to longitudinal vector bosons. Depending on the mass and coupling of the generic tensor, additional interactions of an off-shell tensor to vector bosons arise. Using the Stückelberg procedure, these couplings can be identified with the vector and scalar degree of freedom of the off-shell tensor resonance. It is manifest, that these non-resonant contributions to vector boson scattering processes are suppressed by the mass of the tensor resonance m_W/m_f. Terms proportional to m_W are automatically neglected in the gaugeless limit and are therefore not considered in the implemented `WHIZARD` T-matrix unitarization. However, the description does not violate unitarity for heavy tensors with $m_f \geq 1\,\text{TeV}$ in proton-proton collisions with center of mass energy $\sqrt{s} = 14\,\text{TeV}$ (see (5.51)).

Generic resonances including the T-matrix unitarization have also been implemented into the Monte-Carlo package `WHIZARD` as part of this thesis. Details of the implementation and descriptions of the models can be found in Appendix C.3. Exemplary differential cross section for all resonances have been calculated separately with `WHIZARD` for proton-proton collisions at the LHC and compared with contributions of matched low effective field theory operators, where the resonance has been integrated out. If the resonance is in the reachable energy range of the LHC, the resonance approach is preferable, because the effective field theory can only describe the rise of the resonance. The effective field theory description is insufficient in case of a weakly coupled scalar resonance, where only a deviation from the standard model can be seen at the resonance. However, in case of a strong interacting resonance, the effective field theory coincides sufficiently with the resonance model. In addition to the the pure effective field theory approach the data should also be analyzed using the resonance model. Furthermore, the numerical results of the full processes at the LHC show that resonances could be detected at the LHC within a certain range of mass and coupling values.

In conclusion, this thesis introduced a complete and consistent framework to study new physics in the Higgs sector related to vector boson scattering processes. Additionally, tools for further phenomenological studies at the LHC or other future colliders are provided with the models SSC_2, SSC_AltT and SM_ul, which have been implemented in the public available Monte-Carlo generator `WHIZARD` during this thesis.

Appendices

Chapter A

Mathematical Definitions

A.1. SU(2) Algebra

The generators of the fundamental Isospin-$SU(2)$ representations are the Pauli-matrices τ_1, τ_2, τ_3. Their 2×2 matrix representation reads

$$\tau_1 = \begin{pmatrix} 0 & 1 \\ 1 & 0 \end{pmatrix}, \qquad \tau_2 = \begin{pmatrix} 0 & -\mathrm{i} \\ \mathrm{i} & 0 \end{pmatrix}, \qquad \tau_3 = \begin{pmatrix} 1 & 0 \\ 0 & -1 \end{pmatrix}. \tag{A.1}$$

With the product of two generators obeying

$$\tau_i \tau_j = \delta_{ij} \mathbb{1} + \mathrm{i} \varepsilon_{ijk} \tau_k \tag{A.2}$$

($\varepsilon_{123} = +1$) one can easily calculate the commutator relation

$$\left[\tau_i, \tau_j\right] = 2\mathrm{i} \varepsilon_{ijk} \tau_k, \tag{A.3}$$

the anti-commutator

$$\left\{\tau_i, \tau_j\right\} = 2\delta_{ij} \mathbb{1} \tag{A.4}$$

and the trace of two Pauli matrices

$$\mathrm{tr}\left[\tau_i \tau_j\right] = 2\delta_{ij}. \tag{A.5}$$

The traces of products with more Pauli matrices are then given by

$$\mathrm{tr}\left[\tau_i \tau_j \tau_k\right] = 2\mathrm{i} \varepsilon_{ijk}, \tag{A.6a}$$

$$\mathrm{tr}\left[\tau_i \tau_j \tau_k \tau_l\right] = 2\left(\delta_{ij}\delta_{kl} - \delta_{ik}\delta_{jl} + \delta_{il}\delta_{jk}\right). \tag{A.6b}$$

The following rules for the 3-dimensional Levi-Civita-Tensor are useful

$$\begin{aligned}
\varepsilon_{ijk}\varepsilon_{lmn} =& \begin{vmatrix} \delta_{il} & \delta_{im} & \delta_{in} \\ \delta_{jl} & \delta_{jm} & \delta_{jn} \\ \delta_{kl} & \delta_{km} & \delta_{kn} \end{vmatrix} \\
=& \delta_{il}\delta_{jm}\delta_{kn} + \delta_{im}\delta_{jn}\delta_{kl} + \delta_{in}\delta_{jl}\delta_{km} \\
& - \delta_{in}\delta_{jm}\delta_{kl} - \delta_{im}\delta_{jl}\delta_{kn} - \delta_{il}\delta_{jn}\delta_{km}, && \text{(A.7a)} \\
\varepsilon_{ijk}\varepsilon_{imn} =& \begin{vmatrix} 1 & 0 & 0 \\ 0 & \delta_{jm} & \delta_{jn} \\ 0 & \delta_{km} & \delta_{kn} \end{vmatrix} \\
=& \delta_{jm}\delta_{kn} - \delta_{jn}\delta_{km}, && \text{(A.7b)} \\
\varepsilon_{ijk}\varepsilon_{ijn} =& 2\delta_{kn}, && \text{(A.7c)} \\
\varepsilon_{ijk}\varepsilon_{imn}\varepsilon_{kno} =& \left(\delta_{im}\delta_{jn}\delta_{kl} + \delta_{in}\delta_{jl}\delta_{km} - \delta_{in}\delta_{jm}\delta_{kl} - \delta_{il}\delta_{jn}\delta_{km}\right)\varepsilon_{kno}. && \text{(A.7d)}
\end{aligned}$$

Furthermore, the abbreviations

$$\tau^{\pm} = \frac{1}{2}\left(\tau_1 \pm \mathrm{i}\tau_2\right), \tag{A.8a}$$

$$\tau^{+} = \begin{pmatrix} 0 & 1 \\ 0 & 0 \end{pmatrix}, \tau^{-} = \begin{pmatrix} 0 & 0 \\ 1 & 0 \end{pmatrix} \tag{A.8b}$$

with the commutator relations

$$\frac{1}{2}\left[\tau_3, \tau^{+}\right] = \quad \tau^{+}, \tag{A.9a}$$

$$\frac{1}{2}\left[\tau_3, \tau^{-}\right] = -\tau^{-}, \tag{A.9b}$$

$$\left[\tau^{+}, \tau^{-}\right] = \quad \tau_3 \tag{A.9c}$$

are used.

Dirac Matrices

The Dirac matrices are defined according to the anti commutation relations

$$\{\gamma^{\mu}, \gamma^{\nu}\} = 2g^{\mu\nu}. \tag{A.10}$$

In the chiral basis they can be written as

$$\begin{aligned}
\gamma^{i} &= \begin{pmatrix} 0 & \tau^{i} \\ -\tau^{i} & 0 \end{pmatrix}, \qquad \text{for i} = 1, 2, 3 \\
\gamma^{0} &= \begin{pmatrix} 0 & \mathbb{1} \\ \mathbb{1} & 0 \end{pmatrix}, \qquad \gamma^{5} = \begin{pmatrix} \mathbb{1} & 0 \\ 0 & \mathbb{1} \end{pmatrix}.
\end{aligned} \tag{A.11}$$

Tensor Product

The tensor products of Pauli matrices for the isospin quintet τ_t the isospin singlet τ_v and the isospin scalar τ_s are defined as

$$\tau_t^{++} = \tau^+ \otimes \tau^+, \tag{A.12a}$$

$$\tau_t^{+} = \frac{1}{2}\left(\tau^+ \otimes \tau^3 + \tau^3 \otimes \tau^+\right), \tag{A.12b}$$

$$\tau_t^{0} = \frac{1}{\sqrt{6}}\left(\tau^3 \otimes \tau^3 - \tau^+ \otimes \tau^- - \tau^- \otimes \tau^+\right), \tag{A.12c}$$

$$\tau_t^{-} = \frac{1}{2}\left(\tau^- \otimes \tau^3 + \tau^3 \otimes \tau^-\right), \tag{A.12d}$$

$$\tau_t^{--} = \tau^- \otimes \tau^-, \tag{A.12e}$$

$$\tau_v^{+} = \frac{\mathrm{i}}{2}\left(\tau^+ \otimes \tau^3 - \tau^3 \otimes \tau^+\right), \tag{A.12f}$$

$$\tau_v^{0} = \frac{\mathrm{i}}{\sqrt{2}}\left(\tau^+ \otimes \tau^- - \tau^- \otimes \tau^+\right), \tag{A.12g}$$

$$\tau_v^{-} = -\frac{\mathrm{i}}{2}\left(\tau^- \otimes \tau^3 - \tau^3 \otimes \tau^-\right), \tag{A.12h}$$

$$\tau_s = \frac{1}{2\sqrt{3}}\left(\tau^3 \otimes \tau^3 + 2\tau^+ \otimes \tau^- + 2\tau^- \otimes \tau^+\right), \tag{A.12i}$$

where the Pauli matrix for the isospin singlet is related to

$$\tau^{aa} \equiv \tau^a \otimes \tau^a = 2\sqrt{3}\tau_s\,. \tag{A.13}$$

Here, the Einstein summation convention is implied to sum over the tensor product of the Pauli matrices ($a = 1, 2, 3$). All nonzero traces of products of two tensor products are normalized

$$\mathrm{tr}\left[\tau_t^{++}\tau_t^{--}\right] = \mathrm{tr}\left[\tau_t^{+}\tau_t^{-}\right] = \mathrm{tr}\left[\tau_t^{0}\tau_t^{0}\right] = \mathrm{tr}\left[\tau_v^{+}\tau_v^{-}\right] = \mathrm{tr}\left[\tau_v^{0}\tau_v^{0}\right] = \mathrm{tr}\left[\tau_s\tau_s\right] = 1\,. \tag{A.14}$$

Combining the properties of the tensor product of generic 2×2- matrices A, B, C, D

$$(A \otimes B)(C \otimes D) \tag{A.15}$$

with the definition of the trace

$$\mathrm{tr}\left[A \otimes B\right] = \mathrm{tr}\left[A\right]\mathrm{tr}\left[B\right] \tag{A.16}$$

yields

$$\mathrm{tr}\left[(A \otimes B)(C \otimes D)\right] = \mathrm{tr}\left[AC\right]\mathrm{tr}\left[BD\right]\,. \tag{A.17}$$

This reduces the trace of an isospin singlet to

$$\mathrm{tr}\left[(A \otimes B)\,\tau^{aa}\right] = 2\mathrm{tr}\left[AB\right] - \mathrm{tr}\left[A\right]\mathrm{tr}\left[B\right]. \tag{A.18}$$

Multiplying the two Pauli matrices related to the isospin singlet leads to

$$\tau^{aa}\tau^{bb} = 3\,(\mathbb{1} \otimes \mathbb{1}) - 2\tau^{aa}. \tag{A.19}$$

A.2. Legendre Polynomials

Legendre Polynomials P^ℓ fulfill the properties

$$P^\ell(1) = 1, \tag{A.20a}$$

$$\int_{-1}^{1} \mathrm{d}x P^\ell(x) P^{\ell'}(x) = \frac{2}{2l+1}\delta^{\ell\ell'}. \tag{A.20b}$$

Using the Rodrigues' Formula,

$$P^\ell(x) = \frac{1}{2^\ell \ell!}\frac{d^\ell}{dx^\ell}\left[(x^2-1)^n\right] \tag{A.21}$$

the Legendre Polynomials are explicitly calculated up to $\ell = 3$ in the massless limit $\cos\Theta = 2\frac{t}{s} + 1 = -\left(2\frac{u}{s}+1\right)$,

$$P^0(\cos\Theta) = 1 \qquad\qquad = P^0(s,t,u), \tag{A.22a}$$

$$P^1(\cos\Theta) = \cos\Theta \qquad = 2\frac{t}{s} + 1 \qquad = P^1(s,t,u), \tag{A.22b}$$

$$P^2(\cos\Theta) = \frac{1}{2}\left[3(\cos\Theta)^2 - 1\right] \qquad = 6\frac{t^2}{s^2} + 6\frac{t}{s} + 1 \qquad = P^2(s,t,u), \tag{A.22c}$$

$$P^3(\cos\Theta) = \frac{1}{2}\left[5(\cos\Theta)^3 - 3(\cos\Theta)\right] = 20\frac{t^3}{s^3} + 30\frac{t^2}{s^2} + 12\frac{t}{s} + 1 = P^3(s,t,u). \tag{A.22d}$$

Interchanging u and t can be described by the relation

$$P^\ell(s,t,u) = (-1)^\ell P^\ell(s,u,t). \tag{A.23}$$

A.3. Isospin Basis

The Goldstone bosons $w^\pm, z$ form an isospin triplet. It is convenient to describe the states $|w^\pm\rangle, |z\rangle$ with isospin quantum numbers (I,m). Following [143] the antiparticle state of an isospin state is defined as

$$\overline{|I,m\rangle} = \eta_I(-1)^{I-m} C\,|I,-m\rangle \tag{A.24}$$

with the charge-conjugation operator C and a phase η_I. To fulfill the requirement, that the isospin state is its own antiparticle

$$\overline{|I,m\rangle} = |I,m\rangle, \tag{A.25}$$

the phase is fixed to

$$\eta_I = -1, \tag{A.26}$$

and the charge conjugation operator is defined as

$$\begin{aligned} C|w^{\pm}\rangle &= C\frac{1}{\sqrt{2}}\left(|w^1\rangle \mp \mathrm{i}|w^2\rangle\right) \\ &= \frac{1}{\sqrt{2}}\left(|w^1\rangle \pm \mathrm{i}|w^2\rangle\right) = |w^{\mp}\rangle. \end{aligned} \tag{A.27}$$

Combinings equations (A.27) and (A.24) leads to the relations

$$|w^-\rangle = \quad |1,-1\rangle, \tag{A.28a}$$
$$|w^+\rangle = -|1,+1\rangle \tag{A.28b}$$

A.3.1. Iso-Spin Eigenamplitudes of VBS

The vector boson scattering amplitudes can be realized as $1 \otimes 1$ iso-spin amplitudes in (A.28)

$$\mathcal{A}(w^+w^- \to zz) = -\langle 1,1;1,-1|T|1,0;1,0\rangle \tag{A.29a}$$
$$\mathcal{A}(zz \to zz) = \quad \langle 1,0;1,0|T|1,0;1,0\rangle \tag{A.29b}$$
$$\mathcal{A}(w^+w^- \to w^+w^-) = \langle 1,1;1,-1|T|1,1;1,-1\rangle \tag{A.29c}$$
$$\mathcal{A}(w^+z \to w^+z) = \quad \langle 1,1;1,0|T|1,1;1,0\rangle \tag{A.29d}$$
$$\mathcal{A}(w^+w^+ \to w^+w^+) = \quad \langle 1,1;1,1|T|1,1;1,1\rangle \tag{A.29e}$$

With help of the Clebsch-Gordon decomposition the amplitude $\mathcal{A}(w^+w^- \to zz)$ can be written as a function of iso-spin eigen-amplitudes $\mathcal{A}_I$

$$\begin{aligned} \mathcal{A}(w^+w^- \to zz) &= -\langle 1,-1|\mathrm{T}|0,0\rangle \\ &= \sum_{Im_I,Km_K} \langle 1,-1|I,m_I\rangle\langle I,m_I|\mathrm{T}|K,m_K\rangle\langle K,m_K|0,0\rangle \\ &= \frac{1}{3}\mathcal{A}(I=0,m_I=0) - \frac{1}{3}\mathcal{A}(I=2,m_I=0). \end{aligned} \tag{A.30}$$

Decomposing amplitudes in (A.29) analogously leads to

$$\mathcal{A}(w^+w^- \to zz) = \frac{1}{3}\mathcal{A}_0 - \frac{1}{3}\mathcal{A}_2, \tag{A.31a}$$
$$\mathcal{A}(zz \to zz) = \frac{1}{3}\mathcal{A}_0 + \frac{2}{3}\mathcal{A}_2, \tag{A.31b}$$
$$\mathcal{A}(w^+w^- \to w^+w^-) = \frac{1}{3}\mathcal{A}_0 + \frac{1}{2}\mathcal{A}_1 + \frac{1}{6}\mathcal{A}_2, \tag{A.31c}$$
$$\mathcal{A}(w^+z \to w^+z) = \frac{1}{2}\mathcal{A}_1 + \frac{1}{2}\mathcal{A}_2, \tag{A.31d}$$
$$\mathcal{A}(w^+w^+ \to w^+w^+) = \mathcal{A}_2. \tag{A.31e}$$

A.3.2. Integrals in Isospin-Spin Eigenamplitudes

If the isospin amplitude includes a particle exchange in the t- or u-channel the integral for the partial wave decomposition is defined in [142] by

$$\mathcal{S}_\ell\left(s,m^2\right) = \int_{-s}^{0} \frac{\mathrm{d}t}{s} \frac{t^2}{t-m^2} P_0(t,s,u) P_\ell(s,t,u), \tag{A.32a}$$

$$\mathcal{P}_\ell\left(s,m^2\right) = \int_{-s}^{0} \frac{\mathrm{d}t}{s} \frac{t^2}{t-m^2} P_1(t,s,u) P_\ell(s,t,u), \tag{A.32b}$$

$$\mathcal{D}_\ell\left(s,m^2\right) = \int_{-s}^{0} \frac{\mathrm{d}t}{s} \frac{t^2}{t-m^2} P_2(t,s,u) P_\ell(s,t,u). \tag{A.32c}$$

The corresponding integrals over $\frac{u^2}{u-m^2}$ are equivalent to the integrals in (A.32) multiplied by an additional factor $(-1)^\ell$ because of (A.23). Explicitly calculating (A.32) gives

$$\mathcal{S}_0\left(s,m\right) = m^2 + \frac{m^4}{s}\log\left(\frac{m^2}{s+m^2}\right) - \frac{s}{2}, \tag{A.33a}$$

$$\mathcal{S}_1\left(s,m\right) = 2\frac{m^4}{s} + \frac{m^4}{s^2}\left(2m^2+s\right)\log\left(\frac{m^2}{s+m^2}\right) + \frac{s}{6}, \tag{A.33b}$$

$$\mathcal{S}_2\left(s,m\right) = \frac{m^4}{s^2}\left(6m^2+3s\right) + \frac{m^4}{s^3}\left(6m^4+6m^2s+s^2\right)\log\left(\frac{m^2}{s+m^2}\right), \tag{A.33c}$$

$$\mathcal{P}_0\left(s,m\right) = 1 + \frac{m^2+2s}{s}\log\left(\frac{m^2}{s+m^2}\right), \tag{A.33d}$$

$$\mathcal{P}_1\left(s,m\right) = \frac{m^2+2s}{s^2}\left(2s + \left(2m^2+s\right)\log\left(\frac{m^2}{s+m^2}\right)\right), \tag{A.33e}$$

$$\mathcal{D}_0\left(s,m\right) = m^2 + \frac{11}{2}s + \frac{1}{s}\left(m^4+6m^2s+6s^2\right)\log\left(\frac{m^2}{s+m^2}\right), \tag{A.33f}$$

$$\begin{aligned}\mathcal{D}_1\left(s,m\right) =& 2\frac{m^4}{s} + 12m^2 + \frac{73}{6}s \\ &+ \frac{1}{s^2}\left(2m^2+s\right)\left(m^4+6m^2s+6s^2\right)\log\left(\frac{m^2}{s+m^2}\right).\end{aligned} \tag{A.33g}$$

A.4. Details on T-Matrix Unitarization

Additional details and proofs about the generalization of the K-matrix unitarization scheme to both introduced direct T-matrix unitarization schemes, the linear projection and the Thales projection, are given in this part of the appendix.

A.4.1. Non-Hermitian K-Matrix

If the initial T_0-matrix is not Hermitian, a transformation of a suitable K' has be found that leads to a unitarized T-matrix using the prescription in (4.41)

$$T = \frac{K'}{\mathbb{1} - \mathrm{i}K'/2}\,. \tag{A.34}$$

The most straightforward approach is to neglect the imaginary parts

$$K' = \operatorname{Re} T_0 = \frac{T_0 + T_0^\dagger}{2}\,. \tag{A.35}$$

Whereas, the interpretation of the Cayley transform as an inverse stereographic projection suggests a less drastic approach, which retains the imaginary part. Considering the family $\{T_\kappa\}$ of T_0-matrices that have the same projection from a center $\mathrm{i}\mathbb{1}$

$$\frac{T_\kappa}{2} - \mathrm{i}\mathbb{1} = \kappa\left(\frac{T_0}{2} - \mathrm{i}\mathbb{1}\right)\kappa \tag{A.36}$$

with a positive $\kappa^\dagger = \kappa > 0$. The unique self adjoint member $K' \in \{T_\kappa\}$ of this family has to satisfy

$$K' = (K')^\dagger\,. \tag{A.37}$$

As long as $\operatorname{Im} T_0/2 < \mathbb{1}$, there is a unique solution with a converging power series expansion[1]

$$\kappa = \frac{1}{\sqrt{\mathbb{1} - \frac{1}{2}\operatorname{Im} T_0}}\,, \tag{A.39a}$$

$$K' = \kappa(\operatorname{Re} T_0)\kappa\,. \tag{A.39b}$$

Reinserting equation (A.39) back into (4.41) leads to a unitarization prescription for complex T_0

$$T = \kappa(\operatorname{Re} T_0)\frac{1}{\mathbb{1} - \frac{\mathrm{i}}{2}T_0^\dagger}\kappa^{-1} = \kappa^{-1}\frac{1}{\mathbb{1} - \frac{\mathrm{i}}{2}T_0^\dagger}(\operatorname{Re} T_0)\kappa\,. \tag{A.40}$$

For normal T_0 the operators $\operatorname{Re} T_0$, $\operatorname{Im} T_0$, T_0 and $T_0^\dagger$ commutes and the unitarity transformation simplifies to

$$T = \frac{\operatorname{Re} T_0}{\mathbb{1} - \frac{\mathrm{i}}{2}T_0^\dagger} = \frac{\operatorname{Re} T_0}{\mathbb{1} - \frac{\mathrm{i}}{2}\operatorname{Re} T_0 - \frac{1}{2}\operatorname{Im} T_0}\,. \tag{A.41}$$

This prescription is the direct linear T-matrix unitarization and does not need the intermediate step of calculating the K-matrix within a perturbative expansion.

[1] The Riesz-Dunford functional calculus [116–119] is used to construct projectors on subspaces corresponding to parts of the spectrum of $\operatorname{Im} K/2$

$$P_\Sigma = \int_{\partial\Sigma}\frac{\mathrm{d}z}{2\pi\mathrm{i}}\frac{1}{z\mathbb{1} - \frac{1}{2}\operatorname{Im} T_0}\,, \tag{A.38}$$

where Σ contains the desired part of the spectrum of $\operatorname{Im} K/2$.

A.4.2. Properties of T-matrix unitarized operators

The scattering operators S are unitary, when the interaction matrix T satisfies the optical theorem

$$T^\dagger T = -\mathrm{i}\left(T - T^\dagger\right). \tag{A.42}$$

Furthermore, it is requested, that the transformations have to be idempotent, so that they leave interaction operators invariant, which do not break S-matrix unitarity

$$T\left(T(T_0)\right) = T\left(T_0\right). \tag{A.43}$$

Linear Projection

To proof that direct T-matrix transformation by an inverse stereographic projection for normal T fulfills the unitarity and idempotency, the transformation in (4.41) is rewritten to

$$T\left(T_0\right) = \frac{\mathrm{Re}T_0}{\mathbb{1} - \frac{\mathrm{i}}{2}T_0^\dagger} = \frac{\mathrm{Re}T_0}{\mathbb{1} + \frac{1}{4}T_0T_0^\dagger}\left(\mathbb{1} + \frac{\mathrm{i}}{2}T_0\right). \tag{A.44}$$

Then it is easy to proof, that the linear projection unitarization prescription, satisfies unitarity

$$\begin{aligned} \mathrm{SS}^\dagger &= \mathbb{1} - 2\mathrm{Im}\left(T\right) + \mathrm{TT}^\dagger \\ &= \mathbb{1} - \frac{\left(\mathrm{Re}T_0\right)^2}{\mathbb{1} + \frac{1}{4}T_0T_0^\dagger} + \frac{\left(\mathrm{Re}T_0\right)^2}{\mathbb{1} + \frac{1}{4}T_0T_0^\dagger} = \mathbb{1}\,, \end{aligned} \tag{A.45}$$

and the T-transformation is idempotent

$$\begin{aligned} T\left(T\left(T_0\right)\right) = \frac{\mathrm{Re}T(T_0)}{1 - \frac{\mathrm{i}}{2}T(T_0)^\dagger} &= \frac{\frac{\mathrm{Re}T_0}{\mathbb{1} + \frac{1}{4}T_0T_0^\dagger}\left(\mathbb{1} - \frac{1}{2}\mathrm{Im}T_0\right)}{\mathbb{1} - \frac{\mathrm{i}}{2}\frac{\mathrm{Re}T_0\left(\mathbb{1} - \frac{\mathrm{i}}{2}T_0^\dagger\right)}{\left(\mathbb{1} - \frac{\mathrm{i}}{2}T_0^\dagger\right)\left(\mathbb{1} + \frac{\mathrm{i}}{2}T_0\right)}} \\ &= \frac{\mathrm{Re}T_0}{\mathbb{1} + \frac{1}{4}T_0T_0^\dagger}\left(\mathbb{1} + \frac{\mathrm{i}}{2}T_0\right) = T(T_0)\,. \end{aligned} \tag{A.46}$$

Thales Projection

Analogue to the linear projection the T-operation from (4.64) is rewritten to

$$T\left(T_0\right) = \frac{1}{\mathrm{Re}\left(\frac{1}{T_0}\right) - \frac{\mathrm{i}}{2}\mathbb{1}} = \frac{1}{\mathrm{Re}\left(\frac{1}{T_0}\right)^2 + \frac{1}{4}\mathbb{1}}\left(\mathrm{Re}\left(\frac{1}{T_0}\right) + \frac{\mathrm{i}}{2}\mathbb{1}\right). \tag{A.47}$$

With the latter definition the unitarity of the S-operator is proven by

$$\begin{aligned} \mathrm{SS}^\dagger &= \mathbb{1} - 2\mathrm{Im}\,(T) + \mathrm{TT}^\dagger \\ &= \mathbb{1} - \frac{1}{\mathrm{Re}\left(\frac{1}{T_0}\right)^2 + \frac{1}{4}\mathbb{1}} + \frac{1}{\mathrm{Re}\left(\frac{1}{T_0}\right)^2 + \frac{1}{4}\mathbb{1}} = \mathbb{1}\,. \end{aligned} \tag{A.48}$$

The Thales projection leaves interaction operators invariant, which already satisfy the optical theorem

$$\begin{aligned} T\,(T\,(T_0)) &= \frac{1}{\mathrm{Re}\left(\frac{1}{T(T_0)}\right) - \frac{\mathrm{i}}{2}\mathbb{1}} = \frac{1}{\mathrm{Re}\left(\mathrm{Re}\left(\frac{1}{T_0}\right) - \frac{\mathrm{i}}{2}\mathbb{1}\right) - \frac{\mathrm{i}}{2}\mathbb{1}} \\ &= \frac{1}{\mathrm{Re}\left(\frac{1}{T_0}\right) - \frac{\mathrm{i}}{2}\mathbb{1}} = T\,(T_0)\,. \end{aligned} \tag{A.49}$$

A.4.3. Equations of Motions

Using the derivatives of two general dimension two matrices A and B in the index notation

$$\frac{\partial \mathrm{tr}\,[AB]}{\partial B} = \frac{\partial A^a{}_b B^b{}_a}{\partial B^c{}_d} \tag{A.50}$$

$$= A^d{}_c = A^T, \tag{A.51}$$

the equations of motions for the fields $\mathbf{H}$, $\mathbf{H}^\dagger$, $\mathbf{W}^\mu$ and $\mathbf{B}^\mu$ can be calculated. Using the Euler-Lagrangian for the minimal vector boson scattering Lagrangian (2.32)

$$\partial_\mu \frac{\partial \mathcal{L}_{\mathrm{min}}}{\partial(\partial^\mu \mathbf{H}^\dagger)} = \frac{\partial \mathcal{L}_{\mathrm{min}}}{\partial \mathbf{H}^\dagger}, \tag{A.52a}$$

$$\partial_\mu \frac{\partial \mathcal{L}_{\mathrm{min}}}{\partial(\partial^\mu \mathbf{H})} = \frac{\partial \mathcal{L}_{\mathrm{min}}}{\partial \mathbf{H}} \tag{A.52b}$$

results in the relations

$$\left(\mathbf{D}^2\mathbf{H}\right) = -\mu^2\mathbf{H} + \lambda\,\mathrm{tr}\left[\mathbf{H}^\dagger\mathbf{H}\right]\mathbf{H}, \tag{A.53a}$$

$$\left(\mathbf{D}^2\mathbf{H}\right)^\dagger = -\mu^2\mathbf{H}^\dagger + \lambda\,\mathrm{tr}\left[\mathbf{H}^\dagger\mathbf{H}\right]\mathbf{H}^\dagger. \tag{A.53b}$$

Determining the equations of motions for the gauge fields is more complex. The equation for the gauge fields

$$\partial_\mu \frac{\partial \mathcal{L}_{\mathrm{min}}}{\partial(\partial^\mu \mathbf{W}^\nu)} - \frac{\partial \mathcal{L}_{\mathrm{min}}}{\partial \mathbf{W}^\nu} = 0, \tag{A.54}$$

can be split up in a a part proportional to the field strength $\mathbf{W}^{\mu\nu}$ and in a part proportional to the covariant derivative acting on the Higgs field $\mathbf{D}^\mu\mathbf{H}$. To calculate the contribution of the Euler-Lagrangian of (A.54) for $\mathbf{W}^{\mu\nu}$, the simplification

$$\mathrm{tr}\left[A_{\alpha\beta}\,\partial^\mu \frac{\partial \mathbf{W}^{\alpha\beta}}{\partial(\partial^\mu \mathbf{W}^\nu)}\right] - \mathrm{tr}\left[A_{\alpha\beta}\frac{\partial \mathbf{W}^{\alpha\beta}}{\partial \mathbf{W}^\nu}\right] \tag{A.55}$$

with a general operator $A_{\mu\nu}$ is used. Calculating the first part of (A.55) gives

$$\begin{aligned}
\mathrm{tr}\left[A_{\alpha\beta}\left(\frac{\partial \mathbf{W}^{\alpha\beta}}{\partial \mathbf{W}^{\nu}}\right]\right)^{T} &= \left(\mathrm{tr}\left[A_{\alpha\beta}\frac{\partial\left(-\mathrm{i}g\left[\mathbf{W}^{\alpha},\mathbf{W}^{\beta}\right]\right)}{\partial \mathbf{W}^{\nu}}\right]\right)^{T} \\
&= -\mathrm{i}\frac{g}{2}\Bigg(\mathrm{tr}\Big[A_{\alpha\beta}\frac{\partial}{\partial \mathbf{W}^{\nu}}\Big(\mathbf{W}^{\alpha}\mathbf{W}^{\beta}+\mathbf{W}^{\beta}A_{\alpha\beta}\mathbf{W}^{\alpha} \\
&\qquad -A_{\alpha\beta}\mathbf{W}^{\beta}\mathbf{W}^{\alpha}-\mathbf{W}^{\alpha}A_{\alpha\beta}\mathbf{W}^{\beta}\Big)\Big]\Bigg)^{T} \\
&= -\mathrm{i}g\left(\left(A_{\mu\nu}-A_{\nu\mu}\right)\mathbf{W}^{\mu}-\mathbf{W}^{\mu}\left(A_{\mu\nu}-A_{\nu\mu}\right)\right) \\
&= \left[\mathrm{i}g\mathbf{W}^{\mu},A_{\mu\nu}-A_{\nu\mu}\right]
\end{aligned} \tag{A.56}$$

and the second part of (A.54) can be simplified to

$$\left(\partial^{\mu}\frac{\partial \mathrm{tr}\left[A_{\alpha\beta}\mathbf{W}^{\alpha\beta}\right]}{\partial(\partial^{\mu}\mathbf{W}^{\nu})}\right)^{T} = \left(\partial^{\mu}\frac{\partial \mathrm{tr}\left[A_{\alpha\beta}\left(\partial^{\alpha}\mathbf{W}^{\beta}-\partial^{\beta}\mathbf{W}^{\alpha}\right)\right]}{\partial(\partial^{\mu}\mathbf{W}^{\nu})}\right)^{T} = \partial^{\mu}\left(A_{\mu\nu}-A_{\nu\mu}\right). \tag{A.57}$$

Combining the equations (A.56) and (A.57) reduces (A.55) to

$$\mathrm{tr}\left[A_{\alpha\beta}\partial^{\mu}\frac{\partial \mathbf{W}^{\alpha\beta}}{\partial(\partial^{\mu}\mathbf{W}^{\nu})}\right]-\mathrm{tr}\left[A_{\alpha\beta}\frac{\partial \mathbf{W}^{\alpha\beta}}{\partial \mathbf{W}^{\nu}}\right] = \left[\mathbf{D}^{\mu}_{W},A_{\mu\nu}-A_{\nu\mu}\right] \tag{A.58}$$

The contribution of a general A_{α} proportional to $\mathbf{D}^{\alpha}\mathbf{H}$ to the equation of motion is easily calculated to be

$$\left(\mathrm{tr}\left[A_{\alpha}\frac{\partial \mathbf{D}^{\alpha}\mathbf{H}}{\partial \mathbf{W}^{\nu}}\right]\right)^{T} = \left(\mathrm{tr}\left[A_{\alpha}\frac{\partial\left(-\mathrm{i}g\mathbf{W}^{\alpha}\mathbf{H}\right)}{\partial \mathbf{W}^{\nu}}\right]\right)^{T} = -\mathrm{i}g\mathbf{H}A_{\nu}, \tag{A.59a}$$

$$\left(\mathrm{tr}\left[A_{\alpha}\frac{\partial\left(\mathbf{D}^{\alpha}\mathbf{H}\right)^{\dagger}}{\partial \mathbf{W}^{\nu}}\right]\right)^{T} = \left(\mathrm{tr}\left[A_{\alpha}\frac{\partial\left(\mathrm{i}g\mathbf{H}^{\dagger}\mathbf{W}^{\alpha}\right)}{\partial \mathbf{W}^{\nu}}\right]\right)^{T} = \mathrm{i}gA_{\nu}\mathbf{H}^{\dagger}. \tag{A.59b}$$

Using equations (A.58)and (A.59) the equation of motion for the gauge bosons for the minimal Lagrangian (2.32) can be calculated (the procedure for $\mathbf{B}$ is analogous):

$$\mathbf{D}_{\mu}\mathbf{W}^{\mu\nu} \equiv \left[\mathbf{D}^{W}_{\mu},\mathbf{W}^{\mu\nu}\right] = -\mathrm{i}\frac{g}{2}\left(\mathbf{H}\left(\mathbf{D}^{\nu}\mathbf{H}\right)^{\dagger}-\mathbf{D}^{\nu}\mathbf{H}\mathbf{H}^{\dagger}\right), \tag{A.60a}$$

$$\mathbf{D}_{\mu}\mathbf{B}^{\mu\nu} \equiv \quad \partial_{\mu}\mathbf{B}^{\mu\nu} = -\mathrm{i}\frac{g'}{2}\left(\left(\mathbf{D}^{\nu}\mathbf{H}\right)^{\dagger}\mathbf{H}-\mathbf{H}^{\dagger}\mathbf{D}^{\nu}\mathbf{H}\right). \tag{A.60b}$$

A.5. Dimension eight Operators in Eboli-Basis

A revised dimension 8 operators basis [57] of [56] is listed in this section.

A.5.1. Definitions

The convention 'CD+' is chosen for the covariant derivative

$$D_\mu \Phi \equiv \partial_\mu \Phi + i\frac{g'}{2} B_\mu \Phi + i g W_\mu^i \frac{\tau^i}{2} \Phi, \tag{A.61}$$

and effects the coupling of the longitudinal mode of the gauge bosons. The field strength tensors of the $SU(2)_I$ (W_μ^i) and $U(1)_Y$ (B_μ) contribute to the transversal coupling of the gauge fields

$$\begin{aligned} W_{\mu\nu} &= \frac{i}{2} g \tau^I (\partial_\mu W_\nu^i - \partial_\nu W_\mu^i + g \epsilon_{ijk} W_\mu^j W_\nu^k)\,, \\ B_{\mu\nu} &= \frac{i}{2} g' (\partial_\mu B_\nu - \partial_\nu B_\mu)\,. \end{aligned} \tag{A.62a}$$

In the following the Dimension 8 operators are separated in longitudinal, transversal and mixed contribution, which will refer to the building blocks used.

A.5.2. Operators containing only longitudinal couplings

$$\mathcal{O}_{S,0} = \left[\left(D_\mu \Phi\right)^\dagger D_\nu \Phi \right] \times \left[\left(D^\mu \Phi\right)^\dagger D^\nu \Phi \right], \tag{A.63a}$$

$$\mathcal{O}_{S,1} = \left[\left(D_\mu \Phi\right)^\dagger D^\mu \Phi \right] \times \left[\left(D_\nu \Phi\right)^\dagger D^\nu \Phi \right]. \tag{A.63b}$$

A.5.3. Operators containing mixed couplings

$$\mathcal{O}_{M0} = \mathrm{Tr}\left[W_{\mu\nu} W^{\mu\nu} \right] \times \left[\left(D_\beta \Phi\right)^\dagger D^\beta \Phi \right], \tag{A.64a}$$

$$\mathcal{O}_{M1} = \mathrm{Tr}\left[W_{\mu\nu} W^{\nu\beta} \right] \times \left[\left(D_\beta \Phi\right)^\dagger D^\mu \Phi \right], \tag{A.64b}$$

$$\mathcal{O}_{M2} = \left[B_{\mu\nu} B^{\mu\nu} \right] \times \left[\left(D_\beta \Phi\right)^\dagger D^\beta \Phi \right], \tag{A.64c}$$

$$\mathcal{O}_{M3} = \left[B_{\mu\nu} B^{\nu\beta} \right] \times \left[\left(D_\beta \Phi\right)^\dagger D^\mu \Phi \right], \tag{A.64d}$$

$$\mathcal{O}_{M4} = \left[\left(D_\mu \Phi\right)^\dagger W_{\beta\nu} D^\mu \Phi \right] \times B^{\beta\nu}, \tag{A.64e}$$

$$\mathcal{O}_{M5} = \left[\left(D_\mu \Phi\right)^\dagger W_{\beta\nu} D^\nu \Phi \right] \times B^{\beta\mu}, \tag{A.64f}$$

$$\mathcal{O}_{M6} = \left[\left(D_\mu \Phi\right)^\dagger W_{\beta\nu} W^{\beta\nu} D^\mu \Phi \right], \tag{A.64g}$$

$$\mathcal{O}_{M7} = \left[\left(D_\mu \Phi\right)^\dagger W_{\beta\nu} W^{\beta\mu} D^\nu \Phi \right]. \tag{A.64h}$$

Note, that the operator $\mathcal{O}_{M6}$ is linearly dependent to the operator $\mathcal{O}_{M0}$ and can be neglected.

A.5.4. Operators containing only transversal couplings

$$\mathcal{O}_{T0} = \mathrm{Tr}\left[W_{\mu\nu}W^{\mu\nu}\right] \times \mathrm{Tr}\left[W_{\alpha\beta}W^{\alpha\beta}\right], \tag{A.65a}$$

$$\mathcal{O}_{T1} = \mathrm{Tr}\left[W_{\alpha\nu}W^{\mu\beta}\right] \times \mathrm{Tr}\left[W_{\mu\beta}W^{\alpha\nu}\right], \tag{A.65b}$$

$$\mathcal{O}_{T2} = \mathrm{Tr}\left[W_{\alpha\mu}W^{\mu\beta}\right] \times \mathrm{Tr}\left[W_{\beta\nu}W^{\nu\alpha}\right], \tag{A.65c}$$

$$\mathcal{O}_{T5} = \mathrm{Tr}\left[W_{\mu\nu}W^{\mu\nu}\right] \times B_{\alpha\beta}B^{\alpha\beta}, \tag{A.65d}$$

$$\mathcal{O}_{T6} = \mathrm{Tr}\left[W_{\alpha\nu}W^{\mu\beta}\right] \times B_{\mu\beta}B^{\alpha\nu}, \tag{A.65e}$$

$$\mathcal{O}_{T7} = \mathrm{Tr}\left[W_{\alpha\mu}W^{\mu\beta}\right] \times B_{\beta\nu}B^{\nu\alpha}, \tag{A.65f}$$

$$\mathcal{O}_{T8} = B_{\mu\nu}B^{\mu\nu}B_{\alpha\beta}B^{\alpha\beta}, \tag{A.65g}$$

$$\mathcal{O}_{T9} = B_{\alpha\mu}B^{\mu\beta}B_{\beta\nu}B^{\nu\alpha}. \tag{A.65h}$$

Chapter B

Feynman-Rules

The Feynman rules which are used to calculate the vector boson scattering amplitudes are summarized in this appendix. Focusing only on weak vector boson scattering, the Feynman rules are determined from the Lagrangian, where gluons, photons and fermions are omitted.

B.1. Lagrangian

All Lagrangians are defined within the Higgs matrix realization which was introduced in Chapter 2. The Standard Model interactions is given by

$$\begin{aligned}\mathcal{L}_{\text{SM}} =& -\frac{1}{2}\text{tr}\left[\mathbf{W}_{\mu\nu}\mathbf{W}^{\mu\nu}\right] - \frac{1}{2}\text{tr}\left[\mathbf{B}_{\mu\nu}\mathbf{B}^{\mu\nu}\right] \\ &+ \text{tr}\left[\left(\mathbf{D}_\mu\mathbf{H}\right)^\dagger \mathbf{D}^\mu\mathbf{H}\right] + \mu^2\text{tr}\left[\mathbf{H}^\dagger\mathbf{H}\right] - \frac{\lambda}{2}\left(\text{tr}\left[\mathbf{H}^\dagger\mathbf{H}\right]\right)^2 .\end{aligned} \tag{B.1}$$

Dimension six and eight operators affecting only the Higgs/Goldstone boson sector are discussed in Chapter 3 and are given by

$$\mathcal{L}_{HD} = F_{HD}\,\text{tr}\left[\mathbf{H}^\dagger\mathbf{H} - \frac{v^2}{4}\right]\cdot\text{tr}\left[\left(\mathbf{D}_\mu\mathbf{H}\right)^\dagger\mathbf{D}^\mu\mathbf{H}\right], \tag{B.2a}$$

$$\mathcal{L}_{S,0} = F_{S,0}\,\text{tr}\left[\left(\mathbf{D}_\mu\mathbf{H}\right)^\dagger\mathbf{D}_\nu\mathbf{H}\right]\cdot\text{tr}\left[\left(\mathbf{D}^\mu\mathbf{H}\right)^\dagger\mathbf{D}^\nu\mathbf{H}\right], \tag{B.2b}$$

$$\mathcal{L}_{S,1} = F_{S,1}\,\text{tr}\left[\left(\mathbf{D}_\mu\mathbf{H}\right)^\dagger\mathbf{D}^\mu\mathbf{H}\right]\cdot\text{tr}\left[\left(\mathbf{D}_\nu\mathbf{H}\right)^\dagger\mathbf{D}^\nu\mathbf{H}\right]. \tag{B.2c}$$

In the gaugeless limit ($g, g' \to 0$), they can be rewritten into

$$\mathcal{L}_{HD} = \frac{F_{HD}}{4}\left(h(h+2v) + w^i w^j \delta^{ij}\right)\left(\partial_\mu h \partial^\mu h + \partial_\mu w^{i'} \partial^\mu w^{j'} \delta^{i'j'}\right), \tag{B.3a}$$

$$\mathcal{L}_{S,0} = \frac{F_{S,0}}{4}\Big[\left(\partial_\mu h \partial^\mu h\right)^2 + 2\partial_\mu h \partial^\mu w^i \partial_\nu h \partial^\nu w^j \delta^{ij} + \frac{1}{2}\partial_\mu w^i \partial^\mu w^j \partial_\nu w^{i'} \partial^\nu w^{j'}\left(\delta^{jj'}\delta^{ii'} + \delta^{i'j}\delta^{ij'}\right)\Big], \tag{B.3b}$$

$$\mathcal{L}_{S,1} = \frac{F_{S,1}}{4}\Big[\left(\partial_\mu h \partial^\mu h\right)^2 + 2\partial_\mu h \partial^\mu h \partial_\nu w^i \partial^\nu w^j \delta^{ij} + \partial_\mu w^i \partial^\mu w^j \partial_\nu w^{i'} \partial^\nu w^{j'} \delta^{ij}\delta^{i'j'}\Big]. \tag{B.3c}$$

As an extension to model generic new physics, additional resonances are introduced. The scalar σ and the tensor $f^{\mu\nu}$ represent singlets of the chiral symmetry group, whereas Φ has the quantum numbers $\mathbf{1}\otimes\mathbf{1}$ under $SU(2)_L \times SU(2)_R$. Φ is referred as isotensor for historical reasons, but it actually includes an isovector Φ_v and isoscalar Φ_s besides the isotensor Φ_t. Also the Fierz-Pauli tensor f can be reformulated into a tensor f_f, a vector A_f and a scalar σ_f such, that canonical propagators can be used for each degree of freedoms instead of the complicated tensor propagator

$$\Delta_{\mu\nu,\rho\sigma}(f) = \frac{\mathrm{i}}{k^2 - m^2 + \mathrm{i}\epsilon} P^{\mu_1\mu_2\nu_1\nu_2}(k,m), \tag{B.4a}$$

$$\Delta_{\mu\nu,\rho\sigma}(f') = \frac{\mathrm{i}}{k^2 - m^2 + \mathrm{i}\epsilon}\left(\frac{1}{2}g_{\mu\rho}g_{\nu\sigma} + \frac{1}{2}g_{\mu\sigma}g_{\nu\rho} - \frac{1}{2}g_{\mu\nu}g_{\rho\sigma}\right), \tag{B.4b}$$

$$\Delta_{\mu\nu}(A) = \frac{-\mathrm{i}}{k^2 - m^2 + \mathrm{i}\epsilon} g_{\mu\nu}, \tag{B.4c}$$

$$\Delta(\sigma) = \frac{\mathrm{i}}{k^2 - m^2 + \mathrm{i}\epsilon}, \tag{B.4d}$$

where the projection operator of spin two can be written in terms of the spin-one projection operator,

$$P^{\mu_1\mu_2\nu_1\nu_2}(k,m) = \frac{1}{2}\left[P^{\mu_1\nu_1}(k,m)P^{\mu_2\nu_2}(k,m) + P^{\mu_1\nu_2}(k,m)P^{\mu_1\nu_2}(k,m)\right] - \frac{1}{3}P^{\mu_1\mu_2}(k,m)P^{\nu_1\nu_2}(k,m), \tag{B.5a}$$

$$P^{\mu\nu}(k,m) = \sum_\lambda \bar{\varepsilon}^\mu_\lambda(k,m)\varepsilon^\nu_\lambda(k,m) = g^{\mu\nu} - \frac{k^\mu k^\nu}{m^2}. \tag{B.5b}$$

The couplings of the formally separated tensor resonances f_f, A_f and σ_f to vector boson scattering are related to each other. This is manifest in the Lagrangian for the resonances

$$\mathcal{L}_\sigma = \frac{1}{2}\partial_\mu\sigma\,\partial^\mu\sigma - \frac{1}{2}m_\sigma^2\sigma^2 + \sigma J_\sigma \tag{B.6a}$$

$$\mathcal{L}_\phi = \frac{1}{2}\sum_{i=s,v,t}\mathrm{tr}\left[\partial_\mu\Phi_i\partial^\mu\Phi_i - m_\Phi^2\Phi_i^2\right] + \mathrm{tr}\left[\left(\Phi_t + \frac{1}{2}\Phi_v - \frac{2}{5}\Phi_s\right)J_\phi\right], \tag{B.6b}$$

$$\begin{aligned}\mathcal{L}_f =& \frac{1}{2}\partial_\alpha f_{\mu\nu}\partial^\alpha f^{\mu\nu} - \frac{1}{2}m_f^2 f_{\mu\nu}f^{\mu\nu} - \frac{1}{2}\partial_\alpha f^\mu_{\ \mu}\partial^\alpha f^\nu_{\ \nu} + \frac{1}{2}m_f^2 f^\mu_{\ \mu}f^\nu_{\ \nu}\\ &- \partial^\alpha f_{\alpha\mu}\partial_\beta f^{\beta\mu} - f^\alpha_{\ \alpha}\partial^\mu\partial^\nu f_{\mu\nu} + f_{\mu\nu}J_f^{\mu\nu},\end{aligned} \tag{B.6c}$$

$$\begin{aligned}\mathcal{L}'_f =& \frac{1}{2}f_{f\mu\nu}\left(-\partial^2 - m_f^2\right)f_f^{\mu\nu} + \frac{1}{2}f^\mu_{f\mu}\left(-\frac{1}{2}\left(-\partial^2 - m_f^2\right)\right)f^\nu_{f\nu}\\ &+ \frac{1}{2}A_{f\mu}\left(-\partial^2 - m_f^2\right)A_f^\mu + \frac{1}{2}\sigma_f\left(-\partial^2 - m_f^2\right)\sigma_f\\ &+ \left(f_{f\mu\nu} - \frac{1}{\sqrt{6}}g^{\mu\nu}\sigma + \frac{1}{\sqrt{2}m_f}\left(\partial_\mu A_\nu + \partial_\nu A_\mu\right) + \frac{\sqrt{2}}{\sqrt{3}m_f^2}\partial_\mu\partial_\nu\sigma\right)J_f^{\mu\nu},\end{aligned} \tag{B.6d}$$

$$\begin{aligned}\mathcal{L}_X =& \frac{1}{2}\sum_{i=s,v,t}\mathrm{tr}\Big[\partial_\alpha X_{i\mu\nu}\partial^\alpha X_i^{\mu\nu} - m^2 X_{i\mu\nu}X_i^{\mu\nu} - \partial_\alpha X_{i\ \mu}^{\mu}\partial^\alpha X_{i\ \nu}^{\nu} + m^2 X_{i\ \mu}^{\mu}X_{i\ \nu}^{\nu}\\ &\qquad - 2\partial^\alpha X_{i\alpha\mu}\partial_\beta X_i^{\beta\mu} - 2X_{i\ \alpha}^{\alpha}\partial^\mu\partial^\nu X_{i\mu\nu}\Big]\\ &+ \mathrm{tr}\left[\left(X_{t\mu\nu} + \frac{1}{2}X_{v\mu\nu} - \frac{2}{5}X_{s\mu\nu}\right)J_X^{\mu\nu}\right],\end{aligned} \tag{B.6e}$$

$$\begin{aligned}\mathcal{L}'_X =& \frac{1}{2}\sum_{i=s,v,t}\mathrm{tr}\Big[X'_{i\mu\nu}\left(-\partial^2 - m_X^2\right)X_i'^{\mu\nu} + X'^{\mu}_{i\mu}\left(-\frac{1}{2}\left(-\partial^2 - m_X^2\right)\right)X'^{\nu}_{i\nu}\\ &\qquad + A_{i\mu}\left(-\partial^2 - m_X^2\right)A_i^\mu + \sigma_i\left(-\partial^2 - m_X^2\right)\sigma_i\Big]\\ &+ \mathrm{tr}\Bigg[\left(X'_{t\mu\nu} - \frac{g^{\mu\nu}}{\sqrt{6}}\sigma_t + \frac{\partial_\mu A_{t\nu} + \partial_\nu A_{t\mu}}{\sqrt{2}m_X} + \frac{\sqrt{2}}{\sqrt{3}m_X^2}\partial_\mu\partial_\nu\sigma_t\right)J_X^{\mu\nu}\\ &\quad + \frac{1}{2}\left(X'_{v\mu\nu} - \frac{g^{\mu\nu}}{\sqrt{6}}\sigma_v + \frac{\partial_\mu A_{v\nu} + \partial_\nu A_{v\mu}}{\sqrt{2}m_X} + \frac{\sqrt{2}}{\sqrt{3}m_X^2}\partial_\mu\partial_\nu\sigma_v\right)J_X^{\mu\nu}\\ &\quad - \frac{2}{5}\left(X'_{s\mu\nu} - \frac{g^{\mu\nu}}{\sqrt{6}}\sigma_s + \frac{\partial_\mu A_{s\nu} + \partial_\nu A_{s\mu}}{\sqrt{2}m_X} + \frac{\sqrt{2}}{\sqrt{3}m_X^2}\partial_\mu\partial_\nu\sigma_s\right)J_X^{\mu\nu}\Bigg].\end{aligned} \tag{B.6f}$$

with the Higgs/Goldstone boson current

$$J_\sigma = F_\sigma\,\mathrm{tr}\left[\left(\mathbf{D}_\mu\mathbf{H}\right)^\dagger\mathbf{D}^\mu\mathbf{H}\right], \tag{B.7a}$$

$$J_\phi = F_\phi\left(\left(\mathbf{D}_\mu\mathbf{H}\right)^\dagger\otimes\mathbf{D}^\mu\mathbf{H} + \frac{1}{8}\mathrm{tr}\left[\left(\mathbf{D}_\mu\mathbf{H}\right)^\dagger\mathbf{D}^\mu\mathbf{H}\right]\right)\tau^{aa}, \tag{B.7b}$$

$$J_f^{\mu\nu} = F_f \left(\mathrm{tr}\left[(\mathbf{D}^\mu \mathbf{H})^\dagger \mathbf{D}^\nu \mathbf{H} \right] - \frac{c_f}{4} g^{\mu\nu} \mathrm{tr}\left[(\mathbf{D}_\rho \mathbf{H})^\dagger \mathbf{D}^\rho \mathbf{H} \right] \right) , \tag{B.7c}$$

$$J_X^{\mu\nu} = F_X \Bigg[\frac{1}{2} \left((\mathbf{D}^\mu \mathbf{H})^\dagger \otimes \mathbf{D}^\nu \mathbf{H} + (\mathbf{D}^\nu \mathbf{H})^\dagger \otimes \mathbf{D}^\mu \mathbf{H} \right) - \frac{c_X}{4} g^{\mu\nu} \left(\mathbf{D}_\rho \mathbf{H} \right)^\dagger \otimes \mathbf{D}^\rho \mathbf{H} + \frac{1}{8} \left(\mathrm{tr}\left[(\mathbf{D}^\mu \mathbf{H})^\dagger \mathbf{D}^\nu \mathbf{H} \right] - \frac{c_X}{4} g^{\mu\nu} \mathrm{tr}\left[(\mathbf{D}_\rho \mathbf{H})^\dagger \mathbf{D}^\rho \mathbf{H} \right] \right) \Bigg] \tau^{aa} . \tag{B.7d}$$

B.2. Unitary Gauge

The Feynman rules in unitary gauge of the Lagrangian (B.6) are listed in this section. Only the relevant vertices for the vector boson scattering process are shown. In other words, vertices with more than four fields for effective operators and more than three fields for resonances are neglected.

Standard Model

$$A_{\mu_1} W^+_{\mu_2} W^-_{\mu_3} : \quad -\mathrm{i}e \left[\left(p_{1\,\mu_3} - p_{2\,\mu_3} \right) g_{\mu_1\mu_2} + \left(p_{3\,\mu_2} - p_{1\,\mu_2} \right) g_{\mu_1\mu_3} + \left(p_{2\,\mu_1} - p_{3\,\mu_1} \right) g_{\mu_2\mu_3} \right] , \tag{B.8a}$$

$$Z_{\mu_1} W^+_{\mu_2} W^-_{\mu_3} : \quad -\mathrm{i}c_w g \left[\left(p_{1\,\mu_3} - p_{2\,\mu_3} \right) g_{\mu_1\mu_2} + \left(p_{3\,\mu_2} - p_{1\,\mu_2} \right) g_{\mu_1\mu_3} + \left(p_{2\,\mu_1} - p_{3\,\mu_1} \right) g_{\mu_2\mu_3} \right] , \tag{B.8b}$$

$$h W^+_{\mu_2} W^-_{\mu_3} : \quad \mathrm{i} m_W g g_{\mu_2\mu_3} , \tag{B.8c}$$

$$h Z_{\mu_2} Z_{\mu_3} : \quad \mathrm{i} m_Z g g_{\mu_2\mu_3} , \tag{B.8d}$$

$$W^+_{\mu_1} W^+_{\mu_2} W^-_{\mu_3} W^-_{\mu_4} : \quad -\mathrm{i}g^2 \left(g_{\mu_1\mu_4} g_{\mu_2\mu_3} + g_{\mu_1\mu_3} g_{\mu_2\mu_4} - 2 g_{\mu_1\mu_2} g_{\mu_3\mu_4} \right) , \tag{B.8e}$$

$$Z_{\mu_1} Z_{\mu_2} W^+_{\mu_3} W^-_{\mu_4} : \quad \mathrm{i}c_w^2 g^2 \left(g_{\mu_1\mu_4} g_{\mu_2\mu_3} + g_{\mu_1\mu_3} g_{\mu_2\mu_4} - 2 g_{\mu_1\mu_2} g_{\mu_3\mu_4} \right) , \tag{B.8f}$$

$$A_{\mu_1} A_{\mu_2} W^+_{\mu_3} W^-_{\mu_4} : \quad \mathrm{i}e^2 \left(g_{\mu_1\mu_4} g_{\mu_2\mu_3} + g_{\mu_1\mu_3} g_{\mu_2\mu_4} - 2 g_{\mu_1\mu_2} g_{\mu_3\mu_4} \right) , \tag{B.8g}$$

$$A_{\mu_1} Z_{\mu_2} W^+_{\mu_3} W^-_{\mu_4} : \quad \mathrm{i}e c_w g \left(g_{\mu_1\mu_4} g_{\mu_2\mu_3} + g_{\mu_1\mu_3} g_{\mu_2\mu_4} - 2 g_{\mu_1\mu_2} g_{\mu_3\mu_4} \right) , \tag{B.8h}$$

$$h_{\mu_1} h_{\mu_2} W^+_{\mu_3} W^-_{\mu_4} : \quad \frac{\mathrm{i}}{2} g^2 g_{\mu_3\mu_4} , \tag{B.8i}$$

$$h_{\mu_1} h_{\mu_2} Z_{\mu_3} Z_{\mu_4} : \quad \frac{\mathrm{i}}{2} \frac{g^2}{c_w^2} g_{\mu_3\mu_4} . \tag{B.8j}$$

$\mathcal{L}_{HD}$

$$hW_\mu^+W_\nu^- : \quad \frac{\mathrm{i}g^2v^3}{4}F_{HD}g_{\mu\nu}\,, \tag{B.9a}$$

$$hZ_\mu Z_\nu : \quad \frac{\mathrm{i}g^2v^3}{4c_w^2}F_{HD}g_{\mu\nu}\,, \tag{B.9b}$$

$$h(p_1)h(p_2)h(p_3) : \quad -\mathrm{i}vF_{HD}\left(p_1\cdot p_2 + p_1\cdot p_3 + p_2\cdot p_3\right)\,, \tag{B.9c}$$

$$hhW_\mu^+W_\nu^- : \quad \frac{5\mathrm{i}g^2v^2}{4}F_{HD}g_{\mu\nu}\,, \tag{B.9d}$$

$$hhZ_\mu Z_\nu : \quad \frac{5\mathrm{i}g^2v^2}{4c_w^2}F_{HD}g_{\mu\nu}\,, \tag{B.9e}$$

$$\begin{aligned} h(p_1)h(p_2)h(p_3)h(p_4) : \quad & -\mathrm{i}F_{HD}\left(p_1\cdot p_2 + p_1\cdot p_3 + p_1\cdot p_4\right. \\ & \left. + p_2\cdot p_3 + p_2\cdot p_4 + p_3\cdot p_4\right)\,. \end{aligned} \tag{B.9f}$$

$\mathcal{L}_S$

$$\begin{aligned} W_{\mu_1}^+W_{\mu_2}^+W_{\mu_3}^-W_{\mu_4}^- : \quad & \frac{\mathrm{i}g^4v^4}{16}\left[\left(F_{S,0}+2F_{S,1}\right)\left(g_{\mu_1\mu_3}g_{\mu_2\mu_4}+g_{\mu_1\mu_4}g_{\mu_2\mu_3}\right)\right. \\ & \left. +2F_{S,0}g_{\mu_1\mu_2}g_{\mu_3\mu_4}\right]\,, \end{aligned} \tag{B.10a}$$

$$\begin{aligned} Z_{\mu_1}Z_{\mu_2}W_{\mu_3}^+W_{\mu_4}^- : \quad & \frac{\mathrm{i}g^4v^4}{16c_w^2}\left[F_{S,0}\left(g_{\mu_1\mu_3}g_{\mu_2\mu_4}+g_{\mu_1\mu_4}g_{\mu_2\mu_3}\right)\right. \\ & \left. +2F_{S,1}g_{\mu_1\mu_2}g_{\mu_3\mu_4}\right]\,, \end{aligned} \tag{B.10b}$$

$$\begin{aligned} Z_{\mu_1}Z_{\mu_2}Z_{\mu_3}Z_{\mu_4} : \quad & \frac{\mathrm{i}g^4v^4}{8c_w^4}\left(F_{S,0}+F_{S,1}\right)\left[g_{\mu_1\mu_2}g_{\mu_3\mu_4}g_{\mu_1\mu_3}g_{\mu_2\mu_4}\right. \\ & \left. +g_{\mu_1\mu_4}g_{\mu_2\mu_3}\right]\,, \end{aligned} \tag{B.10c}$$

$$\begin{aligned} h(p_1)h(p_2)W_{\mu_3}^+W_{\mu_4}^- : \quad & -\frac{\mathrm{i}g^2v^2}{4}\left[F_{S,0}\left(p_{1\,\mu_3}p_{2\,\mu_4}+p_{1\,\mu_4}p_{2\,\mu_3}\right)\right. \\ & \left. +2F_{S,1}g_{\mu_3\mu_4}p_1\cdot p_2\right]\,, \end{aligned} \tag{B.10d}$$

$$\begin{aligned} h(p_1)h(p_2)Z_{\mu_3}Z_{\mu_4} : \quad & -\frac{\mathrm{i}g^2v^2}{4c_w^2}\left[F_{S,0}\left(p_{1\,\mu_3}p_{2\,\mu_4}+p_{1\,\mu_4}p_{2\,\mu_3}\right)\right. \\ & \left. +2F_{S,1}g_{\mu_3\mu_4}p_1\cdot p_2\right]\,, \end{aligned} \tag{B.10e}$$

$$\begin{aligned} h(p_1)h(p_2)h(p_3)h(p_4) : \quad & 2\mathrm{i}\left(F_{S,0}+F_{S,1}\right)\left[\left(p_1\cdot p_2\right)\left(p_3\cdot p_4\right)\right. \\ & +\left(p_1\cdot p_3\right)\left(p_2\cdot p_4\right) \\ & \left.+\left(p_1\cdot p_4\right)\left(p_2\cdot p_3\right)\right]\,. \end{aligned} \tag{B.10f}$$

$\mathcal{L}_\sigma$

$$\sigma W_\mu^+ W_\nu^- : \qquad \frac{\mathrm{i}g^2v^2}{4} F_\sigma g_{\mu\nu}\,, \tag{B.11a}$$

$$\sigma Z_\mu Z_\nu : \qquad \frac{\mathrm{i}g^2v^2}{4c_w^2} F_\sigma g_{\mu\nu}\,, \tag{B.11b}$$

$$\sigma h\,(p_1)\, h\,(p_2) : \qquad -\mathrm{i}F_\sigma\, p_1 \cdot p_2\,. \tag{B.11c}$$

$\mathcal{L}_\phi$

$$\phi_t^{\pm\pm} W_\mu^\mp W_\nu^\mp : \qquad \frac{\mathrm{i}g^2v^2}{4} F_\phi g_{\mu\nu}\,, \tag{B.12a}$$

$$\phi_t^{\pm} W_\mu^\mp Z_\nu : \qquad \frac{\mathrm{i}g^2v^2}{4\sqrt{2}c_w} F_\phi g_{\mu\nu}\,, \tag{B.12b}$$

$$\phi_t^0 W_\mu^\mp W_\nu^\pm : \qquad -\frac{\mathrm{i}g^2v^2}{4\sqrt{6}} F_\phi g_{\mu\nu}\,, \tag{B.12c}$$

$$\phi_t^0 Z_\mu Z_\nu : \qquad \frac{\mathrm{i}g^2v^2}{2\sqrt{6}c_w^2} F_\phi g_{\mu\nu}\,, \tag{B.12d}$$

$$\phi_s W_\mu^\mp W_\nu^\pm : \qquad \frac{\mathrm{i}g^2v^2}{8\sqrt{3}} F_\phi g_{\mu\nu}\,, \tag{B.12e}$$

$$\phi_s Z_\mu Z_\nu : \qquad \frac{\mathrm{i}g^2v^2}{8\sqrt{3}c_w^2} F_\phi g_{\mu\nu}\,, \tag{B.12f}$$

$$\phi_v^{\pm} h\,(p)\, W_\mu^\mp : \qquad -\frac{g\,v}{2\sqrt{2}} F_\phi\, p_\mu\,, \tag{B.12g}$$

$$\phi_v^{\pm} h\,(p)\, Z_\mu : \qquad \frac{g\,v}{2\sqrt{2}c_w} F_\phi\, p_\mu\,, \tag{B.12h}$$

$$\phi_s h\,(p_1)\, h\,(p_2) : \qquad \frac{\sqrt{3}}{2}\mathrm{i}F_\phi\, p_1 \cdot p_2\,. \tag{B.12i}$$

$\mathcal{L}_f$

$$f_{\mu\nu} W_\rho^+ W_\sigma^- : \qquad \frac{\mathrm{i}g^2v^2}{8} F_f \left[g_{\mu\sigma} g_{\nu\rho} + g_{\mu\rho} g_{\nu\sigma} - \frac{c_f}{2} g_{\mu\nu} g_{\rho\sigma} \right], \tag{B.13a}$$

$$f_{\mu\nu} Z_\rho Z_\sigma : \qquad \frac{\mathrm{i}g^2v^2}{8c_w^2} F_f \left[g_{\mu\sigma} g_{\nu\rho} + g_{\mu\rho} g_{\nu\sigma} - \frac{c_f}{2} g_{\mu\nu} g_{\rho\sigma} \right], \tag{B.13b}$$

$$f_{\mu\nu} h\,(p_1)\, h\,(p_2) : \qquad -\frac{\mathrm{i}}{2} F_f \left[p_{1\,\mu} p_{2\,\nu} + p_{1\,\mu} p_{2\,\nu} - \frac{c_f}{2} g_{\mu\nu}\, p_1 \cdot p_2 \right]. \tag{B.13c}$$

$\mathcal{L}_f$ in Stückelberg formalism

$$f_{f\mu\nu}W_\rho^+W_\sigma^-: \quad \frac{\mathrm{i}g^2v^2}{8}F_f\left[g_{\mu\sigma}g_{\nu\rho}+g_{\mu\rho}g_{\nu\sigma}-\frac{c_f}{2}g_{\mu\nu}g_{\rho\sigma}\right], \tag{B.14a}$$

$$f_{f\mu\nu}Z_\rho Z_\sigma: \quad \frac{\mathrm{i}g^2v^2}{8c_w^2}F_f\left[g_{\mu\sigma}g_{\nu\rho}+g_{\mu\rho}g_{\nu\sigma}-\frac{c_f}{2}g_{\mu\nu}g_{\rho\sigma}\right], \tag{B.14b}$$

$$f_{f\mu\nu}h\left(p_1\right)h\left(p_2\right): \quad -\frac{\mathrm{i}}{2}F_f\left[p_{1\,\mu}p_{2\,\nu}+p_{1\,\mu}p_{2\,\nu}-\frac{c_f}{2}g_{\mu\nu}p_1\cdot p_2\right]. \tag{B.14c}$$

Because of $\partial_\nu J_f^{\mu\nu}\neq 0$:

$$A_{f\mu}\left(p\right)W_\rho^+W_\sigma^-: \quad \frac{g^2v^2}{4\sqrt{2}m_f}F_f\left(p_\rho g_{\mu\sigma}+p_\sigma g_{\mu\rho}-\frac{cf}{2}p_\mu g_{\sigma\rho}\right), \tag{B.15}$$

$$A_{f\mu}\left(p\right)Z_\rho Z_\sigma: \quad \frac{g^2v^2}{4c_w^2\sqrt{2}m_f}F_f\left(p_\rho g_{\mu\sigma}+p_\sigma g_{\mu\rho}-\frac{cf}{2}p_\mu g_{\sigma\rho}\right), \tag{B.16}$$

$$A_{f\mu}h\left(p_1\right)h\left(p_2\right): \quad \frac{1}{\sqrt{2}m_f}F_f\left[p_1^2p_{2\,\mu}+p_2^2p_{1\,\mu}\right. \tag{B.17}$$

$$\left.+\frac{1}{2}\left(2-c_f\right)p_1\cdot p_2\left(p_1+p_2\right)_\mu\right]. \tag{B.18}$$

Because of $\partial_\mu\partial_\nu J_f^{\mu\nu}\neq 0$ and $J_f{}_\mu^\mu\neq 0$:

$$\sigma_f\left(p\right)W_\rho^+W_\sigma^-: \quad \frac{\mathrm{i}g^2v^2}{4\sqrt{6}}F_f\left[\left(cf-1\right)g_{\rho\sigma}-\frac{1}{m_f^2}\left(2k_\rho k_\sigma-\frac{c_f}{2}k^2g_{\rho\sigma}\right)\right], \tag{B.19a}$$

$$\sigma_f\left(p\right)Z_\rho Z_\sigma: \quad \frac{\mathrm{i}g^2v^2}{4\sqrt{6}c_w^2}F_f\left[\left(cf-1\right)g_{\rho\sigma}-\frac{1}{m_f^2}\left(2k_\rho k_\sigma-\frac{c_f}{2}k^2g_{\rho\sigma}\right)\right], \tag{B.19b}$$

$$\sigma_f h\left(p_1\right)h\left(p_2\right): \quad -\frac{\mathrm{i}}{\sqrt{6}}F_f\left[\left(cf-1\right)\left(p_1\cdot p_2\right)\right.$$

$$-\frac{1}{m_f^2}\Big(2p_1\cdot\left(p_1+p_2\right)p_2\cdot\left(p_1+p_2\right)$$

$$\left.-\frac{c_f}{2}p_1\cdot p_2\left(p_1+p_2\right)^2\Big)\right]. \tag{B.19c}$$

$\mathcal{L}_X$

$$X^{\pm\pm}_{t\mu\nu} W^{\mp}_{\rho} W^{\mp}_{\sigma} : \quad \frac{\mathrm{i}g^2v^2}{8} F_X \left[g_{\mu\sigma} g_{\nu\rho} + g_{\mu\rho} g_{\nu\sigma} - \frac{c_X}{2} g_{\mu\nu} g_{\rho\sigma} \right], \tag{B.20a}$$

$$X^{\pm}_{t\mu\nu} W^{\mp}_{\rho} Z_{\sigma} : \quad \frac{\mathrm{i}g^2v^2}{8\sqrt{2}c_w} F_X \left[g_{\mu\sigma} g_{\nu\rho} + g_{\mu\rho} g_{\nu\sigma} - \frac{c_X}{2} g_{\mu\nu} g_{\rho\sigma} \right], \tag{B.20b}$$

$$X^{0}_{t\mu\nu} W^{\mp}_{\rho} W^{\pm}_{\sigma} : \quad -\frac{\mathrm{i}g^2v^2}{8\sqrt{6}} F_X \left[g_{\mu\sigma} g_{\nu\rho} + g_{\mu\rho} g_{\nu\sigma} - \frac{c_X}{2} g_{\mu\nu} g_{\rho\sigma} \right], \tag{B.20c}$$

$$X^{0}_{t\mu\nu} Z_{\rho} Z_{\sigma} : \quad \frac{\mathrm{i}g^2v^2}{4\sqrt{6}c_w^2} F_X \left[g_{\mu\sigma} g_{\nu\rho} + g_{\mu\rho} g_{\nu\sigma} - \frac{c_X}{2} g_{\mu\nu} g_{\rho\sigma} \right], \tag{B.20d}$$

$$X_{s\mu\nu} W^{\mp}_{\rho} W^{\pm}_{\sigma} : \quad \frac{\mathrm{i}g^2v^2}{16\sqrt{3}} F_X \left[g_{\mu\sigma} g_{\nu\rho} + g_{\mu\rho} g_{\nu\sigma} - \frac{c_X}{2} g_{\mu\nu} g_{\rho\sigma} \right], \tag{B.20e}$$

$$X_{s\mu\nu} Z_{\rho} Z_{\sigma} : \quad \frac{\mathrm{i}g^2v^2}{16\sqrt{3}c_w^2} F_X \left[g_{\mu\sigma} g_{\nu\rho} + g_{\mu\rho} g_{\nu\sigma} - \frac{c_X}{2} g_{\mu\nu} g_{\rho\sigma} \right], \tag{B.20f}$$

$$X^{\pm}_{v\mu\nu} h(p) W^{\mp}_{\rho} : \quad -\frac{g v}{4\sqrt{2}} F_X \left[p_{\mu} g_{\nu\rho} + p_{\nu} g_{\mu\rho} - \frac{c_X}{2} p_{\rho} g_{\mu\nu} \right], \tag{B.20g}$$

$$X_{v\mu\nu} v^{\pm} h(p) Z_{\rho} : \quad \frac{g v}{4\sqrt{2}c_w} F_X \left[p_{\mu} g_{\nu\rho} + p_{\nu} g_{\mu\rho} - \frac{c_X}{2} p_{\rho} g_{\mu\nu} \right], \tag{B.20h}$$

$$X_{s\mu\nu} h(p_1) h(p_2) : \quad \frac{\sqrt{3}}{4} \mathrm{i} F_X \left[p_{1\,\mu} p_{2\,\nu} + p_{1\,\mu} p_{2\,\nu} - \frac{c_X}{2} g_{\mu\nu} p_1 \cdot p_2 \right]. \tag{B.20i}$$

B.3. Gaugeless Limit

The gaugeless limit is suited to calculate the high energy behavior of new physics in the Higgs/Goldstone boson sector, because the subleading transversal polarizations are neglected. All vertices involving Higgs and Goldstone bosons are listed in this section.

$\mathcal{L}_{HD}$

$$
\begin{aligned}
hw^+(p_1)w^-(p_2): &\quad -\mathrm{i}vF_{HD}\,(p_1\cdot p_2)\,, && \text{(B.21a)}\\
hz(p_1)z(p_2): &\quad -\mathrm{i}vF_{HD}\,(p_1\cdot p_2)\,, && \text{(B.21b)}\\
h(p_1)h(p_2)h(p_3): &\quad -\mathrm{i}vF_{HD}\,(p_1\cdot p_2+p_1\cdot p_3+p_2\cdot p_3)\,, && \text{(B.21c)}\\
w^+(p_1)w^+(p_2)w^-(p_3)w^-(p_4): &\quad -\mathrm{i}F_{HD}\,(p_1\cdot p_3+p_1\cdot p_4+p_2\cdot p_3+p_2\cdot p_4)\,, && \text{(B.21d)}\\
w^+(p_1)w^-(p_2)z(p_3)z(p_4): &\quad -\mathrm{i}F_{HD}\,(p_1\cdot p_2+p_3\cdot p_4)\,, && \text{(B.21e)}\\
z(p_1)z(p_2)z(p_3)z(p_4): &\quad -\mathrm{i}F_{HD}\,(p_1\cdot p_2+p_1\cdot p_3+p_1\cdot p_4 && \\
&\qquad +p_2\cdot p_3+p_2\cdot p_4+p_3\cdot p_4)\,, && \text{(B.21f)}\\
h(p_1)h(p_2)w^+(p_3)w^-(p_4): &\quad -\mathrm{i}F_{HD}\,(p_1\cdot p_2+p_3\cdot p_4)\,, && \text{(B.21g)}\\
h(p_1)h(p_2)z(p_3)z(p_4): &\quad -\mathrm{i}F_{HD}\,(p_1\cdot p_2+p_3\cdot p_4)\,, && \text{(B.21h)}\\
h(p_1)h(p_2)h(p_3)h(p_4): &\quad -\mathrm{i}F_{HD}\,(p_1\cdot p_2+p_1\cdot p_3+p_1\cdot p_4 && \\
&\qquad +p_2\cdot p_3+p_2\cdot p_4+p_3\cdot p_4)\,. && \text{(B.21i)}
\end{aligned}
$$

$\mathcal{L}_S$

$$
\begin{aligned}
w^+(p_1)w^+(p_2)w^-(p_3)w^-(p_4): &\quad \mathrm{i}\,(F_{S,0}+2F_{S,1})\,[(p_1\cdot p_3)\,(p_2\cdot p_4) && \\
&\qquad +(p_1\cdot p_4)\,(p_2\cdot p_3)] && \\
&\qquad +2\mathrm{i}F_{S,0}\,(p_1\cdot p_2)\,(p_3\cdot p_4)\,, && \text{(B.22a)}\\
z(p_1)z(p_2)w^+(p_3)w^-(p_4): &\quad \mathrm{i}F_{S,0}\,[(p_1\cdot p_3)\,(p_2\cdot p_4) && \\
&\qquad +(p_1\cdot p_4)\,(p_2\cdot p_3)] && \\
&\qquad +2\mathrm{i}F_{S,1}\,(p_1\cdot p_2)\,(p_3\cdot p_4)\,, && \text{(B.22b)}\\
z(p_1)z(p_2)z(p_3)z(p_4): &\quad 2\mathrm{i}\,(F_{S,0}+F_{S,1})\,[(p_1\cdot p_2)\,(p_3\cdot p_4) && \\
&\qquad +(p_1\cdot p_3)\,(p_2\cdot p_4) && \\
&\qquad +(p_1\cdot p_4)\,(p_2\cdot p_3)]\,, && \text{(B.22c)}
\end{aligned}
$$

$$
\begin{aligned}
h(p_1)h(p_2)w^+(p_3)w^-(p_4): \quad & \mathrm{i}F_{S,0}\left[(p_1\cdot p_3)(p_2\cdot p_4)\right. \\
& \left.+(p_1\cdot p_4)(p_2\cdot p_3)\right] \\
& +2\mathrm{i}F_{S,1}(p_1\cdot p_2)(p_3\cdot p_4)\,, \qquad \text{(B.22d)}\\
h(p_1)h(p_2)z(p_3)z(p_4): \quad & \mathrm{i}F_{S,0}\left[(p_1\cdot p_3)(p_2\cdot p_4)\right. \\
& \left.+(p_1\cdot p_4)(p_2\cdot p_3)\right] \\
& +2\mathrm{i}F_{S,1}(p_1\cdot p_2)(p_3\cdot p_4)\,, \qquad \text{(B.22e)}\\
h(p_1)h(p_2)h(p_3)h(p_4): \quad & 2\mathrm{i}\left(F_{S,0}+F_{S,1}\right)\left[(p_1\cdot p_2)(p_3\cdot p_4)\right. \\
& +(p_1\cdot p_3)(p_2\cdot p_4) \\
& \left.+(p_1\cdot p_4)(p_2\cdot p_3)\right]\,. \qquad \text{(B.22f)}
\end{aligned}
$$

$\mathcal{L}_\sigma$

$$
\left.\begin{array}{l}
\sigma w^+(p_1)\,w^-(p_2)\\
\sigma z(p_1)\,z(p_2)\\
\sigma h(p_1)\,h(p_2)
\end{array}\right\}: \quad -\mathrm{i}F_f\,p_1\cdot p_2\,. \qquad \text{(B.23)}
$$

$\mathcal{L}_\phi$

$$
\begin{aligned}
\phi_t^{\pm\pm}w^\mp(p_1)\,w^\mp(p_2): \quad & -\mathrm{i}F_\phi\,p_1\cdot p_2\,, && \text{(B.24a)}\\
\phi_t^{\pm}w^\mp(p_1)\,z(p_2): \quad & -\frac{\mathrm{i}}{\sqrt{2}}F_\phi\,p_1\cdot p_2\,, && \text{(B.24b)}\\
\phi_t^{0}w^\mp(p_1)\,w^\pm(p_2): \quad & \frac{\mathrm{i}}{\sqrt{6}}F_\phi\,p_1\cdot p_2\,, && \text{(B.24c)}\\
\phi_t^{0}z(p_1)\,z(p_2): \quad & -\frac{\sqrt{2}}{\sqrt{3}}\mathrm{i}F_\phi\,p_1\cdot p_2\,, && \text{(B.24d)}\\
\phi_s w^\mp(p_1)\,w^\pm(p_2): \quad & -\frac{\mathrm{i}}{2\sqrt{3}}F_\phi\,p_1\cdot p_2\,, && \text{(B.24e)}\\
\phi_s z(p_1)\,z(p_2): \quad & -\frac{\mathrm{i}}{2\sqrt{3}}F_\phi\,p_1\cdot p_2\,, && \text{(B.24f)}\\
\phi_v^{\pm}w^\mp(p_1)\,h(p_2): \quad & \frac{\mathrm{i}}{\sqrt{2}}F_\phi\,p_1\cdot p_2\,, && \text{(B.24g)}\\
\phi_v^{0}z(p_1)\,h(p_2): \quad & -\frac{\mathrm{i}}{\sqrt{2}}F_\phi\,p_1\cdot p_2\,, && \text{(B.24h)}\\
\phi_s h(p_1)\,h(p_2): \quad & \frac{\sqrt{3}}{2}\mathrm{i}F_\phi\,p_1\cdot p_2\,. && \text{(B.24i)}
\end{aligned}
$$

$\mathcal{L}_f$

$$\left.\begin{aligned} &f_{\mu\nu} w^+(p_1)\, w^-(p_2) \\ &f_{\mu\nu} z(p_1)\, z(p_2) \\ &f_{\mu\nu} h(p_1)\, h(p_2) \end{aligned}\right\}: \quad -\frac{\mathrm{i}}{2} F_f \left[p_{1\mu} p_{2\nu} + p_{1\mu} p_{2\nu} - \frac{c_f}{2} g_{\mu\nu} p_1 \cdot p_2 \right]. \tag{B.25}$$

$\mathcal{L}_f$ in Stückelberg formalism

$$\left.\begin{aligned} &f_{f\mu\nu} w^+(p_1)\, w^-(p_2) \\ &f_{f\mu\nu} z(p_1)\, z(p_2) \\ &f_{f\mu\nu} h(p_1)\, h(p_2) \end{aligned}\right\}: \quad -\frac{\mathrm{i}}{2} F_f \left[p_{1\mu} p_{2\nu} + p_{1\mu} p_{2\nu} - \frac{c_f}{2} g_{\mu\nu} p_1 \cdot p_2 \right], \tag{B.26a}$$

$$\left.\begin{aligned} &A_{f\mu} w^+(p_1)\, w^-(p_2) \\ &A_{f\mu} z(p_1)\, z(p_2) \\ &A_{f\mu} h(p_1)\, h(p_2) \end{aligned}\right\}: \quad \frac{1}{\sqrt{2} m_f} F_f \left[p_1^2 p_2^\mu + p_2^2 p_1^\mu + \frac{2 - c_f}{2} p_1 \cdot p_2 \, (p_1 + p_2)^\mu \right], \tag{B.26b}$$

$$\left.\begin{aligned} &\sigma_f w^+(p_1)\, w^-(p_2) \\ &\sigma_f z(p_1)\, z(p_2) \\ &\sigma_f h(p_1)\, h(p_2) \end{aligned}\right\}: \quad \begin{aligned} &-\frac{\mathrm{i}}{\sqrt{6}} F_f \left[(cf - 1)\, (p_1 \cdot p_2) \right. \\ &\quad - \frac{1}{m_f^2} \Big(p_1 \cdot p_2 \left(p_1^2 + p_2^2 \right) + 2 p_1^2 p_2^2 \\ &\quad \left. + \frac{2 - c_f}{2} p_1 \cdot p_2 \, (p_1 + p_2)^2 \Big) \right]. \end{aligned} \tag{B.26c}$$

$\mathcal{L}_X$

$$X^{\pm\pm}_{t\mu\nu} w^\mp(p_1)\, w^\mp(p_2): \quad -\frac{\mathrm{i}}{2} F_X \left[p_{1\mu} p_{2\nu} + p_{1\mu} p_{2\nu} - \frac{c_X}{2} g_{\mu\nu} p_1 \cdot p_2 \right], \tag{B.27a}$$

$$X^{\pm}_{t\mu\nu} w^\mp(p_1)\, z(p_2): \quad -\frac{\mathrm{i}}{2\sqrt{2}} F_X \left[p_{1\mu} p_{2\nu} + p_{1\mu} p_{2\nu} - \frac{c_X}{2} g_{\mu\nu} p_1 \cdot p_2 \right], \tag{B.27b}$$

$$X^{0}_{t\mu\nu} w^\mp(p_1)\, w^\pm(p_2): \quad \frac{\mathrm{i}}{2\sqrt{6}} F_X \left[p_{1\mu} p_{2\nu} + p_{1\mu} p_{2\nu} - \frac{c_X}{2} g_{\mu\nu} p_1 \cdot p_2 \right], \tag{B.27c}$$

$$X^{0}_{t\mu\nu} z(p_1)\, z(p_2): \quad -\frac{\mathrm{i}}{\sqrt{6}} F_X \left[p_{1\mu} p_{2\nu} + p_{1\mu} p_{2\nu} - \frac{c_X}{2} g_{\mu\nu} p_1 \cdot p_2 \right], \tag{B.27d}$$

$$X_{s\mu\nu} w^{\mp}(p_1)\, w^{\pm}(p_2): \quad -\frac{\mathrm{i}}{4\sqrt{3}} F_X \left[p_{1\,\mu} p_{2\,\nu} + p_{1\,\mu} p_{2\,\nu} - \frac{c_X}{2} g_{\mu\nu} p_1 \cdot p_2 \right], \tag{B.27e}$$

$$X_{s\mu\nu} z(p_1)\, z(p_2): \quad -\frac{\mathrm{i}}{4\sqrt{3}} F_X \left[p_{1\,\mu} p_{2\,\nu} + p_{1\,\mu} p_{2\,\nu} - \frac{c_X}{2} g_{\mu\nu} p_1 \cdot p_2 \right], \tag{B.27f}$$

$$X^{\pm}_{v\mu\nu} w^{\mp}(p_1)\, h(p_2): \quad \frac{\mathrm{i}}{2\sqrt{2}} F_X \left[p_{1\,\mu} p_{2\,\nu} + p_{1\,\mu} p_{2\,\nu} - \frac{c_X}{2} g_{\mu\nu} p_1 \cdot p_2 \right], \tag{B.27g}$$

$$X^{0}_{v\mu\nu} z(p_1)\, h(p_2): \quad -\frac{\mathrm{i}}{2\sqrt{2}} F_X \left[p_{1\,\mu} p_{2\,\nu} + p_{1\,\mu} p_{2\,\nu} - \frac{c_X}{2} g_{\mu\nu} p_1 \cdot p_2 \right], \tag{B.27h}$$

$$X_{s\mu\nu} h(p_1)\, h(p_2): \quad \frac{\sqrt{3}}{4} \mathrm{i} F_X \left[p_{1\,\mu} p_{2\,\nu} + p_{1\,\mu} p_{2\,\nu} - \frac{c_X}{2} g_{\mu\nu} p_1 \cdot p_2 \right]. \tag{B.27i}$$

B.4. Conversion

This sections contains the conversion of the discussed effective field operators $\mathcal{L}_S$ and $\mathcal{L}_{HD}$ to other bases.

B.4.1. $\mathcal{L}_S$

The conversion from Eboli representation (see Appendix A.5) to matrix representation has to be carried out for every vertex separately, because the Higgs doublet realization does not conserve $SU(2)_C$ as the Higgs matrix representation.

- for WWWW-vertex:

$$F_{S,0} = 2\frac{f_{S,0}}{\Lambda^4}, \tag{B.28a}$$

$$F_{S,0} + 2F_{S,1} = 2\frac{f_{S,1}}{\Lambda^4}, \tag{B.28b}$$

- for WWZZ-vertex:

$$F_{S,0} = \frac{f_{S,0}}{\Lambda^4}, \tag{B.28c}$$

$$F_{S,1} = \frac{f_{S,1}}{\Lambda^4}, \tag{B.28d}$$

- for ZZZZ-vertex:

$$F_{S,0} + F_{S,1} = \frac{f_{S,0} + f_{S,1}}{\Lambda^4}. \tag{B.28e}$$

In contrary, the coefficients α_4 and α_5 of the Appelquist basis (see eq. (3.10)) can be related to $F_{S,0}$ and $F_{S,1}$ for weak vector boson scattering processes via

$$F_{S,0} \widehat{=} 16\frac{\alpha_4}{v^4}, \tag{B.29a}$$

$$F_{S,1} \widehat{=} 16\frac{\alpha_5}{v^4}. \tag{B.29b}$$

This conversion is only valid, if the Higgs contributions of $\mathcal{L}_{S,0}$ and $\mathcal{L}_{S,1}$ can be neglected.

By redefining the operators $\mathcal{O}_S$ of the Eboli basis as in [144]

$$\mathcal{O}'_{S,0} = \frac{1}{2}\left[\left(D_\mu\Phi\right)^\dagger D_\nu\Phi\right] \times \left[\left(D^\mu\Phi\right)^\dagger D^\nu\Phi + \left(D^\nu\Phi\right)^\dagger D^\mu\Phi\right], \tag{B.30a}$$

$$\mathcal{O}_{S,1} = \left[\left(D_\mu\Phi\right)^\dagger D^\mu\Phi\right] \times \left[\left(D_\nu\Phi\right)^\dagger D^\nu\Phi\right], \tag{B.30b}$$

$$\mathcal{O}'_{S,2} = \frac{1}{2}\left[\left(D_\mu\Phi\right)^\dagger D_\nu\Phi\right] \times \left[\left(D^\mu\Phi\right)^\dagger D^\nu\Phi - \left(D^\nu\Phi\right)^\dagger D^\mu\Phi\right], \tag{B.30c}$$

the coupling coefficients can be expressed in terms of coefficients of $\mathcal{L}_{S,0}$ and $\mathcal{L}_{S,1}$ in the Higgs Matrix realization

$$F_{S,0} = \frac{f'_{S,0}}{\Lambda^4}, \tag{B.31a}$$

$$F_{S,1} = \frac{f_{S,1}}{\Lambda^4}. \tag{B.31b}$$

$\mathcal{L}_{HD}$

The total contribution of the operator $\mathcal{L}_{HD}$ to the vector boson scattering amplitude can be separated into a new physics only part and and part which mixes with the Standard Model

$$\mathcal{A}_{HD}(wwzz) = -\frac{s^2}{s-m_H^2}\left(\underbrace{F_{HD}^2\frac{v^2}{4}}_{\text{only NP}} + \underbrace{F_{HD}}_{\text{SM \& NP mixing}}\right). \tag{B.32}$$

The effect of the dimension six operator is equivalent to an additional scalar resonance with the mass of the Standard model Higgs boson. Thus, the coupling F_{HD} can be related to the scalar coupling F_σ

$$F_\sigma = \sqrt{F_{HD}^2 v^2 + 4F_{HD}} \tag{B.33a}$$

$$F_{\text{HD}} = -\frac{2}{v^2}\left(1 \pm \sqrt{\frac{v^2}{4}F_\sigma^2 + 1}\right). \tag{B.33b}$$

Chapter C

WHIZARD Implementation

New models including the T-matrix unitarization scheme via the Thales projection for the effective field theory operators $\mathcal{L}_{S,0}$, $\mathcal{L}_{S,1}$ and the resonances σ, f and ϕ are implemented into the Monte-Carlo generator `WHIZARD` for off-shell vector boson scattering processes as described in Section 4.4.1.

In this appendix, the `WHIZARD` models, which were implemented as part of this thesis, are introduced. Furthermore, the functional principle of `WHIZARD` and `O'MEGA` is explained using the Standard Model as an example. Finally, exemplary parts of the resonance model and T-matrix implementation are given. All files, which are necessary for a generic model implementation in `WHIZARD` are discussed. The file paths mentioned in this appendix are given relative to the main `WHIZARD` folder. Therefore, the resonance model implementation can be also used as a guide to implement further models into `WHIZARD`.

Model	SM-Higgs	Resonance Implementation	Effective Field Theory Representation
NoH_rx	–	Form factor	Non-linear
SM_rx	✓	Form factor	Non-linear
AltH	–	Fields	Non-linear
SSC	✓	Fields	Non-linear
SSC_2	✓	Fields	Higgs-matrix (linear)
SSC_AltT	✓	Fields	Higgs-matrix (linear)

Table C.1.: Overview of new physics models implemented into `WHIZARD` 2.2.6 to study vector boson scattering processes.

C.1. Models

An overview of the available models in WHIZARD, in which the unitarization method for the vector boson scattering processes are included, is given in Table C.1.

The model SM_rx is based on the previous SM_km model. Here, the old K-matrix unitarization scheme of [142] is replaced with the new T-matrix unitarization scheme introduced in Section 4.4.1. During this thesis, the impact of resonances to vector boson scattering processes were introduced directly as physical fields in the model SSC. This was necessary to properly describe the tensor resonance with its contribution to transversal vector boson scattering processes. The ansatz via the form factor implementation into the longitudinal quartic vector boson scattering vertex is not sufficient. New physics contributions of the models SM_rx, SSC and the related no Standard Higgs models NoH_rx and AltH are formulated in the non-linear basis (3.10). Due to the linear Higgs-matrix representation, additional interactions involving at least one Higgs are introduced (see Chapter 3 and 5). The model SSC_2 can be used to simulate these interaction within the discussed T-matrix unitarization (see Section 4.4.1). Its parameters can be set via the WHIZARD script language SINDARIN. An overview of the relevant commands is given in Table C.2a. An extension of the model SSC_2 is the model SSC_AltT. It can be used to analyze the single tensor contributions in the Stückelberg formalism (5.31) and introduces additional Sindarin parameters (see Table C.2b). Additionally, the model SM_ul is implemented to project the isospin-spin bound to other observables like differential cross sections (see Table C.2c for Sindarin paramters).

The introduced models were created as part of this thesis and are included into WHIZARD since release version 2.2.6. Minor correction to the isotensor scalar resonance and isotensor tensor are implemented into the WHIZARD 2.2.8 trunk r7308 and r7332, respectively. These will be available in the next official release WHIZARD 2.2.8.

Parameters	Default value	Description
fs0	0	Coupling strength of dimension eight operator $\mathcal{L}_{S,0}$ in TeV^{-4}
fs1	0	Coupling strength of dimension eight operator $\mathcal{L}_{S,1}$ in TeV^{-4}
gkm_s	0	Coupling strength of isoscalar scalar resonance in TeV^{-1}
gkm_p	0	Coupling strength of isotensor scalar resonance in TeV^{-1}
gkm_f	0	Coupling strength of isoscalar tensor resonance in TeV^{-1}
gkm_t	0	Coupling strength of isotensor tensor resonance in TeV^{-1}
cf	2	Arbitrary coupling parameter for isoscalar tensor
mkm_s	10^{10}	mass of isoscalar scalar resonance in GeV
mkm_p	10^{10}	mass of isotensor scalar resonance in GeV
mkm_f	10^{10}	mass of isoscalar tensor resonance in GeV
mkm_t	10^{10}	mass of isoscalar tensor resonance in GeV
wkm_s	0	width of isoscalar scalar resonance in GeV
wkm_p	0	width of isotensor scalar resonance in GeV
wkm_f	0	width of isoscalar tensor resonance in GeV
wkm_t	0	width of isoscalar tensor resonance in GeV
fkm	1	Flag to enable T-matrix unitarization (0:off, 1:on)
wres	1	Flag to set the width to Breit-Wigner width (0:off, 1:on, only if corresponding width = 0)

(a) Sindarin parameters of the `WHIZARD` model SSC_2.

Parameters	Default value	Description
alt_tt	1	Flag for tensor-tensor (0:off, 1:on)
alt_tv	1	Flag for tensor-vector (0:off, 1:on)
alt_ts	1	Flag for tensor-scalar (trace) (0:off, 1:on)
alt_ts2	1	Flag for tensor-scalar (derivatives) (0:off, 1:on)

(b) Additional Sindarin parameters of the `WHIZARD` model SSC_AltT for the Stückelberg degrees of freedom.

Parameters	Default value	Description
isa_00	0	Saturation of $\mathcal{A}_{00}$ (0:off, 1:on)
isa_02	0	Saturation of $\mathcal{A}_{02}$ (0:off, 1:on)
isa_11	0	Saturation of $\mathcal{A}_{11}$ (0:off, 1:on)
isa_20	0	Saturation of $\mathcal{A}_{20}$ (0:off, 1:on)
isa_22	0	Saturation of $\mathcal{A}_{22}$ (0:off, 1:on)
fkm	1	Flag to enable isospin spin saturation; 0:off, 1:on

(c) Sindarin parameters of the `WHIZARD` model SM_ul.

Table C.2.: Sindarin parameters of introduced `WHIZARD` models.

C.2. The Standard Model in WHIZARD/O'MEGA

The scattering amplitude generation of the Monte Carlo generator WHIZARD and its matrix element generator O'MEGA will be shortly described in this section. As example serves the determination of the sign convention for the covariant derivative. Therefore, the WHIZARD implementation of the triple weak gauge coupling has to be investigated.

In OMEGA, which is written in OCaml, the allowed vertices and its structure of the Standard Model are defined in ./src/omega/src/modellib_SM.ml :

```
let tgc ((g1, g2, g3), t, c) = ((G g1, G g2, G g3), t, c)

let standard_triple_gauge =
  List.map tgc
[ ((Ga, Wm, Wp), Gauge_Gauge_Gauge 1, I_Q_W);
  ((Z, Wm, Wp), Gauge_Gauge_Gauge 1, I_G_ZWW);
  ((Gl, Gl, Gl), Gauge_Gauge_Gauge 1, I_Gs)]

  ...

  | I_Q_W -> "iqw" | I_G_ZWW -> "igzww"
  ...
```

The list tgc has three entries: the coupled fields, the lorentz structure of the coupling and its coupling constant. These are introduced in the WHIZARD file ./src/models/parameters_SM.f90 written in gfortran:

```
    par%cw      = par_array(23)
    par%sw      = par_array(24)
    par%ee      = par_array(25)

     ...

    e = par%ee
    sinthw = par%sw
    sin2thw = par%sw**2
    costhw = par%cw

     ...

    qw = e
    iqw = (0,1)*qw
    gzww = g * costhw
    igzww = (0,1)*gzww
```

These parameters are accessible by the user via WHIZARD's own script language SINDARIN. The parameters are defined with its initial values in ./share/models/SM.mdl:

```
parameter GF      = 1.16639E-5   # Fermi constant
parameter mZ      = 91.1882      # Z-boson mass
parameter mW      = 80.419       # W-boson mass

...

derived v      = 1 / sqrt (sqrt (2.) * GF)# v (Higgs vev)
derived cw     = mW / mZ                  # cos(theta_W)
derived sw     = sqrt (1-cw**2)           # sin(theta_W)
derived ee     = 2 * sw * mW / v          # em-coupling (GF scheme)
```

As mentioned at the beginning the Lorentz structure of the couplings is given in the OMEGA file ./src/omega/src/targets.ml:

```
          | Gauge_Gauge_Gauge coeff ->
              let c = format_coupling coeff c in
              begin match fusion with
              | (F23|F31|F12) ->
                  printf "g_gg(%s,%s,%s,%s,%s)" c wf1 p1 wf2 p2
              | (F32|F13|F21) ->
                  printf "g_gg(%s,%s,%s,%s,%s)" c wf2 p2 wf1 p1
              end
```

The function g_gg contains the prescription, how two fuse two incoming gauge bosons to an outgoing vector boson

$$\begin{aligned} A^{a,\mu}(k_1+k_2) = -\mathrm{i}g\big[&(k_1^\mu - k_2^\mu)A^{a_1}(k_1)\cdot A^{a_2}(k_2) \\ &+ (2k_2+k_1)\cdot A^{a_1}(k_1)A^{a_2,\mu}(k_2) \\ &- A^{a_1,\mu}(k_1)A^{a_2}(k_2)\cdot(2k_1+k_2)\big]. \end{aligned} \tag{C.1}$$

This means, it includes the Lorentz structure of the triple gauge vertex and is defined in ./src/omega/src/omegalib.nw

```
<<Implementation of couplings>>=
pure function g_gg (g, a1, k1, a2, k2) result (a)
  complex(kind=default), intent(in) :: g
  type(vector), intent(in) :: a1, a2
  type(momentum), intent(in) :: k1, k2
  type(vector) :: a
  a = (0, -1) * g * ((k1 - k2) * (a1 * a2) &
             + ((2*k2 + k1) * a1) * a2 - a1 * ((2*k1 + k2) * a2))
end function g_gg
```

To determine the final sign of the vertex, it has to be considered that `OMEGA` will add one i for every propagator and vertex in the function in `./src/omega/src/targets.ml`

```
let print_brakets dictionary amplitude =
  let name = flavors_symbol (flavors amplitude) in
  printf "      %s = 0" name; nl ();
  List.iter (print_braket amplitude dictionary name)
   (F.brakets amplitude);
  let n = List.length (F.externals amplitude) in
  if n mod 2 = 0 then begin
    printf "      @[<2>%s =@, - %s ! %d vertices, %d propagators"
      name name (n - 2) (n - 3); nl ()
  end else begin
    printf "      ! %s = %s ! %d vertices, %d propagators"
      name name (n - 2) (n - 3); nl ()
   end;
 let s = F.symmetry amplitude in
  if s > 1 then
    printf "  @[<2>%s =@, %s@, / sqrt(%d.0 *%s) ! symmetry factor"
     name name s !kind
  else
    printf "  ! unit symmetry factor";
  nl ()
```

C.2.1. Comparison

Considering all the function described earlier the fusion prescriptions of $W^+W^- \to Z$ and $W^+W^- \to \gamma$ can be represented as the analytical expression

$$\begin{aligned} A^\mu(k_- + k_+) =& -\mathrm{i}\cdot iqw\big[(k_-^\mu - k_+^\mu)W^-(k_-)\cdot W^+(k_+) \\ &\quad + (2k_+ + k_-)\cdot W^-(k_-)A^{a_2,\mu}(k_+) \\ &\quad - A^{a_1,\mu}(k_-)W^+(k_+)\cdot(2k_- + k_+)\big] \\ =& \quad +e\big[(k_-^\mu - k_+^\mu)W^-(k_-)\cdot W^+(k_+) \\ &\quad + (2k_+ + k_-)\cdot W^-(k_-)A^{a_2,\mu}(k_+) \\ &\quad - A^{a_1,\mu}(k_-)W^+(k_+)\cdot(2k_- + k_+)\big], \end{aligned} \tag{C.2a}$$

$$\begin{aligned} Z^\mu(k_- + k_+) =& -\mathrm{i}\cdot igzww\big[(k_-^\mu - k_+^\mu)W^-(k_-)\cdot W^+(k_+) \\ &\quad + (2k_+ + k_-)\cdot W^-(k_-)A^{a_2,\mu}(k_+) \\ &\quad - A^{a_1,\mu}(k_-)W^+(k_+)\cdot(2k_- + k_+)\big] \\ =& \quad +g\cdot cw\big[(k_-^\mu - k_+^\mu)W^-(k_-)\cdot W^+(k_+) \\ &\quad + (2k_+ + k_-)\cdot W^-(k_-)A^{a_2,\mu}(k_+) \\ &\quad - A^{a_1,\mu}(k_-)W^+(k_+)\cdot(2k_- + k_+)\big]. \end{aligned} \tag{C.2b}$$

The corresponding Feynman rules of Standard Model are given by

$$\begin{aligned} A_{\mu_1} W^-_{\mu_2} W^+_{\mu_3} : \quad & \mathrm{i}e \left[\left(k_{1\,\mu_3} - k_{2\,\mu_3}\right) g_{\mu_1\mu_2} + \left(k_{3\,\mu_2} - k_{1\,\mu_2}\right) g_{\mu_1\mu_3} \right. \\ & \left. + \left(k_{2\,\mu_1} - k_{3\,\mu_1}\right) g_{\mu_2\mu_3} \right] \qquad \text{(C.3a)} \\ Z_{\mu_1} W^-_{\mu_2} W^+_{\mu_3} : \quad & \mathrm{i}c_w g \left(\left(k_{1\,\mu_3} - k_{2\,\mu_3}\right) g_{\mu_1\mu_2} + \left(k_{3\,\mu_2} - k_{1\,\mu_2}\right) g_{\mu_1\mu_3} \right. \\ & \left. + \left(k_{2\,\mu_1} - k_{3\,\mu_1}\right) g_{\mu_2\mu_3} \right] . \qquad \text{(C.3b)} \end{aligned}$$

Using these rules the fusion prescriptions for the Feynman rules can be derived

$$\begin{aligned} A^\mu(k_1) =& ie\big([W^- \cdot W^+](k_-^{\mu_1} - k_+^\mu) + [(2k_+ + k_-) \cdot W^-]W^{+\mu} \\ & - [(2k_- + k_-) \cdot W^+]W^{-\mu}\big) , \qquad \text{(C.4a)} \\ Z^\mu(k_1) =& i\,c_w g\big([W^- \cdot W^+](k_-^{\mu_1} - k_+^\mu) + [(2k_+ + k_-) \cdot W^-]W^{+\mu} \\ & - [(2k_- + k_-) \cdot W^+]W^{-\mu}\big) . \qquad \text{(C.4b)} \end{aligned}$$

After multiplying another i to (C.2), it coincides with (C.4). Therefore the convention chosen for the `WHIZARD` implementation coincides with "CD-".

C.3. Resonance Model Implementation

The theoretical foundations of the resonances, namely isoscalar scalar σ, isoscalar tensor f, isotensor scalar ϕ, isotensor tensor X and of the dimension eight operators $\mathcal{L}_S$ given in Chapter 5 and Chapter 3, respectively. New Lorentz structures have to be implemented in `O'MEGA` to ensure the correct description of the coupling of these resonance and anomalous vertices to physical vector bosons using unitary gauge (see Appendix B.2). Furthermore, the new particles have to be included into `WHIZARD`.

C.3.1. New Lorentz Structures

New Lorentz structures are defined in the file `./omega/src/omegalib.nw` of `O'MEGA`. For example, the following Lorentz structure is needed for the isoscalar tensor couplings,

$$C_{\mu\nu,\rho\sigma}\left(c_f\right) = g_{\mu\sigma}g_{\nu\rho} + g_{\mu\rho}g_{\nu\sigma} - \frac{c_f}{2} g_{\mu\nu}g_{\rho\sigma} . \qquad \text{(C.5)}$$

O'MEGA needs truncation rules representing the latter coupling of a tensor T with two vectors V_1, V_2

$$\begin{aligned} T_{\mu\nu} &= C_{\mu\nu,\rho\sigma} V_1^\rho V_2^\sigma \\ &= V_{1\,\mu} V_{2\,\nu} + V_{1\,\nu} V_{2\,\mu} - \frac{c_f}{2} V_1^\rho V_{2\,\rho} \\ \Rightarrow T &= V_1 \otimes V_2 + V_2 \otimes V_1 - \frac{c_f}{2} V_1 \cdot V_2 \,, \end{aligned} \tag{C.6a}$$

$$\begin{aligned} V_{1\,\sigma} &= C_{\mu\nu,\rho\sigma} T^{\mu\nu} V_2^\rho \\ &= T_{\sigma\rho} V_2^\rho + T_{\rho\sigma} V_2^\rho \; - \frac{c_f}{2} T_\mu^\mu V_2^\sigma \\ \Rightarrow V_1 &= \left(T + T^T\right) V_1 - \frac{c_f}{2} \mathrm{tr}\left[g^{\mu\nu} T\right] V_1 \,. \end{aligned} \tag{C.6b}$$

These truncation rules are implemented via following code in ./omega/src/omegalib.nw:

```
@ \section{Tensor Couplings}
        <<Declaration of couplings>>=
        public :: t2_vv, v_t2v, t2_vv_cf, v_t2v_cf, &
                  t2_vv_1, v_t2v_1, t2_vv_t, v_t2v_t
...
@
<<Implementation of couplings>>=
        pure function t2_vv_cf (g, lcf, v1, v2) result (t)
          complex(kind=default), intent(in) :: g, lcf
          complex(kind=default) :: tmp_s
          type(vector), intent(in) :: v1, v2
          type(tensor) :: tmp
          type(tensor) :: t_metric, t
          t_metric%t = 0
          t_metric%t(0,0) =   1.0_default
          t_metric%t(1,1) = - 1.0_default
          t_metric%t(2,2) = - 1.0_default
          t_metric%t(3,3) = - 1.0_default
          tmp_s = v1 * v2
          t%t = - (g /2.0_default) * tmp_s * t_metric%t
        end function t2_vv_cf
@
<<Implementation of couplings>>=
        pure function v_t2v_cf (g, lcf, t, v) result (tv)
          complex(kind=default), intent(in) :: g, lcf
          type(tensor), intent(in) :: t
          type(vector), intent(in) :: v
          type(vector) :: tv, tmp_tv
```

```
        tmp_tv = ( t%t(0,0)-t%t(1,1)-t%t(2,2)-t%t(3,3) ) * v
        tv = -( g /2.0_default) * tmp_tv
      end function v_t2v_cf
@
...
```

To include Tensor couplings to two Higgs, following functions are necessary

$$T_{\mu\nu} = g * \left(k_{1\,\mu} k_{2\,\nu} + k_{1\,\nu} k_{2\,\mu}\right) \phi_1\left(k_1\right) \phi_1\left(k_2\right) , \tag{C.7a}$$

$$\phi_1(k_1) = g * \left(T_{\mu\nu} k_1^{\mu} k_2^{\nu} + T_{\nu\mu} k_2^{\mu} k_1^{\nu}\right) \phi_2\left(k_2\right) , \tag{C.7b}$$

$$T_{\mu\nu} = -\frac{g}{2} g^{\mu\nu} k_1^{\rho} k_{2\,\rho} \phi_1\left(k_1\right) \phi_2\left(k_2\right) , \tag{C.7c}$$

$$\phi_1(k_1) = -\frac{g}{2} T_{\nu}^{\nu} \left(k_1 \cdot k_2\right) \phi_2(k_2) . \tag{C.7d}$$

```
<<Implementation of couplings>>=
pure function t2_phi2 (g, phi1, k1, phi2, k2) result (t)
  complex(kind=default), intent(in) :: g, phi1, phi2
  type(momentum), intent(in) :: k1, k2
  type(tensor) :: t
  type(tensor) :: tmp
  tmp = k1.tprod.k2
  t%t = g * (tmp%t + transpose (tmp%t)) * phi1 * phi2
end function t2_phi2
@
<<Implementation of couplings>>=
pure function phi_t2phi (g, t, kt, phi2, k2) result (phi1)
  complex(kind=default), intent(in) :: g, phi2
  type(tensor), intent(in) :: t
  type(momentum), intent(in) :: kt, k2
  type(momentum) :: k1
  complex(kind=default) :: phi1
  type(tensor) :: tmp
  k1 = -kt - k2
  tmp%t = t%t + transpose (t%t)
  phi1 = g * ( (tmp * k2) * k1) * phi2
end function phi_t2phi
@
<<Implementation of couplings>>=
pure function t2_phi2_cf (g, phi1, k1, phi2, k2) result (t)
  complex(kind=default), intent(in) :: g, phi1, phi2
  complex(kind=default) :: tmp_s
  type(momentum), intent(in) :: k1, k2
  type(tensor) :: t_metric, t
```

```
  t_metric%t = 0
  t_metric%t(0,0) =   1.0_default
  t_metric%t(1,1) = - 1.0_default
  t_metric%t(2,2) = - 1.0_default
  t_metric%t(3,3) = - 1.0_default
  tmp_s = (k1 * k2) * phi1 * phi2
  t%t = - (g /2.0_default) * tmp_s * t_metric%t
end function t2_phi2_cf
@
<<Implementation of couplings>>=
pure function phi_t2phi_cf (g, t, kt, phi2, k2) result (phi1)
  complex(kind=default), intent(in) :: g, phi2
  type(tensor), intent(in) :: t
  type(momentum), intent(in) :: kt, k2
  type(momentum) :: k1
  complex(kind=default) ::  tmp_ts, phi1
  k1 = - kt - k2
  tmp_ts =  ( t%t(0,0)-t%t(1,1)-t%t(2,2)-t%t(3,3) )
  phi1 = - ( g /2.0_default) * tmp_ts * (k1 * k2) * phi2
end function phi_t2phi_cf
@
```

Due to the Higgs matrix representation, new Lorentz structure are introduced for the two Higgs, two vector bosons anomalous vertex: `Dim8_Scalar2_Vector2_1`

$$\phi_2(k_2) = ((k_1 \cdot V_1)(k_2 \cdot V_2) + (k_1 \cdot V_1)(k_1 \cdot V_2))\,\phi_1(k_1)\,, \tag{C.8a}$$

$$V_2^\mu = \left(k_1^\mu (k_2 \cdot V_1) + k_2^\mu (k_1 \cdot V_1)\right)\phi_1(k_1)\phi_2(k_2)\,, \tag{C.8b}$$

and `Dim8_Scalar2_Vector2_2`:

$$\phi_2(k_2) = (k_1 \cdot k_2)(V_1 \cdot V_2)\,\phi_1(k_1) \tag{C.9a}$$

$$V_2^\mu = V_1^\mu (k_1 \cdot k_2)\,\phi_1\phi_2\,. \tag{C.9b}$$

The quartic Higgs vertex is defined by the coupling `Dim8_Scalar4`

$$\phi(k_1) = \left[\begin{array}{l}(k_1 \cdot k_2)(k_3 \cdot k_4) + (k_1 \cdot k_3)(k_2 \cdot k_4) \\ + (k_1 \cdot k_4)(k_2 \cdot k_3)\end{array}\right]\phi_2(k_2)\phi_3(k_3)\phi_4(k_4) \tag{C.10}$$

```
...
@ \section{Scalar2-Vector2 Dim-8 Couplings}
<<Declaration of couplings>>=
public :: phi_phi2v_1, v_phi2v_1, phi_phi2v_2, v_phi2v_2
@
<<Implementation of couplings>>=
```

```
pure function phi_phi2v_1 (g, phi1, k1, v1, k_v1, v2, k_v2)
         result (phi2)
  complex(kind=default), intent(in) :: g, phi1
  type(momentum), intent(in) :: k1, k_v1, k_v2
  type(momentum) :: k2
  type(vector), intent(in) :: v1, v2
  complex(kind=default) :: phi2
  k2 = - k1 - k_v1 - k_v2
  phi2 = g * phi1 * &
       ( (k1 * v1) * (k2 * v2) + (k1 * v2) * (k2 * v1) )
end function phi_phi2v_1
@
<<Implementation of couplings>>=
pure function v_phi2v_1 (g, phi1, k1, phi2, k2, v1) result (v2)
  complex(kind=default), intent(in) :: g, phi1, phi2
  type(momentum), intent(in) :: k1, k2
  type(vector), intent(in) :: v1
  type(vector) :: v2
  v2 = g * phi1 * phi2 * &
       ( k1  * (k2 * v1) + k2 * (k1 * v1) )
end function v_phi2v_1
@
<<Implementation of couplings>>=
pure function phi_phi2v_2 (g, phi1, k1, v1,k_v1, v2, k_v2)
         result (phi2)
  complex(kind=default), intent(in) :: g, phi1
  type(momentum), intent(in) :: k1, k_v1, k_v2
  type(vector), intent(in) :: v1, v2
  type(momentum) :: k2
  complex(kind=default) :: phi2
  k2 = - k1 - k_v1 - k_v2
  phi2 = g * phi1 * (k1 * k2) * (v1 * v2)
end function phi_phi2v_2
@
<<Implementation of couplings>>=
pure function v_phi2v_2 (g, phi1, k1, phi2, k2, v1) result (v2)
  complex(kind=default), intent(in) :: g, phi1, phi2
  type(momentum), intent(in) :: k1, k2
  type(vector), intent(in) :: v1
  type(vector) :: v2
  v2 = g * phi1 * phi2 * &
       ( k1  * k2 ) * v1
end function v_phi2v_2
@ \section{Scalar4 Dim-8 Couplings}
```

```
<<Declaration of couplings>>=
public :: s_dim8s3
@
<<Implementation of couplings>>=
pure function s_dim8s3 (g, phi2, k2, phi3, k3, phi4, k4)
         result (phi1)
  complex(kind=default), intent(in) :: g, phi2, phi3, phi4
  type(momentum), intent(in) :: k2, k3, k4
  type(momentum) :: k1
  complex(kind=default) :: phi1
  k1 = - k2 - k3 - k4
  phi1 = ( (k1 * k2) * (k3 * k4) + (k1 * k3) * (k2 * k4) &
         + (k1 * k4) * (k2 * k3) ) * phi2 * phi3 * phi4
end function s_dim8s3
...
```

Furthermore, the coupling of two Higgs to the isoscalar scalar resonance is included

$$\phi_1(k_1) = (k_2 \cdot k_3)\phi_2(k_2)\phi_3(k_3)\,. \tag{C.11}$$

```
@ \section{Scalar3 Dim-5 Couplings}
<<Declaration of couplings>>=
public :: phi_dim5s2
@
<<Implementation of couplings>>=
pure function phi_dim5s2 (g, phi2, k2, phi3, k3) result (phi1)
  complex(kind=default), intent(in) :: g
  type(momentum), intent(in) :: k2, k3
  complex(kind=default), intent(in) :: phi2, phi3
  complex(kind=default) :: phi1
  phi1 = g * phi2 * phi3 * (k2 * k3)
end function phi_dim5s2
```

Necessary Initializations and Definitions

The next step is to define the initialization and color factors of the Lorentz structure according to the function `Tensor_2_Vector_Vector_cf`. Three files have to be changed. First `/omega/src/targets.ml`, because corresponding functions are not included into the virtual machine of `WHIZARD`:

```
...
  | Tensor_2_Vector_Vector_cf _ ->
    failwith "print_current: V3: not implemented"
...
```

Possible color factorization rules have to be included into `/omega/src/colorize.ml`:

```
      | Tensor_2_Vector_Vector_cf c ->
          Tensor_2_Vector_Vector_cf (x * c)
```

Finally, `/omega/src/coupling.mli` has to be changed for a correct initialization and LaTeX documentation:

```
...
  | Tensor_2_Vector_Vector_cf of int (* %
      $T^{\mu\nu} (V_{1,\mu}V_{2,\nu} + V_{1,\nu}V_{2,\mu}
        - \frac{c_f}{2} g_{\mu,\nu}V_1^\rho V_{2,\rho} )$ *)
...
```

The rest of the couplings have also to be implemented analogously into these three files. Starting with `./omega/src/targets.ml`:

```
  | Dim5_Scalar_Scalar2 _ ->
    failwith "print_current: V3: not implemented"
...
  | Tensor_2_Scalar_Scalar _ ->
    failwith "print_current: V3: not implemented"
  | Tensor_2_Scalar_Scalar_cf _ ->
    failwith "print_current: V3: not implemented"
...
  | Dim8_Scalar2_Vector2_1 _ ->
    failwith "print_current: V4: not implemented"
  | Dim8_Scalar2_Vector2_2 _ ->
    failwith "print_current: V4: not implemented"
  | Dim8_Scalar4 _ ->
    failwith "print_current: V4: not implemented"
...
  | Dim5_Scalar_Scalar2 coeff->
    let c = format_coupling coeff c in
    begin match fusion with
    | (F23|F32) -> printf "phi_dim5s2(%s, %s, %s, %s, %s)"
      c wf1 p1 wf2 p2
    | (F12|F13) -> let p12 = Printf.sprintf "(-%s-%s)" p1 p2 in
      printf "phi_dim5s2(%s,%s,%s,%s,%s)" c wf1 p12 wf2 p2
    | (F21|F31) -> let p12 = Printf.sprintf "(-%s-%s)" p1 p2 in
      printf "phi_dim5s2(%s,%s,%s,%s,%s)" c wf1 p1 wf2 p12
    end
...
  | Tensor_2_Scalar_Scalar coeff->
    let c = format_coupling coeff c in
```

```
    begin match fusion with
    | (F23|F32) -> printf "t2_phi2(%s,%s,%s,%s,_%s)"
      c wf1 p1 wf2 p2
    | (F12|F13) -> printf "phi_t2phi(%s,%s,%s,%s,%s)"
      c wf1 p1 wf2 p2
    | (F21|F31) -> printf "phi_t2phi(%s,%s,%s,%s,%s)"
      c wf2 p2 wf1 p1
    end
...
  | Tensor_2_Scalar_Scalar_cf coeff->
    let c = format_coupling coeff c in
    begin match fusion with
    | (F23|F32) -> printf "t2_phi2_cf(%s,%s,%s,%s,_%s)"
      c wf1 p1 wf2 p2
    | (F12|F13) -> printf "phi_t2phi_cf(%s,%s,%s,%s,%s)"
      c wf1 p1 wf2 p2
    | (F21|F31) -> printf "phi_t2phi_cf(%s,%s,%s,%s,%s)"
      c wf2 p2 wf1 p1
    end
...
  | Dim8_Scalar2_Vector2_1 coeff ->
    let c = format_coupling coeff c in
      begin match fusion with
      | F134 | F143 | F234 | F243 ->
          printf "phi_phiv2_1(%s,%s,%s,%s,%s,%s,%s)"
            c wf1 p1 wf2 p2 wf3 p3
      | F314 | F413 | F324 | F423 ->
          printf "phi_phiv2_1(%s,%s,%s,%s,%s,%s,%s)"
            c wf2 p2 wf1 p1 wf3 p3
      | F341 | F431 | F342 | F432 ->
          printf "phi_phiv2_1(%s,%s,%s,%s,%s,%s,%s)"
            c wf3 p3 wf2 p2 wf1 p1
      | F312 | F321 | F412 | F421 ->
          printf "v_phi2v_1(%s,%s,%s,%s,%s,%s)"
            c wf3 p3 wf2 p2 wf1
      | F231 | F132 | F241 | F142 ->
          printf "v_phi2v_1(%s,%s,%s,%s,%s,%s)"
            c wf1 p1 wf3 p3 wf2
      | F123 | F213 | F124 | F214 ->
          printf "v_phi2v_1(%s,%s,%s,%s,%s,%s)"
            c wf1 p1 wf2 p2 wf3
      end

    | Dim8_Scalar2_Vector2_2 coeff ->
```

```
      let c = format_coupling coeff c in
        begin match fusion with
        | F134 | F143 | F234 | F243 ->
          printf "phi_phiv2_2(%s,%s,%s,%s,%s,%s,%s)"
            c wf1 p1 wf2 p2 wf3 p3
        | F314 | F413 | F324 | F423 ->
          printf "phi_phiv2_2(%s,%s,%s,%s,%s,%s,%s)"
            c wf2 p2 wf1 p1 wf3 p3
        | F341 | F431 | F342 | F432 ->
          printf "phi_phiv2_2(%s,%s,%s,%s,%s,%s,%s)"
            c wf3 p3 wf2 p2 wf1 p1
        | F312 | F321 | F412 | F421 ->
          printf "v_phi2v_2(%s,%s,%s,%s,%s,%s)"
            c wf3 p3 wf2 p2 wf1
        | F231 | F132 | F241 | F142 ->
          printf "v_phi2v_2(%s,%s,%s,%s,%s,%s)"
            c wf1 p1 wf3 p3 wf2
        | F123 | F213 | F124 | F214 ->
          printf "v_phi2v_2(%s,%s,%s,%s,%s,%s)"
            c wf1 p1 wf2 p2 wf3
        end
    | Dim8_Scalar4 coeff ->
      let c = format_coupling coeff c in
        begin match fusion with
        | F134 | F143 | F234 | F243 | F314 | F413 | F324 | F423
        | F341 | F431 | F342 | F432 | F312 | F321 | F412 | F421
        | F231 | F132 | F241 | F142 | F123 | F213 | F124 | F214 ->
          printf "s_dim8s3_(%s,%s,%s,%s,%s,%s,%s)"
            c wf1 p1 wf2 p2 wf3 p3
        end
```

and in `./omega/src/colorize.ml`:

```
  let mult_vertex3 x = function
...
  | Dim5_Scalar_Scalar2 c ->
    Dim5_Scalar_Scalar2 (x * c)
  ...
  | Tensor_2_Scalar_Scalar c ->
    Tensor_2_Scalar_Scalar (x * c)
  | Tensor_2_Scalar_Scalar_cf c ->
    Tensor_2_Scalar_Scalar_cf (x * c)
...
  let mult_vertex4 x = function
```

```
...
    | Dim8_Scalar2_Vector2_1 c ->
        Dim8_Scalar2_Vector2_1 (x * c)
    | Dim8_Scalar2_Vector2_2 c ->
        Dim8_Scalar2_Vector2_1 (x * c)
    | Dim8_Scalar4 c ->
        Dim8_Scalar4 (x * c)
...
```

and finally `/omega/src/coupling.mli`:

```
  | Dim5_Scalar_Scalar2 of int (* %
    $\phi_1 \partial_\mu \phi_2 \partial^\mu \phi_3$ *)
...
  | Tensor_2_Scalar_Scalar of int (* %
      $T^{\mu\nu} (\partial_{\mu}\phi_1\partial_{\nu}\phi_2 + %
      \partial_{\nu}\phi_1\partial_{\mu}\phi_2 )$ *)
  | Tensor_2_Scalar_Scalar_cf of int (* %
      $T^{\mu\nu} ( - \frac{c_f}{2} g_{\mu,\nu} %
      \partial_{\rho}\phi_1\partial_{\rho}\phi_2 )$ *)
...
type 'a vertex4 =
...
  | Dim8_Scalar2_Vector2_1 of int
  | Dim8_Scalar2_Vector2_2 of int
  | Dim8_Scalar4 of int
...
```

C.3.2. Model Implementation

The file `./omega/src/modellib_BSM.ml` includes definitions of physics models beyond the Standard Model. Here, only the necessary parts for the generic tensor coupling in dependence of c_f and additional Higgs couplings are listed. For future modularity, additional flags are introduced for these model. The flags have to be initialized in `./omega/src/modellib_BSM.mli`:

```
...
module type SSC_flags =
  sig
    val higgs_triangle : boolcd
    val higgs_hmm : bool
    val triple_anom : bool
    val quartic_anom : bool
    val higgs_anom : bool
```

```
    val k_matrix : bool
    val ckm_present : bool
    val top_anom : bool
    val top_anom_4f : bool
    val cf_arbitrary : bool
    val higgs_matrix : bool
  end

module SSC_kmatrix: SSC_flags

module SSC_kmatrix_2: SSC_flags
...
```

```
module type SSC_flags =
  sig
    val higgs_triangle : bool
    val higgs_hmm : bool
    val triple_anom : bool
    val quartic_anom : bool
    val higgs_anom : bool
    val k_matrix : bool
    val ckm_present : bool
    val top_anom : bool
    val top_anom_4f : bool
    val cf_arbitrary : bool
    val higgs_matrix : bool
  end
...
module SSC_kmatrix_2: SSC_flags =
  struct
    let higgs_triangle = false
    let higgs_hmm = false
    let triple_anom = false
    let quartic_anom = true
    let higgs_anom = false
    let k_matrix = true
    let ckm_present = false
    let top_anom = false
    let top_anom_4f = false
    let cf_arbitrary = true
    let higgs_matrix = true
  end
```

The final implementation of the couplings is done in `./omega/src/modellib_BSM.ml`. Here, the truncation rules for the couplings including their strength are defined:

```
...
type constant =
  ...
  | FS0_HHWW | FS0_HHZZ
  | FS1_HHWW | FS1_HHZZ
  ...
  | G_SZZ_T | G_SSZZ | G_SHH
  ...
  | G_FWW | G_FZZ | G_FWW_CF | G_FZZ_CF
  | G_FWW_T | G_FZZ_T | G_FHH | G_FHH_CF
  | G_TNWW | G_TNZZ | G_TWZ | G_TWW
  | G_TNWW_CF | G_TNZZ_CF | G_TWZ_CF | G_TWW_CF
  ...
  | FS_H4
...
  let rsigma3h =
    [ ((O Rsigma, O H, O H), Dim5_Scalar_Scalar2 1, G_FHH) ]
...
  let rf3cf =
    [ ((O Rf, G Wp, G Wm), Tensor_2_Vector_Vector 1, G_FWW);
      ((O Rf, G Z, G Z), Tensor_2_Vector_Vector 1, G_FZZ);
      ((O Rf, G Wp, G Wm), Tensor_2_Vector_Vector_cf 1, G_FWW_CF);
      ((O Rf, G Z, G Z), Tensor_2_Vector_Vector_cf 1, G_FZZ_CF) ]
...
  let rf3h =
    [ ((O Rf, O H, O H), Tensor_2_Scalar_Scalar 1, G_FHH);
      ((O Rf, O H, O H), Tensor_2_Scalar_Scalar_cf 1, G_FHH_CF) ]
...
  let rt3cf =
    [ ((O Rtn, G Wp, G Wm), Tensor_2_Vector_Vector 1, G_TNWW);
      ((O Rtn, G Z, G Z), Tensor_2_Vector_Vector 1, G_TNZZ) ;
      ((O Rtp, G Z, G Wm), Tensor_2_Vector_Vector 1, G_TWZ) ;
      ((O Rtpp, G Wm, G Wm), Tensor_2_Vector_Vector 1, G_TWW) ;
      ((O Rtm, G Wp, G Z), Tensor_2_Vector_Vector 1, G_TWZ) ;
      ((O Rtmm, G Wp, G Wp), Tensor_2_Vector_Vector 1, G_TWW);
      ((O Rtn, G Wp, G Wm), Tensor_2_Vector_Vector_cf 1,
               G_TNWW_CF);
      ((O Rtn, G Z, G Z), Tensor_2_Vector_Vector_cf 1,
               G_TNZZ_CF) ;
      ((O Rtp, G Z, G Wm), Tensor_2_Vector_Vector_cf 1,
               G_TWZ_CF) ;
```

```
      ((O Rtpp, G Wm, G Wm), Tensor_2_Vector_Vector_cf 1,
               G_TWW_CF) ;
      ((O Rtm, G Wp, G Z), Tensor_2_Vector_Vector_cf 1,
               G_TWZ_CF) ;
      ((O Rtmm, G Wp, G Wp), Tensor_2_Vector_Vector_cf 1,
               G_TWW_CF) ]
...
  let dim8_gauge_higgs4 =
    [ (O H, O H, G Wp, G Wm), Dim8_Scalar2_Vector2_1 1, FS0_HHWW;
      (O H, O H, G Z, G Z), Dim8_Scalar2_Vector2_1 1, FS0_HHZZ;
      (O H, O H, G Wp, G Wm), Dim8_Scalar2_Vector2_2 1, FS1_HHWW;
      (O H, O H, G Z, G Z), Dim8_Scalar2_Vector2_2 1, FS1_HHZZ ]
  ...
  let fs_higgs4 =
    [ (O H, O H, O H, O H), Dim8_Scalar4 1, FS_H4 ]
  ...
    let gauge_higgs4 =
      ( if Flags.higgs_anom then
          standard_gauge_higgs4 @ anomalous_gauge_higgs4
        else
          standard_gauge_higgs ) @
      ( if Flags.higgs_matrix then
          (dim8_gauge_higgs4 )
              else
                [] )
  ...
  let higgs4 =
    ( if Flags.higgs_anom then
        standard_higgs4 @ anomalous_higgs4
      else
        standard_higgs4 ) @
    ( if Flags.higgs_matrix then
        (fs_higgs4 )
      else
              [] )
...
  let vertices3 =
      ...
   ( if Flags.cf_arbitrary then
              (rf3cf @ rt3cf)
           else
        (rf3 @ rt3) )
   rf3t @
   ( if Flags.higgs_matrix then
```

```
            (rsigma3h @ rf3h )
          else
            [] ) @
...
let constant_symbol = function
  ...
    | FS0_HHWW -> "fs0hhww" | FS0_HHZZ -> "fs0hhzz"
    | FS1_HHWW -> "fs1hhww" | FS1_HHZZ -> "fs1hhzz"
    | FS_H4 -> "fsh4"
  ...
    | G_SHH -> "gshh"
        ...
    | G_FWW_CF -> "gfwwcf" | G_FZZ_CF -> "gfzzcf"
    | G_FHH -> "gfhh" | G_FHH_CF -> "gfhhcf"
    | G_FWW_T -> "gfwwt" | G_FZZ_T -> "gfzzt"
    | G_TNWW -> "gtnww" | G_TNZZ -> "gtnzz"
    | G_TNWW_CF -> "gtnwwcf" | G_TNZZ_CF -> "gtnzzcf"
    | G_TWZ -> "gtwz" | G_TWW -> "gtww"
    | G_TWZ_CF -> "gtwzcf" | G_TWW_CF -> "gtwwcf"
  ...
...
```

C.3.3. Defining a particular Model: SSC_2

For the unitarizized description of the new resonances and additional dimension eight Higgs couplings (linear representation), the model `SSC_2` is introduced into `WHIZARD` and `O'MEGA`. Starting with its initialization using the correct flags in the earlier defined `Modellib_BSM`, the file `./omega/src/omega_SSC_2.ml` has to be creating with the content:

```
...
module O = Omega.Make(Fusion.Mixed23)(Targets.Fortran)
  (Modellib_BSM.SSC(Modellib_BSM.SSC_kmatrix_2))
let _ = O.main ()
...
```

and included in the makefile `./omega/src/Makefile.sources`:

```
...
    omega_SSC_2.ml \
...
```

The file `share/models/SSC\_2.mdl` includes all parameters which are accessible by SINDARIN code. As example, the anomalous quartic couplings $F_{S,0}$ and $F_{S,1}$ can be changed by

parameters $s0$ and $s1$. Additionally, possible vertices have to be included, e.g. the coupling of the scalar to two Higgs. The flag `eft_h` is introduced to switch off the couplings to Higgs for comparison with the old model within the non-linear representation.

The discussed extensions are included in `share/models/SSC\_2.mdl` by:

```
        ...
        parameter s0      = 0              # Coefficient of LS0
        parameter s1      = 0              # Coefficient of LS1
        ...
        parameter cf      = 2              # Arbitrary coefficient
                                           # for tensor couplings
        parameter eft_h   = 1              # Switch for EFT couplings
                                           # to Higgs
        ...
        #Sigma - Higgs
        vertex Rsigma H H
        ...
        #Sigma - Higgs
        vertex Rf H H
```

This file has to be added in `./share/Makefile.am` for the compilation of `WHIZARD`.

All parameters of the new `SSC_2` model , included coupling strength of each vertex, are defined in in the file `./src/models/parameters.SSC\_2.f90`, which has to be included in `src/models/Makefile.am`:

```
libmodels_la_SOURCES = \
        ...
        parameters.SSC_2.f90 \
        ...
nodist_execmod_HEADERS = \
        ...
        parameters_ssc_2.$(FC_MODULE_EXT) \
        ...
## The mismatch of filenames and
## module names requires a lot of repetition:
        ...
        parameters_ssc.$(FC_MODULE_EXT): parameters.SSC_2.lo
        @:
```

The new flags and couplings for the new physic couplings, e.g. the dimension eight Higgs coupling, are defined in `src/models/parameters.SSC_2.f90`:

```
private
  complex(default), public :
    ...
    gfwwcf, gfzzcf, &
    gtnww, gtnzz, gtwz, gtww, &
    gtnwwcf, gtnzzcf, gtwzcf, gtwwcf, &
    fs0hhww, fs0hhzz, fs1hhww, fs1hh, fsh4, &
    gshh, gfhh, gfhhcf
...
subroutine import_from_whizard (par_array)
  ...
  real(default), dimension(68), intent(in) :: par_array
  ...
  real(default) :: cf
  real(default) :: eft_h
  ...
  par%cf     = par_array(63)
  par%eft_h  = par_array(64)
  ...
  gkm(13) = par%cf
  gkm(14) = par%eft_h
  ...
  gcf = gkm(13)
  ...
  gshh = - gkm(1)  * gkm(14)
  ...
  gfww = gkm(4) * mass(24) * g / 2
  gfwwcf = gfww * gcf
  gfzz = gkm(4) * mass(23) * g / costhw / 2
  gfzzcf = gfzz * gcf
  gfhh = - gkm(4) / 2.0_default  * gkm(14)
  gfhhcf = gfhh * gcf
  gfwwt = gkm(9) * g**3 / mass(24) / (32.0 * PI)
  gfzzt = gkm(9) * g**3 / costhw**3 / mass(23) /(32.0 * PI)
  gtnww = - gkm(5) * mass(24) * g / 4 / sqrt(3.0_default)
  gtnwwcf = gtnww * gcf
  gtnzz = gkm(5) * mass(23) * g / costhw / 2 / sqrt(3.0_default)
  gtnzzcf = gtnzz * gcf
  gtwz = gkm(5) * mass(23) * g / 4
  gtwzcf = gtwz * gcf
  gtww = gkm(5) * mass(24) * g / 2 / sqrt(2.0_default)
  gtwwcf = gtww * gcf
  ...
```

```
fs0hhww = - g ** 2 * vev ** 2 / 4 * fs0 * gkm(14)
fs1hhww = - g ** 2 * vev ** 2 / 2 * fs1 * gkm(14)
fs0hhzz = - g ** 2 / costhw**2 * vev ** 2 / 4 * fs0 * gkm(14)
fs1hhzz = - g ** 2 / costhw**2 * vev ** 2 / 2 * fs1 * gkm(14)
fsh4 = 2.0_default * ( fs0 + fs1) * gkm(14)
```

Additionally, the parameter file has to be included in `./synchronize.sh`. Then all necessary changes to implement the new `SSC_2` model are executed and the model can be used in `WHIZARD`.

C.4. Unitarization

The Thales-projection T-matrix algorithm is implemented in `WHIZARD` as part of this thesis. To achieve the correct unitarity prescription of longitudinal vector boson scattering amplitudes counter-terms are added for s-channel vertices. In this section, the implementation of the WWHH-vertex is introduced as representative for all weak boson scattering vertices. The unitarization counter terms are introduces as form factors which are calculated in `./omega/src/targets_Kmatrix_2.ml`. An example, how the calculation of the form factors is defined, is given in the next subsection for the $WWHH$-vertex. Here, the implementation of such an calculation scheme in `O'MEGA` is described.

The file `./omega/src/targets_Kmatrix_2.ml` has to be included in `./omega/src/Makefile.sources`:

```
...
OMEGA_TARGETLIB_ML = \
    targets_Kmatrix.ml \
    targets_Kmatrix_2.ml \
...
```

To enable the T-matrix unitarization method for the model SSC_2, it has to be activated in `./src/me_methods/me_methods.nw`:

```
    select case (char (writer%model_name))
    case ("SM_rx", "SM_ul", "SSC", "NoH_rx", "AltH")
       kmatrix_string = " --target:kmatrix_write"
    case ("SSC_2")
       kmatrix_string = " --target:kmatrix_2_write"
    case default
       kmatrix_string = ""
    end select
```

Furthermore, this method has to be added into `./omega/src/targets.ml`:

```
...
let km_write = ref false
let km_pure = ref false
let km_2_write = ref false
let km_2_pure = ref false
...
"kmatrix_write", Arg.Set km_write,
         "write K matrix functions";
"kmatrix_2_write", Arg.Set km_2_write,
         "write K matrix 2 functions";
"kmatrix_write_pure", Arg.Set km_pure,
        "write K matrix pure functions";
"kmatrix_2_write_pure", Arg.Set km_2_pure,
        "write Kmatrix2pure functions";
...
if !km_write || !km_pure then
         (Targets_Kmatrix.Fortran.print !km_pure);
if !km_2_write || !km_2_pure then
        (Targets_Kmatrix_2.Fortran.print !km_2_pure);
...
```

Finally, a file `./omega/src/targets_Kmatrix_2.mli` has to be created, with the content:

```
        module Fortran : sig val print : bool -> unit end
```

C.4.1. Unitarization for WWHH-Vertex

Introducing the form factors dalhz_s, dalhz_t and dalhz_u, which include the contribution of the unitarized operators and resonances with their couplings gkm and masses mkm, the counter term for the vertex $H(p_1)H(p_2)Z_\mu(p_3)Z_\nu(p_4)$ in the s-channel implemented as

$$\begin{aligned} &\text{dalhz\_s}(\text{gkm}, \text{mkm}, p_3 + p_4) p_1^\rho p_{2\,\rho} g^{\mu\nu} \\ +&\text{dalhz\_t}(\text{gkm}, \text{mkm}, p_3 + p_4) p_1^\mu p_2^\nu \\ +&\text{dalhz\_u}(\text{gkm}, \text{mkm}, p_3 + p_4) p_1^\nu p_2^\mu \,. \end{aligned} \tag{C.12}$$

All functions have to be implemented via the file `./omega/src/targets.ml` to `O'MEGA`:

```
  | Scalar2_Vector2_K_Matrix_ms _ ->
    failwith "print_current: V4: K_Matrix not implemented"
...
    let print_scalar2_vector2_km c pa pb wf1 wf2 wf3
     p1 p2 p3 p123 fusion (coeff, contraction) =
```

```
      match contraction, fusion with
      | C_12_34, (F123|F213|F124|F214)
      | C_13_42, (F132|F312|F134|F314)
      | C_14_23, (F142|F412|F143|F413) ->
          printf "(%s%s%s+%s))*(%s*%s)*(%s*%s)*%s"
            (format_coeff coeff) c pa pb p1 p2 wf1 wf2 wf3
      | C_12_34, (F134|F143|F234|F243)
      | C_13_42, (F124|F142|F324|F342)
      | C_14_23, (F123|F132|F423|F432) ->
          printf "(%s%s%s+%s))*(%s*%s)*(%s*%s)*%s"
            (format_coeff coeff) c pa pb p1 p123 wf2 wf3 wf1
      | C_12_34, (F132|F231|F142|F241)
      | C_13_42, (F123|F321|F143|F341)
      | C_14_23, (F124|F421|F134|F431) ->
          printf "(%s%s%s+%s))*(%s*%s)*(%s*%s)*%s"
            (format_coeff coeff) c pa pb p1 p3 wf1 wf3 wf2
      | C_12_34, (F312|F321|F412|F421)
      | C_13_42, (F213|F231|F431|F413)
      | C_14_23, (F214|F241|F314|F341) ->
          printf "(%s%s%s+%s))*(%s*%s)*(%s*%s)*%s"
            (format_coeff coeff) c pa pb p2 p3 wf2 wf3 wf1
      | C_12_34, (F314|F413|F324|F423)
      | C_13_42, (F214|F412|F234|F432)
      | C_14_23, (F213|F312|F243|F342) ->
          printf "(%s%s%s+%s))*(%s*%s)*(%s*%s)*%s"
            (format_coeff coeff) c pa pb p2 p123 wf1 wf3 wf2
      | C_12_34, (F341|F431|F342|F432)
      | C_13_42, (F241|F421|F243|F423)
      | C_14_23, (F231|F321|F234|F324) ->
          printf "(%s%s%s+%s))*(%s*%s)*(%s*%s)*%s"
            (format_coeff coeff) c pa pb p3 p123 wf1 wf2 wf3

    let print_add_scalar2_vector2_km c pa pb wf1 wf2 wf3
     p1 p2 p3 p123 fusion (coeff, contraction) =
      printf "@ + ";
      print_scalar2_vector2_km c pa pb wf1 wf2 wf3
       p1 p2 p3 p123 fusion (coeff, contraction)
...
  | Scalar2_Vector2_K_Matrix_ms (disc, contractions) ->
    let p123 = Printf.sprintf "(-%s-%s-%s)" p1 p2 p3 in
      let pa, pb =
        begin match disc, fusion with
        | 3, (F143|F413|F142|F412|F321|F231|F324|F234) -> (p1, p2)
        | 3, (F314|F341|F214|F241|F132|F123|F432|F423) -> (p2, p3)
```

```
        | 3, (F134|F431|F124|F421|F312|F213|F342|F243) -> (p1, p3)
        | _, (F341|F431|F342|F432|F123|F213|F124|F214) -> (p1, p2)
        | _, (F134|F143|F234|F243|F312|F321|F412|F421) -> (p2, p3)
        | _, (F314|F413|F324|F423|F132|F231|F142|F241) -> (p1, p3)
      end in
    begin match contractions with
    | [] -> invalid_arg
      "Targets.print_current: Scalar2_Vector4_K_Matrix_ms []"
    | head :: tail ->
      printf "(";
      print_scalar2_vector2_km
        c pa pb wf1 wf2 wf3 p1 p2 p3 p123 fusion head;
      List.iter (print_add_scalar2_vector2_km
                   c pa pb wf1 wf2 wf3 p1 p2 p3 p123 fusion)
        tail;
      printf ")"
  end
```

and have to be also defined in `./omega/src/colorize.ml`:

```
            | Scalar2_Vector2_K_Matrix_ms (c, ch2_list) ->
          Scalar2_Vector2_K_Matrix_ms ((x * c),  ch2_list)
```

and `omega/src/coupling.mli`:

```
    | Scalar2_Vector2_K_Matrix_ms of int * (int * contract4) list
```

To ensure that the vertices are only inserted in the s-channel, a procedure will check if s is in the physical region:

```
| V4 (Scalar2_Vector2_K_Matrix_ms (disc, _), fusion, _) ->
    let s12, s23, s13 =
      begin match PT.to_list momenta with
      | [q1; q2; q3] -> (P.Scattering.timelike (P.add q1 q2),
                         P.Scattering.timelike (P.add q2 q3),
                         P.Scattering.timelike (P.add q1 q3))
      | _ -> raise PT.Mismatched_arity
      end in
    begin match disc, s12, s23, s13, fusion with
    | 0, true, false, false,
      (F341|F431|F342|F432|F123|F213|F124|F214)
    | 0, false, true, false,
      (F134|F143|F234|F243|F312|F321|F412|F421)
    | 0, false, false, true,
      (F314|F413|F324|F423|F132|F231|F142|F241) ->
```

```
        true
    | 1, true, false, false, (F341|F431|F342|F432)
    | 1, false, true, false, (F134|F143|F234|F243)
    | 1, false, false, true, (F314|F413|F324|F423) ->
        true
    | 2, true, false, false, (F123|F213|F124|F214)
    | 2, false, true, false, (F312|F321|F412|F421)
    | 2, false, false, true, (F132|F231|F142|F241) ->
        true
    | 3, true, false, false,
      (F143|F413|F142|F412|F321|F231|F324|F234)
    | 3, false, true, false,
      (F314|F341|F214|F241|F132|F123|F432|F423)
    | 3, false, false, true,
      (F134|F431|F124|F421|F312|F213|F342|F243) ->
        true
    | _ -> false
    end
```

Contraction rules for the HHVV coupling have to be inserted in `./omega/src/modellib_BSM`:

```
  let k_matrix_2scalar_2gauge =
    if Flags.k_matrix then
      if Flags.higgs_matrix then
          [ ((O H,O H,G Z,G Z), Scalar2_Vector2_K_Matrix_ms
                (0, [(1, C_12_34)]), D_Alpha_HHZZ_S);
            ((O H,O H,G Wp,G Wm), Scalar2_Vector2_K_Matrix_ms
                (0, [(1, C_12_34)]), D_Alpha_HHWW_S);
            ((O H,G Z,O H,G Z), Scalar2_Vector2_K_Matrix_ms
                (0, [(1, C_13_42)]), D_Alpha_HHZZ_T);
            ((O H,G Wp,O H,G Wm), Scalar2_Vector2_K_Matrix_ms
                (0, [(1, C_13_42)]), D_Alpha_HHWW_T);
            ((O H,G Z,G Z,O H), Scalar2_Vector2_K_Matrix_ms
                (0, [(1, C_14_23)]), D_Alpha_HHZZ_T);
            ((O H,G Wp,G Wm,O H), Scalar2_Vector2_K_Matrix_ms
                (0, [(1, C_14_23)]), D_Alpha_HHWW_T) ]
      else
          []
    else
        []
...
    let gauge_higgs4 =
      ( if Flags.higgs_anom then
          standard_gauge_higgs4 @ anomalous_gauge_higgs4
```

```
      else
        standard_gauge_higgs4 ) @
    ( if Flags.higgs_matrix then
        (dim8_gauge_higgs4 @ k_matrix_2scalar_2gauge )
      else
        [] )
```

Additionally, the form factors of the counter terms are calculated in `./omega/src/targets_Kmatrix_2.ml`:

```
printf "%sfunction dalhw_s (cc,m,k) result (alhw_s)" pure; nl ();
printf "    type(momentum), intent(in) :: k"; nl ();
printf "    real(kind=default), dimension(1:14), intent(in) :: cc"
  ; nl ();
printf "    real(kind=default), dimension(1:5), intent(in) :: m"
  ; nl ();
printf "    complex(kind=default) :: alhw_s"; nl ();
printf "    real(kind=default) :: s"; nl ();
printf "    s = k*k"; nl ();
printf "    alhw_s = - 8.0_default * cc(14) * g**2/vev**2 * &"
  ; nl ();
printf "                ((da00(cc,s,m) &"; nl ();
printf "                - da20(cc,s,m))/24 &"; nl ();
printf "                - 5*(da02(cc,s,m) - da22(cc,s,m))/12)"
  ; nl ();
printf "end function dalhw_s"; nl ();
nl ();
printf "%sfunction dalhw_t (cc,m,k) result (alhw_t)" pure; nl ();
printf "    type(momentum), intent(in) :: k"; nl ();
printf "    real(kind=default), dimension(1:14), intent(in) :: cc"
  ; nl ();
printf "    real(kind=default), dimension(1:5), intent(in) :: m"
  ; nl ();
printf "    complex(kind=default) :: alhw_t"; nl ();
printf "    real(kind=default) :: s"; nl ();
printf "    s = k*k"; nl ();
printf "    alhw_t = - 10.0_default * cc(14) * g**2/ vev**2 * &"
  ; nl ();
printf "                (da02(cc,s,m) - &"; nl ();
printf "                da22(cc,s,m))/4.0_default"; nl ();
printf "end function dalhw_t"; nl ();
nl ();
printf "%sfunction dalhz_s (cc,m,k) result (alhz_s)" pure; nl ();
printf "    type(momentum), intent(in) :: k"; nl ();
```

```
printf "    real(kind=default), dimension(1:14), intent(in) :: cc"
  ; nl ();
printf "    real(kind=default), dimension(1:5), intent(in) :: m"
  ; nl ();
printf "    complex(kind=default) :: alhz_s"; nl ();
printf "    alhz_s = dalhw_s(cc,m,k) / costhw**2"; nl();
printf "end function dalhz_s"; nl ();
nl ();
printf "%sfunction dalhz_t (cc,m,k) result (alhz_t)" pure; nl ();
printf "    type(momentum), intent(in) :: k"; nl ();
printf "    real(kind=default), dimension(1:14), intent(in) :: cc"
  ; nl ();
printf "    real(kind=default), dimension(1:5), intent(in) :: m"
  ; nl ();
printf "    complex(kind=default) :: alhz_t"; nl ();
printf "    alhz_t = dalhw_t(cc,m,k) / costhw**2"; nl();
printf "end function dalhz_t"; nl ();
nl ();
```

Bibliography

[1] Peter W. Higgs. Broken Symmetries and the Masses of Gauge Bosons. *Phys.Rev.Lett.*, 13:508–509, 1964.

[2] T. W. B. Kibble. Kinematics of General Scattering Processes and the Mandelstam Representation. *Phys. Rev.*, 117:1159–1162, 1960.

[3] F. Englert and R. Brout. Broken Symmetry and the Mass of Gauge Vector Mesons. *Phys. Rev. Lett.*, 13:321–323, 1964.

[4] Georges Aad et al. Observation of a new particle in the search for the Standard Model Higgs boson with the ATLAS detector at the LHC. *Phys.Lett.*, B716:1–29, 2012.

[5] Serguei Chatrchyan et al. Observation of a new boson at a mass of 125 GeV with the CMS experiment at the LHC. *Phys.Lett.*, B716:30–61, 2012.

[6] Georges Aad et al. Evidence for the spin-0 nature of the Higgs boson using ATLAS data. *Phys. Lett.*, B726:120–144, 2013.

[7] Vardan Khachatryan et al. Constraints on the spin-parity and anomalous HVV couplings of the Higgs boson in proton collisions at 7 and 8 TeV. *Phys. Rev.*, D92(1):012004, 2015.

[8] Georges Aad et al. Evidence for Electroweak Production of $W^{\pm}W^{\pm}jj$ in pp Collisions at $\sqrt{s} = 8$ TeV with the ATLAS Detector. *Phys. Rev. Lett.*, 113(14):141803, 2014.

[9] CMS Collaboration. Vector boson scattering in a final state with two jets and two same-sign leptons. 2014.

[10] M. Beyer, W. Kilian, P. Krstonosic, Klaus Monig, J. Reuter, E. Schmidt, and H. Schroder. Determination of New Electroweak Parameters at the ILC - Sensitivity to New Physics. *Eur. Phys. J.*, C48:353–388, 2006.

[11] Mauro Moretti, Thorsten Ohl, and Jurgen Reuter. O'Mega: An Optimizing matrix element generator. 2001.

[12] Wolfgang Kilian, Jurgen Reuter, Sebastian Schmidt, and Daniel Wiesler. An Analytic Initial-State Parton Shower. *JHEP*, 04:013, 2012.

[13] Michael E. Peskin and Daniel V. Schroeder. *An Introduction to quantum field theory*. 1995.

[14] Matthew D. Schwartz. *Quantum Field Theory and the Standard Model*. Cambridge University Press, 2014.

[15] Wolfgang Kilian, Thorsten Ohl, and Jurgen Reuter. WHIZARD: Simulating Multi-Particle Processes at LHC and ILC. *Eur.Phys.J.*, C71:1742, 2011.

[16] Jeffrey Goldstone, Abdus Salam, and Steven Weinberg. Broken Symmetries. *Phys.Rev.*, 127:965–970, 1962.

[17] S.L. Glashow. Partial Symmetries of Weak Interactions. *Nucl.Phys.*, 22:579–588, 1961.

[18] Steven Weinberg. A Model of Leptons. *Phys.Rev.Lett.*, 19:1264–1266, 1967.

[19] Abdus Salam. Weak and Electromagnetic Interactions. *Conf.Proc.*, C680519:367–377, 1968.

[20] Gerard 't Hooft. Renormalizable Lagrangians for Massive Yang-Mills Fields. *Nucl. Phys.*, B35:167–188, 1971.

[21] Steven Weinberg. Nonlinear realizations of chiral symmetry. *Phys.Rev.*, 166:1568–1577, 1968.

[22] Thomas Appelquist and Claude W. Bernard. Strongly Interacting Higgs Bosons. *Phys.Rev.*, D22:200, 1980.

[23] Anthony C. Longhitano. Heavy Higgs Bosons in the Weinberg-Salam Model. *Phys.Rev.*, D22:1166, 1980.

[24] Sidney R. Coleman, J. Wess, and Bruno Zumino. Structure of phenomenological Lagrangians. 1. *Phys.Rev.*, 177:2239–2247, 1969.

[25] Jr. Callan, Curtis G., Sidney R. Coleman, J. Wess, and Bruno Zumino. Structure of phenomenological Lagrangians. 2. *Phys.Rev.*, 177:2247–2250, 1969.

[26] W. Kilian. Electroweak symmetry breaking: The bottom-up approach. *Springer Tracts Mod.Phys.*, 198:1–113, 2003.

[27] Benjamin W. Lee, C. Quigg, and H. B. Thacker. The Strength of Weak Interactions at Very High-Energies and the Higgs Boson Mass. *Phys. Rev. Lett.*, 38:883–885, 1977.

[28] Michael E. Peskin and Tatsu Takeuchi. Estimation of oblique electroweak corrections. *Phys.Rev.*, D46:381–409, 1992.

[29] Steven Weinberg. Physical Processes in a Convergent Theory of the Weak and Electromagnetic Interactions. *Phys.Rev.Lett.*, 27:1688–1691, 1971.

[30] Steven Weinberg. General Theory of Broken Local Symmetries. *Phys.Rev.*, D7:1068–1082, 1973.

[31] K.A. Olive et al. Review of Particle Physics. *Chin.Phys.*, C38:090001, 2014.

[32] Thomas Appelquist and Guo-Hong Wu. The Electroweak chiral Lagrangian and new precision measurements. *Phys.Rev.*, D48:3235–3241, 1993.

[33] P. Sikivie, Leonard Susskind, Mikhail B. Voloshin, and Valentin I. Zakharov. Isospin Breaking in Technicolor Models. *Nucl. Phys.*, B173:189, 1980.

[34] Kaoru Hagiwara, R. D. Peccei, D. Zeppenfeld, and K. Hikasa. Probing the Weak Boson Sector in e+ e- → W+ W-. *Nucl. Phys.*, B282:253, 1987.

[35] Celine Degrande, Nicolas Greiner, Wolfgang Kilian, Olivier Mattelaer, Harrison Mebane, et al. Effective Field Theory: A Modern Approach to Anomalous Couplings. *Annals Phys.*, 335:21–32, 2013.

[36] H. Georgi. Effective field theory. *Ann. Rev. Nucl. Part. Sci.*, 43:209–252, 1993.

[37] E. Fermi. Versuch einer Theorie der β-Strahlen. I. *Zeitschrift für Physik*, 88:161–177, March 1934.

[38] F. L. Wilson. Fermi's Theory of Beta Decay. *American Journal of Physics*, 36:1150–1160, December 1968.

[39] Aneesh Manohar and Howard Georgi. Chiral Quarks and the Nonrelativistic Quark Model. *Nucl. Phys.*, B234:189, 1984.

[40] Howard Georgi and Lisa Randall. Flavor Conserving CP Violation in Invisible Axion Models. *Nucl. Phys.*, B276:241, 1986.

[41] Howard Georgi. Generalized dimensional analysis. *Phys. Lett.*, B298:187–189, 1993.

[42] G. Belanger and F. Boudjema. Probing quartic couplings of weak bosons through three vectors production at a 500-GeV NLC. *Phys. Lett.*, B288:201–209, 1992.

[43] G. Belanger and F. Boudjema. gamma gamma → W+ W- and gamma gamma → Z Z as tests of novel quartic couplings. *Phys. Lett.*, B288:210–220, 1992.

[44] W. James Stirling and Anja Werthenbach. Anomalous quartic couplings in neutrino anti-neutrino gamma gamma production via W W fusion at LEP-2. *Phys. Lett.*, B466:369–374, 1999.

[45] Ansgar Denner, S. Dittmaier, M. Roth, and D. Wackeroth. Probing anomalous quartic gauge boson couplings via e+ e- → four fermions + gamma. *Eur. Phys. J.*, C20:201–215, 2001.

[46] CMS Collaboration. A Search for WWgamma and WZgamma production in pp Collisions at sqrt(s) = 8 TeV. 2013.

[47] C. P. Burgess and David London. Uses and abuses of effective Lagrangians. *Phys. Rev.*, D48:4337–4351, 1993.

[48] Gerhard Buchalla, Oscar Cat, and Claudius Krause. Complete Electroweak Chiral Lagrangian with a Light Higgs at NLO. *Nucl.Phys.*, B880:552–573, 2014.

[49] Gerhard Buchalla, Oscar Cat, and Claudius Krause. On the Power Counting in Effective Field Theories. *Phys.Lett.*, B731:80–86, 2014.

[50] G. F. Giudice, C. Grojean, A. Pomarol, and R. Rattazzi. The Strongly-Interacting Light Higgs. *JHEP*, 06:045, 2007.

[51] W. Buchmuller and D. Wyler. Effective Lagrangian Analysis of New Interactions and Flavor Conservation. *Nucl. Phys.*, B268:621–653, 1986.

[52] B. Grzadkowski, M. Iskrzynski, M. Misiak, and J. Rosiek. Dimension-Six Terms in the Standard Model Lagrangian. *JHEP*, 10:085, 2010.

[53] Kaoru Hagiwara, S. Ishihara, R. Szalapski, and D. Zeppenfeld. Low-energy effects of new interactions in the electroweak boson sector. *Phys. Rev.*, D48:2182–2203, 1993.

[54] Kaoru Hagiwara, R. Szalapski, and D. Zeppenfeld. Anomalous Higgs boson production and decay. *Phys. Lett.*, B318:155–162, 1993.

[55] C. Arzt, M. B. Einhorn, and J. Wudka. Patterns of deviation from the standard model. *Nucl. Phys.*, B433:41–66, 1995.

[56] O. J. P. Eboli, M. C. Gonzalez-Garcia, and J. K. Mizukoshi. p p → j j e+- mu+- nu nu and j j e+- mu-+ nu nu at O(alpha(em)**6) and O(alpha(em)**4 alpha(s)**2) for the study of the quartic electroweak gauge boson vertex at CERN LHC. *Phys. Rev.*, D74:073005, 2006.

[57] M. Baak, A. Blondel, A. Bodek, R. Caputo, T. Corbett, et al. Working Group Report: Precision Study of Electroweak Interactions. 2013.

[58] G. Belanger, F. Boudjema, Y. Kurihara, D. Perret-Gallix, and A. Semenov. Bosonic quartic couplings at LEP-2. *Eur. Phys. J.*, C13:283–293, 2000.

[59] M. C. Bergere and Yuk-Ming P. Lam. Equivalence Theorem and Faddeev-Popov Ghosts. *Phys. Rev.*, D13:3247–3255, 1976.

[60] Howard Georgi. On-shell effective field theory. *Nucl. Phys.*, B361:339–350, 1991.

[61] Celine Degrande. A basis of dimension-eight operators for anomalous neutral triple gauge boson interactions. *JHEP*, 02:101, 2014.

[62] Elizabeth E. Jenkins, Aneesh V. Manohar, and Michael Trott. Renormalization Group Evolution of the Standard Model Dimension Six Operators I: Formalism and lambda Dependence. *JHEP*, 1310:087, 2013.

[63] Elizabeth E. Jenkins, Aneesh V. Manohar, and Michael Trott. Renormalization Group Evolution of the Standard Model Dimension Six Operators II: Yukawa Dependence. *JHEP*, 01:035, 2014.

[64] Rodrigo Alonso, Elizabeth E. Jenkins, Aneesh V. Manohar, and Michael Trott. Renormalization Group Evolution of the Standard Model Dimension Six Operators III: Gauge Coupling Dependence and Phenomenology. *JHEP*, 04:159, 2014.

[65] Giampiero Passarino. NLO Inspired Effective Lagrangians for Higgs Physics. *Nucl. Phys.*, B868:416–458, 2013.

[66] Wolfgang Kilian, Thorsten Ohl, Jurgen Reuter, and Marco Sekulla. High-Energy Vector Boson Scattering after the Higgs Discovery. *Phys. Rev.*, D91:096007, 2015.

[67] E. Boos, V. Bunichev, M. Dubinin, and Y. Kurihara. Higgs boson signal at complete tree level in the SM extension by dimension-six operators. *Phys. Rev.*, D89:035001, 2014.

[68] Adam Alloul, Neil D. Christensen, Cline Degrande, Claude Duhr, and Benjamin Fuks. FeynRules 2.0 - A complete toolbox for tree-level phenomenology. *Comput. Phys. Commun.*, 185:2250–2300, 2014.

[69] John M. Cornwall, David N. Levin, and George Tiktopoulos. Derivation of Gauge Invariance from High-Energy Unitarity Bounds on the s Matrix. *Phys. Rev.*, D10:1145, 1974. [Erratum: Phys. Rev.D11,972(1975)].

[70] C. E. Vayonakis. Born Helicity Amplitudes and Cross-Sections in Nonabelian Gauge Theories. *Lett. Nuovo Cim.*, 17:383, 1976.

[71] Michael S. Chanowitz and Mary K. Gaillard. The TeV Physics of Strongly Interacting W's and Z's. *Nucl. Phys.*, B261:379, 1985.

[72] G. Valencia and S. Willenbrock. The Goldstone Boson Equivalence Theorem and the Higgs Resonance. *Phys. Rev.*, D42:853–859, 1990.

[73] J. Reuter, W. Kilian, and M. Sekulla. Simplified Models for Vector Boson Scattering at ILC and CLIC. In *International Workshop on Future Linear Colliders (LCWS13) Tokyo, Japan, November 11-15, 2013*, 2014.

[74] Benjamin W. Lee, C. Quigg, and H. B. Thacker. Weak Interactions at Very High-Energies: The Role of the Higgs Boson Mass. *Phys. Rev.*, D16:1519, 1977.

[75] G.F. Chew. *The Analytic S Matrix: A Basis for Nuclear Democracy.* W. A. Benjamin, 1966.

[76] Marcel Froissart. Asymptotic behavior and subtractions in the Mandelstam representation. *Phys. Rev.*, 123:1053–1057, 1961.

[77] R.J. Eden, P.V. Landshoff, D.I. Olive, and J.C. Polkinghorne. *The Analytic S-Matrix.* Cambridge University Press, 1966.

[78] Geoffrey F. Chew and Stanley Mandelstam. Theory of low-energy pion pion interactions. *Phys. Rev.*, 119:467–477, 1960.

[79] S. Aramaki and T. Osawa. On the existence of poles in the unphysical sheet. *Prog. Theor. Phys.*, 29:451–460, 1963.

[80] David I. Olive. Exploration of s-matrix theory. *Phys. Rev.*, 135:B745–B760, Aug 1964.

[81] A. P. Balachandran and J. Nuyts. Simultaneous partial-wave expansion in the Mandelstamm variables: Crossing symmetry for partial waves. *Phys. Rev.*, 172:1821–1827, 1968.

[82] R. Roskies. Crossing restrictions on pi pi partial waves. *Nuovo Cim.*, A65:467–490, 1970.

[83] P. Dita. On the Construction of Analytic and Crossing Symmetric Partial Waves. *Int. J. Theor. Phys.*, 16:201, 1977.

[84] Anke Biekötter, Alexander Knochel, Michael Krämer, Da Liu, and Francesco Riva. Vices and virtues of higgs effective field theories at large energy. *Phys. Rev. D*, 91:055029, Mar 2015.

[85] Michael S. Chanowitz and Mary K. Gaillard. Multiple production of w and z as a signal of new strong interactions. *Physics Letters B*, 142(12):85 – 90, 1984.

[86] V. Barger, A. L. Stange, and R. J. N. Phillips. Multiple-weak-boson signals at hadron supercolliders. *Phys. Rev. D*, 45:1484–1502, Mar 1992.

[87] H. Padé. Sur la répresentation approchée d'une fonction par des fractions rationelles. *Ann. École Nor.*, 3:193, 1892.

[88] J.L. Basdevant, D. Bessis, and J. Zinn-Justin. Pad approximants in strong interactions. two-body pion and kaon systems. *Il Nuovo Cimento A*, 60(2):185–238, 1969.

[89] J. L. Basdevant, D. Bessis, and J. Zinn-Justin. Pade approximants in strong interactions. two-body pion and kaon systems. *Nuovo Cim.*, A60:185–238, 1969.

[90] J. Bagger, V. Barger, K. Cheung, J. Gunion, T. Han, G. A. Ladinsky, R. Rosenfeld, and C. P. Yuan. Strongly interacting WW system: Gold-plated modes. *Phys. Rev. D*, 49:1246–1264, Feb 1994.

[91] Duane A. Dicus and Wayne W. Repko. Padé approximants and unitarity in w^+w^- and z^0z^0 scattering. *Phys. Rev. D*, 42:3660–3667, Dec 1990.

[92] A. Dobado, Maria J. Herrero, and Tran N. Truong. Study of the strongly interacting higgs sector. *Physics Letters B*, 235(12):129 – 133, 1990.

[93] A. Dobado, M.J. Herrero, and J. Terron. The role of chiral lagrangians in strongly interacting w_l,$w_l$signals at pp supercolliders. *Zeitschrift für Physik C Particles and Fields*, 50(2):205–219, 1991.

[94] A. Dobado, M.J. Herrero, and J. Terron. $w^{\pm}$ $z_{\mathbf{0}}$ signals from the strongly interacting symmetry breaking sector. *Zeitschrift für Physik C Particles and Fields*, 50(3):465–471, 1991.

[95] Tran N. Truong. Chiral perturbation theory and final-state theorem. *Phys. Rev. Lett.*, 61:2526–2529, Nov 1988.

[96] Tran N. Truong. Remarks on unitarization methods. *Phys. Rev. Lett.*, 67:2260–2263, Oct 1991.

[97] A. Dobado and J. R. Peláez. Inverse amplitude method in chiral perturbation theory. *Phys. Rev. D*, 56:3057–3073, Sep 1997.

[98] A. Dobado, M. J. Herrero, J. R. Peláez, and E. Ruiz Morales. Cern lhc sensitivity to the resonance spectrum of a minimal strongly interacting electroweak symmetry breaking sector. *Phys. Rev. D*, 62:055011, Aug 2000.

[99] Domènec Espriu and Federico Mescia. Unitarity and causality constraints in composite higgs models. *Phys. Rev. D*, 90:015035, Jul 2014.

[100] Tran N. Truong. Radiative corrections to W(L) W(L) scattering in the standard model. *Phys. Lett.*, B258:402–408, 1991.

[101] Dieter Zeppenfeld and Scott Willenbrock. Probing the three-vector-boson vertex at hadron colliders. *Phys. Rev. D*, 37:1775–1786, Apr 1988.

[102] U. Baur and D. Zeppenfeld. Unitarity Constraints on the Electroweak Three Vector Boson Vertices. *Phys. Lett.*, B201:383, 1988.

[103] Terrance Figy and Dieter Zeppenfeld. Qcd corrections to jet correlations in weak boson fusion. *Physics Letters B*, 591(34):297 – 303, 2004.

[104] V. Hankele, G. Klämke, D. Zeppenfeld, and T. Figy. Anomalous higgs boson couplings in vector boson fusion at the cern lhc. *Phys. Rev. D*, 74:095001, Nov 2006.

[105] W. Heitler. The influence of radiation damping on the scattering of light and mesons by free particles. i. *Mathematical Proceedings of the Cambridge Philosophical Society*, 37:291–300, 7 1941.

[106] Julian Schwinger. Quantum electrodynamics. i. a covariant formulation. *Phys. Rev.*, 74:1439–1461, Nov 1948.

[107] Suraj N. Gupta. Theory of longitudinal photons in quantum electrodynamics. *Proc. Phys. Soc.*, A63:681–691, 1950.

[108] S.N. Gupta. *Quantum Electrodynamics*. Gordon and Breach Science Publishers, 1981.

[109] Suraj N. Gupta, James M. Johnson, and Wayne W. Repko. W, Z and Higgs scattering at SSC energies. *Phys. Rev.*, D48:2083–2096, 1993.

[110] Micheal S. Berger and Michael S. Chanowitz. Strong W+ W+ scattering at the SSC. *Phys. Lett.*, B263:509–516, 1991.

[111] Michael S. Chanowitz. Quantum corrections from nonresonant W W scattering. *Phys. Rept.*, 320:139–146, 1999.

[112] F. Bloch and A. Nordsieck. Note on the Radiation Field of the electron. *Phys. Rev.*, 52:54–59, 1937.

[113] D. R. Yennie, Steven C. Frautschi, and H. Suura. The infrared divergence phenomena and high-energy processes. *Annals Phys.*, 13:379–452, 1961.

[114] P. P. Kulish and L. D. Faddeev. Asymptotic conditions and infrared divergences in quantum electrodynamics. *Theor. Math. Phys.*, 4:745, 1970. [Teor. Mat. Fiz.4,153(1970)].

[115] H. D. Dahmen, P. Manakos, T. Mannel, and T. Ohl. Unitary approximation for radiative high-energy scattering processes: application to Bhabha scattering. *Z. Phys.*, C50:75–84, 1991.

[116] F. Riesz. *Über die linearen Transformationen des Hilbertschen Raumes. Acta Sci. Math. (Szeged)*, 5:1-1:23–54, 1930.

[117] I.M. Gelfand. Normierte ringe. *Rec. Math. [Mat. Sbornik] N.S.*, 9(51):3–24, 1941.

[118] N. Dunford and J. T. Schwartz. *Linear Operators Part I: General Theory.* John Wiley & Sons, New York, 1988.

[119] N. Dunford and J. T. Schwartz. *Linear Operators; Part II Spectral Theory.* John Wiley & Sons, New York, 1988.

[120] Neil D. Christensen, Claude Duhr, Benjamin Fuks, Jurgen Reuter, and Christian Speckner. Introducing an interface between WHIZARD and FeynRules. *Eur. Phys. J.*, C72:1990, 2012.

[121] Wolfgang Kilian, Thorsten Ohl, Jurgen Reuter, and Marco Sekulla. Resonances at the LHC beyond the Higgs:The Scalar/Tensor Case. DESY 15-183, SI-HEP-2015-22, KA-TP-19-2015, KEK Preprint 2015-1869, 2015.

[122] Ignatios Antoniadis. A Possible new dimension at a few TeV. *Phys. Lett.*, B246:377–384, 1990.

[123] Nima Arkani-Hamed, Savas Dimopoulos, and G. R. Dvali. The Hierarchy problem and new dimensions at a millimeter. *Phys. Lett.*, B429:263–272, 1998.

[124] Ignatios Antoniadis, Nima Arkani-Hamed, Savas Dimopoulos, and G. R. Dvali. New dimensions at a millimeter to a Fermi and superstrings at a TeV. *Phys. Lett.*, B436:257–263, 1998.

[125] Nima Arkani-Hamed, Howard Georgi, and Matthew D. Schwartz. Effective field theory for massive gravitons and gravity in theory space. *Annals Phys.*, 305:96–118, 2003.

[126] Kurt Hinterbichler. Theoretical Aspects of Massive Gravity. *Rev. Mod. Phys.*, 84:671–710, 2012.

[127] David B. Kaplan and Howard Georgi. SU(2) x U(1) Breaking by Vacuum Misalignment. *Phys. Lett.*, B136:183, 1984.

[128] Thomas Appelquist and J. Carazzone. Infrared Singularities and Massive Fields. *Phys. Rev.*, D11:2856, 1975.

[129] Howard E. Haber and Yosef Nir. Multiscalar Models With a High-energy Scale. *Nucl. Phys.*, B335:363, 1990.

[130] Howard E. Haber. Nonminimal Higgs sectors: The Decoupling limit and its phenomenological implications. In *Joint U.S.-Polish Workshop on Physics from Planck Scale to Electro-Weak Scale (SUSY 94) Warsaw, Poland, September 21-24, 1994*, 1994.

[131] C. Fronsdal. On the theory of higher spin fields. *Il Nuovo Cimento (1955-1965)*, 9(2):416–443, 1958.

[132] Steven Weinberg. Feynman Rules for Any Spin. *Phys. Rev.*, 133:B1318–B1332, 1964.

[133] Shi-Zhong Huang, Peng-Fei Zhang, Tu-Nan Ruan, Yu-Can Zhu, and Zhi-Peng Zheng. Feynman propagator for a particle with arbitrary spin. *Eur. Phys. J.*, C42:375–389, 2005.

[134] M. Fierz and W. Pauli. On relativistic wave equations for particles of arbitrary spin in an electromagnetic field. *Proc. Roy. Soc. Lond.*, A173:211–232, 1939.

[135] L. P. S. Singh and C. R. Hagen. Lagrangian formulation for arbitrary spin. 1. The boson case. *Phys. Rev.*, D9:898–909, 1974.

[136] E. C. G. Stueckelberg. Interaction energy in electrodynamics and in the field theory of nuclear forces. *Helv. Phys. Acta*, 11:225–244, 1938.

[137] E. C. G. Stueckelberg. La Mecanique du point materiel en theorie de relativite et en theorie des quanta. *Helv. Phys. Acta*, 15:23–37, 1942.

[138] Henri Ruegg and Marti Ruiz-Altaba. The Stueckelberg field. *Int. J. Mod. Phys.*, A19:3265–3348, 2004.

[139] James Bonifacio, Pedro G. Ferreira, and Kurt Hinterbichler. Transverse diffeomorphism and Weyl invariant massive spin 2: Linear theory. *Phys. Rev.*, D91:125008, 2015.

[140] I. L. Buchbinder and V. A. Krykhtin. Gauge invariant Lagrangian construction for massive bosonic higher spin fields in D dimensions. *Nucl. Phys.*, B727:537–563, 2005.

[141] C. P. Burgess and David London. Light spin one particles imply gauge invariance. 1992.

[142] Ana Alboteanu, Wolfgang Kilian, and Juergen Reuter. Resonances and Unitarity in Weak Boson Scattering at the LHC. *JHEP*, 11:010, 2008.

[143] A.D. Martin and T.D. Spearman. *Elementary particle theory.* North-Holland Pub. Co., 1970.

[144] Maximilian Löschner. Unitarisation of Anomalous Couplings in Vector Boson Scattering. Master's thesis, Karlsruhe Institute of Technology, Germany, 2014.

Danksagung

Abschließend möchte ich allen danken, die mich während meiner Promotion unterstützt haben. Mein besonderer Dank gilt meinem Doktorvater Prof. Dr. Wolfgang Kilian für die mir gebotene Gelegenheit mit ihm neue Theorien im Higgs Sektor zu erforschen, sowie die Möglichkeit mich mit Physikern anderer Institute weltweit fachlich auszutauschen. Für die fruchtbare Zusammenarbeit in diesem Forschungsgebiet danke ich ebenfalls den beiden weiteren `WHIZARD` Hauptautoren, Prof. Dr. Thorsten Ohl und Dr. Jürgen R. Reuter.

Vielen Dank an alle Mitglieder der TP1 Gruppe, insbesondere Prof. Dr. Thomas Mannel. Ich erinnere mich gerne an die Hilfsbereitschaft und die freundliche Atmosphäre in Siegen.

An dieser Stelle möchte ich der JSPS, dem DAAD und meiner Gastgeberin Prof. Dr. Mihoko Nojiri danken, die mir einen zweimonatigen Aufenthalt während meiner Promotionszeit am KEK in Japan ermöglicht haben. In diesem Zusammenhang möchte ich einen herzlichen Dank an Dr. Johannes Heinonen aussprechen, der mir sogar kritische und hilfreiche Anregungen zu meiner Arbeit nach Japan gesendet hat. Einen Dank richte ich ebenfalls an die fleißigen Korrekturleser Dr. Sven Faller und Robin Roth.

Zusätzlich danke ich meinen Kommolitonen, allen meinen Freunden und meiner Freundin für Rückhalt und Geduld.

Ein ganz besonderer Dank gilt meiner ganzen Familie, insbesondere meinen Eltern und meinem Bruder, die mich nicht nur während der Promotionszeit, sondern während meines kompletten Studiums, uneingeschränkt unterstützt haben!